MIGRACIJA KRITIČNIH RADIONUKLIDOV NA VPLIVNEM OBMOČJU BIVŠEGA RUDNIKA URANA ŽIROVSKI VRH

Marko Štrok

Doktorska disertacija
Mednarodna podiplomska šola Jožefa Stefana
Ljubljana, Slovenija, marec 2011

Komisija za oceno doktorske disertacije:

prof. dr. Peter Stegnar, predsednik, Institut »Jožef Stefan«, Ljubljana

prof. dr. Boris Pihlar, član, FKKT UL, Ljubljana

doc. dr. Ljudmila Benedik, član, Institut »Jožef Stefan«, Ljubljana

doc. dr. Borut Smodiš, član, Institut »Jožef Stefan«, Ljubljana

MEDNARODNA PODIPLOMSKA ŠOLA JOŽEFA STEFANA
JOŽEF STEFAN INTERNATIONAL POSTGRADUATE SCHOOL

Marko Štrok

MIGRACIJA KRITIČNIH RADIONUKLIDOV NA VPLIVNEM OBMOČJU BIVŠEGA RUDNIKA URANA ŽIROVSKI VRH

Doktorska disertacija

MIGRATION OF CRITICAL RADIONUCLIDES IN THE AREA OF FORMER URANIUM MINE ŽIROVSKI VRH

Doctoral Dissertation

Mentor: doc. dr. Borut Smodiš

Ljubljana, Slovenija, marec 2011

Kazalo

Povzetek

Izvedel sem študijo migracije kritičnih naravnih radionuklidov na območju bivšega rudnika urana Žirovski vrh v Sloveniji. Med kritične naravne radionuklide spadajo dolgoživi naravni radionuklidi iz uran-radijeve razpadne vrste in sicer ^{238}U, ^{234}U, ^{230}Th, ^{226}Ra, ^{210}Pb in ^{210}Po. Na območju bivšega rudnika urana Žirovski vrh v Sloveniji se nahajata dve odlagališči ostankov rudarjenja in stranskih produktov pridobivanja uranovega koncentrata. V okviru doktorskega dela sem obravnaval eno izmed njih in sicer odlagališče Boršt, na katerem je bila odložena hidrometalurška jalovina (jalovina, ki je ostala po izluževanju rude z žvepleno kislino), ki vsebuje povišane vsebnosti naravnih radionuklidov iz uranove razpadne vrste. Zaradi različnih procesov v naravi lahko pride do migracije naravnih radionuklidov iz odlagališča v okolico kar predstavlja nevarnost za okoliško prebivalstvo.

Zato sem na odlagališču hidrometalurške jalovine Boršt odvzel vzorce tal, trave in dreves. Po predhodni pripravi vzorcev, sem iz njih s pomočjo radiokemijske separacije ločil dolgožive radionuklide ^{238}U, ^{234}U, ^{230}Th, ^{226}Ra, ^{210}Pb in ^{210}Po. Meritve ^{238}U, ^{234}U, ^{230}Th, ^{226}Ra, in ^{210}Po sem izvedenl s pomočjo spektrometrije alfa, meritve ^{210}Pb pa s proporcionalnim števcem. Prav tako sem izvedel dva sekvenčna ekstrakcijska postopka, ki omogočata določitev vsebnosti naravnih radionuklidov v različnih frakcijah (vodotopna frakcija, organska frakcija, karbonati, Fe, Mn oksidi in preostanek). Obenem sem rezultate obeh postopkov med seboj statistično primerjal. Rezultate vsebnosti naravnih radionuklidov v travah sem uporabil za določitev faktorjev prenosa med tlemi in travo. Preveril sem tudi možnost uporabe trave za sledenje migracije naravnih radionuklidov v tleh. Rezultate vsebnosti naravnih radionuklidov v različnih delih dreves pa sem uporabil za določitev koncentracijskih razmerij.

Prav tako sem izvedel analize ^{238}U, ^{234}U, ^{230}Th, ^{226}Ra, ^{210}Pb in ^{210}Po v vzorcih tal, travne silaže, sena in mleka iz okolice bivšega rudnika urana Žirovski vrh. Vsebnosti naravnih radionuklidov v mleku sem primerjal z referenčno lokacijo in mlekom v prahu, ki je na voljo v trgovinah. Izračunal sem efektivne letne doze zaradi zaužitja za odrasle in dojenčke do enega leta starosti za vzorce mleka iz okolice bivšega rudnika urana Žirovski vrh ter jih primerjal z vzorcem mleka iz referenčne lokacije in vzorci mleka v prahu. Izračunal sem tudi koncentracijska razmerja med travno silažo in senom ter mlekom.

Ugotovil sem, da sekvenčna ekstrakcijska postopka, razen za organsko frakcijo in preostanka v primeru ^{238}U, dajeta statistično različne rezultate. Kljub temu nam omogočata ugotoviti, da se ^{238}U, ^{230}Th in ^{210}Pb zadržujejo v eni izmed zamočvirjenih lokacij pod odlagališčem Boršt. Glede na specifične aktivnosti v hidrometalurški jalovini je na območju odlagališča Boršt najbolj mobilen ^{238}U, sledijo pa mu ^{226}Ra, ^{210}Pb, ^{230}Th in ^{210}Po. Rezultati faktorjev prenosa iz tal v travo so bili primerljivi z vrednostmi iz literature, v primeru ^{238}U ter ^{226}Ra pa bi bilo mogoče uporabiti travo za sledenje migracije naravnih radionuklidov. Vsebnost naravnih radionuklidov je najvišja v enoletnih iglicah in listih dreves, kar pomeni, da drevesa koncentrirajo radionuklide v starejših iglicah in listih. Rezultati vsebnosti naravnih radionuklidov v vzorcih mleka iz območja bivšega rudnika urana Žirovski vrh ne kažejo na povišane vrednosti v primerjavi z ostalimi vzorci. Največjo skupno efektivno letno ingestijsko dozo pa sem določil v vzorcu mleka v prahu

iz Pomurskih mlekarn in je za dojenčke do enega leta starosti znašala 648 μSv/leto. Ugotovil sem tudi, da več kot 90 % skupnih efektivnih letnih doz zaradi zaužitja v vseh primerih prispevata ^{210}Po in ^{210}Pb.

Abstract

A study of the migration of critical radionuclide in the area of the former uranium mine of Žirovski vrh in Slovenia was performed. Critical natural radionuclides are defined as the long-lived natural radionuclides from the uranium-radium decay chain, which are ^{238}U, ^{234}U, ^{230}Th, ^{226}Ra, ^{210}Pb and ^{210}Po. In the area of the former uranium mine at Žirovski vrh, two waste piles with uranium mining and milling wastes exist. The study area of this doctoral work was focused on one of these two piles, the Boršt waste pile, where uranium mill tailings are deposited. Uranium mill tailings contain elevated levels of natural radionuclides from the uranium decay chain. Different processes in nature can cause migration of natural radionuclides from the waste pile into the surroundings which can represent a hazard for the nearby local population.

Therefore, soil, grass and tree samples were collected at the Boršt waste pile. After pretreatment of the samples, radiochemical separations of the long-lived radionuclides ^{238}U, ^{234}U, ^{230}Th, ^{226}Ra, ^{210}Pb and ^{210}Po were performed. ^{238}U, ^{234}U, ^{230}Th, ^{226}Ra, and ^{210}Po were measured by alpha-particle spectrometry and ^{210}Pb a with gas-flow proportional counter. In addition, two sequential extraction protocols, which allow determination of natural radionuclide concentrations in different fractions (water soluble, organic, carbonate, Fe, Mn oxides and residual fraction), were also performed. The results of the two protocols were statistically compared. The results for the natural radionuclide activity concentrations in grass were used for calculation of soil-to-plant transfer factors. The possibility of using grass for tracing the migration of natural radionuclides in soil was evaluated. Results of the natural radionuclide concentrations in different tree compartments (wood, shoots and foliage) were used for the calculation of concentration ratios.

Analysis of ^{238}U, ^{234}U, ^{230}Th, ^{226}Ra, ^{210}Pb and ^{210}Po in soil, silage, hay and milk samples from the surrounding area of the former uranium mine were performed. Activity concentrations of natural radionuclides in milk were compared with a reference location and with powdered milk samples bought from shops. Yearly effective ingestion doses for adults and infants up to one year old for milk samples from the surrounding area of the former uranium mine were calculated and compared with the milk sample from the reference location and with the commercial powdered milk samples. Concentration ratios between silage, hay and milk samples were also calculated.

The results showed that the two sequential extraction protocols give statistically different results, with the exception of the organic fraction and residue in the case of ^{238}U. However, both protocols revealed that ^{238}U, ^{230}Th and ^{210}Pb are retained in a swampy area below the Boršt waste pile. According to the activity concentrations in uranium mill tailings on the Boršt waste pile, ^{238}U is the most mobile, followed by ^{226}Ra, ^{210}Pb, ^{230}Th and ^{210}Po. Soil-to-grass transfer factors were comparable with literature values. In the case of ^{238}U and ^{226}Ra, grass shows potential for use as an indicator for radionuclide migration in soil. The highest activity concentration in the case of tree samples were found in one years old needles and leaves, which means that trees concentrate radionuclides in older needles and leaves. Activity concentrations of the radionuclides analysed in milk samples from the area surrounding the former uranium mine at Žirovski

vrh are in general not higher than in other samples. The highest combined yearly effective ingestion dose was found in the powdered milk sample from the Pomurske mlekarne diary of 648 μSv/year for infants. In addition, more than 90 % of the combined annual effective ingestion doses in all cases was due to ^{210}Po and ^{210}Pb.

Seznam kratic

HMJ	=	hidrometalurška jalovina
IUPAC	=	International Union of Pure and Applied Chemistry
BCR	=	Bureau Communautaire de Référence
SI	=	Systéme International
IAEA	=	International Atomic Energy Agency
NPL	=	National Physical Laboratory
PIPS	=	Passivated Implanted Planar Silicon

1 Uvod

Naravni radionuklidi se nahajajo povsod v okolju. V posameznih geoloških formacijah je njihova koncentracija povišana, kot na primer na območju Žirovskega vrha, kjer se je v preteklosti vršilo intenzivno pridobivanje urana iz uranove rude. Zapuščina preteklega rudarjenja je jalovina, ki je preostanek izluževanja urana iz rude in je odložena v bližini rudnika na odlagališčih Boršt in Jazbec. V jalovini lahko najdemo tako ostanke urana, ki ni bil v popolnosti izlužen iz nje, in tudi vse ostale radionuklide iz uranove razpadne vrste, kot na primer ^{238}U, ^{234}U, ^{230}Th, ^{226}Ra, ^{210}Pb in ^{210}Po. Odlagališči jalovine sta v času pisanja te doktorske disertacije že sanirani do te mere, da ni pričakovati večjega vpliva radionuklidov na okolico. Vendar padavine, erozija tal, zaledne vode in mnogi drugi procesi lahko v prihodnosti povzročijo migracijo določenih radionuklidov iz odlagališč v okolico. Odlagališči namreč ležita v subalpskem področju, kjer je količina padavin relativno velika, v neposredni bližini pa živijo ljudje, ki bi lahko bili ob nepredvidljivi migraciji radionuklidov iz odlagališč izpostavljeni višjim koncentracijam naravnih radionuklidov. Zato je potrebno poznati kakšna je mobilnost radionuklidov odloženih na odlagališčih v specifičnih lokalnih razmerah. Prav tako odlagališči jalovine predstavljata naravni laboratorij v katerem povišane koncentracije naravnih radionuklidov omogočajo raziskovanje raznih procesov kroženja in migracije radionuklidov, ki jih na območjih z nizkimi vsebnostmi radionuklidov ni mogoče izvesti ali je njihova izvedba otežena.

Na **odlagališču Jazbec** je bila odložena revna ruda in rdeča oborina. Revna ruda je bila okarakterizirana kot ruda, ki je vsebovala manj kot 450 g/t U_3O_8, rdeča oborina pa je bila eden izmed stranskih produktov v procesu izluževanja urana (Florjančič, 2000). Na začetku doktorskega dela (november 2006), so se na odlagališču Jazbec že izvajala končna sanacijska dela, ki so vključevala ureditev brežin odlagališča, ureditev radonske zapore, drenaž, vrhnjega sloja in zatravitve odlagališča. Zato raziskovalno delo na tem odlagališču ni bilo možno.

V nasprotju z odlagališčem Jazbec, pa na **odlagališču Boršt** zaključnih sanacijskih del v času začetka doktorskega dela še niso začeli izvajati. Zato sem območje odlagališča Boršt izbral za izvajanje raziskav migracije naravnih radionuklidov. Na odlagališču Boršt so v preteklosti odlagali hidrometalurško jalovino (HMJ), ki je bila odpadni produkt po izluževanju urana z žvepleno kislino. Brežine odlagališča so bile pokrite s 30 – 40 cm zemlje, na katerih je rasla naravna vegetacija (pretežno trava, bori in smreke, v manjši meri pa tudi javor ter nekatere grmovnice). Izcedne vode s povišano vsebnostjo naravnih radionuklidov so se izlivale v bližnji potok Todraščica, površinske vode iz odlagališča pa so odvajali v zadrževalni bazen, kjer se je vršila sedimentacija trdnih delcev, preliv pa je prav tako odtekal v potok Todraščica.

Industrijsko pridobivanje uranovega koncentrata iz uranove rude je v Rudniku urana Žirovski vrh potekalo med leti 1984 in 1990, ko je bilo z dekretom prekinjeno izkoriščanje urana. Shemo pridobivanja uranovega koncentrata prikazuje slika 1. Po drobljenju in mletju uranove rude, je bil iz nje izlužen uran s pomočjo H_2SO_4. Odpadni produkt izluževanja je bila HMJ, ki je bila, kot že rečeno, odložena na odlagališču Boršt. Uran je bil ekstrahiran iz lužnice, ki je ostala po izluževanju urana z žvepleno kislino, s pomočjo terciarnih aminov in kerozina. Iz preostalega rafinata iz solventne ekstrakcije so oborili hidrokside (rdeče blato) s pomočjo apna. Iz eluata pa so z amoniakom oborili

uranov koncentrat in ga posušili (Florjančič, 2000).

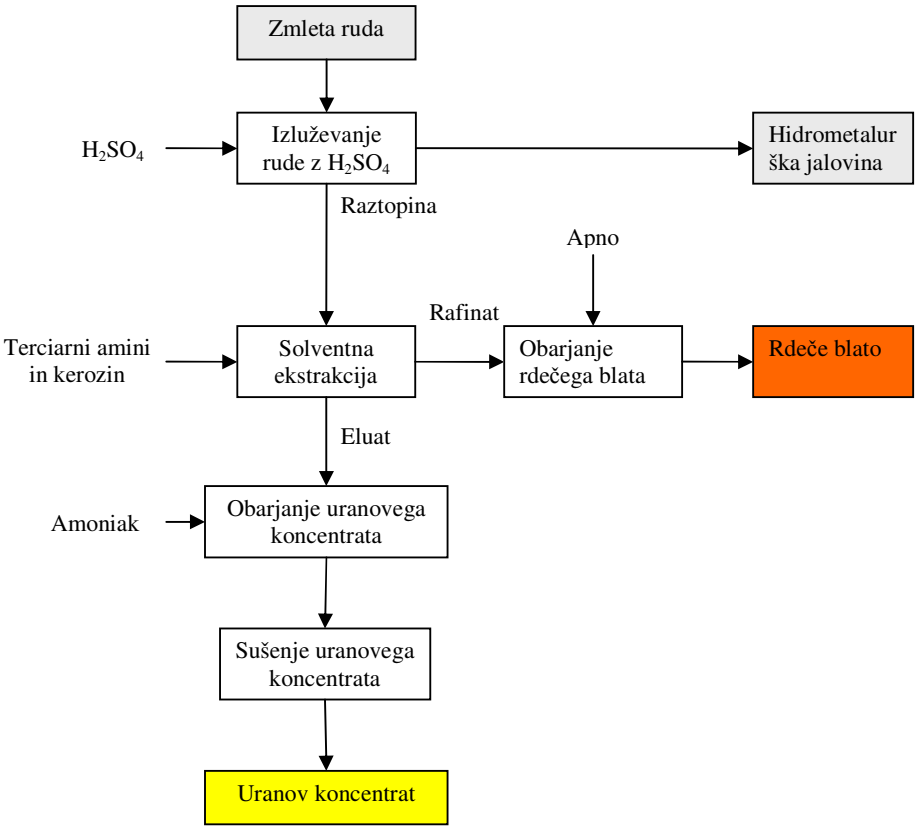

Slika 1: *Poenostavljena shema pridobivanja uranovega koncentrata.*

V času industrijskega pridobivanja uranovega koncentrata je bilo na odlagališču Boršt odloženih 0,6 milijonov ton HMJ z vsebnostjo (995 ± 80) Bq/kg ^{238}U, (3930 ± 580) Bq/kg ^{230}Th in (8630 ± 340) Bq/kg ^{226}Ra (Križman et al., 1995). Poleg teh radionuklidov, vsebuje HMJ tudi vse ostale radionuklide iz uran-radijeve in aktinijeve razpadne vrste. Na sliki 2 so tako prikazani uran-radijevi dolgoživi radionuklidi ^{238}U, ^{234}U, ^{230}Th, ^{226}Ra, ^{210}Pb in ^{210}Po, ki so bili predmet raziskav predstavljenih v doktorski disertaciji.

Uran ima atomsko število 92 in je najtežji naravni element. Njegovi trije naravni izotopi so ^{238}U (99,28 %), ^{235}U (0,71 %) in ^{234}U (0,0054 %). Znan je kot tretji v vrsti aktinidov, pri katerih se polni notranja 5 f orbitala. Vsi trije uranovi naravni izotopi razpadajo z razpadom α z energijami razpada 4,3 MeV (^{238}U), 4,7 MeV (^{235}U) in 4,9 MeV (^{234}U). Na območju Žirovskega vrha je prevladujoči uranov mineral uranova smola ($4UO_2 \cdot UO_3$ do $2UO_2 \cdot 3UO_3$), ki je kolomorfna, pretežno izotropizirana oblika uraninita in je sive barve z nekoliko rjavim odtenkom (Florjančič, 2000). Kovinski uran je svetlikajoča se kovina srebrne barve, ki ima tališče pri 1132 °C in vrelišče pri 3818 °C. Uran lahko obstaja v vodnih raztopinah v štirih oksidacijskih stanjih in sicer kot U^{3+} (rdeč), U^{4+} (zelen), UO_2^+ (nestabilen) in UO_2^{2+} (rumen). Oksidacijsko redukcijski potencial uranovih ionov v kisli raztopini je predstavljen v formuli 1. (Hampel, 1968).

$$UO_2^{2+} \xrightarrow{+0{,}063\ V} UO_2^{+} \xrightarrow{+0{,}58\ V} U^{4+} \xrightarrow{-0{,}631\ V} U^{3+} \xrightarrow{-1.80\ V} U \qquad (1)$$

$$\uparrow \xleftarrow{+0{,}32\ V}$$

Obstaja tudi uran z oksidacijskim številom 2, vendar le v nekaterih trdnih spojinah, kot na primer UO ali US, ion s tem oksidacijskim stanjem v raztopini pa ne obstaja. U^{3+} ion je zelo nestabilen, saj sprošča vodik iz vode, prav tako UO_2^+, ki predstavlja U^{5+} in običajno disproporcionira na U^{4+} ter UO_2^{2+}. Kljub temu, da je nestabilen, pa v raztopinah najdemo U^{5+} v organskih in anorganskih (s kloridnimi, sulfatnimi ali karbonatnimi ioni) kompleksih. Najpomembnejši oksidacijski stanji urana sta 4+ in 6+, zato kemizem urana lahko povežemo z dvema oksidoma v teh oksidacijskih stanjih in sicer UO_2 in UO_3. Prvi se raztaplja v kislih raztopinah, pri čemer oblikuje U^{4+} ione in tvori trdne soli kot UCl_4 in $U(SO_4)_2 \cdot 9H_2O$. Ion UO_2^{2+} tvori v kislih raztopinah uranilne derivate tipa $UO_2(NO_3)_2 \cdot 6H_2O$ in UO_2Cl_2. Sorodni so tudi derivati trioksida, uranati in poliuranati. Znani so tudi uranati alkalnih kovin, kot na primer $M_2U_2O_7$. (Hampel, 1968)

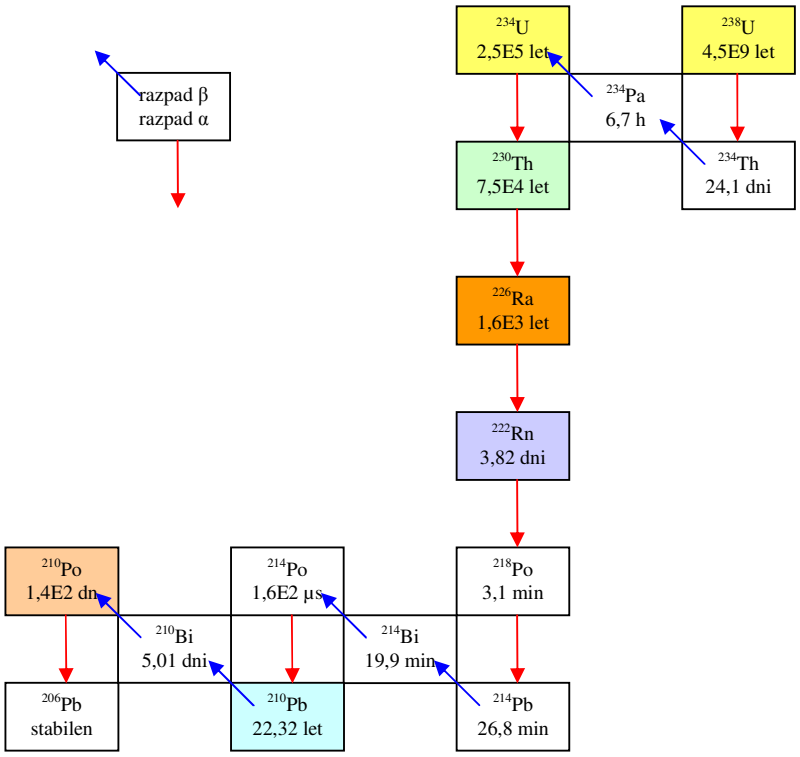

Slika 2: *Uran-radijeva razpadna vrsta.*

Trivalentne uranove spojine ni mogoče oboriti iz vodnega U^{3+}, ker je podvržen hitri oksidaciji do U^{6+}. Običajne vodotopne soli U^{4+} so kloridi, bromidi, sulfati in perklorati; vse te raztopine so hidrolizirane. Kloridni in bromidni ioni oblikujejo šibke komplekse v razredčenih raztopinah medtem, ko so sulfatni ionski kompleksi močnejši. Uranov (IV) oksalat, fosfat, fluorid, molibdat, arzenat, ferocianid in hidroksid so netopni v nevtralnih pogojih. Zanimiva oksidna kationa MO_2^{2+} in MO_2^+ se pojavljata praktično le pri aktinidih. Uranilni ion UO_2^{2+} se obnaša kot enostavni, dvakrat pozitivno nabiti ion in lahko v mnogih primerih nadomešča Ca^{2+}. Obstajajo tudi dokazi o bolj zapletenih polimernih vrstah tega iona, kot na primer $U_2O_5^{2+}$ in $U_3O_8^{2+}$, ki se oblikujejo v koncentriranih uranilnih raztopinah kot rezultat hidrolize. (Hampel, 1968).

Atomsko število **torija** je 90. Razni torijevi izotopi se pojavljajo v vseh naravnih razpadnih vrstah, vendar so vsi radioaktivni. Najbolj znan je ^{232}Th, ki je na začetku torijeve razpadne vrste. V uranovi razpadni vrsti, ki je prikazana na sliki 2, najdemo še ^{234}Th in ^{230}Th. Z vidika teme doktorske disertacije je najpomembnejši ^{230}Th, saj ima precej dolg razpolovni čas (slika 2) medtem, ko je ^{232}Th na Žirovskem vrhu prisoten le v

zelo nizkih koncentracijah. Podobno kot uranovi izotopi, tudi ^{230}Th razpada z razpadom α z energijo 4,8 MeV.

V splošnem je torij v kemijskih reakcijah prisoten kot štirikrat pozitivno nabiti ion. Torij je drugi v vrsti aktinidov, pri čemer imajo vsi elementi razen aktinija in torija elektrone v 5 f orbitali v osnovnem stanju. Pri tvorbi spojin ima torij močne kovinske lastnosti in tvori binarne spojine praktično z vsemi nekovinskimi elementi. ThO_2 lahko dobimo s termičnim razpadom oksalatov, hidroksidov in nitratov, s hidrolizo halidov ter s segrevanjem kovinskega torija na zraku ali kisiku. Ostale torijeve okside je tudi možno pripraviti, vendar v normalnem kemijskem obnašanju torija ne igrajo pomembne vloge. Torijev dioksid je osnova za tvorbo soli z organskimi in anorganskimi kislinami. Ker torij obstaja v raztopini kot majhen, visoko nabit kation, je izpostavljen obsežnim interakcijam z vodo in mnogimi anioni. Torij obstaja le v oksidacijskem stanju 4+, zato ni potrebno upoštevati redoks reakcij. Vodotopne soli torija so nitrati, sulfati, kloridi in perklorati. Najpomembnejše netopne spojine torija pa so hidroksidi, fluoridi, in fosfati (Hyde, 1960).

Radij je najtežji element alkalnih zemelj. Njegovo atomsko število je 88. Izmed vseh radijevih izotopov je najpomembnejši ^{226}Ra, ki je razpadni produkt ^{238}U (slika 2). Tudi ^{226}Ra razpada z razpadom α z energijo 4,9 MeV. Kemijske lastnosti radija so določene z njegovo pozicijo v drugi skupini periodnega sistema. Njegovi oksidacijski stanji sta 0 in 2+, redoks potencial pa -2,916 V, kar je podobno kot pri kalciju, stronciju in bariju. Tudi kemijsko obnašanje radija je podobno tem elementom. Vendar pa močna radioaktivnost radija povzroča veliko radiacijskih poškodb v kristalih, ki vsebujejo radij. Tako so $Ra(IO_3)_2$ kristali za razliko od brezbarvnega $Ba(IO_3)_2$, rjave barve zaradi prisotnosti prostega joda, ki je posledica radiacijske redukcije. Radij obstaja v raztopinah le v oksidacijskem stanju 2+. Zaradi njegovega bazičnega karakterja ga je zelo težko kompleksirati. To je tudi vzrok, da je večina radijevih spojin enostavnih ionskih soli. Radijevi klodiri, bromidi in nitrati so topni v vodi, toda njihova topnost pada z naraščajočo koncentracijo kloridnih, bromidnih ali nitratnih ionov. Radijev klorid in bromid sta manj topna od pripadajočih barijevih soli, radijev nitrat pa je bolj topen od barijevega (Kirby in Salutsky, 1964).

Svinec ima atomsko število 82 in se nahaja v četrti skupini periodnega sistema elementov in ima tališče pri 327 °C ter vrelišče pri 1737 °C. Radioaktivni izotop svinca ^{210}Pb razpada z razpadom beta z maksimalno energijo 63 keV. V vodnih raztopinah se svinec ponavadi nahaja v divalentni obliki, saj je tetravalentna oblika nestabilna ali netopna (Gibson, 1961). Najpomembnejša topna svinčeva sol je $Pb(NO_3)_2$, ki jo lahko pridobimo z raztapljanjem kovinskega svinca v dušikovi kislini. Tudi svinčev acetat je topen in kristalizira v obliki $Pb(C_2H_3O_2)_2{\cdot}3H_2O$. Ta snov le delno disociira v vodnih raztopinah, zato postanejo mnoge slabo topne svinčeve soli v raztopinah, ki vsebujejo acetatni ion bolje topne. Pri tem pride do tvorbe bodisi nedisociiranega svinčevega acetata, bodisi ob presežku acetatnih ionov do tvorbe kompleksov $Pb(C_2H_3O_2)_3^-$ ali $Pb(C_2H_3O_2)_4^{2-}$. Zaradi te lastnosti svinčevega acetata, se velikokrat uporablja pri analitiki, saj pomaga pri raztopitvi slabo topnih svinčevih spojin. Zraven sulfatov, kromatov, sulfidov in karbonatov, spadajo tudi halidi med slabo topne svinčeve soli. Topnost svinčevih halidov se zmanjšuje v vrstnem redu, kot so navedeni: $PbCl_2$, $PbBr_2$, PbI_2, PbF_2. (Hampel, 1968).

Polonij ima atomsko število 84, nima stabilnih izotopov in spada med najredkejše naravne elemente. ^{210}Po, ki je zadnji radionuklid v uranovi razpadni vrsti, razpada z razpadom α z energijo 4,8 MeV. Polonij ima tališče pri 254 °C in vrelišče pri 962 °C, kjer tvori brezbarvne pare s Po_2 molekulami. Kljub temu je znano, da je polonij hlapen pri mnogo nižjih temperaturah, pri čemer je hlapnost odvisna od tega, s katerimi kemijskimi vrstami je povezan. Tako Mabuchi (1958) ugotavlja, da polonij, ki je povezan s spojinami iz organskih reagentov (difenilkarbazid, difenilkarbazon, difeniltiokarbazon, tiourea,

difeniltiourea,...), sublimira že pri temperaturah pod 160 °C in zračnem tlaku. Pri anorganskih spojinah (kalijev jodid in HCl) pa do sublimacije ni prišlo niti pri 200 °C in zračnem tlaku. Podobno ugotavljata Jia in Torri (2007), ki sta za razkroj zemelj uporabila talino vzorca z Na_2CO_3 in Na_2O_2 pri 600 °C in izmerila, da je bila hlapnost polonija okrog 14 %. Čas trajanja taljenja sta spreminjala od 0 do 120 min in pri tem nista opazila povečevanja hlapnosti s časom.

Kemizem polonija kaže največ podobnosti s kemizmom telurja. Polonij počasi oksidira na zraku. Pri tem se tvori pretežno PoO_2. Raztaplja se v koncentrirani žveplovi in selenovi kislini. Koncentrirana dušikova kislina in zlatotopka raztapljata polonij tako, da ga oksidirata do Po^{4+}. V razredčeni klorovodikovi kislini se polonij raztaplja tako, da tvori rdeč do roza Po^{2+}, ki se nato oksidira do rumenega Po^{4+} zaradi radiolitske reakcije. Polonij obstaja v valencah -2, 0, +2, +3, +4 in +6. Polonijeve soli so bolj bazične od pripadajočih selenovih ali telurjevih spojin. (Hampel, 1968).

Detekcija naravnih radionuklidov je odvisna od vrste radioaktivnega sevanja, ki ga oddajajo posamezni radionuklidi in je posledica razpada le teh. Tako v osnovi lahko razdelimo radionuklide med tiste ki razpadajo na bodisi delce alfa ali beta, nekateri med njimi pa ob tem oddajajo tudi sevanje gama. Za detekcijo sevanja gama se za vzorce najpogosteje uporablja spektrometrija gama, za detekcijo delcev alfa spektrometrija alfa, proporcionalni števec ali tekočinski scintilacijski števec. Pri detekciji delcev alfa je spektrometrija alfa veliko boljša od ostalih dveh možnosti saj omogoča prikaz spektra, ki nam olajša identifikacijo posameznih radionuklidov, prav tako pa so vrednosti ozadja veliko nižje kar omogoča mnogo nižje meje detekcije. Za detekcijo delcev beta pa se pri vzorcih iz okolja najpogosteje uporabljata proporcionalni števec z nizkim ozadjem in tekočinski scintilacijski števec. V primeru detekcije delcev beta omogoča proporcionalni števec z nizkim ozadjem nižje vrednosti ozadja in posledično nižje meje detekcije v primerjavi s tekočim scintilacijskim detektorjem. V doktorskem delu sem za detekcijo ^{238}U, ^{234}U, ^{230}Th, ^{226}Ra in ^{210}Po uporabil spektrometer alfa, za detekcijo ^{210}Pb pa proporcionalni števec.

Porazdelitev, mobilnost in biološka dostopnost radionuklidov je odvisna ne le od aktivnosti, ampak tudi od oblike v kateri se nahajajo v okolju. Spremembe pogojev v okolju lahko močno vplivajo na obnašanje radionuklidov zato, ker pride do spremembe oblike v kateri se pojavljajo v okolju. Tako lahko nekateri radionuklidi preidejo v bolj topno obliko, spet drugi se lahko oborijo in postanejo biološko nedostopni. Obliko v kateri se nahajajo radionuklidi v vzorcu oziroma v okolju lahko dobimo s pomočjo speciacijske analize (Ure in Davidson, 2002). IUPAC (2000) opredeljuje speciacijsko analizo kot analitske aktivnosti, ki so potrebne za identifikacijo in/ali meritev množine ene ali več individualnih kemijskih zvrsti v vzorcu. Prvi korak k speciacijski analizi je frakcionacija, ki je proces klasifikacije analita ali skupine analitov v določenem vzorcu glede na njegove fizikalne (velikost, topnost) in kemijske (reaktivnost, sposobnost vezave) lastnosti.

V doktorski disertaciji sem uporabil in primerjal dva najpogosteje uporabljana **sekvenčna ekstrakcijska postopka** in sicer Schultzeva modifikacija Tessierjevega postopka (Schultz et al., 1998) ter revidiran BCR postopek (Rauret et al., 1999). Pri sekvenčni ekstrakciji razvrščamo analit glede na njegovo topnost v različnih topilih, zato jo glede na IUPAC-ovo (2000) definicijo uvrščamo med frakcionacije in je zelo uporabna kot začetna stopnja speciacije radionuklidov v zemlji. Pri sekvenčni ekstrakciji izvedemo celo vrsto zaporednih ekstrakcij istega vzorca z različnimi ekstraktanti. Največja prednost sekvenčne ekstrakcije je izboljšana selektivnost reagentov, saj razporedimo ekstrakcijske stopnje tako, da najprej ekstrahiramo vzorec z najblažjimi reagenti in na koncu z najbolj reaktivnimi.

Eni izmed prvih začetnikov sekvenčne ekstrakcije so bili Tessier et al. (1979), ki so

razvili postopek sekvenčne ekstrakcije za kovine v sledovih v vzorcih sedimentov. Postopek temelji na selektivnem raztapljanju določenega elementa, ki je prisoten v vzorcu v različnih topilih. Tessierjev postopek predvideva pet stopenj, kjer kot rezultat dobimo vsebnost analita v petih frakcijah: izmenljiva, vezana na karbonate, vezana na Fe-Mn okside, vezana na organsko snov ter preostanek. Vse frakcije so odvisne od uporabljenih reagentov in se ne nanašajo na točno določeno kemijsko frakcijo. Takšno razvrščanje nam pove koliko analita je biodostopnega in mobilnega za prenos v ostale dele ekosistema. Obenem je postopek dokaj enostaven, zato se je uporaba tega postopka v svetu močno razširila tudi na preučevanje tal in ostalih kemijskih elementov ter tudi na radionuklide. Število objav, v katerih je bila uporabljena ena izmed metod sekvenčne ekstrakcije, je bilo v letu 2006 že večje od 200 (Bacon in Davidson, 2008).

V času od razvoja Tessierjevega postopka do danes so se pojavile mnoge modifikacije tega postopka, kot tudi drugi postopki. Raziskovalci so namreč spreminjali in modificirali razne postopke ter razvijali nove z namenom, da bi postopek bolj ustrezal njihovim potrebam. To je privedlo do tega, da rezultati med seboj niso bili primerljivi. Zato so Ure et al. (1993) razvili tako imenovani BCR tristopenjski postopek z namenom, da bi poenotili postopke sekvenčnih ekstrakcij ter tako dobili ponovljive rezultate. Temu je v letu 1999 sledila še revizija BCR tristopenjskega postopka, ki so jo naredili Rauret et al. (1999). Za študije mobilnosti radionuklidov pa se kljub razvoju BCR postopka najpogosteje uporablja Tessierjev postopek ter modifikacija tega postopka, ki so jo izvedli Schultz et al. (1998).

Pri pregledu literature lahko ugotovimo, da nobena izmed študij, ki se ukvarjajo z radionuklidi ne uporablja BCR postopka ali revizijo le tega, čeprav je bil predstavljen z namenom poenotenja sekvenčnih ekstrakcijskih postopkov. Večina raziskovalcev pri raziskavah mobilnosti dolgoživih naravnih radionuklidov v zemljah in sedimentih uporablja Tessierjev postopek (Aguado et al., 2004; Trautmannsheimer et al., 1998) ali Schultzov postopek (Blanco et al., 2005). Mnogo je tudi raziskovalcev, ki uporabljajo druge postopke, ki so po navadi ena izmed modifikacij Tessierjevega postopka (Al-Masri et al., 2006; Galindo et al., 2007; Desideri et al., 2008). Na splošno pa so raziskave mobilnosti dolgoživih naravnih radionuklidov veliko redkejše v primerjavi z umetnimi radionuklidi ali težkimi kovinami.

Zanimivo možnost pri sledenju migracije radionuklidov predstavlja tudi **uporaba izotopskega razmerja ^{234}U/^{238}U**. V ravnotežnih pogojih bi namreč lahko predpostavili, da sta specifični aktivnosti ^{234}U in ^{238}U enaki, vendar vedno ni tako. Kot razlog neravnotežju med ^{234}U in ^{238}U Bourdon et al. (2003), Adloff in Rössler (1991) ter Suksi et al. (2006) navajajo odbojni efekt, ki sproži premik razpadnega produkta iz delca v okolje in povečano mobilnost razpadnega produkta zaradi oksidacije ^{234}U v območjih, ki niso blizu fazne meje. Shematski prikaz odbojnega efekta in oksidacije ^{234}U prikazuje slika 3. Posledica tega efekta je znižanje izotopskega razmerja ^{234}U/^{238}U v delcu in povečanje v njegovi okolici. Skladno s tem lahko pričakujemo v HMJ in v področjih kontaminiranih s HMJ, da bo izotopsko razmerje ^{234}U/^{238}U enako 1, saj je bila HMJ podvržena drobljenju in mletju ter izluževanju s H_2SO_4 in omenjen efekt ne more potekati. V področjih kjer ni vpliva HMJ pa lahko pričakujemo izotopsko razmerje ^{234}U/^{238}U v tleh v preostanku iz sekvenčne ekstrakcije, ki je manjše od 1 ter v mobilnih frakcijah večje od 1.

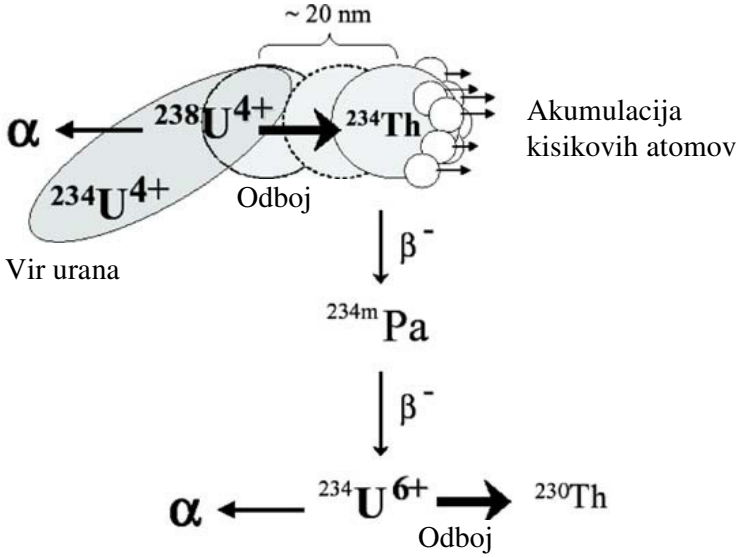

Slika 3: *Shematski prikaz odbojnega efekta in oksidacije ^{234}U (Suksi et al., 2006).*

Brežine odlagališča Boršt je na začetku študij, ki so predstavljene v tem doktorskem delu prekrivala naravna vegetacija, kar je predstavljalo priložnost za raziskave privzema naravnih radionuklidov v travo in drevesa. Tako sem določil **faktorje prenosa** radionuklidov iz tal v trave in jih primerjal z rezultati iz literature. Faktor prenosa predstavlja razmerje med aktivnostjo posameznega radionuklida v rastlini in aktivnostjo v tleh. Uporaben je predvsem kot parameter v modelih za oceno prenosa radionuklidov po prehranski verigi. Faktor prenosa iz tal v trave je v veliki meri odvisen od vrste tal zato so razlike med faktorji prenosa iz tal v trave iz različnih lokacij po svetu lahko tudi več velikostnih razredov. Tako so na primer faktorji prenosa iz tal v trave za ^{238}U v podatkih iz literature v razponu od 3.07E-4 do 4.56E-1 (Vandenhove et al., 2009). Zato je bilo pomembno določiti faktorje prenosa iz tal v trave v okolju v katerem se nahaja odlagališče Boršt. Ker bosta po končani sanaciji odlagališči prekriti s travo, sem preveril tudi možnost uporabe trave za spremljanje migracije naravnih radionuklidov iz odlagališč. Iz stališča privzema radionuklidov pa so zanimiva tudi drevesa, ki so rasla na brežinah odlagališča Boršt, saj so zaradi relativno tanke plasti zemlje, s katero je bila pokrita jalovina, praktično rasla s koreninami v samem jalovišču. V literaturi je zaslediti kar nekaj študij povezanih z drevesi, ki so rasla na različnih odlagališčih odpadkov rudarjenja urana (Petrova, 2006; Madruga et al., 2001; Rodríguez et al., 2010 in Thiry et al. 2005). Tako sem, kjer je to bilo mogoče, dobljene rezultate primerjal z že objavljenimi.

V bližini odlagališč Boršt in Jazbec živijo ljudje, ki so zaskrbljeni zaradi vpliva le teh na njihovo zdravje. Ena izmed možnih prenosnih poti radionuklidov, katerim je izpostavljeno okoliško prebivalstvo, je tudi prenos preko krme, ki jo pridelujejo v bližnji okolici bivšega rudnika Žirovski vrh, v krave, ki jih imajo domačini in posledično v mleko. Zato so bili odvzeti vzorci mleka pri štirih kmetih, ki krmijo krave s krmo, ki jo pridelajo v bližini bivšega rudnika urana Žirovski vrh. V odvzetih vzorcih mleka sem določil vsebnosti kritičnih naravnih radionuklidov (^{238}U, ^{234}U, ^{226}Ra, ^{210}Pb in ^{210}Po) in jih primerjal z vrednostmi v vzorcu mleka iz referenčne lokacije, ki je bil odvzet v Bukovščici. Izračunal sem tudi dozno obremenitev za odrasle prebivalce ter dojenčke, kot posledico pitja mleka. Pri dojenčkih mleko predstavlja še posebno velik delež pri prehrani in so lahko zaradi večjega vnosa posledično bolj obremenjeni pri povišanih vsebnostih naravnih radionuklidov. Zato sem vrednosti iz vzorcev mleka iz okolice Žirovskega vrha primerjal z vrednostmi v mleku v prahu, ki sem ga kupil v trgovinah v Ljubljani in je namenjeno za pripravo hrane za dojenčke.

Kljub temu, da je mleko zelo pomembno živilo v prehrani ljudi, so raziskave naravnih radionuklidov v mleku zelo redke in po pregledu dostopne literature nisem našel nobenega članka, ki bi se ukvarjal s to problematiko. Obstaja pa veliko študij o vsebnosti in prenosu umetnih radionuklidov v mleko, kot sta na primer ^{90}Sr in ^{131}I, ki se lahko sprostita v naravno okolje preko različnih človeških aktivnosti (jedrske elektrarne, jedrske nesreče, eksplozije jedrskih bomb…). V okolici rudnika urana Žirovski vrh so v preteklosti v okviru programa nadzora radioaktivnosti že bile izvedene meritve radionuklidov v mleku. Omenjene meritve so bile izvedene s spektrometrijo gama, rezultati pa so bili omejeni le na ^{226}Ra in ^{210}Pb, pa še pri teh dveh radionuklidih so zaradi premajhne občutljivosti metode vrednosti bile pod mejo detekcije (< 0,03 Bq/kg svežega mleka za ^{226}Ra in < 0,2 Bq/kg svežega mleka za ^{210}Pb) (Omahen et al., 2006). Zato sem naravne radionuklide v mleku v doktorskem delu določil s pomočjo radiokemijske separacije in meritve bodisi s pomočjo spektrometra alfa (^{238}U, ^{234}U, ^{226}Ra, in ^{210}Po) ali proporcionalnega števca (^{210}Pb). Omenjene metode omogočajo tudi do desetkrat nižje meje detekcije in so posledično bolj primerne za določitev naravnih radionuklidov v vzorcih mleka. Ker so raziskave naravnih radionuklidov v mleku zelo redke, sem izvedel tudi določitev koncentracijskih razmerij med krmo in mlekom, za kar so bili odvzeti vzorci tal, sena, travne silaže in mleka na kmetiji, ki se nahaja v bližini bivšega rudnika urana Žirovski vrh.

2 Namen dela

Namen doktorskega dela je bil doprinesti, razširiti in poglobiti trenutna spoznanja glede obnašanja naravnih radionuklidov v okolju. Na posameznih področjih, ki jih obravnava doktorsko delo so namreč študije, ki jih je moč zaslediti v dostopni literaturi, zelo omejene ali pa sploh ne obstajajo. Namen doktorskega dela je poglobljeno obravnavati obnašanje naravnih radionuklidov na območju bivšega rudnika urana Žirovski vrh. Tako je namen dela ugotoviti migracijo in mobilnost kritičnih radionuklidov (^{238}U, ^{234}U, ^{230}Th, ^{226}Ra, ^{210}Pb in ^{210}Po) na vplivnem območju bivšega rudnika urana Žirovski vrh v tleh in prenos teh radionuklidov v travo, drevesa in mleko. Prav tako sem v doktorskem delu statistično primerjal dva sekvenčna ekstrakcijska postopka z namenom ugotovitve primernosti uporabe sekvenčnih ekstrakcijskih postopkov za določanje vsebnosti naravnih radionuklidov v določeni frakciji. Namen doktorskega dela je tudi oceniti ustreznost uporabe trave za spremljanje migracije radionuklidov iz odlagališča ter določiti vsebnost radionuklidov v drevesih, ki so rasla na odlagališču Boršt. V doktorskem delu sem ocenil tudi efektivno letno ingestijsko dozo, ki jo prejmejo odrasli in dojenčki do enega leta starosti pri uživanju mleka iz okolice območja bivšega rudnika urana Žirovski vrh. To dozo sem primerjal z vzorcem iz referenčne lokacije ter vzorci mleka v prahu, ki so dostopni v trgovinah z namenom ugotovitve ali bivši rudnik urana Žirovski vrh vpliva na vsebnosti naravnih radionuklidov v vzorcih mleka. V doktorskem delu sem določil tudi faktorje prenosa med tlemi in travo kakor tudi koncentracijska razmerja med hidrometalurško jalovino in določenimi deli dreves in koncentracijska razmerja med krmo in mlekom.

3 Materiali in metode

3.1 Kemikalije

Vse uporabljene kemikalije, razen kjer ni posebno navedeno, so bile p.a. kvalitete. Seznam uporabljenih kemikalij je sledeč:

- Koncentrirana HNO_3 (65 %) proizvajalca Sigma-Aldrich.
- Koncentrirana HCl (37 %) proizvajalca Sigma-Aldrich.
- Koncentrirana HF (48 %) proizvajalca E. Merck.
- Koncentrirana H_2SO_4 (96 %) proizvajalca Sigma-Aldrich.
- Raztopina NH_4OH (25 %) proizvajalca E. Merck.
- Raztopina H_2O_2 (30 %) proizvajalca E. Merck.
- $MgCl_2 \cdot 6H_2O$ proizvajalca E. Merck.
- NaOCl (10 – 12 %), reagent grade, proizvajalca Sigma-Aldrich.
- Natrijev acetat (NaAc) proizvajalca Alkaloid Skopje.
- Ocetna kislina (HAc) (100 %) proizvajalca E. Merck.
- NH_2OHHCl proizvajalca E. Merck.
- Na_2O_2 proizvajalca Sigma-Aldrich.
- Na_2CO_3 proizvajalca Sigma-Aldrich.
- Etanol (95 %) proizvajalca Carlo Erba Reagenti.
- NH_4HAc proizvajalca Kemika Zagreb.
- Askorbinska kislina proizvajalca Sigma-Aldrich.
- $Al(NO_3)_3 \cdot 9H_2O$ proizvajalca E. Merck.
- Oksalna kislina proizvajalca Alkaloid Skopje.
- $Pb(NO_3)_2$ proizvajalca E. Merck.
- EDTA proizvajalca Carlo Erba Reagenti.
- NaOH proizvajalca E. Merck.
- $BaCl_2 \cdot 2H_2O$ proizvajalca Carlo Erba Reagenti.
- Na_2SO_4 proizvajalca Carlo Erba Reagenti.
- $FeCl_3 \cdot 6H_2O$ proizvajalca E. Merck.
- Nd_2O_3 proizvajalca E. Merck.
- Plin P-10 (90 % argon, 10 % metan) proizvajalca Messer Slovenija.
- Tekoči pH indikator s pH območjem 0 – 5 proizvajalca E. Merck.
- 15 % raztopina $TiCl_3$ proizvajalca E. Merck.

3.2 Certificirane standardne raztopine in radioaktivni viri

Pri doktorskem delu sem uporabil sledeče certificirane standardne raztopine in radioaktivne vire:

- ^{232}U v 1 M HNO_3, proizvajalca Eckert & Ziegler Analytics, s specifično aktivnostjo 729 Bq/g na dan 27.11.2007 in relativno razširjeno negotovostjo (k = 2) 5,0 % (številka certifikata: 76225-482).

- ^{229}Th v 0,5 M HNO_3, proizvajalca Eckert & Ziegler Analytics, s specifično aktivnostjo 77,8 Bq/g na dan 27.11.2007 in relativno razširjeno negotovostjo (k = 2) 3,5 % (številka certifikata: 76224-482).
- ^{133}Ba v 0,1 M HCl z dodanim 30 µg/g Ba nosilcem, proizvajalca Eckert & Ziegler Analytics, s specifično aktivnostjo 11 kBq/g na dan 27.11.2007 in relativno razširjeno negotovostjo (k = 2) 1,7 % (številka certifikata: 76218-482).
- ^{210}Pb v 1 M HNO_3, proizvajalca Eckert & Ziegler Analytics, s specifično aktivnostjo 699 Bq/g na dan 27.11.2007 in relativno razširjeno negotovostjo (k = 2) 3,3 % (številka certifikata: 76220-482).
- ^{209}Po v 2 M HCl, proizvajalca Eckert & Ziegler Analytics, s specifično aktivnostjo 36,3 Bq/g na dan 27.11.2007 in relativno razširjeno negotovostjo (k = 2) 2,0 % (številka certifikata: 76221-482).
- Elektrodepoziran vir premera 24,1 mm proizvajalca Analytics, z aktivnostjo ^{238}U (1,70 ± 0,05) Bq, ^{234}U (1,68 ± 0,05) Bq, ^{239}Pu (1,62 ± 0,05) Bq in ^{241}Am (1,53 ± 0,05) Bq na dan 1.5.2004 (številka certifikata: 67978-121).

Vse certificirane standardne referenčne raztopine in viri so imeli specifične aktivnosti ali aktivnosti, sledljive do osnovnih SI enot.

3.3 Reagenti

Uporabil sem sledeče reagente:

- Raztopina 0,4 M $MgCl_2$, pH 5; raztopimo 81,32 g $MgCl_2 \cdot 6H_2O$ v 500 mL deionizirane vode in razredčimo z deionizirano vodo do 1000 mL.
- 5 – 6 % NaOCl, pH 7,5; k 0,5 L deionizirane vode dodamo 0,5 L 10 – 12 % NaOCl.
- Raztopina 1 M NaAc v 25 % HAc, pH 4; raztopimo 83 g NaAc v 500 mL deionizirane vode, dodamo 250 mL konc. HAc in razredčimo z deionizirano vodo do 1000 mL.
- Raztopina 0,04 M NH_2OHHCl, pH 2; raztopimo 2,78 g NH_2OHHCl v 950 mL deionizirane vode, uravnamo pH na 2 z dodatkom koncentrirane HNO_3 in razredčimo z deionizirano vodo do 1000 mL.
- 0,11 M HAc; k 950 mL deionizirane vode dodamo 6,25 mL 100 % ocetne kisline in razredčimo do 1000 mL z deionizirano vodo.
- Raztopina 0,5 M NH_2OHHCl v 0,05 M HNO_3; raztopimo 34,75 g NH_2OHHCl v 500 mL deionizirane vode, dodamo 3,47 mL koncentrirane HNO_3 in razredčimo z deionizirano vodo do 1000 mL.
- Raztopina 1 M NH_4HAc; raztopimo 77,08 g NH_4HAc v 950 mL deionizirane vode, uravnamo pH na 2 z dodatkom koncentrirane HNO_3 in razredčimo z deionizirano vodo do 1000 mL.
- Deionizirana voda.
- Sledilec ^{232}U s specifično aktivnostjo (0,3836 ± 0,0096) Bq/mL na dan 27.11.2007; k 1,0184 g certificirane standardne raztopine ^{232}U s specifično aktivnostjo 729 Bq/g dodamo 90 mL deionizirane vode, 7 mL koncentrirane HNO_3 in razredčimo z deionizirano vodo do 100 mL. Nato odvzamemo 5,1675 g tako pripravljene raztopine, dodamo 80 mL deionizirane vode in 7 mL koncentrirane HNO_3 ter razredčimo z deionizirano vodo do 100 mL.
- Sledilec ^{229}Th s specifično aktivnostjo (0,3898 ± 0,0069) Bq/mL na dan 27.11.2007; k 0,5009 g certificirane standardne raztopine ^{229}Th s specifično aktivnostjo 77,8 Bq/g dodamo 90 mL deionizirane vode, 3,5 mL koncentrirane

HNO_3 in razredčimo z deionizirano vodo do 100 mL.

- Sledilec ^{133}Ba s specifično aktivnostjo (110,4 ± 1,0) Bq/mL na dan 27.11.2007; k 0,9951 g certificirane standardne raztopine ^{133}Ba s specifično aktivnostjo 11 kBq/g dodamo 80 mL deionizirane vode, 10 mL 0,3 mg/mL Ba^{2+}, 0,8 mL koncentrirane HCl in razredčim z deionizirano vodo do 100 mL.
- Sledilec ^{209}Po s specifično aktivnostjo (0,3760 ± 0,0038) Bq/mL na dan 27.11.2007; k 1,0359 g certificirane standardne raztopine ^{209}Po s specifično aktivnostjo 36,3 Bq/g dodamo 80 mL deionizirane vode, 16 mL koncentrirane HCl in razredčimo z deionizirano vodo do 100 mL.
- Raztopina $Pb(NO_3)_2$ s koncentracijo 50 mg/mL Pb^{2+}; raztopimo 7,99 g $Pb(NO_3)_2$ v 80 mL deionizirane vode in razredčimo z deionizirano vodo do 100 mL.
- Raztopina 0,1 M EDTA / 0,5 M NaOH; raztopimo 2 g NaOH v 80 mL deionizirane vode, dodamo 2,922 g EDTA, ki jo prav tako raztopimo in razredčimo z deionizirano vodo do 100 mL.
- Raztopina Ba nosilca s koncentracijo 0,3 mg/mL Ba^{2+}; najprej pripravimo raztopino s koncentracijo 3 mg/mL Ba^{2+} tako, da 0,533 g $BaCl_2 \cdot 2H_2O$ raztopimo v 40 mL deionizirane vode in razredčimo z deionizirano vodo do 50 mL. Nato odvzamemo 10 mL raztopine s koncentracijo 3 mg/mL Ba^{2+} in jo razredčimo z deionizirano vodo do 100 mL.
- Ocetna kislina 1:1; k 250 mL deionizirane vode dodamo 250 mL 100 % ocetne kisline.
- Nasičena raztopina Na_2SO_4; dodamo toliko Na_2SO_4 k 300 mL deionizirane vode dokler ne dosežemo točke nasičenja.
- 0,125 mg/mL $BaSO_4$ substrat; k 80 mL deionizirane vode dodamo 2,5 mL raztopine s koncentracijo 3 mg/mL Ba^{2+}, 10 kapljic koncentrirane H_2SO_4 in razredčimo z deionizirano vodo do 100 mL.
- Raztopina Fe^{3+} s koncentracijo 5 mg/mL; raztopimo 2,42 g $FeCl_3 \cdot 6H_2O$ v 90 mL deionizirane vode in razredčimo z deionizirano vodo do 100 mL.
- Raztopina 3 M HNO_3 / 1 M $Al(NO)_3$; raztopimo 373 g $Al(NO_3)_3 \cdot 9H_2O$ v 500 mL deionizirane vode, dodamo 208,3 mL koncentrirane HNO_3 in razredčimo z deionizirano vodo do 1000 mL.
- Ekstrakcijski material TEVA proizvajalca Triskem International z velikostjo delcev od 100 do 150 μm.
- Ekstrakcijski material UTEVA proizvajalca Triskem International z velikostjo delcev od 100 do 150 μm.
- Ekstrakcijski material Sr Resin proizvajalca Triskem International z velikostjo delcev od 100 do 150 μm.
- 3 M HNO_3; k 750 mL deionizirane vode dodamo 208,3 mL koncentrirane HNO_3 in razredčimo z deionizirano vodo do 1000 mL.
- 2,5 M HNO_3; k 800 mL deionizirane vode dodamo 173 mL koncentrirane HNO_3 in razredčimo z deionizirano vodo do 1000 mL.
- 9 M HCl; k 250 mL deionizirane vode dodamo 743,8 mL koncentrirane HCl in razredčimo z deionizirano vodo do 1000 mL.
- 6 M HCl; k 500 mL deionizirane vode dodamo 495,9 mL koncentrirane HCl in razredčimo z deionizirano vodo do 1000 mL.
- 1 M HCl; k 900 mL deionizirane vode dodamo 82,6 mL koncentrirane HCl in razredčimo z deionizirano vodo do 1000 mL.
- Raztopina Nd^{3+} s koncentracijo 0,5 mg/mL; najprej pripravimo raztopino Nd^{3+} s koncentracijo 5 mg/mL tako, da 0,5832 g Nd_2O_3 raztopimo v 70 mL deionizirane vode in 20 mL koncentrirane HCl in nato razredčimo z deionizirano vodo do 100 mL. Nato odvzamemo 10 mL raztopine Nd^{3+} s koncentracijo 5 mg/mL in jo

razredčimo z deionizirano vodo do 100 mL.
- 10 μg/mL NdF_3 substrat; k 1 mL raztopini Nd^{3+} s koncentracijo 5 mg/mL in 460 mL 1 M HCl dodamo 40 mL koncentrirane HF.
- 0,58 M HF; k 98 mL deionizirane vode dodamo 2 mL koncentrirane HF.
- Raztopina 5 M HCl / 0,05 M oksalne kisline; raztopimo 6,3 g oksalne kisline v 500 mL deionizirane vode in dodamo 413,2 mL koncentrirane HCl ter razredčimo z deionizirano vodo do 1000 mL.
- Raztopina Pb sledilca s koncentracijo 12 mg Pb/mL; raztopimo 1,9176 g $Pb(NO_3)_2$ v 80 mL deionizirane vode in razredčimo z deionizirano vodo do 100 mL.
- 2 M HCl; k 800 mL deionizirane vode dodamo 165,3 mL koncentrirane HCl in razredčimo z deionizirano vodo do 1000 mL.
- 6 M HNO_3; k 550 mL deionizirane vode dodamo 416,7 mL koncentrirane HNO_3 in razredčimo z deionizirano vodo do 1000 mL.

3.4 Aparature, pripomočki in laboratorijski material

Uporabil sem sledeče aparature, pripomočki in laboratorisjki material:

- Plastične centrifugirke (50 mL).
- Teflonske centrifugirke (60 mL).
- Analitska tehtnica Mettler – Toledo AE 163 DR z merilnim obsegom od 0,01 g do 162/31 g, najmanjšim razdelkom d = 0,1/0,01 mg, preskusnim razdelkom e = 1 mg in točnostnim razredom I.
- Ročna kosa.
- Lopata.
- Sušilnik Instrumentaria Zagreb ST-05.
- Kuhinjska tehtnica Soehnle z merilnim obsegom do 5 kg in najmanjšim razdelkom d = 1 g.
- Keramična terilnica.
- Sejalnik proizvajalca Fritsch.
- Sito z velikostjo zank 2 mm proizvajalca Fritsch.
- Mlin za mletje Fritsch Rotor Speed Mill pulverisette 14.
- Motorna žaga Stihl.
- Stresalnik Ika HS 501 digital.
- Centrifuga Tehtnica Centric 322A.
- Stresalnik v vodni kopeli Julabo SW22.
- Peč za pripravo alkalnih talin Clasic Clare 4.0.
- Peč za žganje vzorcev proizvajalca Bosio.
- 0,1 μm polisulfonski filter premera 25 mm proizvajalca Pall.
- Plastični filtrirni lijak proizvajalca Pall.
- Steklena presesalna bučka proizvajalca Schott Duran.
- Plastična vodna črpalka proizvajalca Schott Duran.
- Ultrazvočna kopel Elma S15H Elmasonic.
- Aluminijasta ploščica premera 25 mm.
- Lepilo na vodni osnovi Giotto Gelik.
- Namizna svetilka.
- Led.
- Keramični lončki.
- Karbonski lončki Sigradur glassy carbon (50 mL).
- Grelno – mešalne plošče Tehtnica Rotamix SHP-10, Tehtnica Rotamix 550 MMH

in Ika C-MAG HS 10.
- Plastična 10 mL kolona Poly-Prep proizvajalca Bio-Rad.
- Steklena 16 mL kolona Econo-Pack proizvajalca Bio-Rad.
- Kvantitativni filtrirni papir črni trak podjetja Whatman.
- Aluminijasta merilna ploščica s premerom 25 mm za pripravo vira za meritve ^{210}Pb.
- Bakrena ploščica premera 18 mm.
- Srebrna ploščica premera 18 mm.
- Plastično držalo za bakrene in srebrne ploščice za spontano depozicijo polonija.
- Pipeta za pipetiranje volumnov od 0,1 do 1 mL Socorex Acura 825.
- Pipeta za pipetiranje volumnov od 0,5 do 5 mL Socorex Acura 835.
- Spektrometer alfa Alpha Analyst proizvajalca Canberra z 8 merilnimi komorami z PIPS detektorji.
- Vakuumska črpalka TRIVAC D 2,5 E 140000 proizvajalca Leybold.
- Spektrometer gama z detektorjem iz visoko čistega germanija proizvajalca Ortec z 8,6 % relativnim izkoristkom pri 1,33 MeV ^{60}Co.
- Večkanalni analizator Spectrum Master 919 proizvajalca Ortec.
- Proporcionalni števec Tennelec LB4100-W proizvajalca Canberra z 8 pretočnimi plinskimi proporcionalnimi detektorji.
- Hladilnik proizvajalca LTH.

Poleg navedene laboratorijske opreme sem uporabil še običajen laboratorijski material, kot so čaše, bučke, merilni valji, urna stekla, razne plastične posodice in podobno.

3.5 Vzorčenje in priprava vzorcev

Vzorce tal sem vzorčil na šestih lokacijah na območju odlagališča Boršt. Vzorce tal sem odvzel na globini 0 – 15 cm, njihova povprečna masa pa je znašala 5 kg. Vzorčevalne lokacije so prikazane na sliki 4. Lokaciji 1 in 2 ležita v dveh zamočvirjenih področjih, skozi kateri teče izcedna voda iz odlagališča s povišano vsebnostjo naravnih radionuklidov. Zato sem pričakoval, da se bodo radionuklidi v teh dveh lokacijah zadrževali. Lokacija 3 leži izven odlagališča na nekoliko povišanem delu in ni pod vplivom izcednih vod iz odlagališča, zato sem jo obravnaval kot nekontaminirano lokacijo. Lokacije od 4 do 6 pa ležijo na brežinah odlagališča in predstavljajo vzorce prekrivke odlagališča, ki je bila debela 30 do 40 cm.

Slika 4: *Zračni posnetek odlagališča Boršt; številke označujejo vzorčevalne lokacije*.

Po vzorčenju sem vzorce tal pripravil skladno s standardom ISO 11464 (1994). Vzorce sem stehtal, posušil v sušilniku pri 80 °C in ponovno stehtal. Zatem sem večje kose zemlje strtl v terilnici in vzorce presejal skozi sito z velikostjo zank 2 mm. Pri tem sem odstranil kamne in korenine. Vzorec sem zatem homogeniziral, reprezentativni vzorec pa odvzel z delitvijo na štiri dele, iz katerih sem izmenično odvzel 200 g vzorca. Del vzorca sem poslal na Center za pedologijo in varstvo okolja, Oddelka za agronomijo, Biotehniške fakultete v Ljubljani, kjer so izvedli pedološke raziskave vzorcev.

Vzorce trave sem odvzel septembra na enakih lokacijah kot vzorce tal in sicer s košnjo površine velike približno 2 m^2. Travo sem pokosil približno 3 cm nad tlemi in je pred nadaljnjo obdelavo nisem opral. Zatem sem vzorce trave posušil v sušilniku pri 80 °C ter zmlel in homogeniziral. Drevesa sem poljubno vzorčil na brežinah odlagališča Boršt. Vzorčil sem šest rdečih borov (*Pinus sylvestris*), šest smrek (*Picea abies*) in edini beli javor (*Acer pseudoplatanus*), ki je rasel na brežinah odlagališča. Bori in smreke so bili stari od 9 do 13 let, javor pa 15 let. Pri vsakem vzorcu drevesa sem odvzel les, ki je bil odžagan od 5 do 30 cm nad tlemi, mladi poganjki ter eno leto stare iglice in liste. Vse vzorce sem posušil v sušilniku pri 80 °C, narezal in zmlel ter homogeniziral. Vzorci trav in dreves pred sušenjem niso bili sprani z vodo, zato obstaja možnost kontaminacije vzorcev.

Odvzeti so bili tudi štirje vzorci mleka iz okolice rudnika urana Žirovski vrh in referenčne lokacije v Bukovščici. Volumen posameznega vzorca je znašal okrog 5 L. Pred uparjanjem so bili vzorci mleka stehtani, zatem pa uparjeni do suhega v uparjalnikih na Odseku za fiziko nizkih in srednjih energij Instituta Jožef Stefan, pri 60 °C. Po uprajanju so bili ponovno stehtani ter do začetka analize shranjeni v plastičnih vrečkah v hladilniku. V trgovinah v Ljubljani sem kupil tudi štiri vzorce mleka v prahu, ki se uporablja za pripravo hrane za dojenčke in sicer mleko v prahu Pomurskih mlekarn, ter tri

vzorce mleka v prahu podjetja Hipp iz Gmundena v Avstiji. Mleko v prahu podjetja Hipp je bilo okarakterizirano, kot proizvod iz biološke pridelave in se je razlikovalo v sestavi glede na starostno skupino dojenčkov, kateri je namenjeno. Tako je mleko v prahu Hipp PRE namenjeno novorojenčkom od rojstva pa do šestega meseca, Hipp 2 dojenčkom od šestega do desetega meseca in Hipp 3 za dojenčke po desetem mesecu. Sestavine v Hipp prehrani za dojenčke so zraven posnetega mleka tudi rastlinska olja, laktoza, škrob, delno demineralizirana sirotka v prahu (vse iz biološke proizvodnje) in kalcijev klorid, vitamin C, kalcijev hidroksid, železov laktat, cinkov sulfat, niacin, vitamin E, pantotenska kislina, bakrov sulfat, folna kislina, vitamin K, vitamin A, natrijev jodat, vitamin B_6, vitamin B_1, manganov sulfat, natrijev selenit, biotin in vitamin D. Vzorce mleka v prahu sem pred začetkom analize posušil pri 60 °C z namenom odstranitve morebitne vlage.

Za potrebe določitve koncentracijskih razmerij med krmo in mlekom so bili na eni kmetiji odvzeti trije vzorci tal, ki reprezentativno predstavljajo tla, na katerih kmetija prideluje krmo za krave. Vzorci tal so bili odvzeti na globini 0 – 15 cm, njihova povprečna masa pa je znašala 5 kg. Nadaljnja priprava vzorcev tal je bila enaka kot pri vzorcih tal odvzetih na območju odlagališča Boršt in je bila skladna s standardom ISO 11464 (1994). Odvzel sem tudi vzorce sena in travne silaže, s katero so trenutno krmili krave ter vzorec mleka. Volumen vzorca mleka je bil okrog 5 L in je bil pripravljen na enak način, kot ostali vzorci mleka, ki so bili odvzeti iz okolice rudnika urana Žirovski vrh in referenčne lokacije v Bukovščici. Vzorca sena in travne silaže pa sem pripravil na enak način, kot vzorce trave, ki sem jih odvzel na območju odlagališča Boršt.

3.6 Sekvenčna ekstrakcijska postopka

Oba sekvenčna ekstrakcijska postopka, ki sem ju uporabil sta prikazana v tabelah 1 in 2. Iz praktičnih razlogov bom skozi tekst Schultzevo modifikacijo Tessierjevega sekvenčnega ekstrakcijskega postopka označeval kot postopek S, revidiran BCR sekvenčni ekstrakcijski postopek pa kot postopek B. Takoj opazimo znatne razlike med obema postopkoma. Pri postopku B je namreč razmerje med ekstraktantom in vzorcem petkrat večje kot pri postopku S, tudi ekstrakcijski čas je veliko večji (16 ur pri postopku B v primerjavi z 1-6 ur pri postopku S). Ob tem sta pri postopku B izmenljiva frakcija ter karbonatna frakcija združeni. Tudi pri primerjavi uporabljenih ekstraktantov so opazne razlike.

Tabela 1: *Schultzeva modifikacija Tessierjevega sekvenčnega ekstrakcijskega postopka (postopek S) (Schultz et al., 1998).*

Ciljna frakcija	Ekstrakcijski reagent	Razmerje reagent / vzorec (m/m)	Temp. (°C)	Čas stresanja (h)
Izmenljiva	0,4 M $MgCl_2$ pH 5	15:1	Sobna temp.	1
Organska snov	5-6 % NaOCl pH 7,5	15:1	96	0,5 x 2
Karbonati	1 M NaAc v 25 % HAc pH 4	15:1	Sobna temp.	2 x 2
Fe/Mn oksidi	0,04 M NH_2OHHCl pH 2 (HNO_3)	15:1	Sobna temp.	5
Preostanek	Talina Na_2O_2 in HNO_3 / HCl / HF / H_2SO_4		900	

Tabela 2: *Revidiran BCR sekvenčni ekstrakcijski postopek (postopek B) (Rauret et al., 1999).*

Ciljna frakcija	Ekstrakcijski reagent	Razmerje reagent / vzorec (m/m)	Temp. (°C)	Čas stresanja (h)
Karbonati	0,11 M HAc	40:1	Sobna temp.	16
Fe/Mn oksidi	0,5 M NH_2OHHCl 0,05 M HNO_3	40:1	Sobna temp.	16
Organska snov	8,8 M H_2O_2	10:1	Sobna temp.	1
			85	1
	8,8 M H_2O_2	10:1	85	1
	1 M NH_4HAc	50:1	Sobna temp	16
Preostanek	Talina Na_2O_2 in HNO_3 / HCl / HF / H_2SO_4		900	

Sekvenčna ekstrakcijska postopka sem izvedel skladno z referencama Schultz et al. (1998) in Rauret et al. (1999). Tako sem v primeru postopka S, 1,5 g vzorca prenesel v teflonsko centrifugirko in čez noč navlažil z dodatkom 0,6 mL deionizirane vode. Zatem sem po vrsti izvedel ekstrakcijske stopnje, kot jih prikazuje tabela 1. Pri vsaki stopnji sem dodal 22,5 mL ekstrakcijskega reagenta in vzorec stresal na stresalniku pri 180 obr/min, skladno s časom stresanja, ki ga prikazuje tabela 1. Pri frakciji za organsko snov sem vzorec stresal v vodni kopeli pri temperaturi 96 °C. Po koncu stresanja posamezne ekstrakcijske stopnje, sem vzorec 30 min centrifugiral pri 3000 obr/min in zatem prefiltriral skozi 0,1 μm polisulfonski filter. Preostanek vzorca sem podvrgel naslednjemu ekstrakcijskemu reagentu v postopku, radionuklide v filtratu pa sem ločil skladno z radiokemijskim separacijskim postopkom.

V primeru postopka B sem v teflonsko centrifugirko natehtal 1 g vzorca in dodal 40 mL prvega ekstrakcijskega reagenta (tabela 2). Zatem sem vzorec 16 ur stresal na stresalniku pri 30 obr/min. Nato sem ekstraktant z 20 min centrifugiranjem pri 3000 obr/min ločil od trdnega preostanka in prefiltriral skozi 0,1 μm polisulfonski filter. Radionuklide v filtratu sem ločil skladno z radiokemijskim separacijskim postopkom. Preostanek sem spral z 20 mL deionizirane vode in 15 min stresal pri 30 obr/min ter ponovno 20 min centrifugiral pri 3000 obr/min. Zatem sem dodal naslednji ekstrakcijski reagent (tabela 2) in ves prejšnji postopek ponovil. Pri ekstrakciji organske snovi sem najprej preostanek 1 h razkrajal z dodatkom 10 mL H_2O_2 pri sobni temperaturi. Zatem sem vzorec položil v vodno kopel in razkrajal še 1 h pri 85 °C. Nato sem odstranil pokrov centrifugirke, ki je bil pred tem narahlo položen na njej, in volumen raztopine odparil do 3 mL pri isti temperaturi. Nato sem dodal naslednjih 10 mL H_2O_2 in vzorec ponovno razkral pri 85 °C za 1 h. Temu je sledilo ponovno uparjanje, vendar tokrat do 1 mL. Po ohlajanju sem vzorcu dodal 50 mL 1 M NH_4HAc in vzorec 16 h stresal na stresalniku pri 30 obr/min. Ločbo ekstraktanta od preostanka sem opravil na enak način kot pri ostalih frakcijah.

3.7 Simultana radiokemijska separacija ^{238}U, ^{234}U, ^{230}Th in ^{226}Ra

Za vse raztopine, ki so ostale pri vsaki izmed sekvenčnih ekstrakcijskih stopenj sem uporabil enak separacijski postopek, ki je povzet na sliki 5. ^{226}Ra sem ločil od ostalih radionuklidov z uporabo postopkov opisanih v Lozano et al. (1997). Uranove in torijeve izotope pa sem ločil s pomočjo ekstrakcijske kromatografije s TEVA in UTEVA ekstrakcijskim materialom.

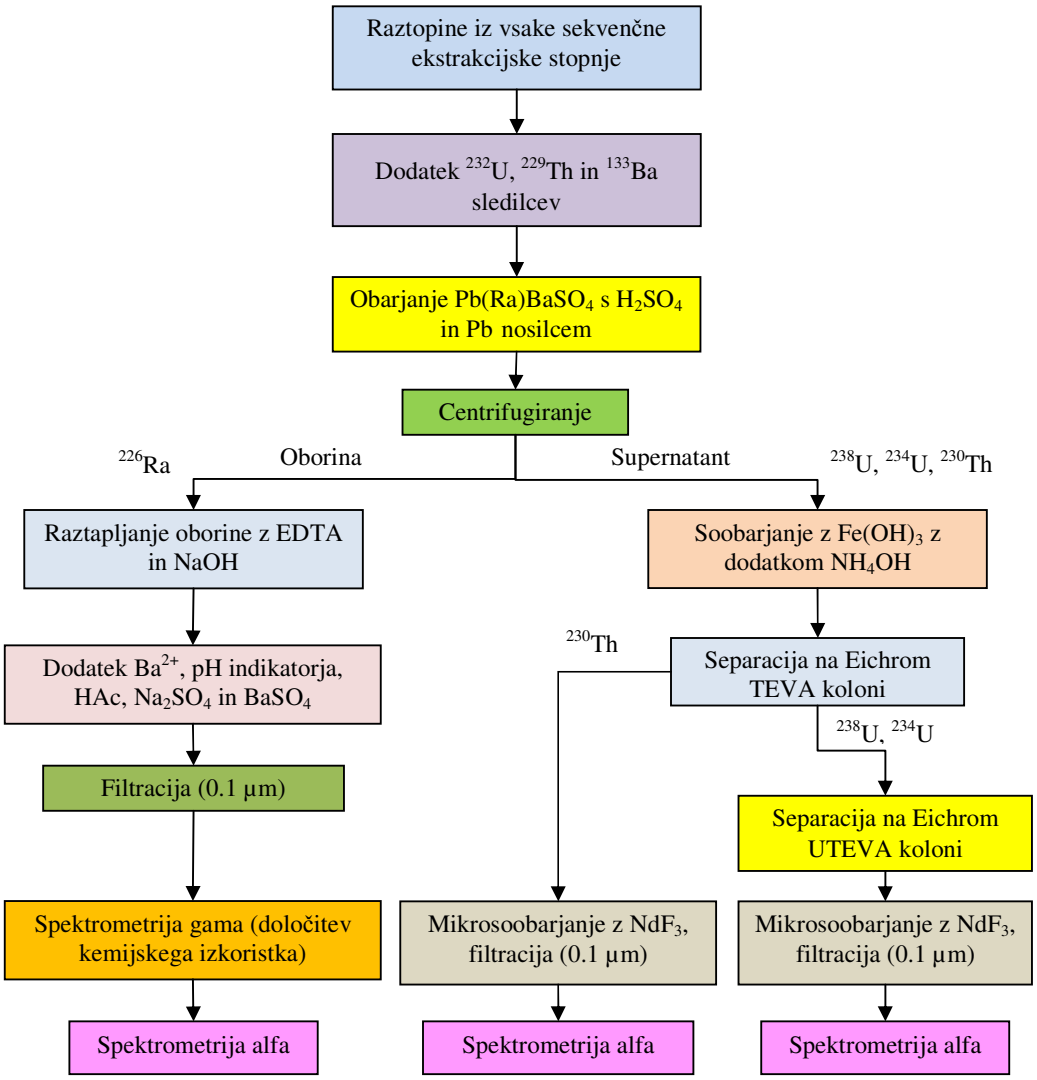

Slika 5: *Radiokemijski separacijski postopek ^{238}U, ^{234}U, ^{230}Th in ^{226}Ra za raztopine iz vsake sekvenčne ekstrakcijske stopnje.*

Najprej sem filtratom iz vsake sekvenčne ekstrakcijske stopnje dodal sledilce kemijskega izkoristka in sicer ^{232}U za sledenje kemijskega izkoristka za uranove izotope, ^{229}Th za sledenje kemijskega izkoristka za ^{230}Th in ^{133}Ba za sledenje kemijskega izkoristka ^{226}Ra. Dodane aktivnosti ^{232}U in ^{229}Th so bile odvisne od aktivnosti posameznega vzorca in so znašale od 0,03 Bq do 0,1 Bq. Pomembno je namreč, da je velikost vrha sledilca v spektru alfa primerljiva velikosti vrhovom vzorca, da ne pride do neželenega efekta prekrivanja vrhov. Dodana aktivnost ^{133}Ba pa je bila vedno enaka in je znašala 60 Bq. Kemijski izkoristek v primeru ^{226}Ra sem namreč določil s pomočjo relativne meritve ^{133}Ba s spektrometrom gama in ni motil meritve ^{226}Ra s spektrometrom alfa. Vse sledilce kemijskega izkoristka sem pripravil iz certificiranih standardnih raztopin, ki so imele podano aktivnost sledljivo do osnovnih SI enot. S tem je bila dosežena tudi sledljivost vseh meritev.

Po dodatku sledilcev sem radij in barij sooboril s $PbSO_4$ tako, da sem vzorcu dodal 1 mL koncentrirane H_2SO_4 in 1 mL raztopine $Pb(NO_3)_2$ s koncentracijo 50 mg/mL Pb^{2+}. Po 30 min sem vzorec 5 min centrifugiral pri 3000 obr/min in supernatant, ki je vseboval uran in torij, oddekantiral ter shranil za nadaljnjo obdelavo. Oborino, ki je vsebovala radij

pa sem spral z deionizirano vodo, da bi odstranil odvečno H_2SO_4 in ponovno 5 min centrifugiral pri 3000 obr/min. Po koncu centrifugiranja sem supernatant zavrgel. Postopek spiranja in centrifugiranja sem ponovil tolikokrat, dokler ni bila vrednost pH supernatanta nevtralna. Zatem sem oborino raztopil z dodatkom 4 mL 0,1 M EDTA / 0,5 M NaOH. Če slučajno količina 0,1 M EDTA / 0,5 M NaOH ni bila zadostna, da bi se oborina popolnoma raztopila, sem dodal dodatno količino le te, dokler ni bila dosežena popolna raztopitev oborine. Potem sem vzorcu dodal 0,3 mL Ba nosilca s koncentracijo 0,3 mg/mL Ba^{2+} in kapljico tekočega indikatorja pH z območjem pH 0 – 5, kar je raztopino obarvalo modro. Zatem sem vrednost pH prilagodil z dodatkom 1 mL ocetne kisline 1:1, kar se je odrazilo v spremembi barve raztopine v modrozeleno. Pri tem je pH raztopine znašal med 3 in 4, kar omogoče selektivno obarjanje $Ba(Ra)SO_4$. Zatem sem dodal še 4 mL nasičene raztopine Na_2SO_4 in 0,3 mL 0,125 mg/mL substrata $BaSO_4$. S tem sem radij mikrosooboril v obliki $Ba(Ra)SO_4$. Po 30 min sem vzorec prefiltriral skozi 0,1 μm polisulfonski filter in spiral trikrat z 2 mL deionizirane vode. Filter sem nato prilepil na Al ploščico s pomočjo lepila na vodni osnovi in posušil pod grelno svetilko. Ko je bil filter posušen, je bil vir pripravljen za meritve.

Supernatantu, ki je vseboval uran in torij sem dodal amoniak, dokler ni bil dosežen pH 9 – 10 ter 1 mL raztopine Fe^{3+} s koncentracijo 5 mg/mL. S tem sta se uran in torij sooborila z $Fe(OH)_3$. Po 30 min sem vzorec 5 min centrifugiral pri 3000 obr/min. Po centrifugiranju sem supernatant zavrgel, oborino pa spral z deionizirano vodo in ponovno 5 min centrifugiral pri 3000 obr/min. Ta postopek sem ponovil tolikokrat, dokler ni bil pH supernatanta nevtralen. Ekstrakcijsko kromatografijo sem izvedel skladno s Horwitz et al. (1993). Oborino sem raztopil s pomočjo 10 mL 3 M HNO_3 / 1 M $Al(NO)_3$ in prenesel na ekstrakcijsko kolono TEVA, ki sem jo predhodno kondicioniral z dodatkom 5 mL 3 M HNO_3. Nato sem centrifugirko, v kateri je bil vzorec, spral s 5 mL 2,5 M HNO_3, ki sem jih zatem nanesel na kolono. Temu je sledilo spiranje kolone z dodatkom 30 mL 2,5 M HNO_3. Pri teh pogojih kolona TEVA zadržuje torij, ne pa tudi urana, zato sem zbiral vse eluate do te stopnje v čisto centrifugirko in jih shranil za nadaljnjo separacijo urana. Zatem sem torij spral iz kolone TEVA s pomočjo 20 mL 9 M HCl in 5 mL 6 m HCl. Torij sem mikrosooboril skladno s postopki opisanimi v Sill in Williams (1981) ter Hindman (1983). Eluate, v katerih je bil torij, sem zbiral v čisto centrifugirko, kjer sem jim dodal 0,1 mL Nd^{3+} s koncentracijo 0,5 mg/mL in 1 mL koncentrirane HF. S tem sem mikrosooboril torij z NdF_3. Centrifugirko z vzorcem sem položil za 30 min v ledeno kopel. Zatem sem vzorec prefiltriral skozi 0,1 μm polisulfonski filter, ki sem ga predhodno spral z 10 mL 10 μg/mL NdF_3 substratom. Centrifugirko sem spral dvakrat z 2 mL 0,58 M HF in dvakrat z 2 mL deionizirane vode. Vse te raztopine sem nato zaporedoma spustil skozi filter, ki sem ga na koncu spral še z 2 mL deionizirane vode. Filter sem nato zalepil na aluminijasto ploščico s pomočjo lepila na vodni osnovi in ga posušil pod grelno svetilko. Po sušenju je bil vir pripravljen za meritve.

Eluate, ki so vsebovali uran, sem spustil skozi ekstrakcijsko kolono UTEVA, ki sem jo predhodno kondicioniral s 5 mL 3 M HNO_3. Nato sem centrifugirko, v kateri je bil vzorec, spral s 5 mL 3 M HNO_3 in jih zatem nanesel na kolono. Zatem sem spiral kolono z zaporednim dodajanjem 5 mL 3 M HNO_3, 2 mL 9 M HCl in 20 mL 5 M HCl / 0,05 M oksalne kisline. V teh stopnjah kolona UTEVA zadržuje uran, ostali radiouklidi pa se spirajo, zato sem vse eluate zavrgel. Uran sem nato iz kolone eluiral z dodakom 15 mL 1 M HCl. Uran sem mikrosooboril skladno s postopki opisanimi v Sill in Williams (1981) ter Hindman (1983). K eluatu sem dodal 0,1 mL Nd^{3+} s koncentracijo 0,5 mg/mL, 1 mL 15 % $TiCl_3$ in 1 mL koncentrirane HF. S tem sem mikrosooboril uran z NdF_3. Centrifugirko z vzorcem sem položil za 30 min v ledeno kopel. Zatem sem vzorec prefiltriral skozi 0,1 μm polisulfonski filter, ki sem ga predhodno spral z 10 mL 10 μg/mL NdF_3 substratom. Centrifugirko sem spral dvakrat z 2 mL 0,58 M HF in dvakrat z 2 mL

deionizirane vode. Vse te raztopine sem nato zaporedoma spustil skozi filter, ki sem ga na koncu spral še z 2 mL deionizirane vode. Filter sem nato zalepil na aluminijasto ploščico s pomočjo lepila na vodni osnovi in posušil pod grelno svetilko. Po sušenju je bil vir pripravljen za meritve.

Postopek za radiokemijsko separacijo ^{238}U, ^{234}U, ^{230}Th in ^{226}Ra za preostanek iz sekvenčnih ekstrakcijskih postopkov in za vzorce trav, dreves ter mleka je povzet na sliki 6. Vzorec sem najprej žaril 4 h v peči pri 650 °C z namenom odstranitve organske snovi in zatem razkrojil z uporabo principov opisanih v Jia et al. (2004) in Sill (1961). Tako sem 0,5 g žganega vzorca natehtal v ogljikov lonček, skupaj z 2 g Na_2CO_3 in 2 g Na_2O_2 ter v 5 min stalil pri 900 °C v peči za pripravo alkalnih talin. Po ohlajanju sem talini dodal sledilce kemijskega izkoristka ^{232}U, ^{229}Th in ^{133}Ba. Tudi tukaj je bila dodana aktivnost ^{232}U in ^{229}Th odvisna od aktivnosti urana in torija v vzorcu, dodana aktivnost ^{133}Ba pa je bila v vseh primerih 60 Bq. Tudi v tem primeru sem vse standarde pripravil iz certificiranih standardnih raztopin s sledljivo aktivnostjo do osnovnih SI enot. Zatem sem talino raztopil z dodatkom 2 mL deionizirane vode in 2 mL koncentrirane HNO_3 ter jo prenesel v teflonsko čašo. Nato sem vzorcu dodal 5 mL koncentrirane HNO_3, 5 mL koncentrirane HCl in 5 mL koncentrirane HF. Vse skupaj sem zatem uparil pri 200 °C. Zatem sem dodal 5 mL H_2O_2 in ponovno uparil vzorec pri 200 °C. Postopek dodajanja kislin in peroksida ter uparjanja sem ponovil še dvakrat. Nato sem vzorcu dodal 8 mL koncentrirane H_2SO_4 in nastalo raztopino uparil pri 300 °C. Po tem sem vzorec raztopil s pomočjo 2 mL koncentrirane HNO_3 in 10 mL deionizirane vode ter ga naprej procesiral na enak način, kot raztopine iz posamezne sekvenčne ekstrakcijske stopnje, seveda brez ponovnega dodajanja sledilcev.

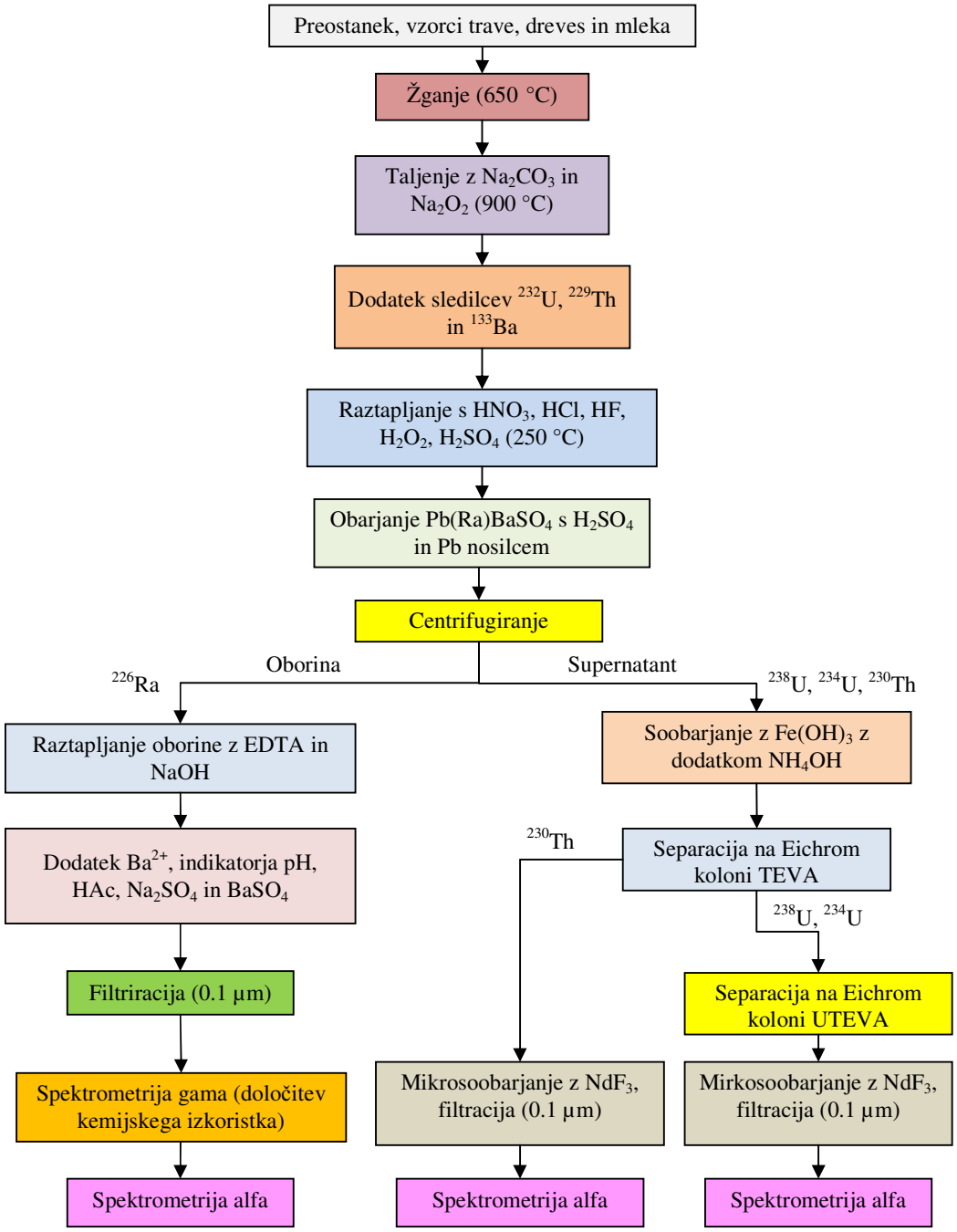

Slika 6: *Radiokemijski separacijski postopek ^{238}U, ^{234}U, ^{230}Th in ^{226}Ra za preostanke iz vsake sekvenčne ekstrakcijske stopnje in za vzorce trav ter dreves.*

3.8 Separacija ^{210}Pb

Pri določitvi ^{210}Pb sem k filtratom iz vsake sekvenčne ekstrakcijske stopnje, z izjemo za organsko snov pri postopku S, najprej dodal 2 mL Pb sledilca s koncentracijo 12 mg Pb^{2+}/mL. Za tem sem vzorcu dodal toliko koncentrirane HCl, da je bila dosežena 2 M vsebnost HCl v vzorcu. Filtrate za organsko snov pri postopku S pa sem najprej uparil do suhega pri 100 °C. Zatem sem dodal 6 mL koncentrirane HCl in ponovno uparil vzorec do suhega. Nato sem preostanek raztopil v 25 mL 2 M HCl in vzorcu dodal 2 mL Pb

sledilca s koncentracijo 12 mg Pb/mL.

^{210}Pb sem ločil od ostalih radionuklidov skladno s postopkom, ki so ga razvili Vajda et al. (1997) in delno modificirali Vreček et al. (2004). Tako sem »Sr Resin« ekstrakcijsko kolono kondicioniral z dodatkom 100 mL 2 M HCl. Nato sem dodal vzorec na kolono, za tem pa jo spral z 90 mL 2 M HCl in 60 mL 6 M HNO_3. Pri teh pogojih kolona »Sr Resin« zadržuje svinec, ostali radionuklidi pa prehajajo skozi, zato sem vse eluate zavrgel. Svinec sem eluiral iz kolone z dodatkom 90 mL 6 m HCl. Eluat sem nato uparil do suhega pri 100 °C in preostanek raztopil v 25 mL deionizirane vode. Raztopino sem nato prefiltriral skozi kvantitativni filter, svinec pa oboril iz filtrata z dodatkom 2 mL koncentrirane H_2SO_4. Po 30 min sem vzorec 5 min centrifugiral pri 3000 obr/min. Po centrifugiranju sem supernatant zavrgel, oborino pa spral z deionizirano vodo in ponovno centrifugiral 5 min pri 3000 obr/min. Postopek spiranja in centrifugiranja sem ponovil tolikokrat, dokler ni bila vrednost pH supernatanta nevtralna. Zatem sem oborino prenesel v predhodno stehtano aluminijasto merilno ploščico in ponovno 5 min centrifugiral pri 3000 obr/min. Po koncu centrifugiranja sem odpipetiral supernatant in ploščico z oborino posušil pod grelno lučko. Ko je bila oborina suha, sem ploščico z oborino ponovno stehtal. Tako sem dobil maso $PbSO_4$ oborine, ki je služila za gravimetrično določitev kemijskega izkoristka separacije ^{210}Pb.

Postopek separacije ^{210}Pb iz preostankov iz sekvenčnih ekstrakcijskih postopkov, vzorcev trav in dreves je bil enak. Predhodno stehtan vzorec sem najprej prenesel v erlenmajer bučko. Masa vzorca je bila odvisna od aktivnosti ^{210}Pb in je znašala od 1 do 10 g. Nato sem vzorcu dodal 2 mL Pb sledilca s koncentracijo 12 mg Pb/mL, 25 mL koncentrirane HNO_3 in 5 mL koncentrirane HCl. Vzorec sem pokril z urnim steklom in ga čez noč razkrajal pri sobni temperaturi. Naslednji dan sem pokrit vzorec 30 min razkrajal pri 200 °C. Po ohlajanju sem dodal vzorcu 10 mL H_2O_2 in vzorec za 10 min segrel na 100 °C. Po ohlajanju sem vzorec prefiltriral skozi filter črni trak. Nerazkrojeno filtrno pogačo sem prenesel nazaj v erlenmajer bučko in ves postopek razkroja ponovil. Na koncu sem oba filtrata združil in ju do suhega uparil pri 100 °C. Za tem sem sušino raztopil v 25 mL 2 M HCl in ^{210}Pb ločil od ostalih radionuklidov na enak način, kot to opisuje prejšnji odstavek.

Pri separaciji ^{210}Pb iz vzorcev mleka sem k 100 g mleka v prahu dodal 2 mL Pb sledilca s koncentracijo 12 mg Pb^{2+}/mL, 250 mL koncentrirane HNO_3 in 50 mL koncentrirane HCl. Vzorec sem pokril z urnim steklom in ga čez noč razkrajal pri sobni temperaturi. Naslednji dan sem pokrit vzorec 30 min razkrajal pri 200 °C. Po ohlajanju sem dodal vzorcu 20 mL H_2O_2 in ga za 10 min segrel na 100 °C. Po ohlajanju sem vzorec prefiltriral skozi kvantitativni filter. Trdno filtrno pogačo sem zavrgel, filtrat pa uparil do suhega pri 100 °C. Zatem sem preostanek raztopil v 100 mL 2 M HCl in prefiltriral skozi kvantitativni filter. ^{210}Pb v filtratu sem ločil od ostalih radionuklidov na enak način, kot pri ostalih vzorcih s pomočjo postopka, ki so ga razvili Vreček et al. (2004).

3.9 Separacija ^{210}Po

Najprej sem k filtratom iz sekvenčnih ekstrakcijskih stopenj dodal sledilec kemijskega izkoristka ^{209}Po. Dodana aktivnost je bila odvisna od aktivnosti ^{210}Po v posameznem vzorcu in je znašala od 0,03 Bq do 0,1 Bq. Sledilec kemijskega izkoristka sem pripravil iz certificirane standardne raztopine z aktivnostjo sledljivo do osnovnih SI enot. Filtrate za karbonatne frakcije in frakcije za organsko snov sekvenčnih ekstrakcijskih postopkov, sem najprej uparil do suhega pri 80 °C in raztopil v 100 mL deionizirane vode. Ostale frakcije obeh sekvenčnih ekstrakcijskih postopkov pa sem razredčil do 100 mL z deionizirano vodo brez predhodnega uparjanja. Zatem sem vsem raztopinam dodal 2 mL koncentrirane HCl, 0,5 g askorbinske kisline in 0,5 g hidroksilamonijevega klorida za

maskiranje. Nato sem štiri ure spontano depoziral polonij na bakreno ali srebrno ploščico pri 80 °C, ki sem jo vstavil v poseben nosilec (Benedik in Vreček, 2001) in istočasno mešal raztopino z magnetnim mešalom. Po koncu spontane depozicije sem bakreno ali srebrno ploščico spral z deionizirano vodo ter jo posušil na zraku. Ko se je posušila, je bila pripravljena za meritve.

Podobno kot za ^{210}Pb, sem tudi za ^{210}Po separacija preostankov sekvenčnih ekstrakcijskih postopkov, vzorcev trav, dreves in mleka izvedel na enak način. Tako sem predhodno stehtan vzorec najprej prenesel v erlenmajer bučko. Masa vzorca je bila odvisna od aktivnosti ^{210}Po in je znašala od 1 do 5 g. Nato sem vzorcu dodal sledilec kemijskega izkoristka ^{209}Po. Dodana aktivnost je bila odvisna od aktivnosti ^{210}Po v posameznem vzorcu in je znašala od 0,03 Bq do 0,1 Bq. Sledilec kemijskega izkoristka sem pripravil iz certificirane standardne raztopine z aktivnostjo sledljivo do osnovnih SI enot. Zatem sem vzorcu dodal 25 mL koncentrirane HNO_3 in 5 mL koncentrirane HCl. Vzorec sem pokril z urnim steklom in ga čez noč razkrajal pri sobni temperaturi. Naslednji dan sem pokrit vzorec 30 min razkrajal pri 200 °C. Po ohlajanju sem vzorcu dodal 10 mL H_2O_2 in ga 10 min segreval na 100 °C. Po ohlajanju sem vzorec prefiltriral skozi kvantitativni filter. Nerazkrojeno filtrno pogačo sem prenesel nazaj v erlenmajer bučko in ves postopek razkroja ponovil. Na koncu sem oba filtrata združil in ju do suhega uparil pri 80 °C. Zatem sem vzorec raztopil v 100 mL deionizirane vode. Nato sem dodal 2 mL koncentrirane HCl, 0,5 g askorbinske kisline in 0,5 g hidroksilamonijevega klorida. Polonij sem nato štiri ure spontano depoziral na bakreno ploščico pri 80 °C in hkrati mešal raztopino z magnetnim mešalom. Po koncu spontane depozicije sem bakreno ploščico spral z deionizirano vodo ter posušil na zraku. Ko se je posušila, je bila pripravljena za meritve.

3.10 Meritve

Meritve mase sem izvedel s pomočjo analitske tehtnice Mettler – Toledo AE 163, ki je bila umerjena s certificiranimi utežmi. Meritve volumna sem izvedel z merilnimi valji s certificiranimi volumni, bučkami ter pipetami, ki sem jih umeril s pomočjo analitske tehtnice Mettler – Toledo AE 163.

Meritve aktivnosti sevalcev alfa ^{238}U, ^{234}U, ^{230}Th, ^{226}Ra in ^{210}Po sem izvedenel s pomočjo spektrometra alfa proizvajalca Canberra, ki je prikazan na sliki 7. Med sevalce alfa uvrščamo radionuklide, ki razpadajo z razpadom alfa, ki je na primeru ^{238}U prikazan v formuli 2. Iz formule 2 je razvidno, da ^{238}U razpada v ^{234}Th in delec alfa (^{4}He), pri tem pa se sprosti še energija Q_1. Pri razpadu je delec alfa, ki je mnogo lažji od ^{234}Th, odbit z določeno energijo stran od ^{234}Th. Detekcija radionuklidov, ki razpadajo z razpadom alfa poteka preko detekcije odbitega delca alfa, ki nastane pri razpadu. V mojem primeru sem za detekcijo delcev alfa uporabil polprevodniški silicijev detektor. Kinetična energija delca alfa se ob interakciji s polprevodniškim silicijevim detektorjem spremeni v električni sunek, ki ga nato elektronika ojači in razvrsti glede na njegovo energijo.

$$^{238}_{92}\mathrm{U} \rightarrow {}^{234}_{90}\mathrm{Th} + {}^{4}_{2}\mathrm{He} + Q_1 \qquad (2)$$

Slika 7: *Spektrometer alfa Alpha Analyst proizvajalca Canberra.*

Spektrometer alfa Alpha Analyst ima vgrajenih osem merilnih komor, od katerih imata po dve skupen vakuumski priključek (slika 7). Znotraj vsake komore je nameščen polprevodniški silicijev detektor PIPS (Passivated Implanted Planar Silicon) premera 2,4 cm. Detektor PIPS je sestavljen iz tanke plasti silicija tipa – n, nanešenega na podlago iz sintetične smole, na katerega je vakuumsko naparjena plast zlata, ki služi kot prevodna plast. Debelina okna detektorja je manj kot 0,5 nm, kar omogoča detekcijo delcev alfa. Ob vstopu v plast silicija delci alfa z ionizacijo ustvarijo prevodne elektrone in elektronske luknje (energija tvorba para 3,5 eV) in s tem napetostni sunek, ki ga po ojačanju analizira večkanalni analizator. Detektorji imajo geometrijo 2 π, kar pomeni, da je maksimalni teoretični izkoristek detektorja 50 %, saj do detektorja lahko teoretično pride le polovica delcev alfa (slika 8).

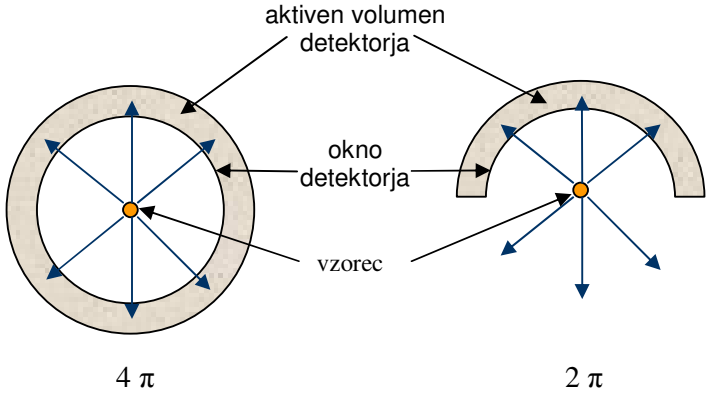

Slika 8: *Shematski prikaz geometrije 4 π in 2 π.*

Spektrometer alfa je opremljen z vakuumsko črpalko TRIVAC D 2,5 E 140000, ki sodi v družino dvostopenjskih oljnih rotacijskih črpalk in skrbi za vzdrževanje vakuuma v

merilnih komorah. Vakuum v merilnih komorah je potreben zato, ker so delci alfa sorazmerno veliki in se zelo hitro ustavijo v zraku. Tako je potrebno pred začetkom meritve izčrpati zrak iz merilnih komor, da je število delcev alfa, ki dosežejo detektor, večje. Vsaka merilna komora ima 12 rež v katere vstavimo predal na katerega položimo vzorec. Prva reža je od detektorja oddaljena 0,1 cm, vsaka naslednja reža je od predhodne oddaljena 0,4 cm, torej je oddaljenost vzorca od detektorja lahko od 0,1 cm pa vse do 4,5 cm. Z manjšo razdaljo med vzorcem in detektorjem se povečuje izkoristek detekcije ter zmanjšuje ločljivost spektrov, saj je prostorski kot delcev alfa večji (slika 9). Zaradi relativno nizkih aktivnosti, ki so bile predmet meritev, sem vse meritve izvedel na oddaljenosti 0,1 cm od detektorja. Pod komorami z detektorji se nahaja sistemski kontrolnik z vso pripadajočo elektroniko za obdelavo in zajemanje rezultatov in uravnavanje vakuuma v komorah.

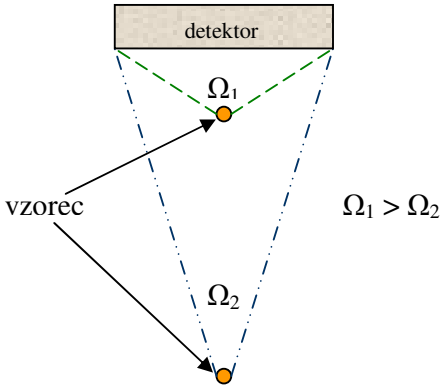

Slika 9: *Spreminjanje prostorskega kota z razdaljo od detektorja.*

Zajemanje in obdelavo spektrov sem izvedel s pomočjo programske opreme Genie 2000 proizvajalca Canberra. Spektrometer alfa je bil opremljen tudi s programom Alpha Analyst, ki omogoča računalniško upravljanje s spektrometrom alfa. To v praksi pomeni, da uporabnik le vstavi vzorec v merilno komoro, izbere ustrezen protokol meritve ter vnese podatke o vzorcu; program nato avtomatsko vzpostavi potreben vakuum v merilni komori, začne meritev, zajema spekter alfa ter ga na koncu tudi obdela in ustvari poročilo o rezultatih meritve.

Ozadje posameznih detektorjev spektrometra alfa sem določil z 10000 minutno meritvijo praznih merilnih komor in je znašalo v povprečju 1,2E-4 sunka na sekundo v energijskem območju od 3 MeV do 8 MeV. Določitev izkoristka detekcije spektrometra alfa, kakor tudi energijsko kalibracijo, sem izvedel s pomočjo certificiranega standardnega izvora z elektrodepoziranimi ^{238}U, ^{234}U, ^{239}Pu in ^{241}Am (številka certifikata: 67978-121). Aktivnosti omenjenih radionuklidov so znašale (1,70 ± 0,05) Bq za ^{238}U, (1,68 ± 0,05) Bq za ^{234}U, (1,62 ± 0,05) Bq za ^{239}Pu in (1,53 ± 0,05) Bq za ^{241}Am na dan 1.5.2004 in so bile sledljive do osnovnih SI enot. Izmerjeni izkoristki detekcije posameznih detektorjev pri razdalji 0,1 cm od detektorja v energijskem območju ^{226}Ra (od 4,2 MeV do 4,8 MeV) so prikazani v tabeli 3 in so v povprečju znašali 28,75 %. Spekter alfa certificiranega standardnega izvora z elektrodepoziranimi ^{238}U, ^{234}U, ^{239}Pu in ^{241}Am je prikazan na sliki 10. Tipično za vrhove v spektru alfa je, da imajo tako imenovani rep na nižje energijskem delu, kar je lepo razvidno tudi pri vrhovih na sliki 10, kjer so vrhovi na levi strani nekoliko širši kot na desni.

Tabela 3: *Izkoristki detekcije za posamezne detektorje pri razdalji 0,1 cm od detektorja za ^{226}Ra.*

Oznaka detektorja	Izkoristek detektorja za ^{226}Ra (%)
A_1_1A	28,44
A_1_1B	27,79
A_1_2A	29,68
A_1_2B	28,73
A_1_3A	28,37
A_1_3B	28,63
A_1_4A	28,59
A_1_4B	29,79

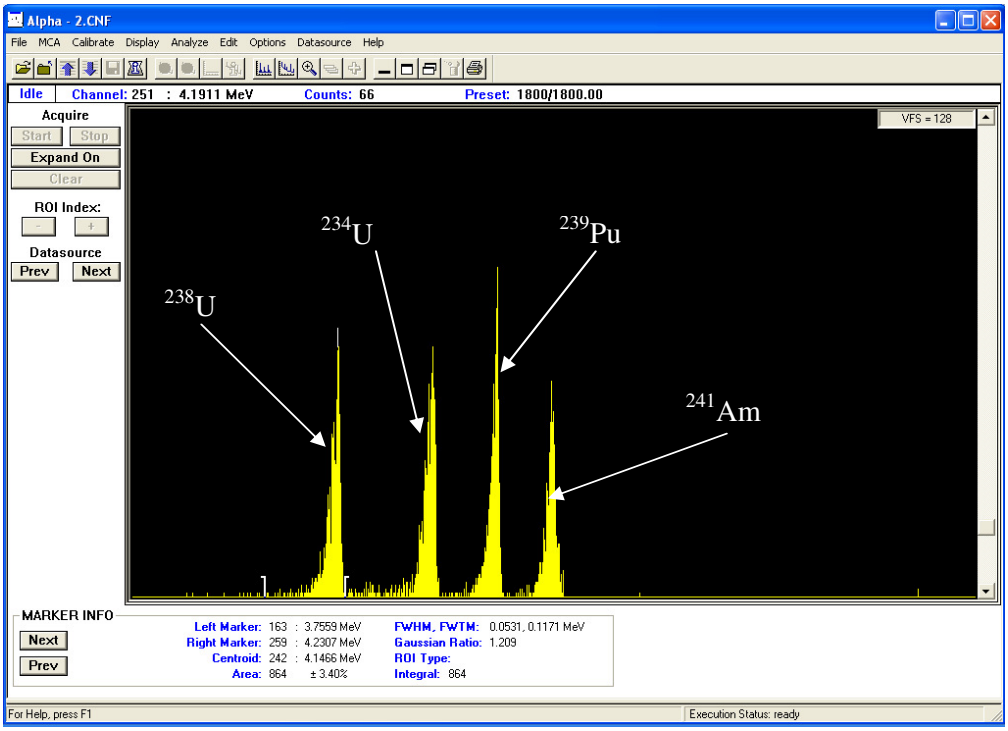

Slika 10: *Spekter alfa certificiranega standardnega izvora z elektrodepoziranimi ^{238}U, ^{234}U, ^{239}Pu in ^{241}Am.*

Tipičen spekter alfa uranovih izotopov prikazuje slika 11, kjer so od leve proti desni vidni vrhovi ^{238}U, ^{235}U, ^{234}U in vrh sledilca kemijskega izkoristka ^{232}U.

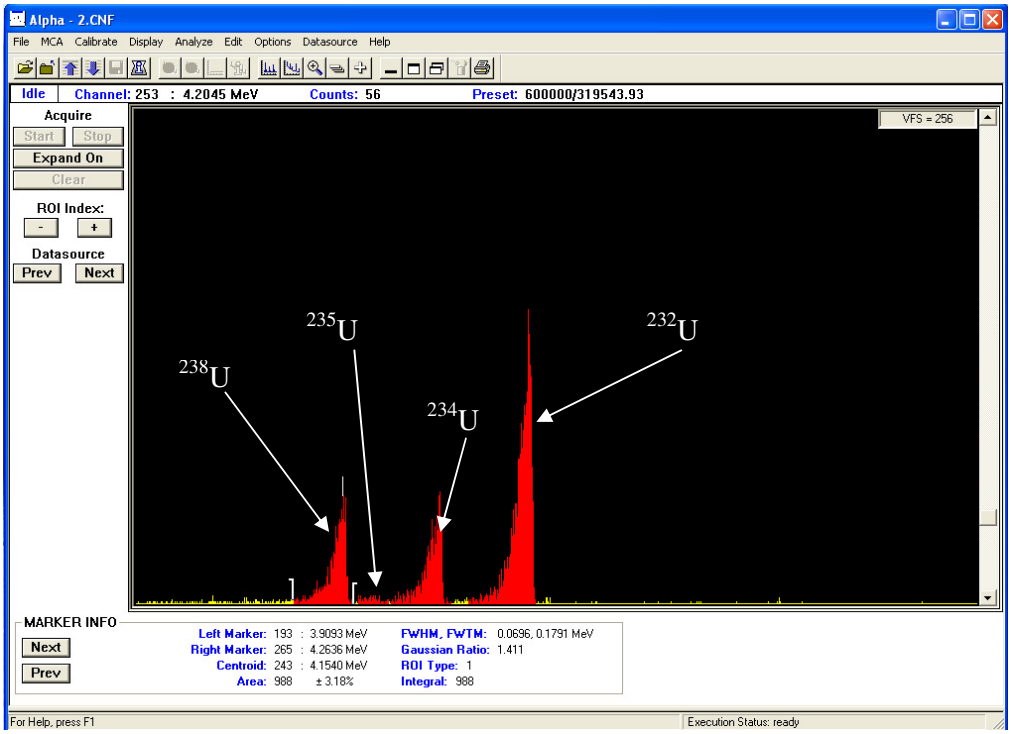

Slika 11: *Spekter alfa uranovih izotopov.*

Podobno kot v primeru urana, prikazuje slika 12 spekter alfa za torijeve izotope, kjer so od leve proti desni prikazani ^{232}Th, ^{230}Th, sledilec kemijskega izkoristka ^{229}Th in ^{228}Th ter njegovi razpadni produkti ^{224}Ra, ^{220}Rn in ^{216}Po. Vrh ^{228}Th je večji od vrha ^{232}Th zato, ker sem torijeve izotope ločil sočasno z uranovimi izotopi, kjer sem dodal sledilec kemijskega izkoristka ^{232}U, čigar razpadni produkt je ^{228}Th. Zato specifične aktivnosti ^{228}Th pri sočasni separaciji urana in torija ni mogoče določiti, saj je le ta povečana za dodaten ^{228}Th, ki nastaja iz ^{232}U.

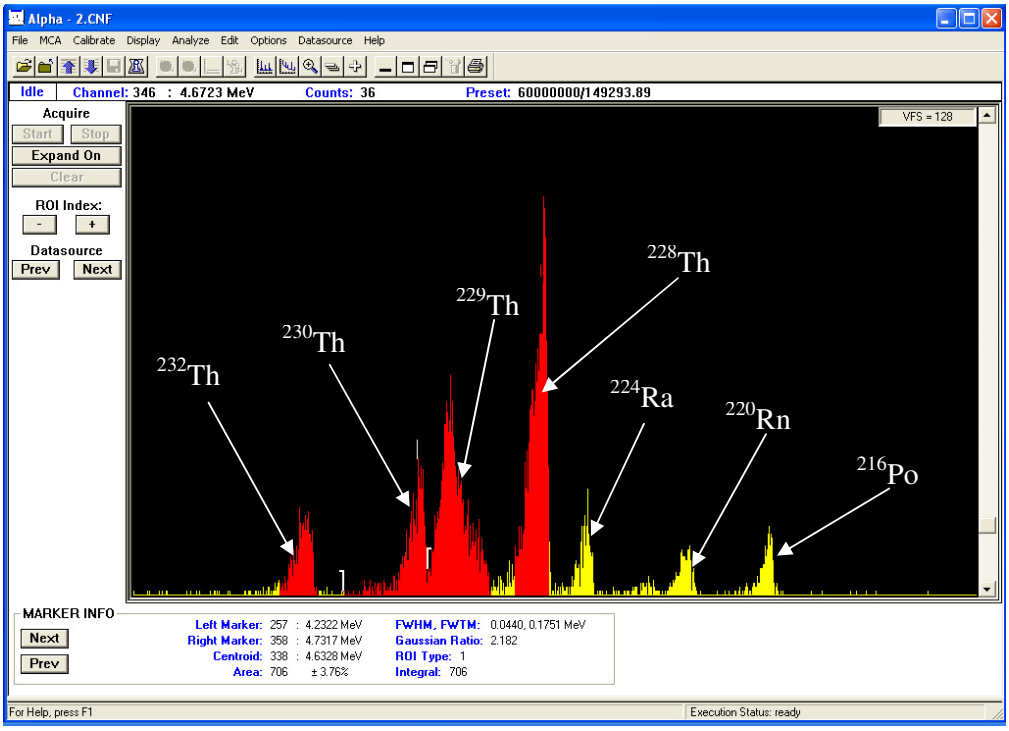

Slika 12: *Spekter alfa torijevih izotopov.*

Slika 13 prikazuje spekter alfa za ^{226}Ra, kjer so lepo vidni tudi razpadni produkti ^{226}Ra in sicer ^{222}Rn, ^{218}Po ter ^{214}Po.

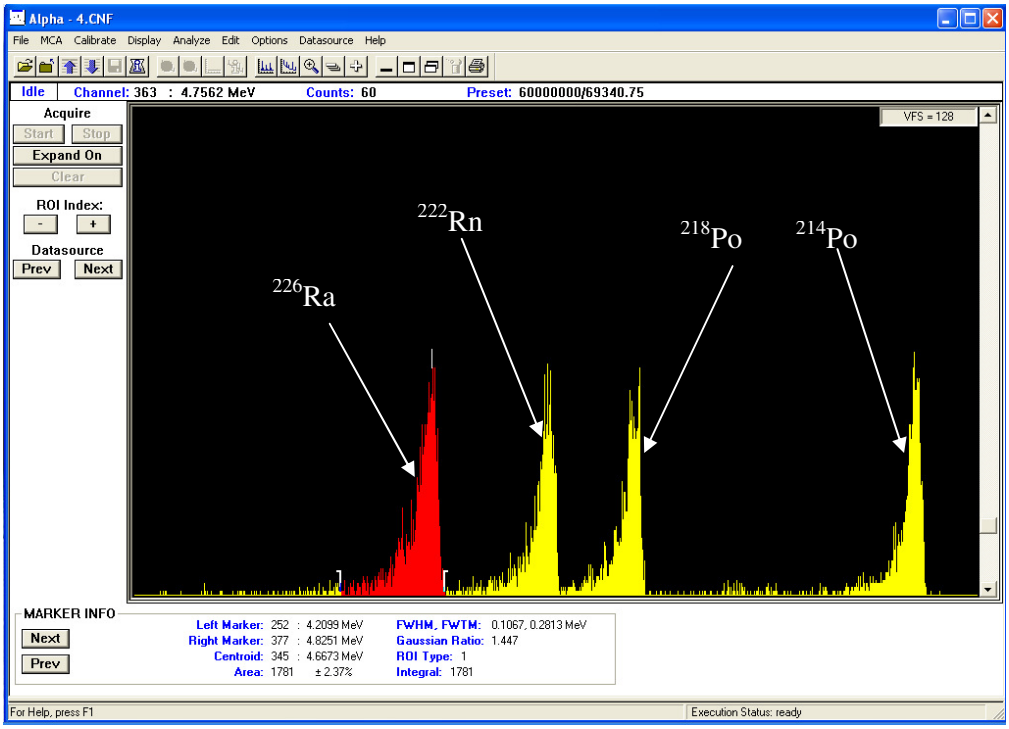

Slika 13: *Spekter alfa ^{226}Ra.*

Na sliki 14 je prikazan spekter alfa za sledilec kemijskega izkoristka ^{209}Po ter ^{210}Po. Ob primerjavi slike 14 s slikami 11-13 je razvidno, da so vrhovi v primeru polonija veliko

ožji. Razlog za to je veliko manjša samoabsorpcija polonija v viru, ki sem ga pripravil s spontano depozicijo, kot pa v primeru urana, torija in radija. Njihove vire sem namreč pripravil s postopkom mikrosoobarjanja, kjer je samoabsoprcija v viru nekoliko večja.

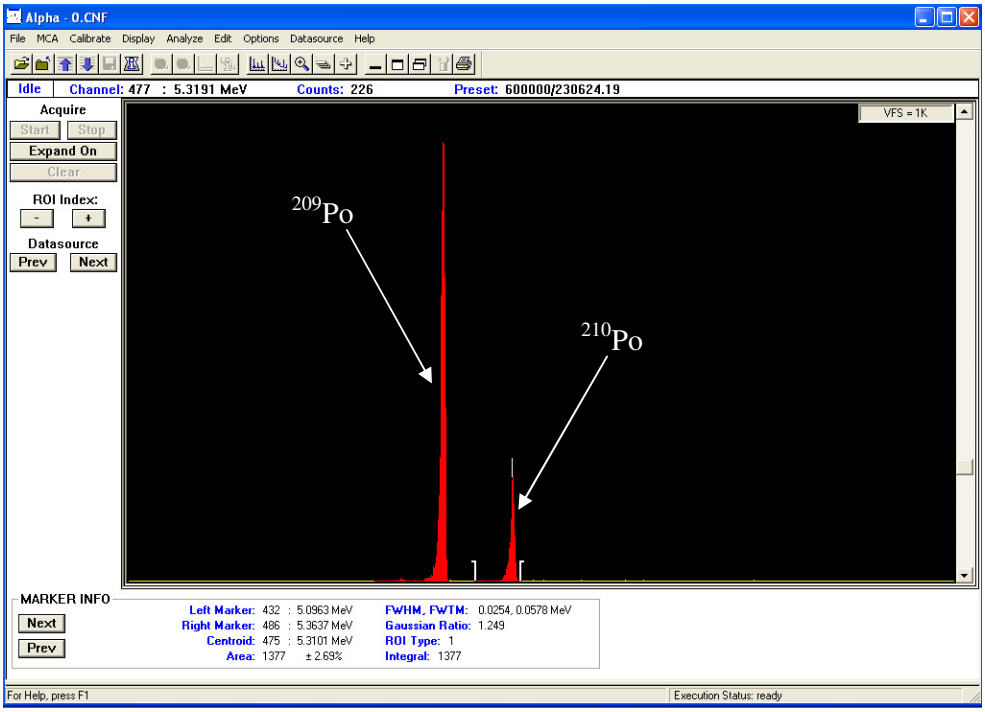

Slika 14: *Spekter alfa polonijevih izotopov.*

Program Genie 2000 uporablja za izračun minimalne aktivnosti, ki jo detektor še lahko zazna Currie-jevo enačbo (Currie, 1968), ki je predstavljena v enačbi 3:

$$MDA = \frac{k^2 + 2L_C}{t_m \varepsilon_m m} \qquad (3)$$

Kjer je:

MDA minimalna aktivnost, ki jo števec še lahko zazna v Bq
k konstanta standardnega odmika za dosego določene stopnje zaupanja in znaša pri 95 % stopnji zaupanja 1,645
t_m čas meritve v s
ε_m izkoristek detekcije meritve
m masa vzorca v kg
L_C minimalna aktivnost, pri kateri lahko z gotovostjo trdimo, da je aktivnost vzorca večja od 0 Bq

Minimalne aktivnosti, ki jih števec še lahko zazna so za ^{238}U, ^{234}U, ^{230}Th, ^{226}Ra in ^{210}Po v povprečju znašale 2,2E-4 Bq.

Določitev kemijskega izkoristka za ^{226}Ra sem izvedel z meritvijo aktivnosti ^{133}Ba na spektrometru gama z detektorjem iz visoko čistega germanija proizvajalca Ortec, ki je zaščiten pred zunanjim sevanjem s 5 cm svinčenim ščitom. Germanijev kristal detektorja ima premer 41,9 mm, dolžina le tega pa znaša 38,7 mm. Relativni izkoristek spektrometra gama znaša 8,6 % pri 1,33 MeV ^{60}Co. Detektor je bil povezan z večkanalnim analizatorjem Spectrum Master 919 podjetja Ortec in je prikazan na sliki 15. Zajemanje

spektra sem izvedel s pomočjo programa Maestro, prav tako proizvajalca Ortec. Program Maestro omogoča osnovno zajemanje spektra, kakor tudi določanje površine posameznega vrha, kar popolnoma zadošča potrebam določitve kemijskega izkoristka za ^{226}Ra. Tega sem namreč določil relativno, kar pomeni, da sem površino vrha ^{133}Ba pri 356 keV v vzorcu primerjal s površino vrha ^{133}Ba pri 356 keV v standardu enake geometrije, ki ni bil podvržen kemijski separaciji. Slednjega sem pripravil z uparjanjem sledilca kemijskega izkoristka ^{133}Ba na aluminijasto ploščico. Po uparjanju sem površino vira zalepil z lepilnim trakom, kar je onemogočilo odpadanje sušine iz aluminijaste ploščice. Pri relativnih meritvah ni potrebe po absolutni kalibraciji spektrometra gama, potrebna je le dovolj dobra energijska kalibracija, ki je bila izvedena s pomočjo točkastih izvorov sevalcev gama.

Slika 15: *Spektrometer gama.*

Na sliki 16 je prikazan spekter gama, na katerem je povečan in označen vrh ^{133}Ba pri 356 keV, ki sem ga uporabil za določitev kemijskega izkoristka ^{226}Ra. Tukaj vidimo, da je oblika vrhov v spektru gama drugačna, kot pri spektrih alfa (slike 10 – 14), saj v primeru spektra gama vrhovi nimajo tako imenovanih repov in so praktično Gaussove oblike.

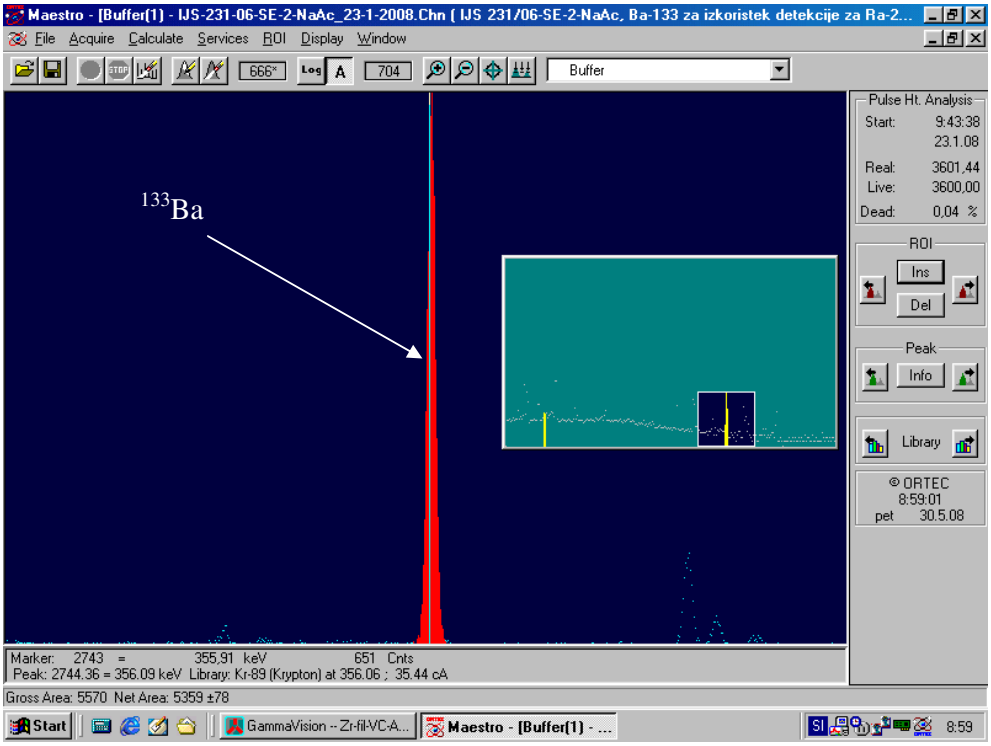

Slika 16: *Vrh ^{133}Ba v spektru gama pri 356 keV.*

Meritve ^{210}Pb sem izvedel s pomočjo proporcionalnega števca Tennelec LB4100-W proizvajalca Canberra (slika 17), zajemanje rezultatov pa s pomočjo programa OSUM, prav tako proizvajalca Canberra. Proporcionalni števec ima osem proporcionalnih detektorjev premera 5,7 cm, ki lahko neodvisno drug od drugega opravljajo meritve. Ploščinska gostota okna detektorjev je 80 μg/cm^2. Geometrija detektorjev je 2π, za prepihovanje detektorjev pa se uporablja plin P10 (90% argona, 10% metana). Največji premer pripravljenih virov za meritve lahko znaša 5,2 cm. Detektorji so zaščiteni z 10 cm debelim svinčenim ščitom, ki služi za zmanjševanje ozadja. Osem detektorjev je razdeljenih v dva predala, kjer se v vsakem nahajajo štirje detektorji. Nad štirimi detektorji se nahaja tako imenovani »guard« detektor, ki meri visoko energijsko kozmično sevanje in ga avtomatsko odšteva od sunkov posameznega detektorja. V samem ohišju števca se nahaja še sistemski kontrolnik v katerem sta dva glavna ojačevalnika, dva predojačevalnika, mikroprocesor in visokonapetostna enota. Ta elektronika skrbi za obdelavo sunka in kot rezultat posreduje podatek o številu sunkov ter o času meritve programu OSUM. Preko tega programa uporabnik krmili števec in nadzira operacije, ki jih števec izvaja.

Slika 17: *Proporcionalni števec Canberra Tennelec LB4100-W.*

Kljub temu, da je geometrija detektorjev proporcionalnega števca 2π, je lahko zaradi odboja delcev beta od merilne ploščice izkoristek detektorja večji od 50 %. Omenjeni efekt prikazuje slika 18, kjer vidimo, da se lahko delci beta z dovolj veliko energijo odbijejo od merilne ploščice nazaj proti detektorju, kjer so lahko detektirani.

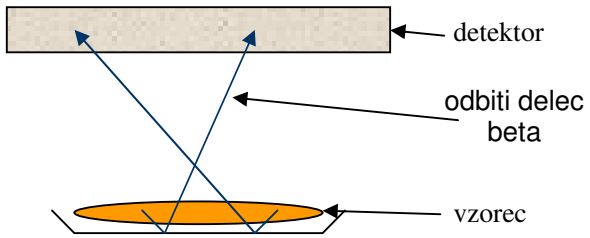

Slika 18: *Proporcionalni števec Canberra Tennelec LB4100-W.*

Proporcionalni števec izkorišča učinek ionizacije delcev beta, ki prodirajo skozi plin. Sestavljen je iz anode in katode, med katerima je plin, skozi katerega prodirajo delci beta, ki sprožijo v plinu primarno ionizacijo. Tako nastali elektroni potujejo pod vplivom napetosti proti anodi, kationi pa proti katodi. Ker je napetost pri kateri deluje proporcionalni števec dovolj visoka, imajo elektroni nastali pri primarni ionizaciji, ki potujejo proti anodi, dovolj kinetične energije, da sprožijo sekundarno ionizacijo v plinu, kar sproži plaz ionizacij ob anodi. Multiplikacija elektronov zlahka doseže vrednosti 10^4. Ko elektroni dosežejo anodo, nastane pulz naboja, ki je ob tako veliki multiplikaciji lahko merljiv. Delovanje proporcionalnega števca shematsko prikazuje slika 19. Nastalo število elektronov pri sekundarni ionizaciji je proporcionalno številu elektronov, ki so nastali pri primarni ionizaciji, kar omogoča detekcijo delca beta (L'Annunziata, 1998).

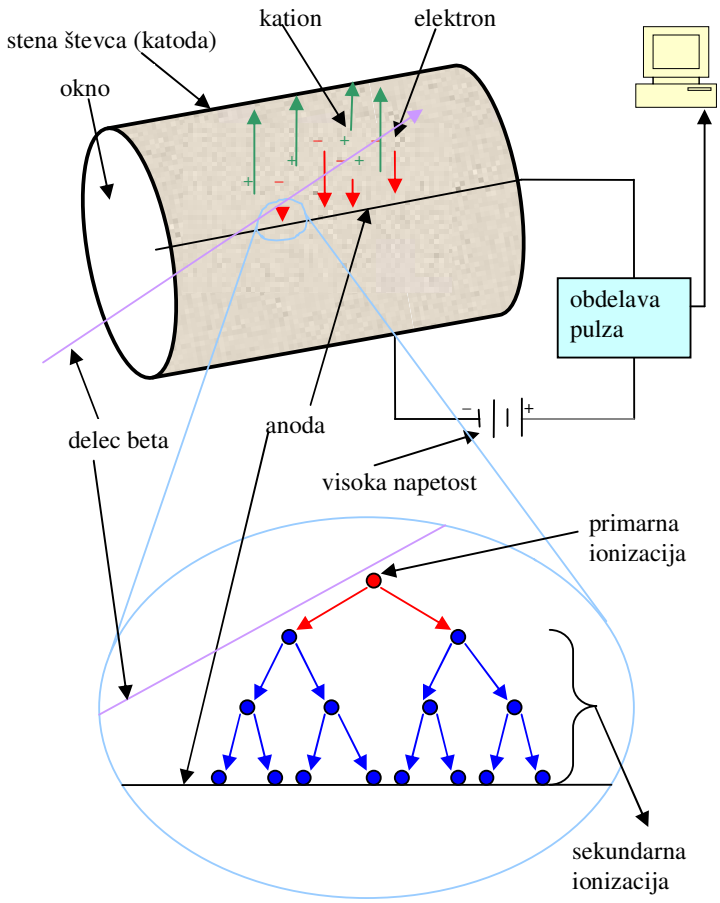

Slika 19: *Shematski prikaz delovanja proporcionalnega števca.*

Plin, ki se uporablja za proporcionalni števec, ne sme tvoriti anionov ter ne sme vsebovati komponent, ki privlačijo elektrone. Te pogoje najbolje zadovoljujejo žlahtni plini. Ker po nastanku ionskega para pri ionizaciji kation ostane v vzbujenem stanju, preide v osnovno stanje z oddajanjem fotonov, ki lahko naprej sprožijo dodatne plazove elektronov, kar pokvari proporcionalnost. Zato morajo biti ti fotoni zadušeni z drugim mehanizmom, kot na primer z disociacijo. Tako se žlahtnim plinom dodaja majhen delež večatomskega plina. Najpogosteje uporabljena mešanica je tako imenovani plin P10, ki vsebuje 90 % argona in 10 % metana. Ker se molekule metana porabljajo, je potrebno konstantno dovajati svež plin, izrabljenega pa odvajati (L'Annunziata, 1998).

Za razliko od spektrometra alfa in spektrometra gama pa proporcionalni števec ne omogoča prikaz energijskega spektra zaznanih sunkov. Njegova energijska obdelava sunkov je omejena le na razvrščanje sunkov med višje energijske in nižje energijske sunke, kjer se višje energijski nanašajo na delce alfa, nižje energijski pa na delce beta (slika 20).

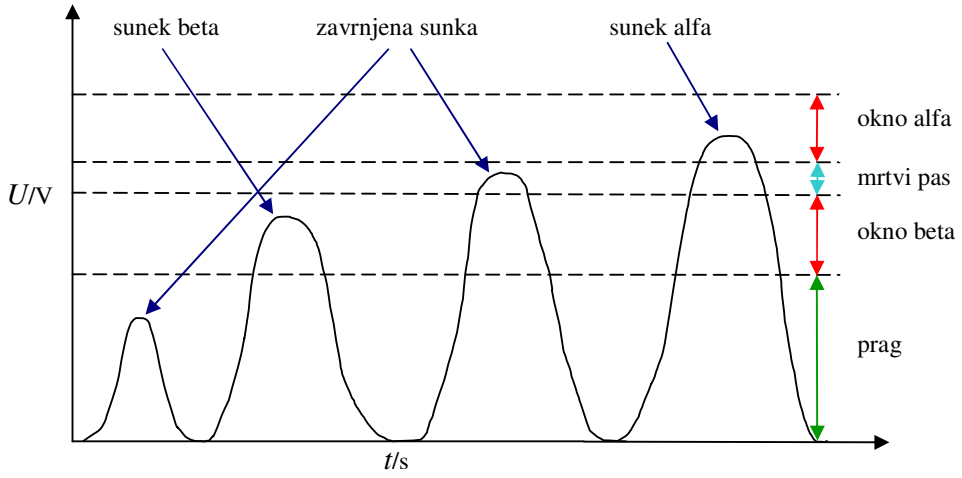

Slika 20: *Analiza sunkov v sistemu proporcionalnega števca LB4100–W.*

Za razliko od sevanja alfa in gama, kjer so energije sevanja diskretne, pa so le te pri sevanju beta kontinuirne. Razlog temu je nastanek antinevtrina pri razpadu beta, ki je na primeru ^{210}Pb predstavljen na formuli 4. Tako se energija, ki se sprosti pri razpadu porazdeli med novonastali atom, elektron (delec beta) ter antinevtrino in je lahko pri vsakem razpadu različna. Iz slike 21 lahko tako na primeru ^{210}Bi vidimo, da je energija delcev beta lahko zelo različna in znaša v tem primeru vse do 1162 keV s povprečno vrednostjo 389 keV.

$$^{210}_{82}\mathrm{Pb} \rightarrow ^{210}_{83}\mathrm{Bi} + \mathrm{e}^{-} + \bar{\nu} + Q_2 \qquad (4)$$

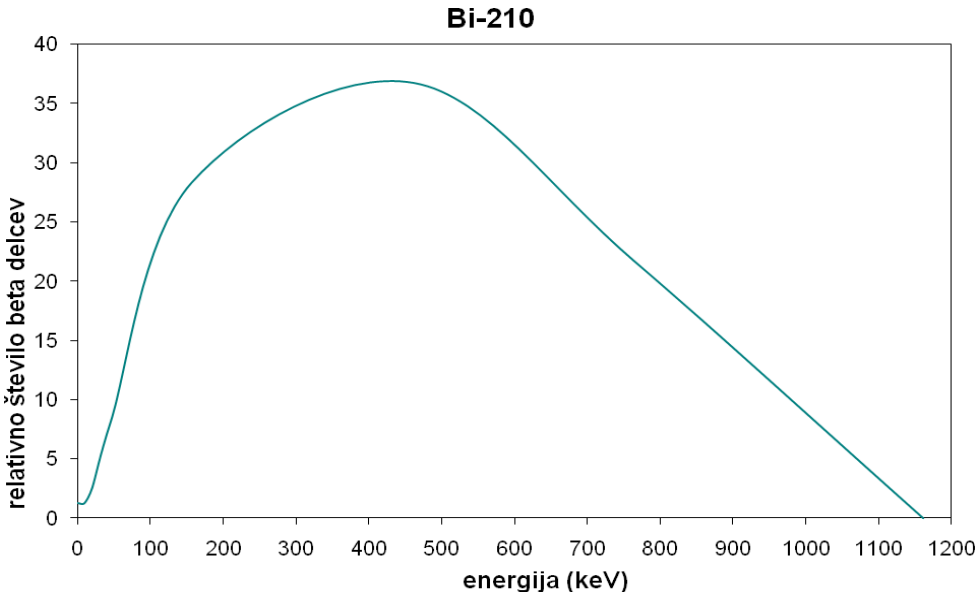

Slika 21: *Kontinuirni energijski spekter ^{210}Bi.*

Kalibracijo proporcionalnega števca in določitev izkoristka detekcije pri meritvah ^{210}Pb sem izvedel s certificirano standardno raztopino ^{210}Pb z aktivnostjo sledljivo do osnovnih SI enot. Vzorce za kalibracijo sem pripravil na enak način kot ostale vzorce.

Kalibracija omogoča korekcije tako za samoabsorpcijo delcev beta v vzorcu, kot tudi za porast ^{210}Bi iz ^{210}Pb. Zaradi relativno nizke energije delcev beta, ki nastanejo pri razpadu ^{210}Pb (maksimalna energija delcev beta znaša le 63 keV), je potrebno določiti ^{210}Pb posredno preko ^{210}Bi, ki je prav tako sevalec beta, vendar z mnogo višjo maksimalno energijo sevanja beta (slika 21). Posledica tega je, da je izkoristek detekcije za ^{210}Bi veliko večji kot za ^{210}Pb. Vendar pa je zaradi razpolovnega časa ^{210}Bi, ki znaša 5,01 dni (slika 2) potrebno počakati vsaj mesec dni, da se vzpostavi trajno radioaktivno ravnotežje med ^{210}Pb in ^{210}Bi. Posledica tega je, da se izkoristek detekcije spreminja v času od separacije, dokler se ne vzpostavi trajno radioaktivno ravnotežje med ^{210}Pb in ^{210}Bi. Problem pri kalibraciji predstavlja tudi samoabsorpcija delcev beta v viru $PbSO_4$, ki raste z večjo maso vira. Tako je izkoristek detekcije manjši pri večji masi vzorca. Ker je masa $PbSO_4$ odvisna od kemijskega izkoristka, se le ta spreminja od vzorca do vzorca in je lahko zelo različna.

Omenjene težave sem premostil s kalibracijo proporcionalnega števca, ki omogoča tako korekcije za porast ^{210}Bi iz ^{210}Pb in posledično povečevanje izkoristka detekcije, kot tudi korekcije zaradi različne samoabsorpcije v virih, ki so posledica različnega kemijskega izkoristka. Tako sem pripravil vire z različno ploščinsko gostoto $PbSO_4$ in znano dodano aktivnostjo ^{210}Pb ter jih pomeril v proporcionalnem števcu. Nato sem eksperimentalne rezultate uporabil za določitev enačbe izkoristka detekcije s pomočjo programa CurveExpert 1.3, ki omogoča izračun izkoristka detekcije v poljubnem času po radiokemijski separaciji in pri poljubni masi vira $PbSO_4$. Omenjeni rezultati so predstavljeni v enačbi 5, ki omogoča izračun skupnega izkoristka ^{210}Pb in ^{210}Bi ($\varepsilon_{\text{Pb-210+Bi210}}$) v odvisnosti od ploščinske gostote $PbSO_4$ ($\rho_{A,\text{PbSO4}}$) in časa po radiokemijski separaciji ^{210}Pb ($t_{2,\text{Pb-210}}$), kjer je $\lambda_{\text{Bi-210}}$ razpadna konstanta ^{210}Bi. Na sliki 22 so tako s točkami predstavljeni rezultati eksperimentalnih meritev pri različnih ploščinskih gostotah $PbSO_4$ in s krivuljami rezultati dobljeni z enačbo 5 pri določeni ploščinski gostoti $PbSO_4$. Iz slike 22 je razvidno, da enačba 5 zelo dobro opisuje spremembe izkoristka detekcije za ^{210}Pb in ^{210}Bi s časom, kot tudi zaradi različne samoabsorpcije.

$$\begin{aligned}\varepsilon_{\text{Pb}-210+\text{Bi}-210} = &-0{,}0492\left(-1{,}8007-\exp\left(-0{,}0373\rho_{A,\text{PbSO4}}\right)\right)\\ &-0{,}2648\left(-0{,}7469-\exp\left(-0{,}1811\rho_{A,\text{PbSO4}}\right)\right)\\ &\cdot\left(1-\exp\left(-\lambda_{\text{Bi}-210}t_{2,\text{Pb}-210}\right)\right)\end{aligned} \qquad (5)$$

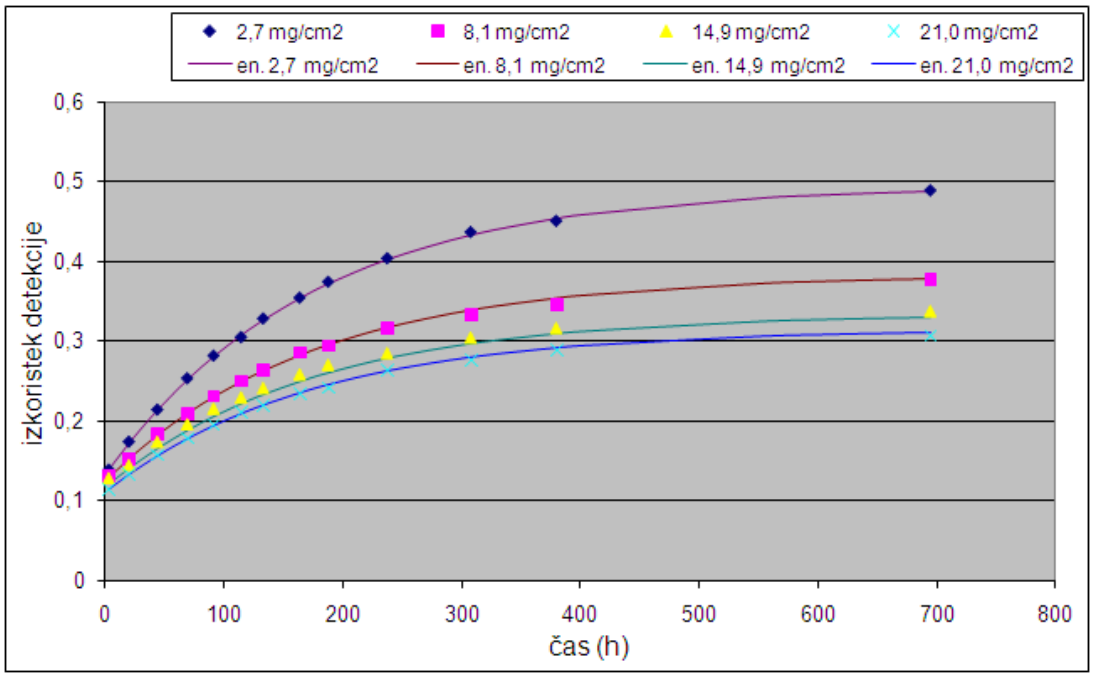

Slika 22: *Sprememba izkoristka detekcije za ^{210}Pb in ^{210}Bi pri različnih ploščinskih gostotah $PbSO_4$.*

Minimalno aktivnost, ki jo detektor še lahko zazna sem v primeru proporcionalnega števca določil skladno z enačbami 6 – 9. Takšen način določitve meje detekcije priporoča proizvajalec proporcionalnega števca.

$$MDA = \frac{k^2 + 2L_C}{t_m \varepsilon_m m} \tag{6}$$

$$L_C = k s_0 \tag{7}$$

$$s_0 = \frac{s_{RB}}{\varepsilon_m} \tag{8}$$

$$s_{RB}^2 = s_B^2 + \frac{R_B t_m \left(1 + R_B t_m z^2\right)}{t_m^2} \tag{9}$$

Kjer je:

MDA	minimalna aktivnost, ki jo števec še lahko zazna v Bq
k	konstanta standardnega odmika za dosego določene stopnje zaupanja in znaša pri 95 % stopnji zaupanja 1,645
t_m	čas meritve v s
ε_m	izkoristek detekcije meritve
m	masa vzorca v kg
L_C	minimalna aktivnost, pri kateri lahko z gotovostjo trdimo, da je aktivnost vzorca večja od 0 Bq
s_0	standardni odmik meritve vzorca z ničelno aktivnostjo
s_{RB}	standardni odmik gostote sunkov ozadja v času meritve
S_B	standardni odmik meritve ozadja
R_B	gostota sunkov ozadja

Minimalna aktivnost, ki jo števec še lahko zazna je pri meritvah ^{210}Pb v povprečju znašala 5,4E-3 Bq.

Merilne negotovosti pri vseh meritvah sem določil skladno s priporočili Eurachem (2000) in IAEA (2004). Upošteval sem vse vire merilne negotovosti, na koncu pa izračunal kombinirano standardno negotovost, ki sem jo podal s faktorjem pokritja $k = 1$. V nadaljevanju je predstavljen izračun negotovosti za primer določitve vsebnosti ^{238}U v tleh, kjer je merjenec specifična aktivnost ^{238}U v talnem vzorcu izražena v Bq/kg suhe mase na dan vzorčenja, analit pa je ^{238}U. Specifična aktivnost merjenca sem izračunal skladno z enačbo 10:

$$a_{\mathrm{A}} = \frac{A_{\mathrm{A}}}{m_{\mathrm{a}} q} f_1 f_2 f_3 f_4 \tag{10}$$

Kjer je:

a_A specifična aktivnost analita na dan vzorčenja v Bq/kg suhe mase
A_A aktivnost analita v mikrosooborjenem vzorcu v Bq
m_a masa sežganega vzorca, ki je bila uporabljena za analizo v kg
q razmerje med suho maso in sežgano maso vzorca
f_1 korekcija za razpad analita v času od vzorčenja do začetka meritve
f_2 korekcija za razpad analita med časom meritve t_G
f_3 korekcija za razpad sledilca kemijskega izkoristka od časa kalibracije sledilca do začetka meritve
f_4 korekcija za razpad sledilca kemijskega izkoristka med časom meritve t_G

Aktivnost analita sem izračunal z enačbo 11:

$$A_{\mathrm{A}} = c_{\mathrm{T}} V_{\mathrm{T}} \left(\frac{R_{\mathrm{GA}} - R_{\mathrm{BA}}}{R_{\mathrm{GT}} - R_{\mathrm{BT}}} \right) \left(\frac{p_{\alpha \mathrm{T}}}{p_{\alpha \mathrm{A}}} \right) \tag{11}$$

Kjer je:

c_T certificirana koncentracija raztopine sledilca kemijskega izkoristka v Bq/mL na dan kalibracije standarda
V_T volumen raztopine sledilca kemijskega izkoristka v mL
R_{GA} skupna hitrost štetja analita v s^{-1} v času štetja t_G
R_{BA} hitrost štetja analita v slepem vzorcu v s^{-1} v času štetja t_B
R_{GT} skupna hitrost štetja sledilca kemijskega izkoristka v s^{-1} v času štetja t_G
R_{BT} hitrost štetja sledilca kemijskega izkoristka v slepem vzorcu v s^{-1} v času štetja t_B
$p_{\alpha T}$ vsota verjetnosti emisije delcev alfa za tiste črte alfa v spektru sledilca, ki se nahajajo v območju kanalov v spektru alfa za določitev skupne hitrosti štetja (ponavadi zelo blizu 1)
$p_{\alpha A}$ Vsota verjetnosti emisije delcev alfa za tiste črte alfa v spektru analita, ki se nahajajo v omočju kanalov v spektru alfa za določitev skupne htrosti štetja (ponavadi zelo blizu 1)

Korekcijski faktorji za razpad so definirani v enačbah 12 – 15:

$$f_1 = \exp\left(\lambda_{\mathrm{A}} \left(t_{\mathrm{S}} - t_{\mathrm{E}}\right)\right) \tag{12}$$

$$f_2 = \frac{\lambda_{\mathrm{A}} t_{\mathrm{G}}}{1 - \exp\left(-\lambda_{\mathrm{A}} t_{\mathrm{G}}\right)} \tag{13}$$

$$f_3 = \exp\left(-\lambda_T \left(t_S - t_C\right)\right) \quad (14)$$

$$f_4 = \frac{\lambda_T t_G}{1 - \exp\left(-\lambda_T t_G\right)} \quad (15)$$

Kjer je:

λ_A razpadna konstanta analita v s^{-1}
λ_T razpadna konstanta sledilca kemijskega izkoristka v s^{-1}
t_E čas konca vzorčenja
t_S čas začetka meritve
t_C čas kalibracije standarda, ki je bil uporabljen kot sledilec kemijskega izkoristka
t_G trajanje meritve vzorca v s

Podatki o vzorcu, kakor tudi parametri, ki so znani pred začetkom analize so sledeči:

$t_S - t_E$: $6{,}307 \times 10^{6}$ s
$t_S - t_C$: $1{,}577 \times 10^{8}$ s
λ_A : $4{,}919 \times 10^{-18}$ s^{-1}
λ_T : $3{,}188 \times 10^{-10}$ s^{-1}
$p_{\alpha A}$: 1
$p_{\alpha T}$: 1
c_T : 0,33 Bq/mL , nanaša se na datum kalibracije standarda
V_T : 0,1 mL
R_{BA} : $8{,}0 \times 10^{-6}$ s^{-1} , hitrost štetja analita v slepem vzorcu, ugotovljena iz nekaj ločenih analiz slepega vzorca in izračunana skladno z enačbo 22
$u(R_{BA})$: $6{,}4 \times 10^{-6}$ s^{-1} , standardna negotovost R_{BA}, ugotovljena iz nekaj ločenih analiz slepega vzorca in izračunana skladno z enačbo 23
R_{BT} : $7{,}0 \times 10^{-5}$ s^{-1} , hitrost štetja sledilca kemijskega izkoristka v slepem vzorcu, ugotovljena iz nekaj ločenih analiz slepega vzorca in izračunana skladno z enačbo 24
$u(R_{BT})$: $5{,}6 \times 10^{-5}$ s^{-1} , standardna negotovost R_{BT} , ugotovljena iz nekaj ločenih analiz slepega vzorca in izračunana skladno z enačbo 25

Izmerjeni podatki in parametri iz analize so sledeči:

tara :	41,9266 g
bruto suha masa vzorca :	104,8129 g
neto suha masa vzorca, m_D :	62,8863 g
bruto masa vzorca po sežigu :	97,1492 g
neto masa vzorca po sežigu, m_A :	55,2226 g
$q = \frac{m_D}{m_A}$:	1,1388
tara pri tehtanju mase sežganega vzorca :	4,8541 g
bruto masa sežganega vzorca :	5,3656 g
neto masa sežganega vzorca za analizo, m_a:	0,5115 g

t_G : $3{,}680 \times 10^{5}$ s
t_B : $3{,}680 \times 10^{5}$ s
R_{GA} : $3{,}571 \times 10^{-3}$ s^{-1}
R_{GT} : $9{,}114 \times 10^{-3}$ s^{-1}

Vire negotovosti sem identificiral s pomočjo vzročno-posledičnega diagrama, ki je prikazan na sliki 23.

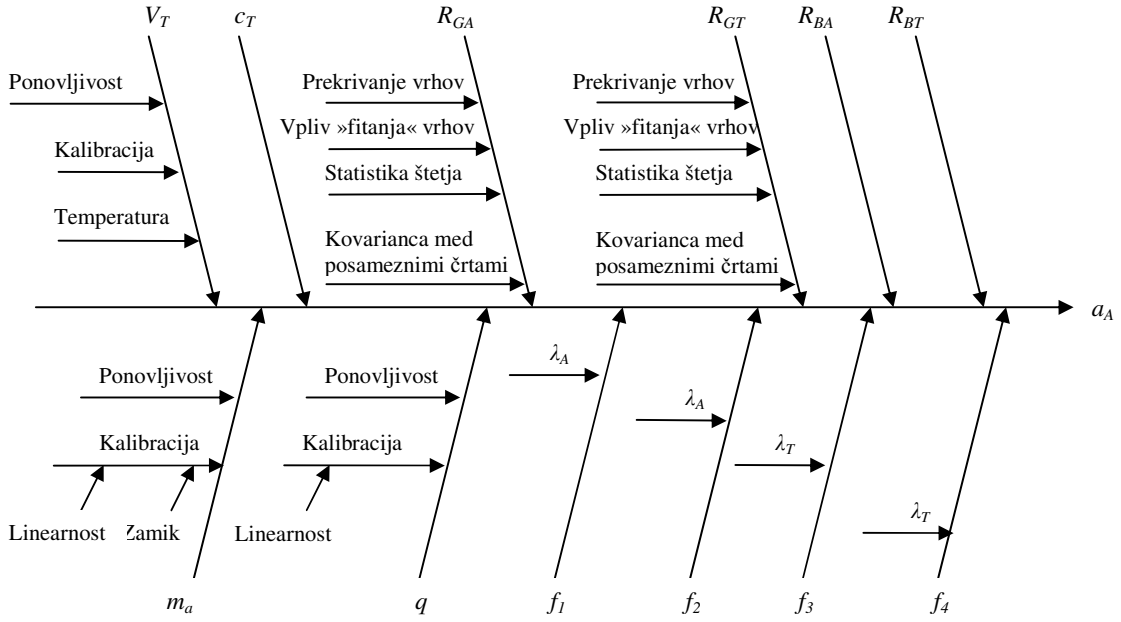

Slika 23: *Vzročno-posledični diagram za ugotavljanje virov negotovosti za meritev* ^{238}U.

Kombinirano standardno negotovost razmerja med masami $q = m_D / m_A$ pri sežigu sem izračunal s pomočjo enačb 16 – 18:

$$\frac{u(q)}{q} = \sqrt{\left(\frac{u(m_D)}{m_D}\right)^2 + \left(\frac{u(m_A)}{m_A}\right)^2} \quad (16)$$

$$u(m_D) = \sqrt{u^2(bruto\ suha\ masa\ vzorca) + u^2(tara)} \quad (17)$$

$$u(m_A) = \sqrt{u^2(bruto\ masa\ sežganega\ vzorca\ \ po\ sežigu) + u^2(tara)} \quad (18)$$

Kjer je:

$u(q)$ kombinirana standardna negotovost razmerja med masami
$u(m_D)$ kombinirana standardna negotovost mase suhega vzorca v g
$u(m_A)$ kombinirana standardna negotovost mase sežganega vzorca v g

Kombinirano standardno negotovost mase sežganega vzorca, uporabljenega za analizo (m_a) sem izračunal s pomočjo enačbe 19:

$$u(m_a) = \sqrt{u^2(bruto\ masa\ sežganega\ vzorca) + u^2(tara)} \quad (19)$$

Relativna standardna negotovost certificirane koncentracije sledilca kemijskega izkoristka $u(c_T) / c_T$ je znašala 0,024.

Komponente negotovosti volumna sledilca V_T, ki sem ga odvzel s pipeto iz raztopine sledilca kemijskega izkoristka so:

- Relativna standardna negotovost internega volumna (0,1 mL), ki je podana od

proizvajalca je znašala 2,0E-3; zaradi trikotne porazdelitve je delimo s $\sqrt{6}$, kar nato znese 1,0E-3.

- Serija meritev volumnov in mas je rezultirala v relativni standardni negotovosti 2,5E-3.
- Variiranje v temperaturi okolja za ± 3 °C je rezultiralo v standardni negotovosti 3,1E-4 mL.

Te tri komponente negotovosti volumna sledilca so rezultirale v kombinirani relativni standardni negotovosti volumna dodanega sledilca ($u(V_T) / V_T$) 2,6E-3.

Pri izračunih standardnih negotovostih povezanih s površino vrha sem predpostavil, da se vrh sledilca kemijskega izkoristka in analita ne prekrivata. Tako sem standardno negotovost skupne hitrosti štetja analita R_{GA} izračunal po enačbi 20:

$$u(R_{GA}) = \sqrt{\frac{R_{GA}}{t_G}} \tag{20}$$

Standardno negotovost skupne hitrosti štetja sledilca kemijskega izkoristka sem izračunal s pomočjo enačbe 21:

$$u(R_{GT}) = \sqrt{\frac{R_{GT}}{t_G}} \tag{21}$$

Pogosto je variacija serije meritev slepih vzorcev večja, kot lahko predpostavimo iz same statistike štetja, ki sledi Poissonovi porazdelitvi. Zato je priporočljivo določiti negotovosti iz serije n meritev slepih vzorcev. Hitrost štetja analita v slepem vzorcu (R_{BA}) in njegovo standardno negotovost ($u(R_{BA})$) sem izračunal s pomočjo enačb 22 in 23:

$$R_{BA} = \frac{\sum_{i=1}^{n} R_{BA,i}}{n} \tag{22}$$

$$u(R_{BA}) = \sqrt{\frac{\sum_{i=1}^{n} \left(R_{BA,i} - R_{BA}\right)^2}{n-1}} \tag{23}$$

Podobno je določena tudi hitrost štetja sledilca kemijskega izkoristka v slepem vzorcu (R_{BT}) in pripadajoča standardna negotovost ($u(R_{BT})$), ki ju podajata enačbi 24 in 25:

$$R_{BT} = \frac{\sum_{i=1}^{n} R_{BT,i}}{n} \tag{24}$$

$$u(R_{BT}) = \sqrt{\frac{\sum_{i=1}^{n} \left(R_{BT,i} - R_{BT}\right)^2}{n-1}} \tag{25}$$

Relativna standardna negotovost razpadne konstante analita ($u(\lambda_A) / \lambda_A$) znaša 6,7E-4, sledilca kemijskega izkoristka ($u(\lambda_T) / \lambda_T$) pa 5,8E-3.

Standardne negotovosti korekcijskih faktorjev f_1, f_2, f_3 in f_4 so definirane z enačbami 26 – 29:

$$u(f_1) = f_1\left(t_S - t_E\right)u(\lambda_A) \tag{26}$$

$$u(f_2) = f_2\left(1 - f_2\exp\left(-\lambda_A t_G\right)\right)\frac{u(\lambda_A)}{\lambda_A} \tag{27}$$

$$u(f_3) = f_3\left(t_S - t_C\right)u(\lambda_T) \tag{28}$$

$$u(f_4) = f_4\left(1 - f_4\exp\left(-\lambda_T t_G\right)\right)\frac{u(\lambda_T)}{\lambda_T} \tag{29}$$

Pri izračunu merjenca iz enačb 10 in 11 sledi:

$A_A = 0,01298$ Bq

$a_A = 21,1915$ Bq/kg suhe mase

Pri izračunu relativne kombinirane standardne negotovosti $u_C(a_A)$ / a_A specifične aktivnosti analita na dan vzorčenja sem uporabil enačbe 30 – 35:

$$\frac{u_c(a_A)}{a_A} = \sqrt{\left(\frac{u_c(A_A)}{A_A}\right)^2 + \left(\frac{u(m_a)}{m_a}\right)^2 + \left(\frac{u(q)}{q}\right)^2 + \left(\frac{u(f_1)}{f_1}\right)^2 + \left(\frac{u(f_2)}{f_2}\right)^2 + \left(\frac{u(f_3)}{f_3}\right)^2 + \left(\frac{u(f_4)}{f_4}\right)^2} \tag{30}$$

$$\frac{u_c(A_A)}{A_A} = \sqrt{\left(\frac{u_c(c_T)}{c_T}\right)^2 + \left(\frac{u(V_T)}{V_T}\right)^2 + \left(\frac{u(y)}{y}\right)^2} \tag{31}$$

$$y = \frac{R_{GA} - R_{BA}}{R_{GT} - R_{BT}} \tag{32}$$

$$\frac{u(y)}{y} = \sqrt{\left(\frac{u(R_{GA} - R_{BA})}{(R_{GA} - R_{BA})}\right)^2 + \left(\frac{u(R_{GT} - R_{BT})}{(R_{GT} - R_{BT})}\right)^2} \tag{33}$$

$$\left(\frac{u(R_{GA} - R_{BA})}{(R_{GA} - R_{BA})}\right)^2 = \frac{u^2(R_{GA}) + u^2(R_{BA})}{(R_{GA} - R_{BA})^2} \tag{34}$$

$$\left(\frac{u(R_{GT} - R_{BT})}{(R_{GT} - R_{BT})}\right)^2 = \frac{u^2(R_{GT}) + u^2(R_{BT})}{(R_{GT} - R_{BT})^2} \tag{35}$$

Če vstavimo ustrezne podatke v enačbe 30 – 35 dobimo kot rezultat kombinirano standardno negotovost merjenjca ob faktorju pokritja $k = 1$:

$$\frac{u_c(a_A)}{a_A} = \sqrt{\left(\frac{5,4\cdot10^{-4}\text{ Bq}}{0,01298\text{ Bq}}\right)^2 + \left(\frac{1,4\cdot10^{-4}\text{ g}}{0,5115\text{ g}}\right)^2 + \left(\frac{3,9\cdot10^{-6}}{1,1388}\right)^2 + \left(\frac{2,1\cdot10^{-14}}{1}\right)^2 + \left(\frac{1,2\cdot10^{-15}}{1}\right)^2 + \left(\frac{3,4\cdot10^{-4}}{0,95}\right)^2 + \left(\frac{8,4\cdot10^{-7}}{1}\right)^2}$$

$u_C(a_A) = 0,9$ Bq/kg suhe mase

In končni rezultat lahko izrazimo kot:

$a_A = (21,2 \pm 0,9)$ Bq/kg suhe mase

4 Rezultati

4.1 Fizikalno kemijske meritve vzorcev tal

V tabeli 4 so predstavljeni rezultati fizikalno kemijskih parametrov vzorcev tal, ki so bili določeni v Centru za pedologijo in varstvo okolja, Oddelka za agronomijo, Biotehniške fakultete v Ljubljani. Iz rezultatov je razvidno, da je bila vrednost pH tal rahlo kisla, z izjemo lokacije 4, kjer je bila nevtralna. Rezultati vsebnosti organske snovi so bili relativno nizki in so znašali od 2,1 % v lokaciji 6 pa vse do 5,9 % v lokaciji 3. Prav tako je bila vsebnost karbonatov v tleh nizka, z izjemo lokacije 4, kjer je znašala 7,9 %. Velikostno porazdelitev delcev prikazujejo deleži peska, melja in gline. Pesek predstavljajo delci velikosti od 0,0625 mm do 2 mm, melj delci velikosti od 0,0039 do 0,0625 mm in glina delci manjši od 0,0039 mm. Velikostna porazdelitev delcev v tleh iz lokacij 4 in 6 je primerljiva, medtem, ko imajo tla v lokaciji 3 več melja, tla v lokaciji 1 pa več peska. V tleh iz lokacije 2 so vsi trije velikostni razredi približno enako zastopani. Glede na teksturni razred spadajo tla iz lokacije 1 med peščeno ilovnate, tla iz lokacije 3 med meljno ilovnate, tla iz ostalih lokacij pa med ilovnata.

Tabela 4: *Rezultati fizikalno kemijskih parametrov vzorcev tal.*

Lokacija	pH v $CaCl_2$	Organska snov (%)	Karbonati (%)	Pesek (%)	Melj (%)	Glina (%)
1	5,4	5,4	1,6	62,0	27,5	10,5
2	4,5	3,8	0,8	37,2	36,3	26,5
3	4,5	5,9	1,2	12,5	68,2	19,3
4	7,0	3,8	7,9	46,7	34,9	18,4
6	5,9	2,1	<0,5	49,9	31,3	18,8

4.2 Rezultati in primerjava sekvenčnih ekstrakcijskih postopkov v zemljah

Primerjava obeh sekvenčnih ekstrakcijskih postopkov za vse analizirane radionuklide v vzorcih zemelj je prikazana na slikah 24 – 33. Kemijski izkoristki separacij so znašali od 47 do 95 % za ^{238}U, od 46 do 92 % za ^{230}Th, od 54 do 87 % za ^{226}Ra, od 50 do 79 % za ^{210}Pb in od 69 do 100 % za ^{210}Po. Na slikah 24 – 33 sem rezultate postopka S za vseh šest lokacij nanesel na os x, rezultate postopka B pa na os y. Nanesel sem tudi premico y=x, ki nam pomaga ugotoviti ujemanje rezultatov obeh postopkov. V primeru, ko oba postopka dajeta enak rezultat, bi ležale točke na tej premici. Zaradi večje jasnosti sem rezultate za posamezen radionuklid prikazal na dveh slikah. Na grafih sem prikazal tudi negotovosti posameznih meritev in to v obliki kombinirane standardne negotovosti s faktorjem pokritja $k = 1$. Kjer negotovosti niso vidne, so manjše od simbola. Postopek S vključuje tudi izmenljivo frakcijo, kar pa ni slučaj v primeru postopka B, zato sem zaradi primerljivosti rezultate v primeru postopka S za izmenljivo in karbonatno frakcijo seštel

in so predstavljeni kot karbonatna frakcija.

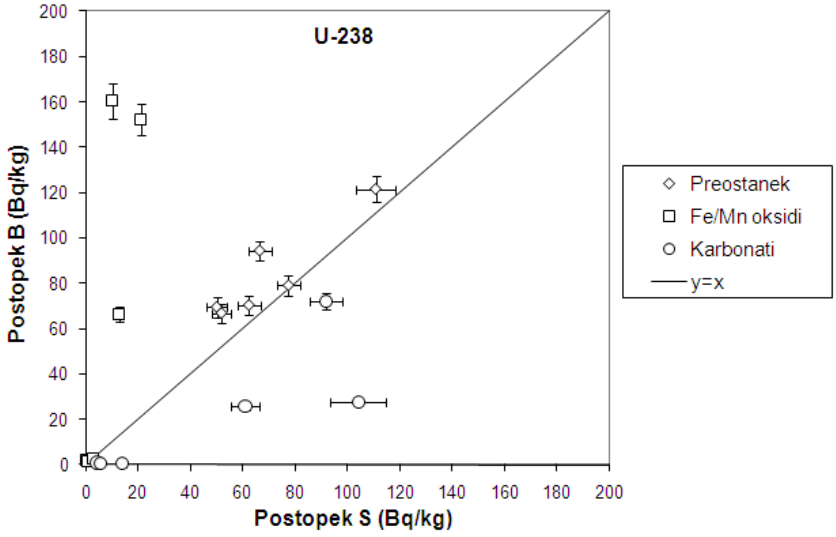

Slika 24: *Primerjava obeh postopkov za ^{238}U za preostanek, Fe/Mn okside in karbonate.*

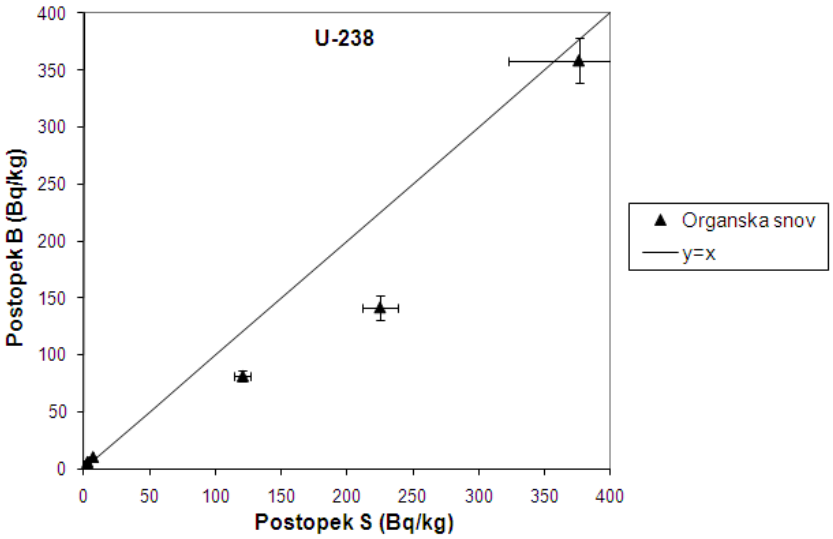

Slika 25: *Primerjava obeh postopkov za ^{238}U za organsko snov.*

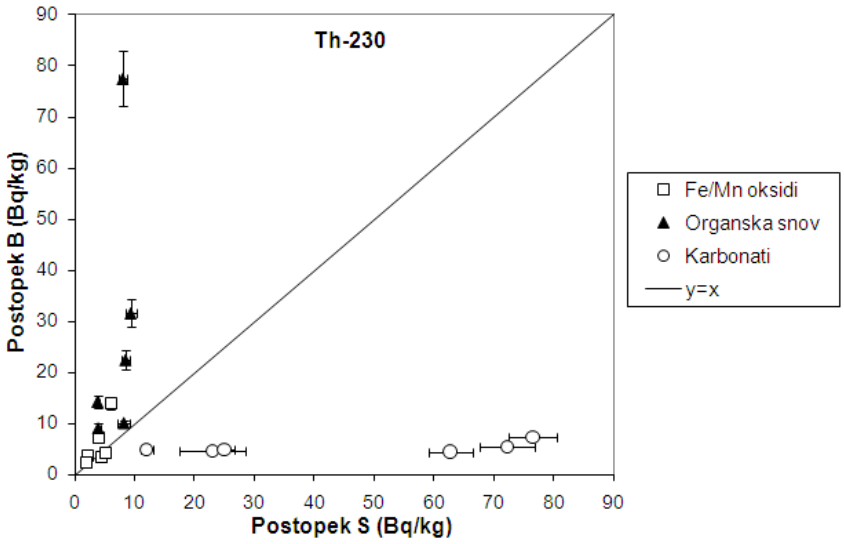

Slika 26: *Primerjava obeh postopkov za ^{230}Th za Fe/Mn okside, organsko snov in karbonate.*

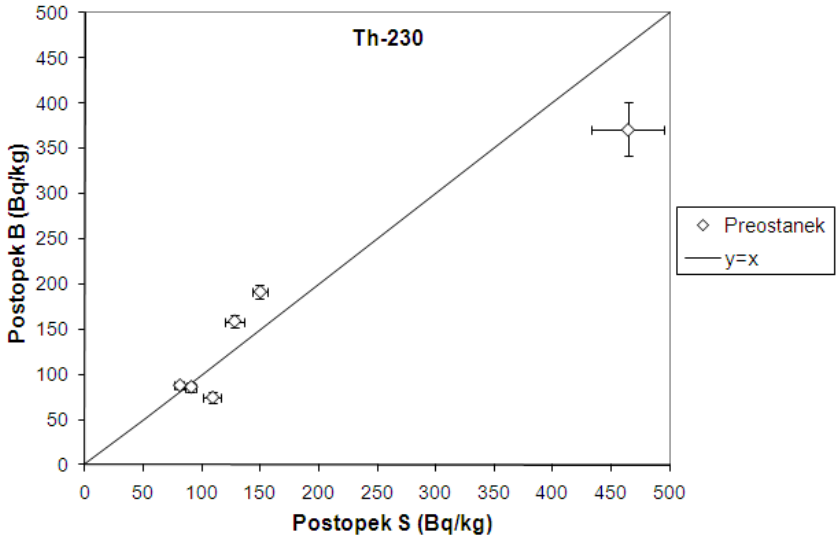

Slika 27: *Primerjava obeh postopkov za ^{230}Th za preostanek.*

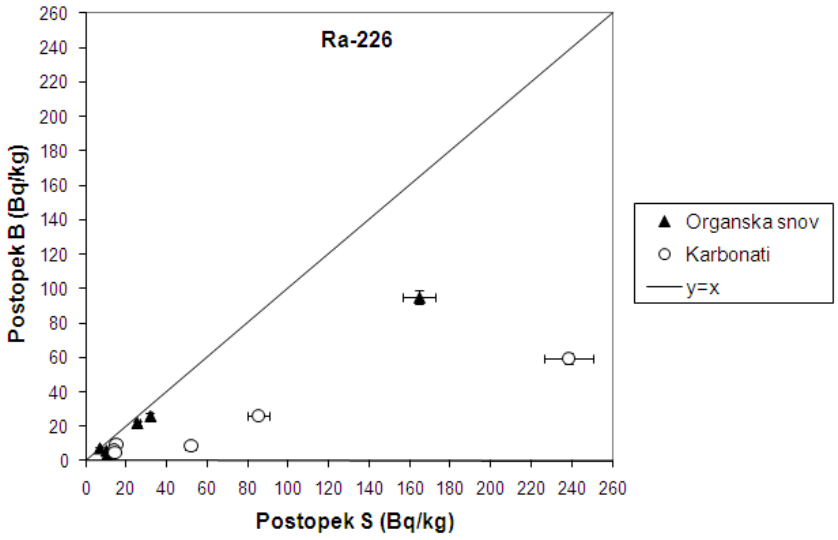

Slika 28: *Primerjava obeh postopkov za ^{226}Ra za organsko snov in karbonate.*

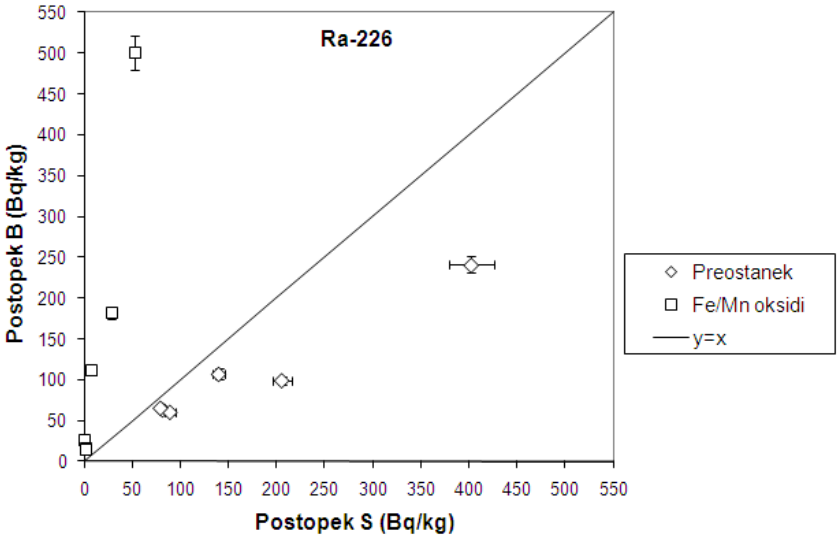

Slika 29: *Primerjava obeh postopkov za ^{226}Ra za preostanek in Fe/Mn okside.*

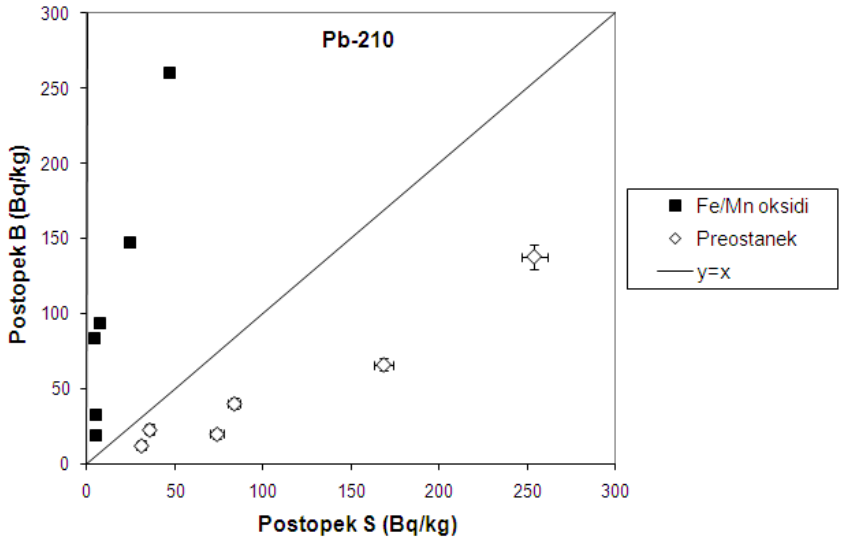

Slika 30: *Primerjava obeh postopkov za ^{210}Pb za Fe/Mn okside in preostanek.*

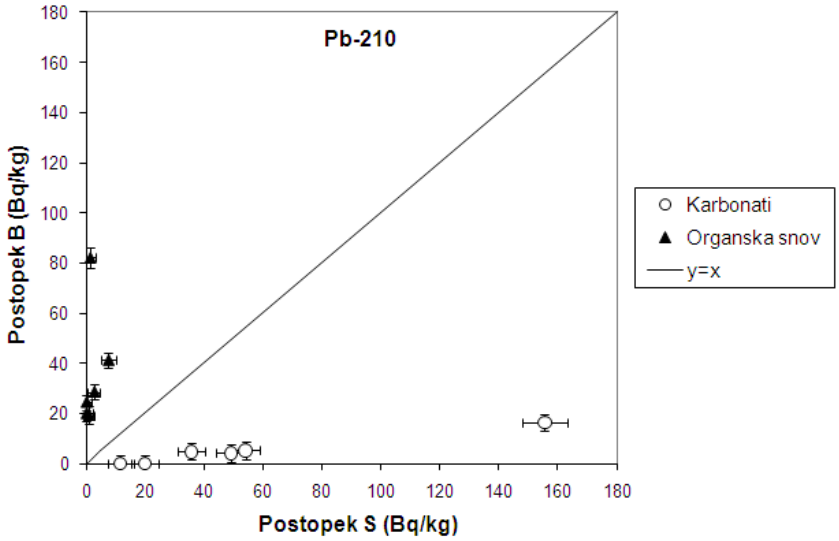

Slika 31: *Primerjava obeh postopkov za ^{210}Pb za karbonate in organsko snov.*

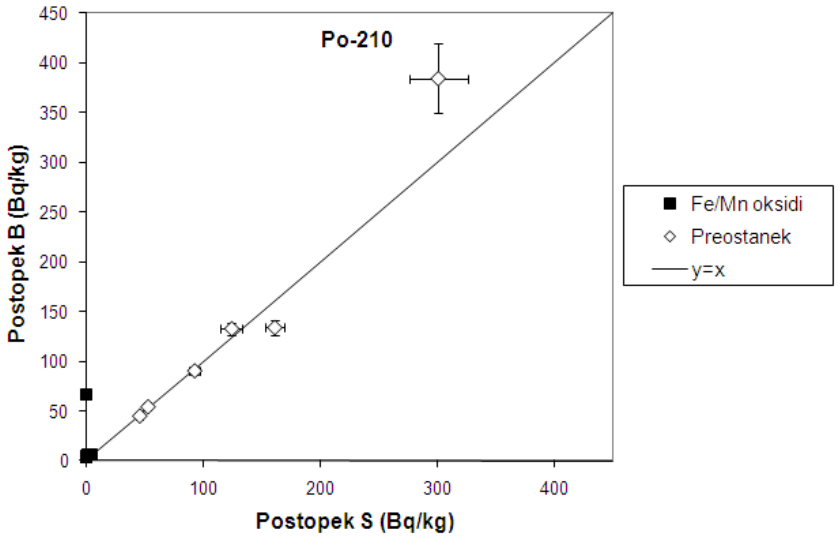

Slika 32: *Primerjava obeh postopkov za ^{210}Po za Fe/Mn okside in preostanek.*

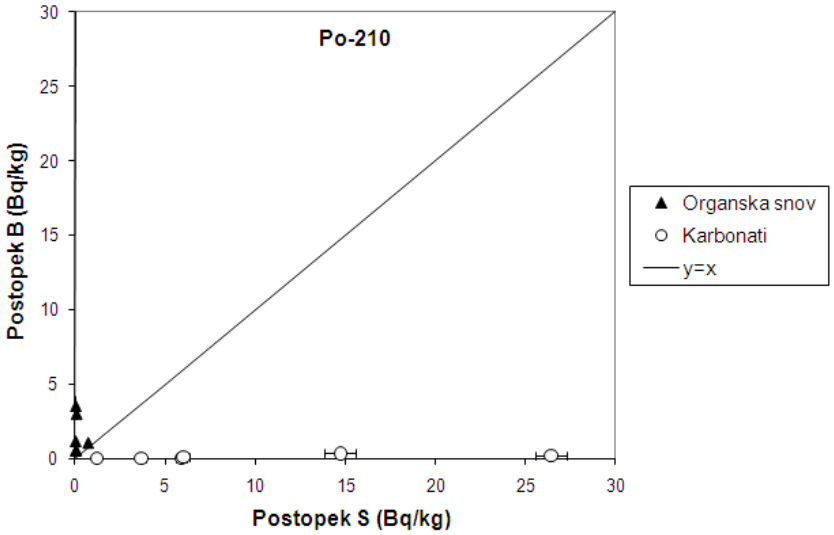

Slika 33: *Primerjava obeh postopkov za ^{210}Po za organsko snov in karbonate.*

V mnogih primerih sem lahko že iz slik 24 – 33 z lahkoto ugotovil, da postopka nista primerljiva (na primer rezultati za karbonatno frakcijo pri ^{210}Po, ki jih prikazuje slika 33). Pri nekaterih, kot na primer pri preostanku v primeru ^{210}Po (slika 32), pa to ni tako očitno. Zato sem izvedel statistično primerjavo rezultatov dveh postopkov skladno s pristopom, ki ga opisujeta Bland in Altman (1986). Ta pristop temelji na primerjanju razlik rezultatov dveh postopkov. Tako sem na grafih na slikah 34 – 53 prikazal razliko med rezultati postopka S in B v odvisnosti od povprečnih vrednosti rezultatov obeh postopkov pri posameznih frakcijah. Poleg tega sem na grafih predstavil še povprečne vrednosti razlik med obema postopkoma (povprečje (S-B)), dvakratni standardni odmik razlik med obema postopkoma (2SD) in 20 % maksimalne vrednosti povprečij med obema postopkoma. Poenostavljeno povedano, če postopek S daje višje vrednosti od postopka B, so povprečne razlike med obema postopkoma pozitivne in, če postopek B daje višje vrednosti so povprečne razlike med obema postopkoma negativne. V primeru, ko bi oba

postopka dajala popolnoma enake rezultate pa bi bilo povprečje razlik enako 0. Seveda je v realnosti to težko izvedljivo, ker vsako meritev spremlja določena negotovost, kar na koncu privede do določenih odstopanj. Tako je potrebno za ovrednotenje sprejemljivosti odstopanj, določiti nek kriterij v okviru katerega sta postopka še primerljiva. V mojem primeru sem kot osnovo za določitev tega kriterija izbral kombinirano standardno negotovost posameznih rezultatov, ki je znašala od 3 do 20 %. Razlog za takšno odstopanje relativnih negotovosti rezultatov temelji v negotovosti zaradi statistike štetja, ki sledi Poissonovi porazdelitvi in je večja pri manjših aktivnostih ter manjša pri večjih. Najpogosteje zastopana negotovost je znašala okrog 10 %, zato sem jo izbral kot kriterij, kar pri faktorju pokritja $k = 2$ znaša 20 %. To vrednost sem tudi predstavil s prekinjeno črto na posameznih grafih na slikah 34 – 53. Skladno s tem postopka nista primerljiva, če je dvakratnik standardnega odmika (2SD) večji od 20 %.

Tako sem lahko iz slik 34 – 37, ki prikazujejo rezultate primerljivosti obeh postopkov za ^{238}U ugotovil, da postopek S daje višje vrednosti od postopka B v primeru karbonatne frakcije in organske snovi, postopek B pa v primeru Fe/Mn oksidov in preostanka. Iz slik 34 – 37 je tudi razvidno, da je dvakratnik standardnega odmika manjši od 20 % v primeru organske snovi in preostanka, torej postopka S in B za ti dve frakciji dajeta statistično primerljive rezultate. Nasprotno pa velja za karbonatno frakcijo in Fe/Mn okside, kjer postopka v primeru ^{238}U dajeta statistično različne rezultate.

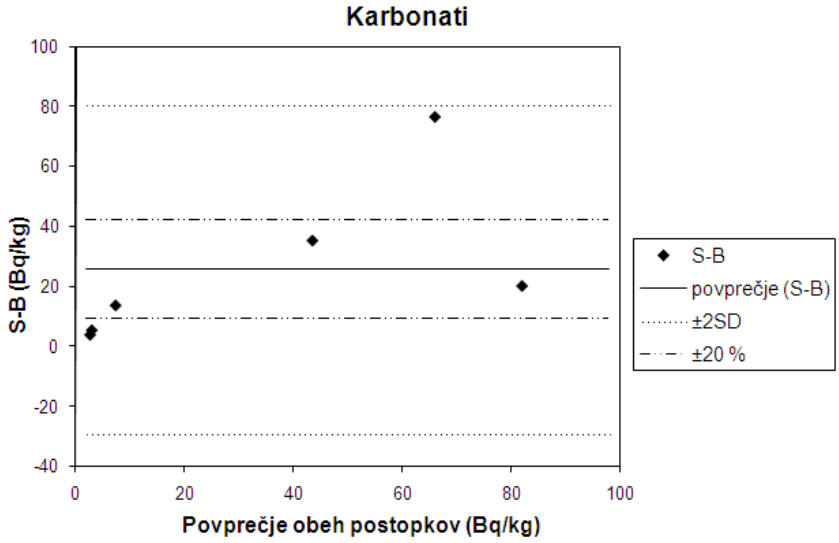

Slika 34: *Primerjava razlik posameznih meritev v odvisnosti od povprečnih vrednosti meritev obeh postopkov za ^{238}U za karbonatno frakcijo.*

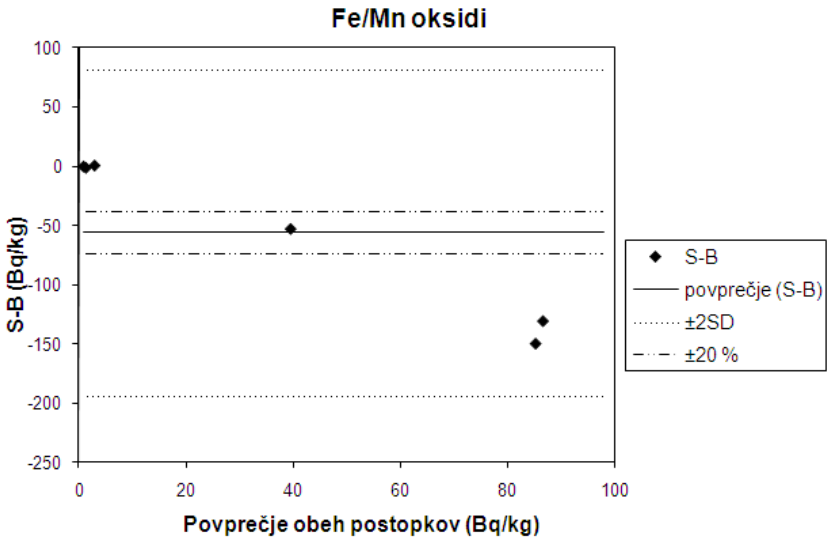

Slika 35: *Primerjava razlik posameznih meritev v odvisnosti od povprečnih vrednosti meritev obeh postopkov za ^{238}U za Fe/Mn oksidno frakcijo.*

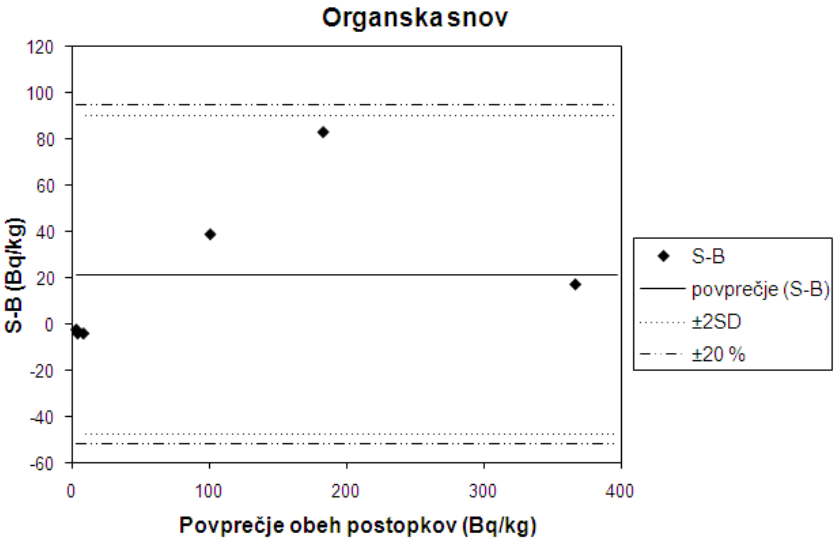

Slika 36: *Primerjava razlik posameznih meritev v odvisnosti od povprečnih vrednosti meritev obeh postopkov za ^{238}U za organsko frakcijo.*

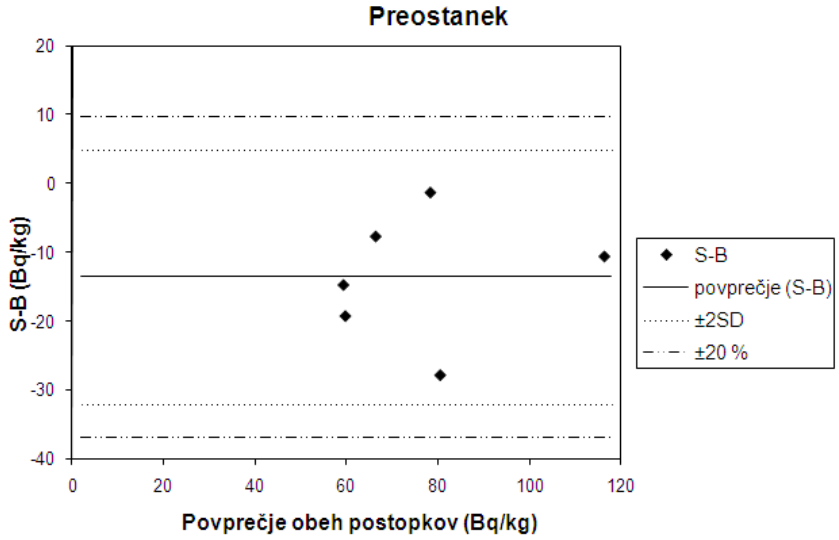

Slika 37: *Primerjava razlik posameznih meritev v odvisnosti od povprečnih vrednosti meritev obeh postopkov za ^{238}U za preostanek.*

Podobno kot za ^{238}U so na slikah 38 – 41 prikazani rezultati za ^{230}Th. Iz njih sem ugotovil, da postopek S daje višje rezultate v primeru karbonatne frakcije in preostanka, postopek B pa v primeru Fe/Mn oksidov ter organske snovi. Ugotovil sem tudi, da dajeta postopka pri vseh frakcijah statistično različne rezultate.

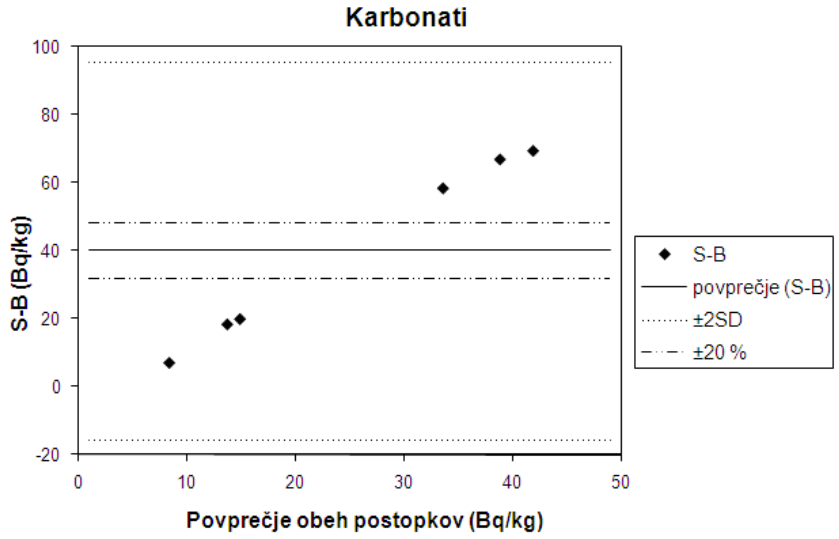

Slika 38: *Primerjava razlik posameznih meritev v odvisnosti od povprečnih vrednosti meritev obeh postopkov za ^{230}Th za karbonatno frakcijo.*

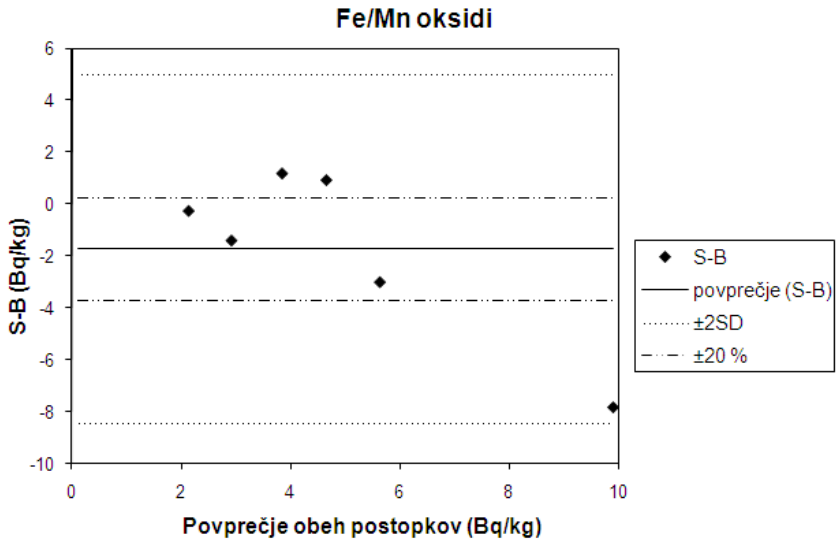

Slika 39: *Primerjava razlik posameznih meritev v odvisnosti od povprečnih vrednosti meritev obeh postopkov za ^{230}Th za Fe/Mn oksidno frakcijo.*

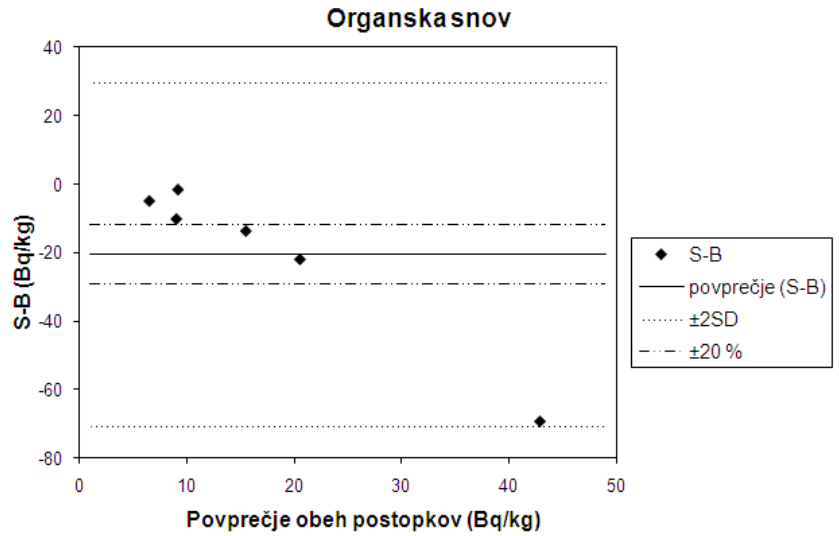

Slika 40: *Primerjava razlik posameznih meritev v odvisnosti od povprečnih vrednosti meritev obeh postopkov za ^{230}Th za organsko frakcijo.*

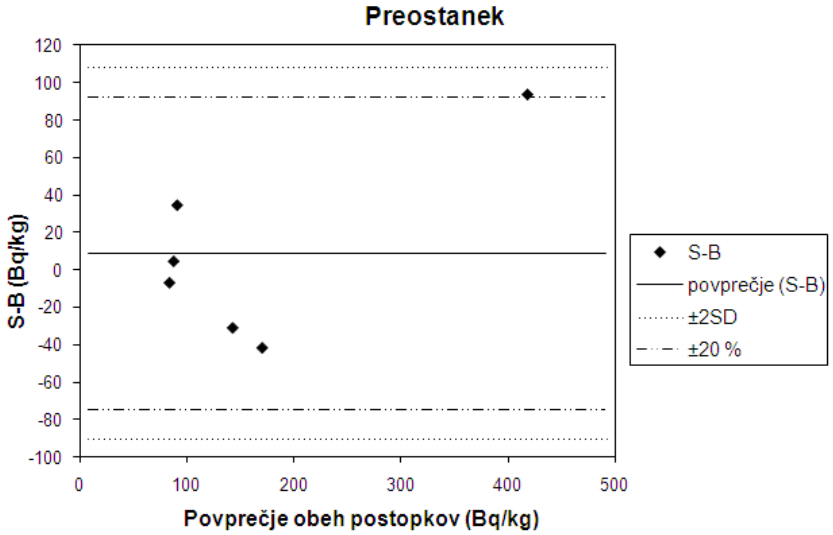

Slika 41: *Primerjava razlik posameznih meritev v odvisnosti od povprečnih vrednosti meritev obeh postopkov za ^{230}Th za preostanek.*

Rezultati ujemanja obeh postopkov za ^{226}Ra so prikazani na slikah 42 – 45. Tudi tukaj je razvidno, da postopek S daje višje rezultate v primeru karbonatne frakcije, organske snovi in preostanka, nižje od postopka B pa le v primeru Fe/Mn oksidov. Tudi v primeru ^{226}Ra sem ugotovil, da je dvakratnik standardnega odmika večji od 20 % pri vseh frakcijah, kar pomeni, da dajeta postopka statistično različne rezultate.

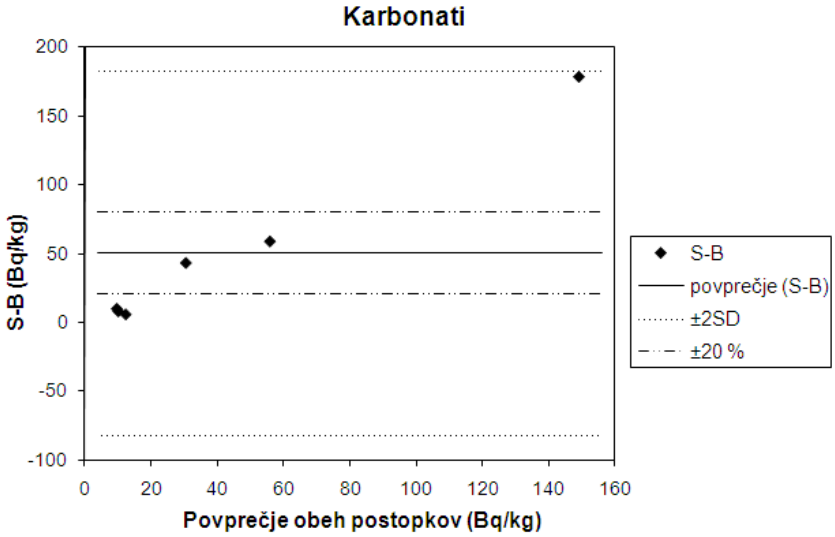

Slika 42: *Primerjava razlik posameznih meritev v odvisnosti od povprečnih vrednosti meritev obeh postopkov za ^{226}Ra za karbonatno frakcijo.*

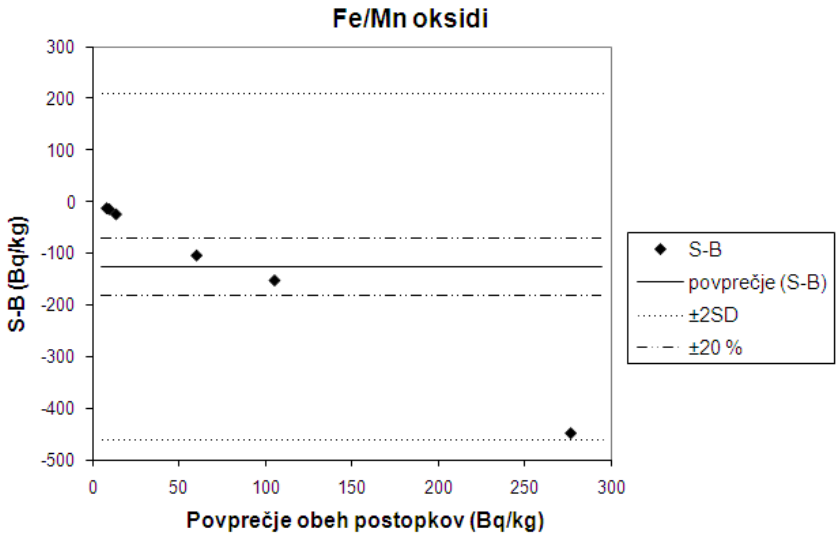

Slika 43: *Primerjava razlik posameznih meritev v odvisnosti od povprečnih vrednosti meritev obeh postopkov za ^{226}Ra za Fe/Mn oksidno frakcijo.*

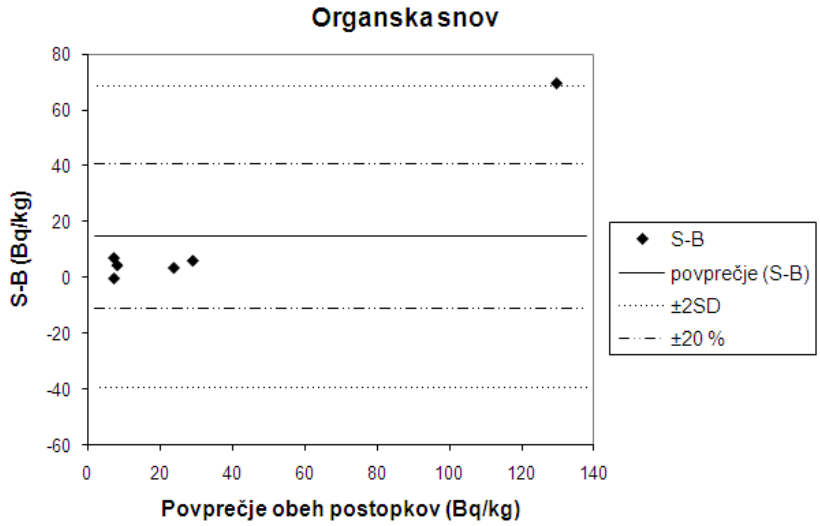

Slika 44: *Primerjava razlik posameznih meritev v odvisnosti od povprečnih vrednosti meritev obeh postopkov za ^{226}Ra za organsko frakcijo.*

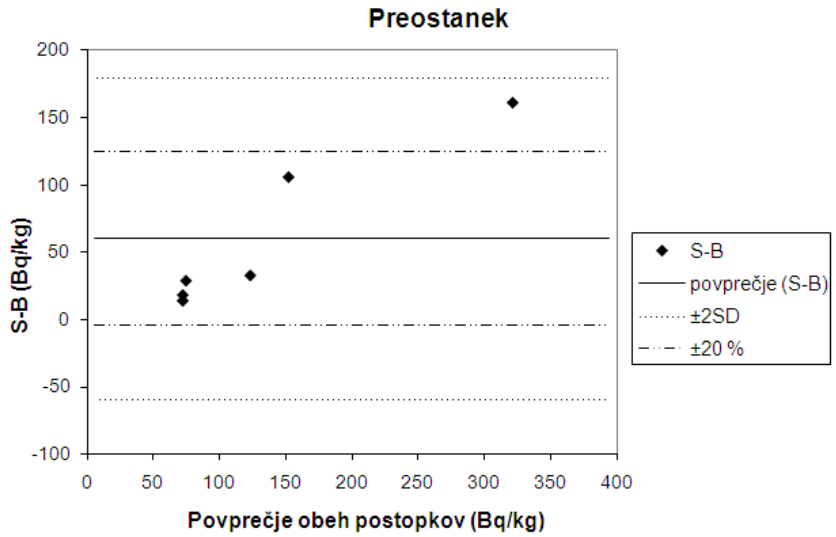

Slika 45: *Primerjava razlik posameznih meritev v odvisnosti od povprečnih vrednosti meritev obeh postopkov za ^{226}Ra za preostanek.*

Podobno sem ugotovil tudi za ujemanje obeh postopkov v primeru ^{210}Pb, ki ga prikazujejo slike 46 – 49, kjer je tudi dvakratnik standardnega odmika pri vseh frakcijah večji od 20 %. Torej so tudi v primeru ^{210}Pb rezultati obeh postopkov za vse frakcije statistično različni. Višje vrednosti daje postopek S v primeru karbonatne frakcije in pri preostanku, postopek B pa pri Fe/Mn oksidih in pri organski snovi.

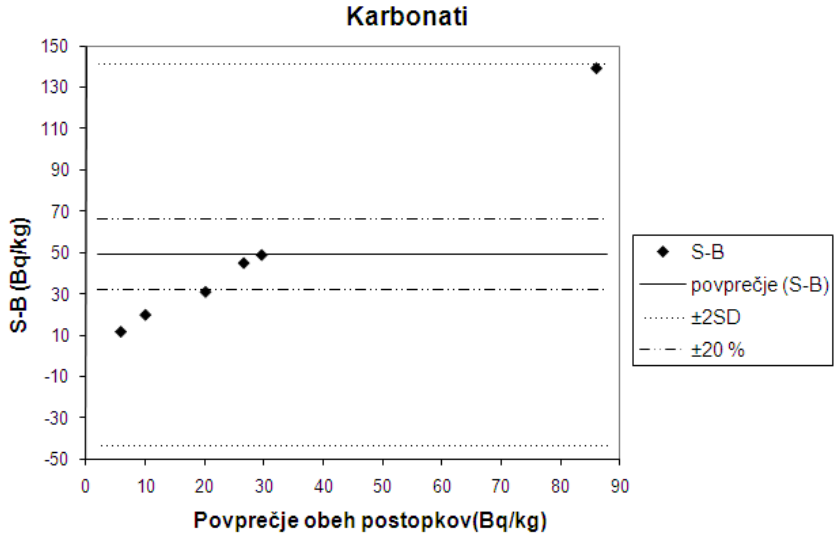

Slika 46: *Primerjava razlik posameznih meritev v odvisnosti od povprečnih vrednosti meritev obeh postopkov za ^{210}Pb za karbonatno frakcijo.*

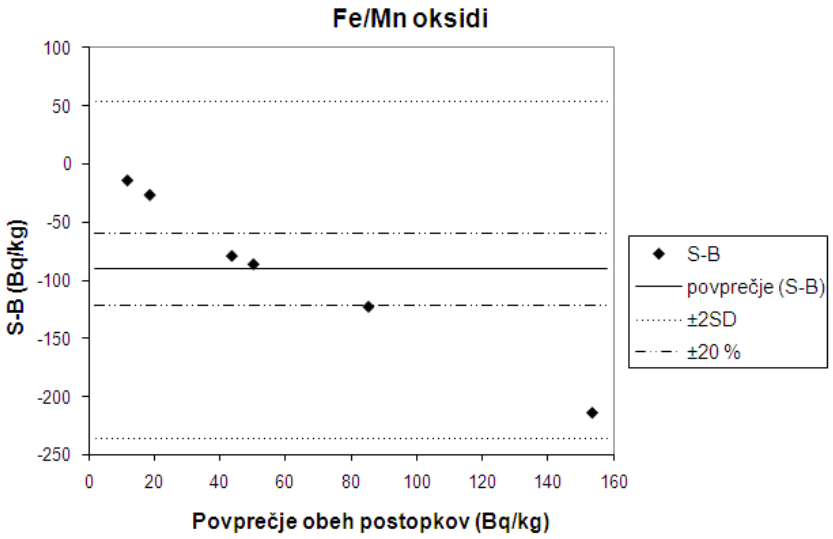

Slika 47: *Primerjava razlik posameznih meritev v odvisnosti od povprečnih vrednosti meritev obeh postopkov za ^{210}Pb za Fe/Mn oksidno frakcijo.*

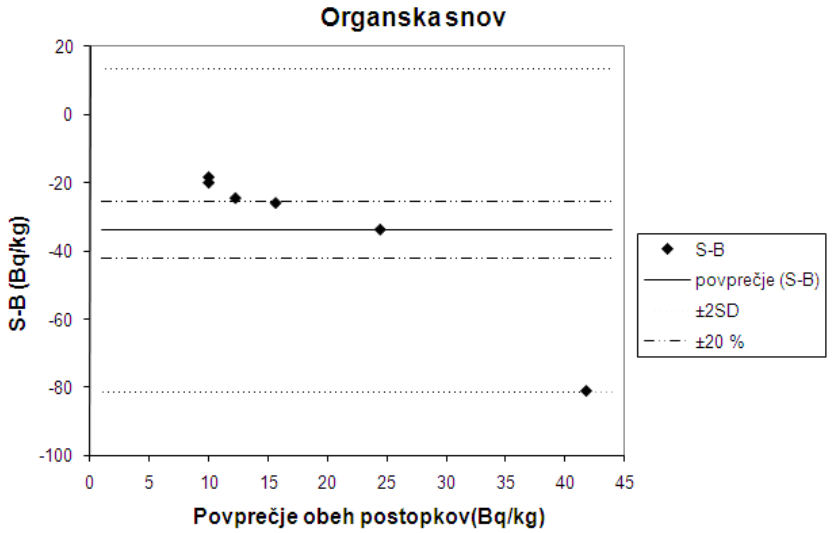

Slika 48: *Primerjava razlik posameznih meritev v odvisnosti od povprečnih vrednosti meritev obeh postopkov za ^{210}Pb za organsko frakcijo.*

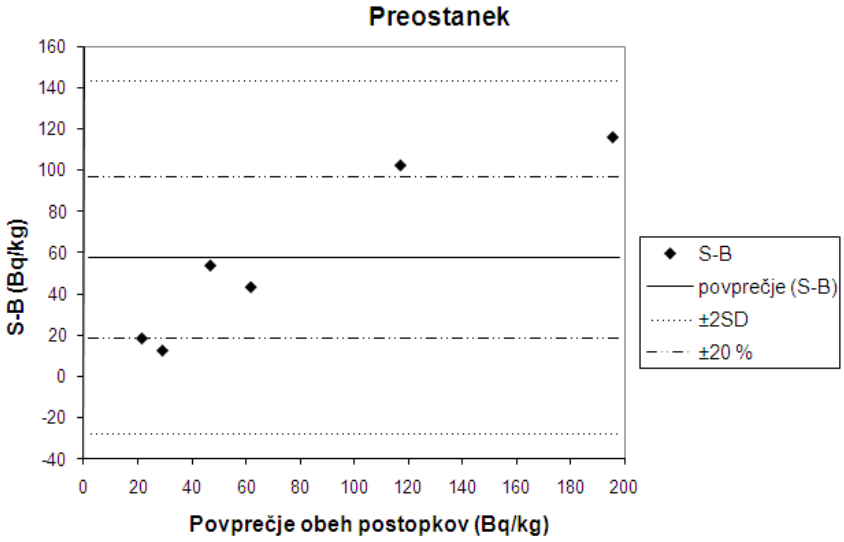

Slika 49: *Primerjava razlik posameznih meritev v odvisnosti od povprečnih vrednosti meritev obeh postopkov za ^{210}Pb za preostanek.*

Na slikah 50 – 53 so prikazani rezultati primerljivosti obeh postopkov za ^{210}Po. Ugotovil sem, da postopek S daje višje vrednosti v primeru karbonatne frakcije, postopek B pa pri vseh ostalih frakcijah. Prav tako sem ugotovil, da so dvakratniki standardnega odmika pri vseh frakcijah večji od 20 %, kar pomeni, da dajeta postopka statistično različne rezultate.

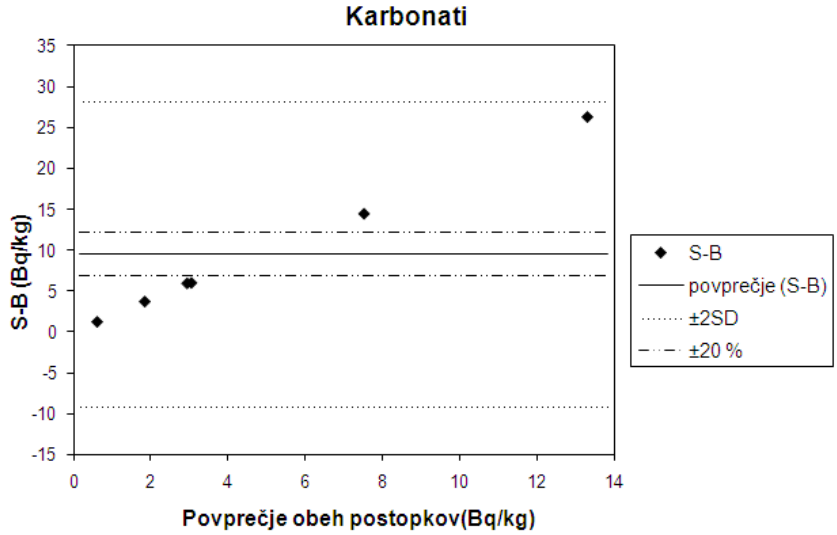

Slika 50: *Primerjava razlik posameznih meritev v odvisnosti od povprečnih vrednosti meritev obeh postopkov za ^{210}Po za karbonatno frakcijo.*

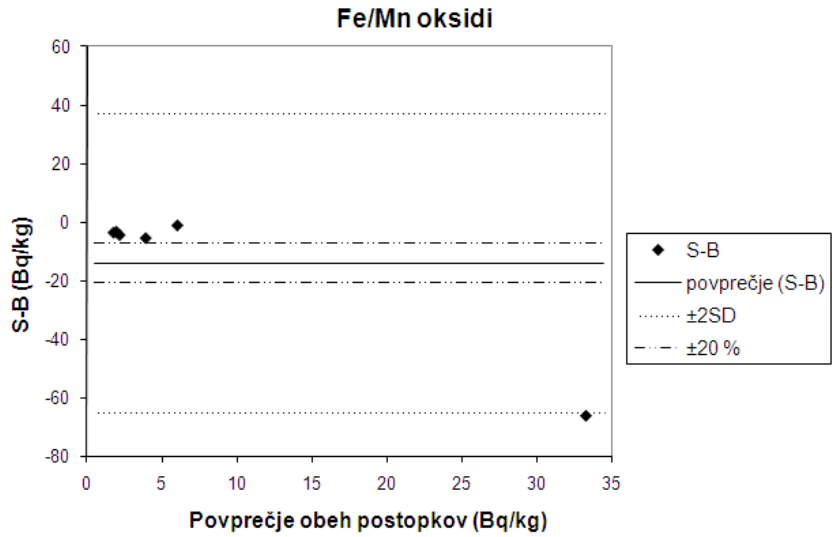

Slika 51: *Primerjava razlik posameznih meritev v odvisnosti od povprečnih vrednosti meritev obeh postopkov za ^{210}Po za Fe/Mn oksidno frakcijo.*

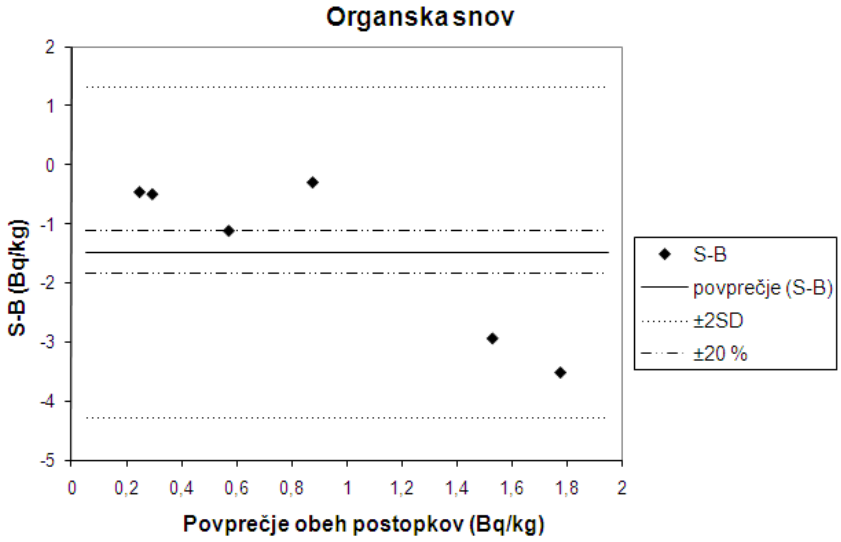

Slika 52: *Primerjava razlik posameznih meritev v odvisnosti od povprečnih vrednosti meritev obeh postopkov za ^{210}Po za organsko frakcijo.*

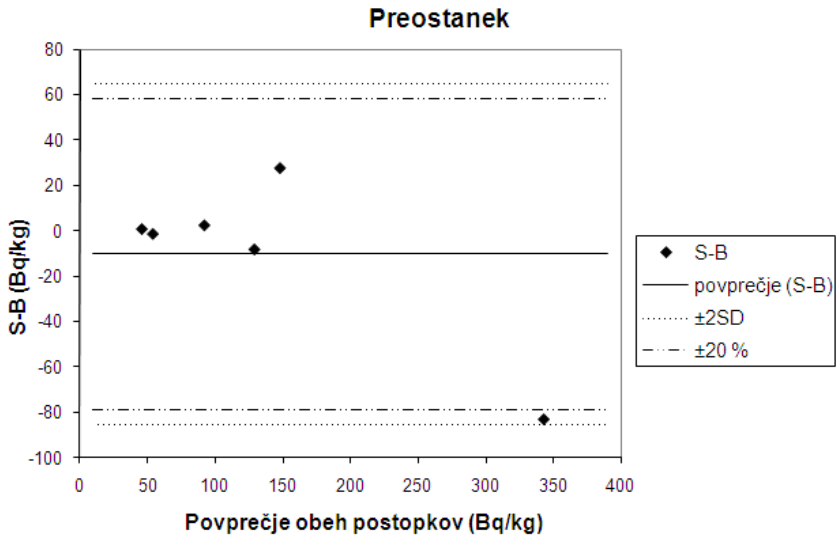

Slika 53: *Primerjava razlik posameznih meritev v odvisnosti od povprečnih vrednosti meritev obeh postopkov za ^{210}Po za preostanek.*

V tabeli 5 so še enkrat povzeti in numerično prikazani rezultati primerjave obeh postopkov. Prva kolona prikazuje radionuklide, druga posamezne frakcije, v tretji so predstavljeni rezultati povprečnih vrednosti razlik med obema postopkoma, četrta pa prikazuje dvakratnik standardnega odmika razlik med obema postopkoma. V peti so prikazane maksimalne vrednosti povprečij med obema postopkoma, ki so potrebne za izračun relativnih vrednosti dvakratnika standardnega odmika; le te so predstavljene v šesti koloni. V primeru, da znašajo te razlike manj od 20 % pomeni, da sta po izbranih kriterijih postopka statistično primerljiva, v nasprotnem primeru pa ne. Tako lahko povzamem, da dajeta postopka, razen v primeru ^{238}U za organsko snov in preostanek, statistično različne rezultate.

Tabela 5: *Rezultati statistične ocene ujemanja obeh sekvenčnih ekstrakcijskih postopkov.*

Radionuklid	Frakcija	povpr (S-B) [Bq/kg]	2SD [Bq/kg]	Maks (povpr (S,B)) [Bq/kg]	2SD/ max(S, B) [%]	Ujemanje
^{238}U	Karbonati	25,7	54,9	82,0	67	NE
	Fe/Mn oksidi	-56,2	138	86,7	159	NE
	Organska snov	21,6	68,9	367	19	DA
	Preostanek	-13,6	18,5	116	16	DA
^{230}Th	Karbonati	40,0	55,5	41,9	132	NE
	Fe/Mn oksidi	-1,7	6,7	9,9	68	NE
	Organska snov	-20,4	50,1	42,9	117	NE
	Preostanek	8,9	99,3	418	24	NE
^{226}Ra	Karbonati	50,8	133	149	89	NE
	Fe/Mn oksidi	-126	335	277	121	NE
	Organska snov	15,0	53,9	130	42	NE
	Preostanek	60,7	120	322	37	NE
^{210}Pb	Karbonati	49,2	92,5	86,0	107	NE
	Fe/Mn oksidi	-90,5	145	154	94	NE
	Organska snov	-33,9	47,4	41,8	113	NE
	Preostanek	57,7	85,6	196	44	NE
^{210}Po	Karbonati	9,5	18,6	13,3	140	NE
	Fe/Mn oksidi	-13,9	51,2	33,3	154	NE
	Organska snov	-1,5	2,8	1,8	157	NE
	Preostanek	-10,4	75,1	343	22	NE

Pri pregledu vseh rezultatov primerjave postopkov (slike 34 – 53) sem ugotovil, da daje postopek S pri vseh radionuklidih višje rezultate za karbonatno frakcijo od postopka B, ki pa daje v pri vseh radionuklidih višje rezultate za Fe/Mn okside.

Iz slik 34 – 53 smo se lahko prepričali, da dajeta oba postopka v večini primerov statistično različne rezultate. Vendar pa sem lahko iz njih kljub temu marsikaj zanimivega zaključil. Tako slike 54 – 63 ter priloge 2 – 5 prikazujejo rezultate obeh postopkov v šestih vzorčevalnih lokacijah. Rezultati za posamezen radionuklid so na slikah 54 – 63 predstavljeni v dveh grafih, od katerih prvi prikazuje deleže posamezne frakcije v celotni aktivnosti, drugi pa celotne aktivnosti posamezne frakcije. Zaradi večje preglednosti, negotovosti meritev pri posameznih frakcijah niso prikazane. Tako sem lahko za ^{238}U ugotovil (sliki 54 in 55), da je bila najvišja celotna specifična aktivnost, definirana kot vsota vseh frakcij, v lokaciji 4, ki leži na dnu odlagališča v smeri spiranja radionuklidov. Povišane celotne specifične aktivnosti v primerjavi z lokacijo 3, ki ni pod vplivom odlagališča, sem opazil še v primeru lokacije 6 in 1. Kljub temu, da oba sekvenčna ekstrakcijska postopka dajeta različne rezultate za karbonatno frakcijo in Fe/Mn okside, pa sem lahko iz slike 54 ugotovil, da je porazdelitveni profil med lokacijami 1, 4 in 6 podoben. Prav tako sem lahko ugotovil podobnosti med lokacijami 2, 3 in 5. V primeru lokacij 1, 4 in 6 je prevladujoča frakcija ^{238}U v primeru postopka S vezana na organsko snov (od 40 do 60 %), v primeru lokacij 2, 3 in 5 pa se ^{238}U nahaja pretežno v preostanku (od 70 do 90 %).

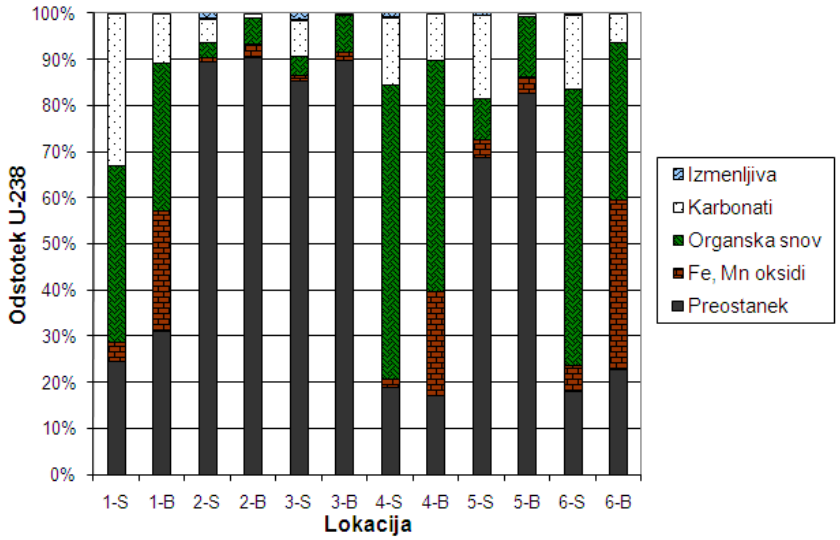

Slika 54: *Porazdelitveni profili ^{238}U v vzorcih zemelj po lokacijah in posameznih sekvenčnih ekstrakcijskih postopkih.*

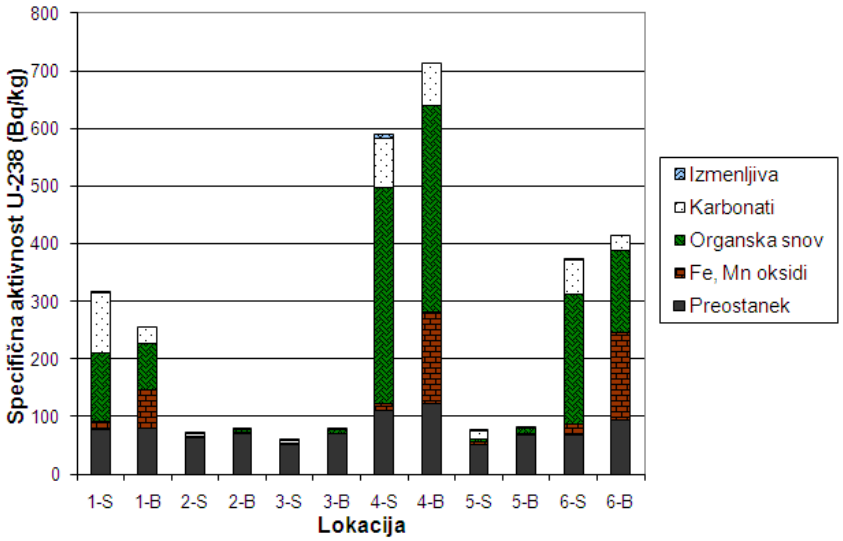

Slika 55: *Specifične aktivnosti ^{238}U v vzorcih zemelj po lokacijah in sekvenčnih ekstrakcijskih postopkih.*

Podobno so prikazani tudi rezultati za ^{230}Th na slikah 56 in 57, kjer ponovno ugotavljam najvišjo celotno specifično aktivnost v vzorcu iz lokacije 4. Povišane celotne specifične aktivnosti v primerjavi z lokacijo 3 je v primeru ^{230}Th zaznati še v lokacijah 5 in 6, postopek S pa daje tudi nekoliko višje specifične aktivnosti tudi v vzorcu iz lokacije 1. Porazdelitveni profil lokacij na sliki 56 pokaže, da je v vseh lokacijah največ ^{230}Th v preostanku (od 50 do 86 %).

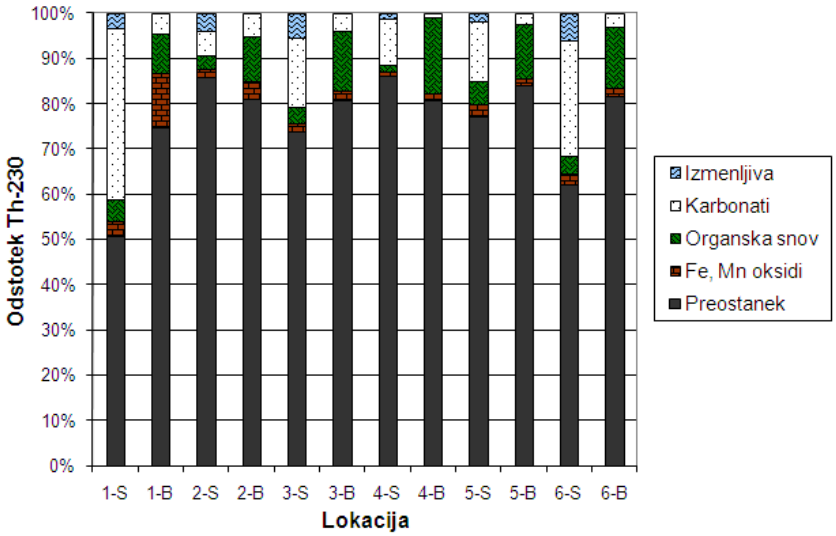

Slika 56: *Porazdelitveni profili ^{230}Th v vzorcih zemelj po lokacijah in posameznih sekvenčnih ekstrakcijskih postopkih.*

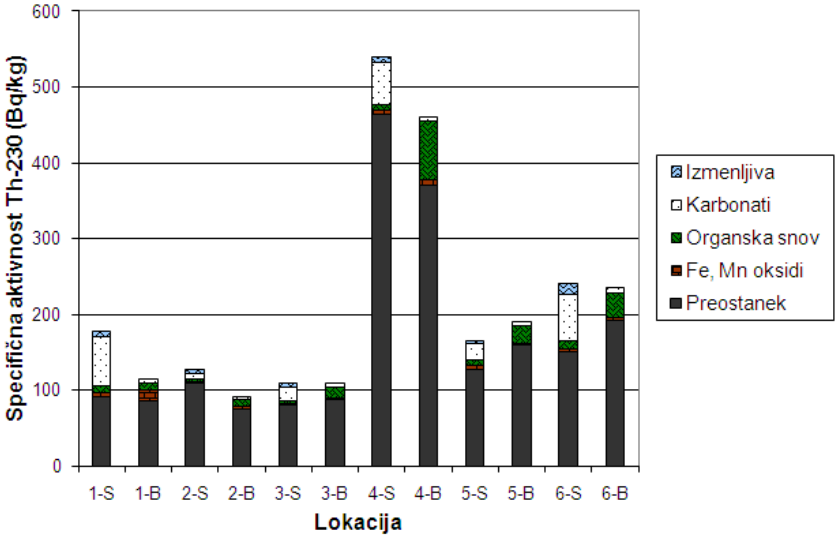

Slika 57: *Specifične aktivnosti ^{230}Th v vzorcih zemelj po lokacijah in sekvenčnih ekstrakcijskih postopkih.*

Tudi v primeru ^{226}Ra sem najvišjo celotno specifično aktivnost ugotovil v lokaciji 4 (slika 59), povišane celotne specifične aktivnosti v primerjavi z lokacijo 3 pa sem ugotovil tudi v lokacijah 5 in 6. Vrednosti celotnih specifičnih aktivnosti v lokacijah 1 in 2 pa so primerljive z lokacijo 3. Pri primerjavi porazdelitvenih profilov na sliki 58 sem opazil, da je v lokacijah 1, 2 in 3 več ^{226}Ra v preostanku (od 60 do 80 %), kot pa v lokacijah 4, 5 in 6 (30 do 60 %).

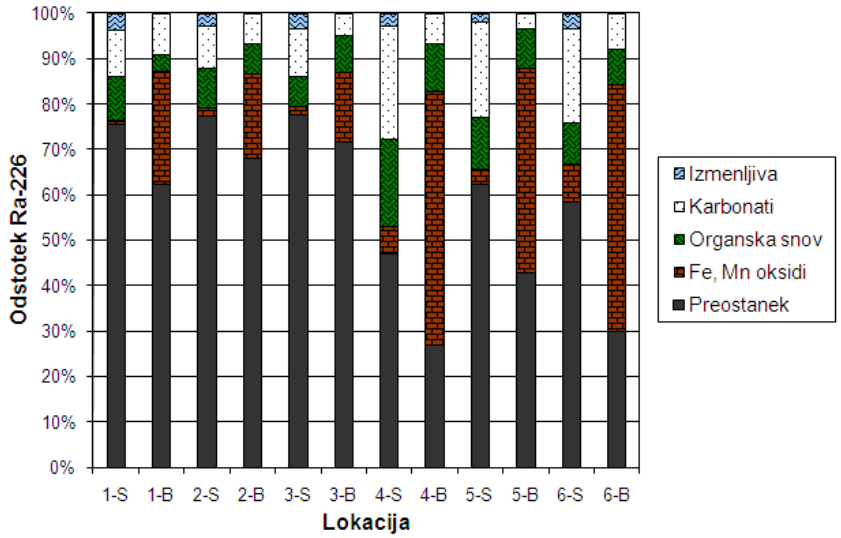

Slika 58: *Porazdelitveni profili ^{226}Ra v vzorcih zemelj po lokacijah in posameznih sekvenčnih ekstrakcijskih postopkih.*

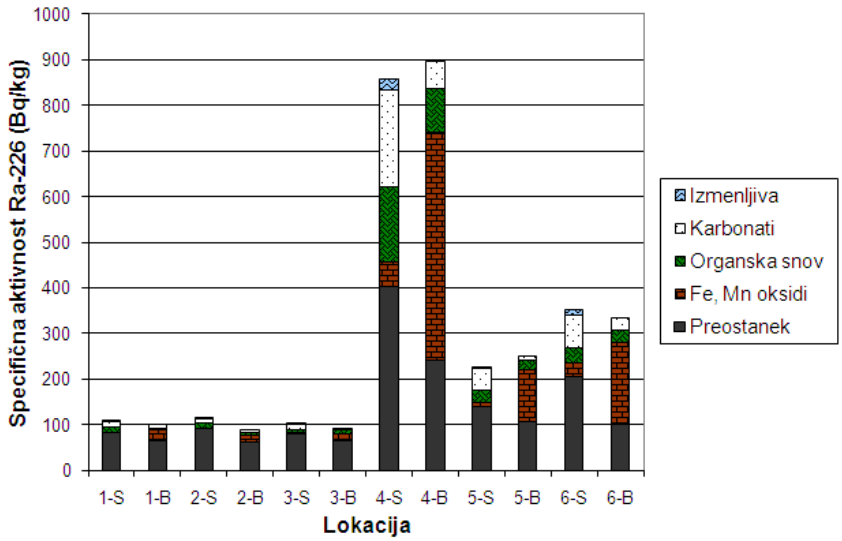

Slika 59: *Sspecifične aktivnosti ^{226}Ra v vzorcih zemelj po lokacijah in sekvenčnih ekstrakcijskih postopkih.*

Sliki 60 in 61 prikazujeta rezultate obeh sekvenčnih ekstrakcijskih postopkov za ^{210}Pb, kjer sem prav tako ugotovil, da je najvišja vsebnost celotne specifične aktivnosti ^{210}Pb v lokaciji 4. Povišane celotne specifične aktivnosti v primerjavi z lokacijo 3, je zaznati tudi v lokacijah 1, 5 in 6. Rezultati porazdelitvenih profilov v primeru ^{210}Pb (slika 60) pa so kontradiktorni. Pri postopku S je namreč prevladujoča frakcija, v kateri se nahaja ^{210}Pb, preostanek (od 55 do 70 %), pri postopku B, pa Fe/Mn oksidi (od 40 do 60 %).

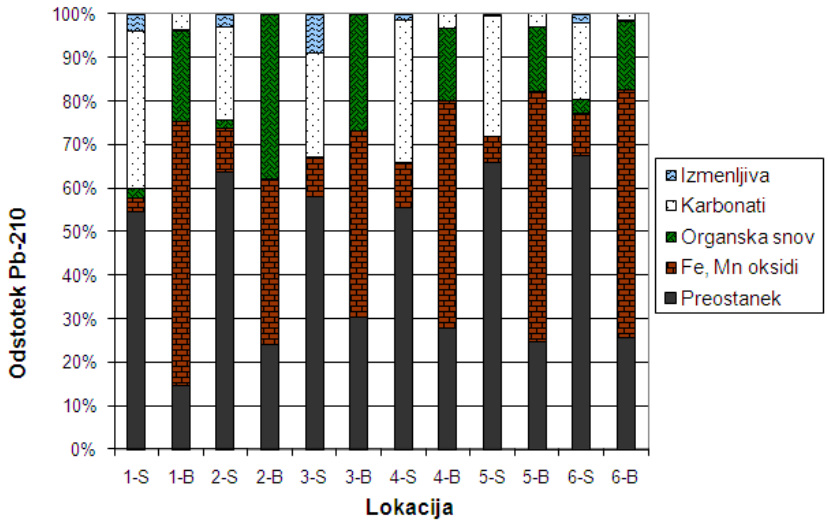

Slika 60: *Porazdelitveni profili ^{210}Pb v vzorcih zemelj po lokacijah in posameznih sekvenčnih ekstrakcijskih postopkih.*

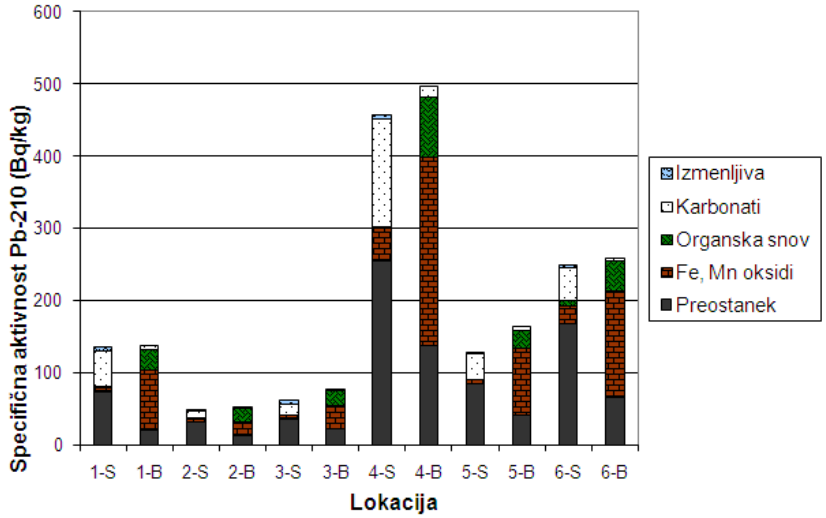

Slika 61: *Specifične aktivnosti ^{210}Pb v vzorcih zemelj po lokacijah in sekvenčnih ekstrakcijskih postopkih.*

Rezultate sekvenčnih ekstrakcijskih postopkov za ^{210}Po prikazujeta sliki 62 in 63. Ker so bile izvedene analize ^{210}Po približno tri leta po vzorčenju, so celotne specifične aktivnosti ^{210}Po v trajnem radioaktivnem ravnotežju s ^{210}Pb. Zato rezultatov celotnih specifičnih aktivnosti v sliki 63 ni mogoče povezati z dejanskim stanjem ^{210}Po ob času vzorčenja. Kljub temu pa ugotavljam, da so porazdelitveni profili v primeru ^{210}Po (slika 62) drugačni kot v primeru ^{210}Pb (slika 60). Tako se v primeru ^{210}Po le ta nahaja pretežno v preostanku (od 70 do 98 %).

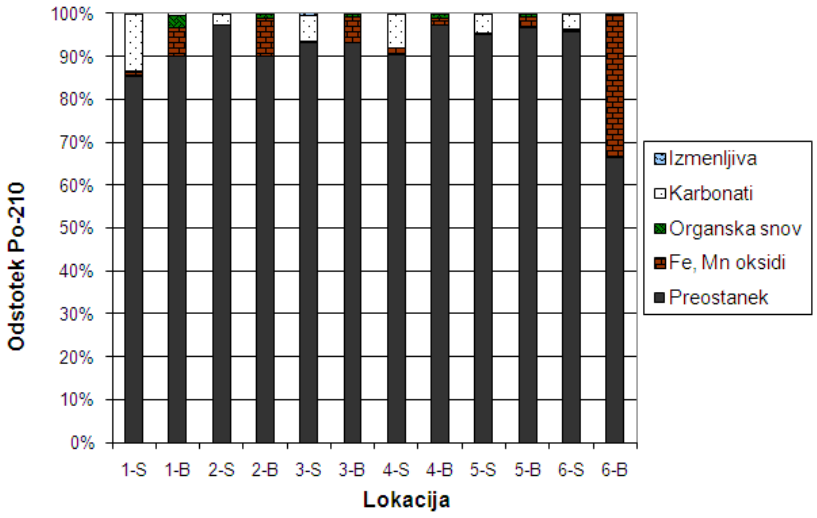

Slika 62: *Porazdelitveni profili ^{210}Po v vzorcih zemelj po lokacijah in posameznih sekvenčnih ekstrakcijskih postopkih.*

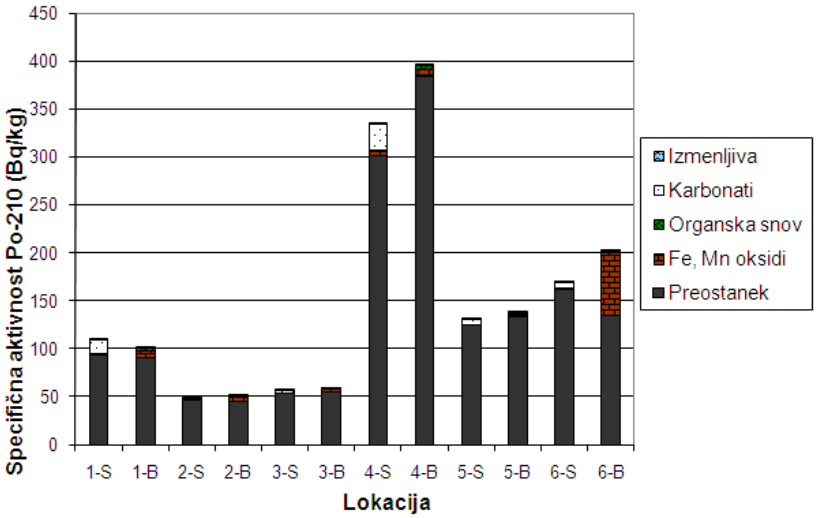

Slika 63: *Specifične aktivnosti ^{210}Po v vzorcih zemelj po lokacijah in sekvenčnih ekstrakcijskih postopkih.*

Ob pregledu skupnih značilnosti vseh obravnavanih radionuklidov ugotavljam, da je bila v vseh primerih celotna specifična aktivnost najvišja v lokaciji 4. Skupne značilnosti vseh radionuklidov so tudi povišane celotne specifične aktivnosti v lokaciji 6 v primerjavi z lokacijo 3 ter primerljive celotne specifične aktivnosti v vzorcih iz lokacije 2. V primeru ^{230}Th, ^{226}Ra in ^{210}Pb sem zaznal tudi povišane celotne specifične aktivnosti v lokaciji 5, ter v primeru ^{238}U, ^{226}Ra in ^{210}Pb v lokaciji 1.

4.3 Izotopsko razmerje ^{234}U/^{238}U

Rezultate izotopskega razmerja ^{234}U/^{238}U prikazuje slika 64. Graf prikazuje izotopsko razmerje ^{234}U/^{238}U za mobilne frakcije in za preostanek iz sekvenčne ekstrakcije s

postopkom S. V mobilni frakciji so združeni rezultati sekvenčne ekstrakcije s postopkom S za izmenljivo frakcijo, karbonatno frakcijo, organsko snov in Fe/Mn okside. Razvidno je, da je izotopsko razmerje večje od 1 v primeru mobilnih frakcij v lokacijah 2 in 3, pri ostalih lokacijah pa je izotopsko razmerje enako 1. Pri preostanku je razvidno nižje izotopsko razmerje od 1 v lokacijah 1, 2 in 3 ter enako 1 v lokacijah 4, 5 in 6.

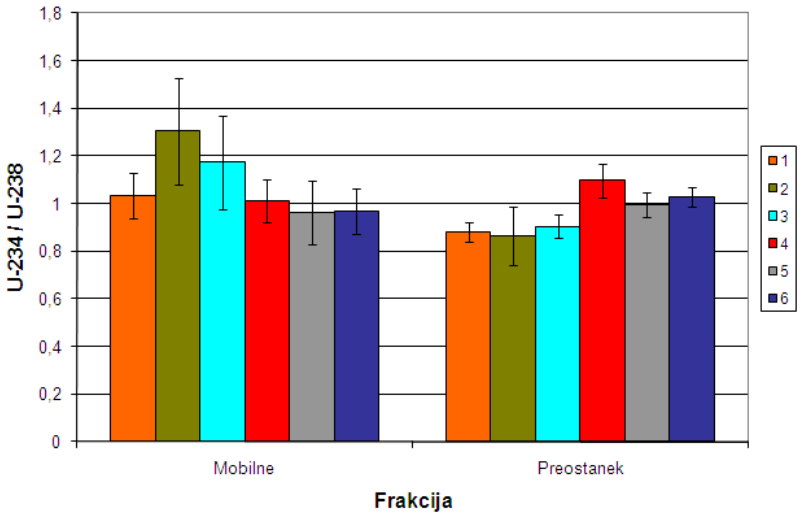

Slika 64: *Izotopska razmerija* $^{234}U/^{238}U$.

4.4 Vsebnosti naravnih radionuklidov v travah

Faktorje prenosa iz tal v travo, ki predstavljajo razmerje med specifično aktivnostjo posameznega radionuklida v travi in specifično aktivnostjo v tleh, kakor tudi vsebnosti ^{238}U, ^{230}Th, ^{226}Ra in ^{210}Pb v travi in v tleh prikazujejo slike 65 – 72 ter priloge 6-8. Kemijski izkoristki separacij so znašali od 55 do 86 % za ^{238}U, od 68 do 90 % za ^{230}Th, od 43 do 66 % za ^{226}Ra in od 55 do 62 % za ^{210}Pb. Rezultati za posamezni radionuklid so predstavljeni v dveh grafih, od katerih prvi prikazuje faktorje prenosa iz tal v travo v odvisnosti od specifične aktivnosti v tleh, drugi pa specifično aktivnost v travi v odvisnosti od specifične aktivnosti v tleh. Številke ob posamezni točki označujejo vzorčevalne lokacije, ki so predstavljene na sliki 4. Negotovosti so podane kot kombinirane standardne negotovosti s faktorjem pokritja $k = 1$. V primerih, ko negotovost na grafu ni vidna, je manjša od simbola. Rezultati za ^{210}Po niso vključeni, saj je ob času analize preteklo približno tri leta od časa vzorčenja. To pomeni, da sta ^{210}Po in ^{210}Pb v trajnem radioaktivnem ravnotežju in ni več mogoče razločiti med njima, saj sta njuni specifični aktivnosti v vzorcih enaki.

Slika 65 prikazuje faktorje prenosa iz tal v travo za ^{238}U. Iz nje je razvidno, da sta faktorja prenosa v vzorcih iz lokacij 1 in 2 približno 7 krat večja kot pri ostalih lokacijah, v katerih so faktorji prenosa približno enaki, čeprav je specifična aktivnost v tleh zelo različna. Na sliki 66 so predstavljene vrednosti specifične aktivnosti ^{238}U v travah v odvisnosti od specifičnih aktivnosti v tleh. Iz te slike so spet razvidne večje specifične aktivnosti v travi v vzorcih iz lokacij 1 in 2, ter mnogo nižje v ostalih lokacijah, ki so v linearni korelaciji s specifičnimi aktivnostmi v tleh.

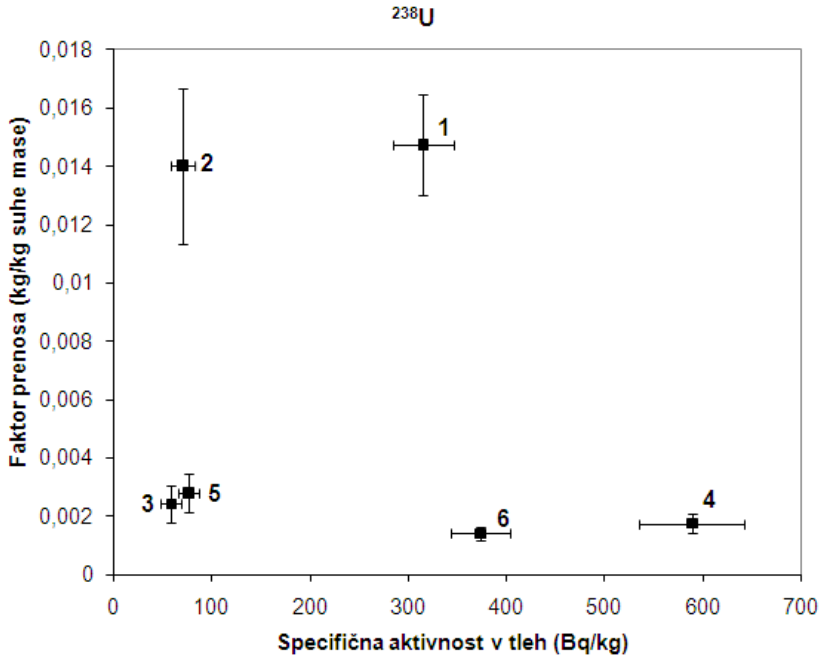

Slika 65: *Faktorji prenosa ^{238}U v odvisnosti od specifične aktivnosti ^{238}U v tleh.*

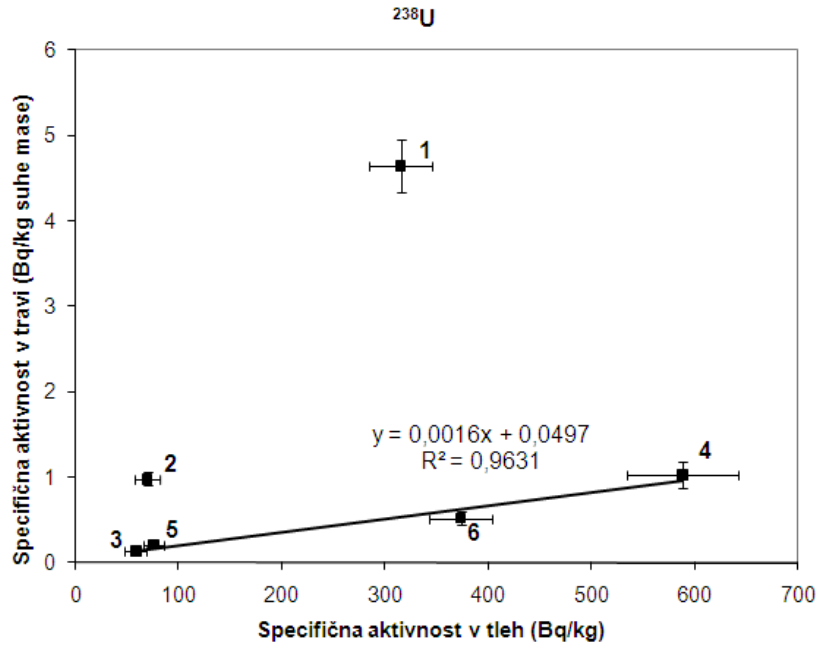

Slika 66: *Specifične aktivnosti ^{238}U v travi v odvisnosti od specifične aktivnosti ^{238}U v tleh.*

Podobno so predstavljeni tudi rezultati za ^{230}Th, kjer na sliki 67 vidimo upad faktorjev prenosa iz tal v travo s povečanjem specifične aktivnosti v tleh. Na sliki 68, kjer so predstavljene vrednosti specifične aktivnosti ^{230}Th v travah v odvisnosti od specifičnih aktivnosti v tleh pa vidimo, da le te med seboj niso korelirane.

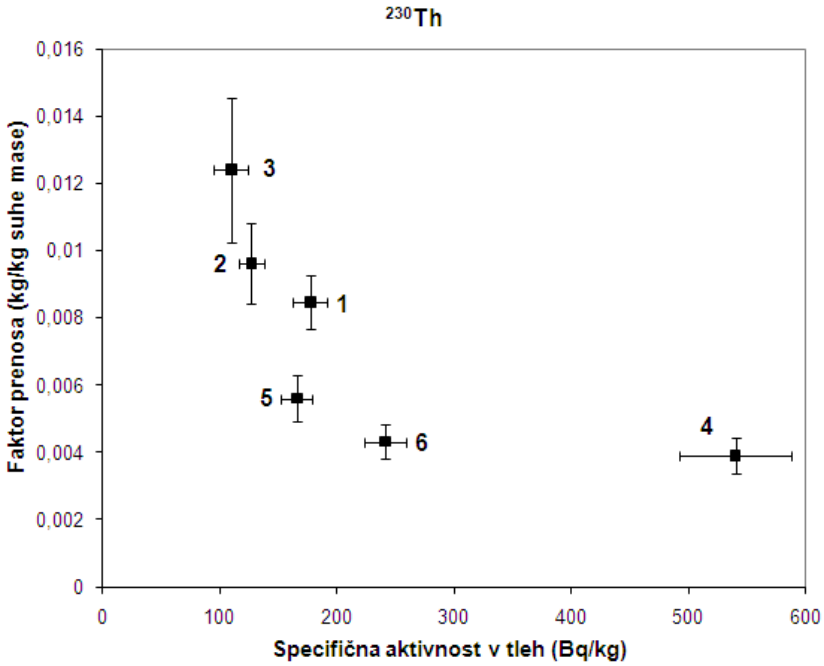

Slika 67: *Faktorji prenosa ^{230}Th v odvisnosti od specifične aktivnosti ^{230}Th v tleh.*

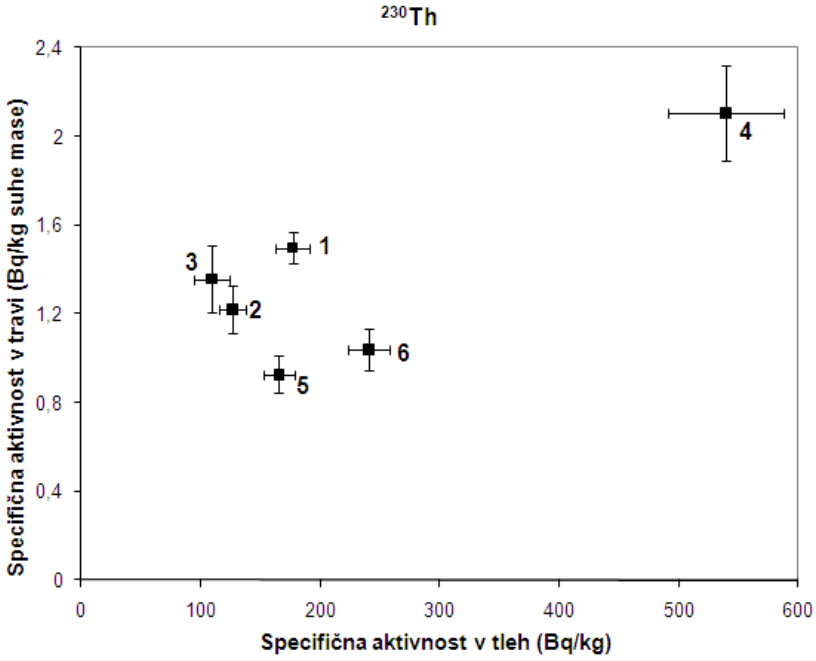

Slika 68: *Specifične aktivnosti ^{230}Th v travi v odvisnosti od specifične aktivnosti ^{230}Th v tleh.*

Rezultate za faktorje prenosa iz tal v travo za ^{226}Ra prikazuje slika 69, kjer sem opazil mnogo nižje faktorje prenosa za lokacije 1, 2 in 3 v primerjavi z ostalimi. Rezultati na sliki 70 prikazujejo linearno korelacijo specifičnih aktivnosti v travi in tleh za lokacije 4, 5 in 6, ter mnogo nižje vrednosti za ostale tri lokacije.

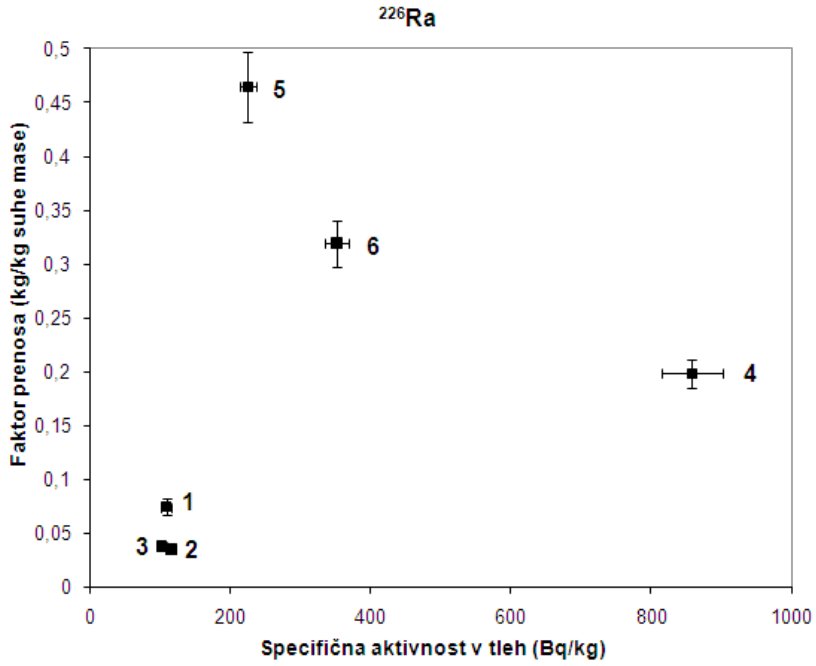

Slika 69: *Faktorji prenosa ^{226}Ra v odvisnosti od specifične aktivnosti ^{226}Ra v tleh.*

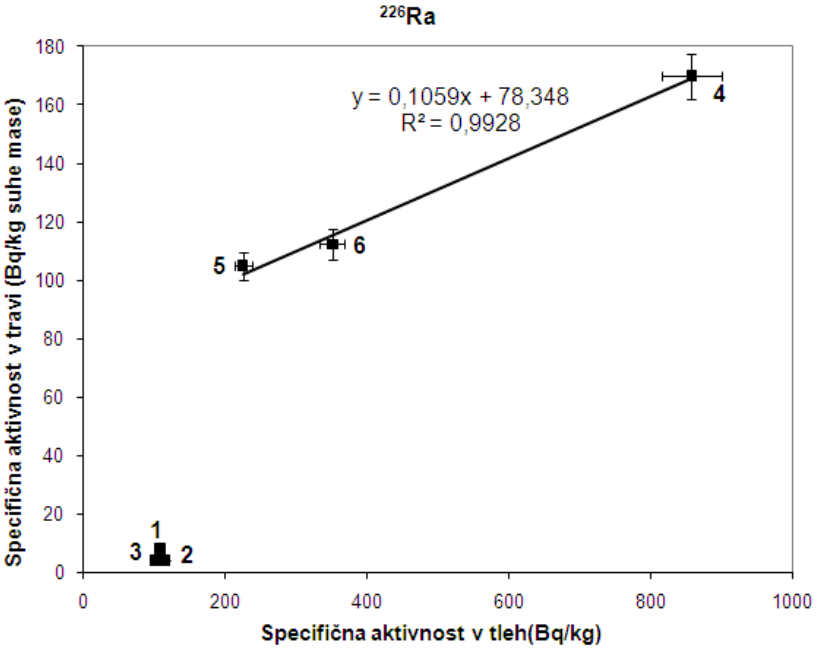

Slika 70: *Specifične aktivnosti ^{226}Ra v travi v odvisnosti od specifične aktivnosti ^{226}Ra v tleh.*

Podobno kot v primeru ^{230}Th, tudi v primeru ^{210}Pb faktorji prenosa iz tal v travo padajo z naraščajočo specifično aktivnostjo ^{210}Pb v tleh, kar prikazuje slika 71. Specifične aktivnosti ^{210}Pb v travi in tleh pa niso korelirane (slika 72).

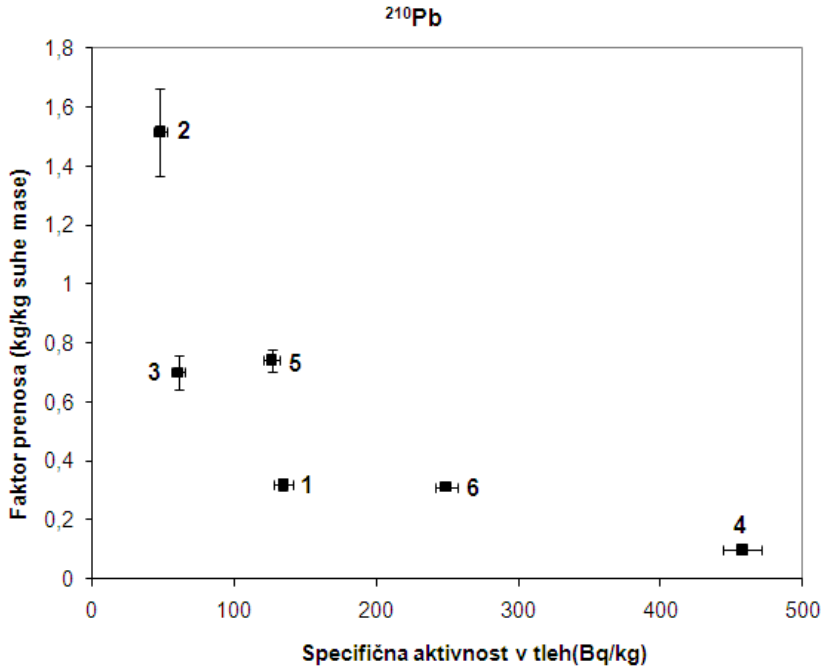

Slika 71: *Faktorji prenosa ^{210}Pb v odvisnosti od specifične aktivnosti ^{210}Pb v tleh.*

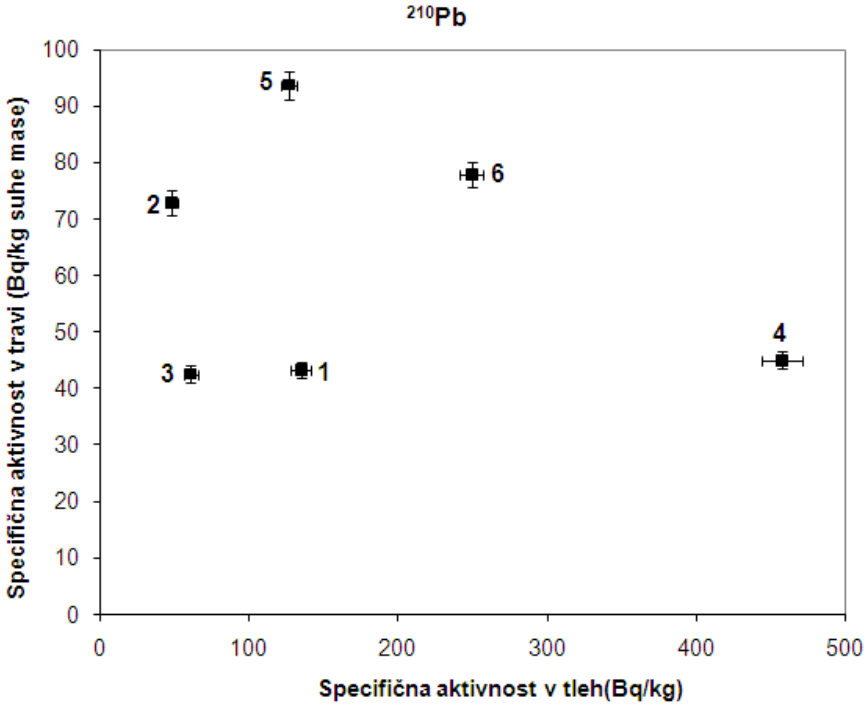

Slika 72: *Specifične aktivnosti ^{210}Pb v travi v odvisnosti od specifične aktivnosti ^{210}Pb v tleh.*

Faktorji prenosa iz tal v travo so znašali od 1,40E-3 do 1,47E-2 za ^{238}U, od 3,90E-3 do 1,24E-2 za ^{230}Th, od 3,46E-2 do 4,65E-1 za ^{226}Ra in od 9,83E-2 do 1,52E+0 za ^{210}Pb. Ugotovljeni faktorji prenosa so v glavnem primerljivi z objavljenimi rezultati iz literature, kjer znašajo od 3,07E-4 do 4,56E-1 za ^{238}U, od 7,40E-4 do 6,52E-1 za ^{230}Th, od 9,63E-2 do 7,19E-1 za ^{226}Ra in od 2,23E-3 do 1,00E+0 za ^{210}Pb (Vandenhove et al., 2009).

4.5 Vsebnosti naravnih radionuklidov v drevesih

Vsebnosti ^{238}U, ^{230}Th, ^{226}Ra in ^{210}Pb v borih, smrekah in javorju so predstavljene na slikah 73 – 84 ter v prilogah 9 in 10. Kemijski izkoristki separacije so znašali od 50 do 90 % za ^{238}U, od 69 do 100 % za ^{230}Th, od 35 do 59 % za ^{226}Ra in od 55 do 100 % za ^{210}Pb. Pri borih in smrekah so rezultati na slikah 73 – 84 predstavljeni v obliki »box plot« diagramov, v primeru javorja pa to ni bilo možno saj je na odlagališču Boršt raslo le eno takšno drevo. Tako so pri javorju rezultati podani za eno drevo skupaj s kombinirano standardno negotovostjo s faktorjem pokritja $k = 1$. »Box plot« diagrami pa prikazujejo maksimalno in minimalno vrednost, zgornji in spodnji kvartil ter mediano. Podobno kot pri vzorcih trav sem tudi v primeru dreves analize vzorcev izvedel približno tri leta po vzorčenju, zato določitev specifične aktivnosti ^{210}Po ni bila več možna.

Rezultati za ^{238}U so prikazani na slikah 73 – 75, pri katerih prvi prikazuje rezultate za vzorce lesa, drugi za vzorce poganjkov in tretji za enoletne iglice ali liste. Ugotovil sem, da so specifične aktivnosti ^{238}U v enoletnih iglicah ali listih največje, tem sledijo specifične aktivnosti v poganjkih, najmanjše pa so vrednosti v lesu. Z namenom ugotovitve ali so razlike med posameznimi deli dreves tudi statistično relevantne sem uporabil Kruskal-Wallisov ANOVA test, ki se uporablja v primerih, ko so variance heterogene. Omenjeni test je pokazal, da so rezultati za vsebnosti ^{238}U v enoletnih iglicah ali listih, poganjkih in lesu statistično različne ($P_{\text{U-238}} < 0{,}0001$). Največje maksimalne specifične aktivnosti ^{238}U v lesu in enoletnih iglicah ali listih so bile določene pri boru, temu je sledil javor in smreka. Pri poganjkih pa sem največje maksimalne specifične aktivnosti ^{238}U ugotovil pri javorju, zatem pa pri smreki in pri boru. Z namenom ugotovitve statističnih razlik med bori in smrekami sem uporabil Studentov t test, ki je pri ^{238}U pokazal, da so rezultati za omenjeni vrsti dreves v primeru poganjkov ter enoletnih iglic in listov statistično različni pri 95 % zaupanju, v primeru lesa pa pri 96 % zaupanju (tabela 6).

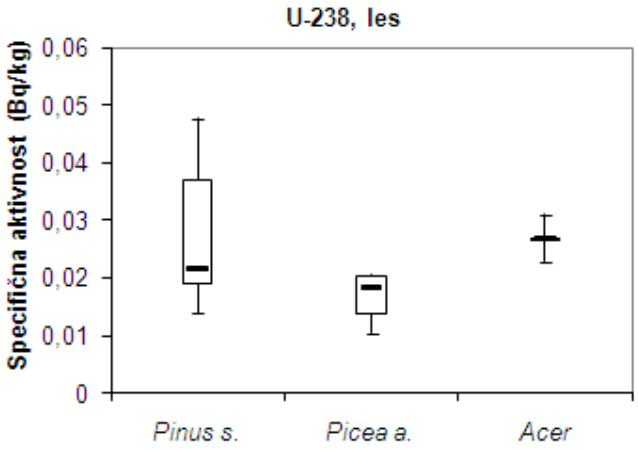

Slika 73: *Specifične aktivnosti ^{238}U v lesu.*

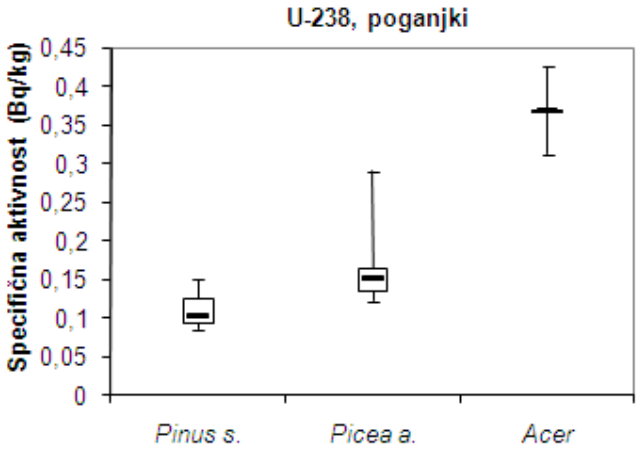

Slika 74: *Specifične aktivnosti ^{238}U v poganjkih.*

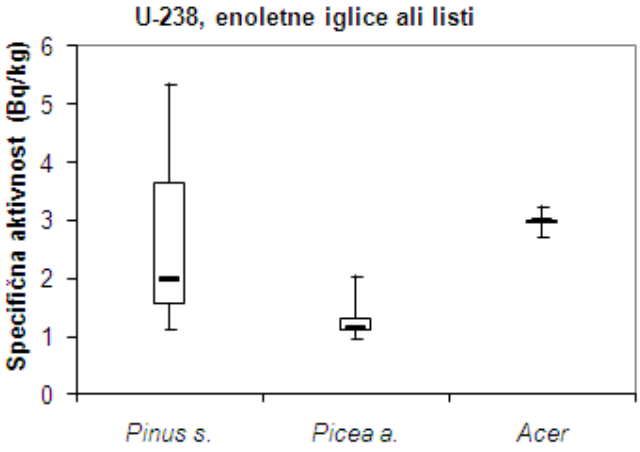

Slika 75: *Specifične aktivnosti ^{238}U v enoletnih iglicah ali listih.*

Tabela 6: *Rezultati Studentovega t testa z verjetnostmi (P), da so rezultati med bori in smrekami enaki.*

Vrsta	*P* (les)	*P* (poganjki)	*P* (enoletne iglice ali listi)
^{238}U	0,0582	0,0360	0,0498
^{230}Th	0,0080	0,0982	0,1901
^{226}Ra	0,0171	0,0500	0,0315
^{210}Pb	0,1367	0,1330	0,0216

Podobno kot za ^{238}U, so na slikah 76 – 78 predstavljeni tudi rezultati za ^{230}Th, kjer sem največje specifične aktivnosti prav tako ugotovil v primeru enoletnih iglic ali listov, njim pa so sledili poganjki in les. Rezultati Kruskal-Wallisovega ANOVA testa so tudi pri ^{230}Th pokazali, da so vrednosti enoletnih iglic ali listov, poganjkov ter lesa statistično različne ($P_{Th\text{-}230} < 0{,}0001$). Največje maksimalne specifične aktivnosti ^{230}Th v lesu in enoletnih iglicah ali listih, sem določil pri smreki, njej pa sta sledila javor in bor. Pri

poganjkih sem največje maksimalne specifične aktivnosti ^{230}Th določil pri javorju, temu pa sta sledila smreka in bor. Rezultati Studentovega t testa za ^{230}Th v borih in smrekah so pokazali, da so pri 95 % zaupanju le pri lesu rezultati statistično različni med obema vrstama (tabela 6).

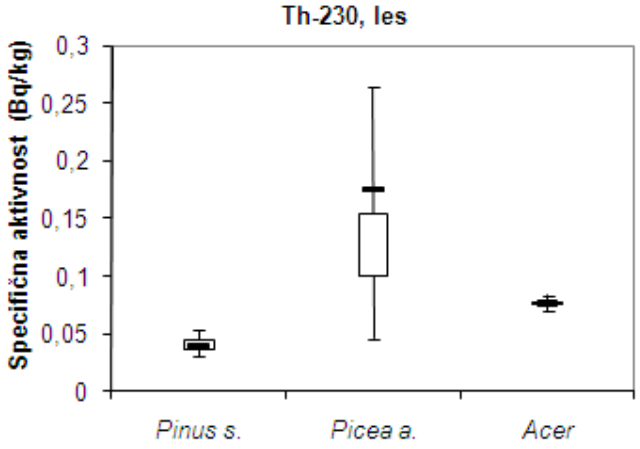

Slika 76: *Specifične aktivnosti ^{230}Th v lesu.*

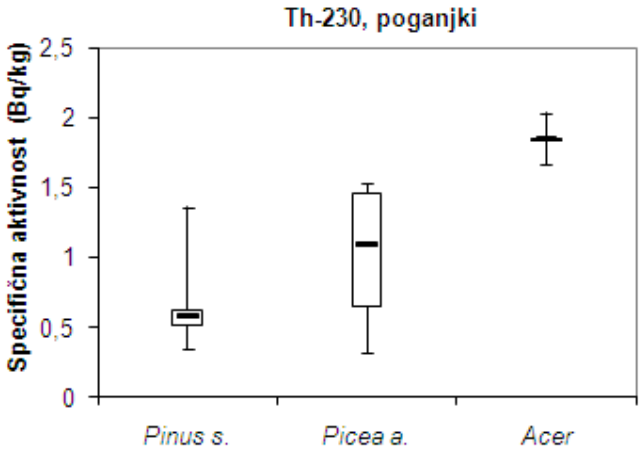

Slika 77: *Specifične aktivnosti ^{230}Th v poganjkih.*

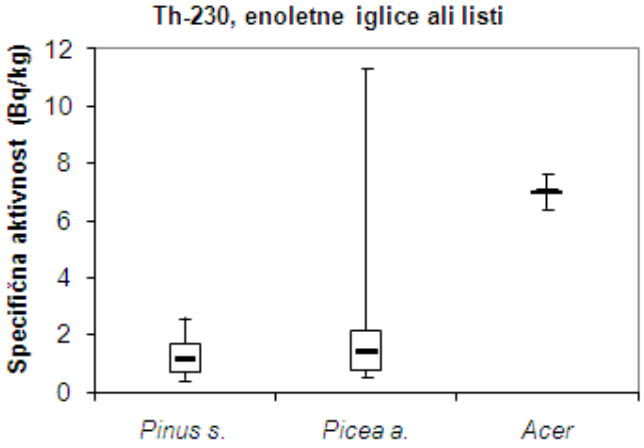

Slika 78: *Specifične aktivnosti ^{230}Th v enoletnih iglicah ali listih.*

Specifična aktivnost ^{226}Ra je bila prav tako največja pri enoletnih iglicah ali listih, zatem pa v poganjkih in v lesu (slike 79 – 81). Tudi tukaj so rezultati Kruskal-Wallisovega ANOVA testa pokazali, da so rezultati za ^{226}Ra v enoletnih iglicah ali listih, poganjkih in lesu statistično različni ($P_{Ra\text{-}226}$ = 0,026). V vseh delih rastlin sem največje maksimalne specifične aktivnosti ^{226}Ra določil pri smreki, njej pa sta sledila javor in bor. Zanimive so zelo majhne specifične aktivnosti ^{226}Ra pri boru v primerjavi s smreko, ki so bile za 62 krat manjše pri lesu, 101 krat manjše pri poganjkih in 42 krat manjše pri enoletnih iglicah. Rezultati Studentovega t testa so pri ^{226}Ra pokazali, da pri 95 % zaupanju obstajajo statistične razlike pri vseh treh vrstah vzorcev (tabela 6).

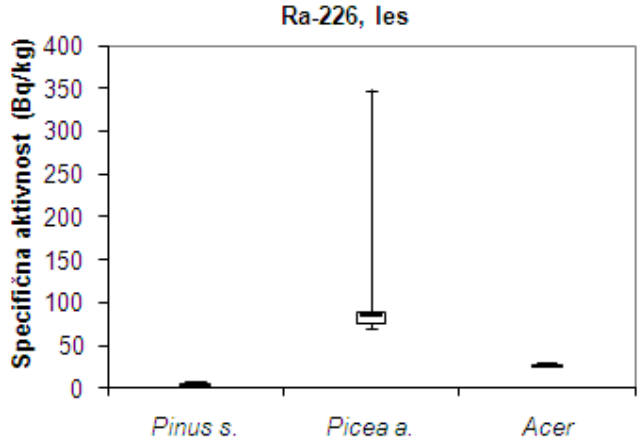

Slika 79: *Specifične aktivnosti ^{226}Ra v lesu.*

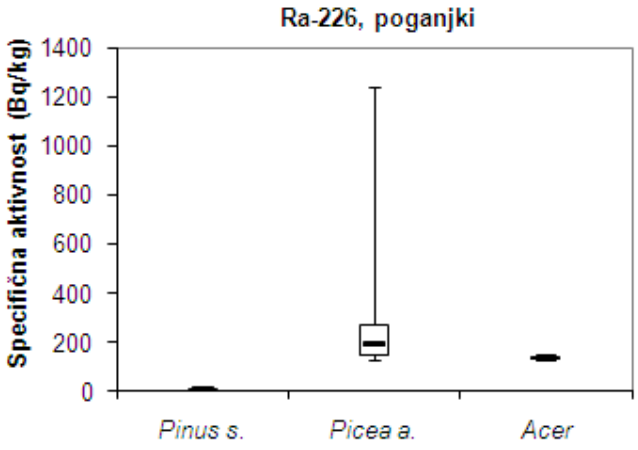

Slika 80: *Specifične aktivnosti ^{226}Ra v poganjkih.*

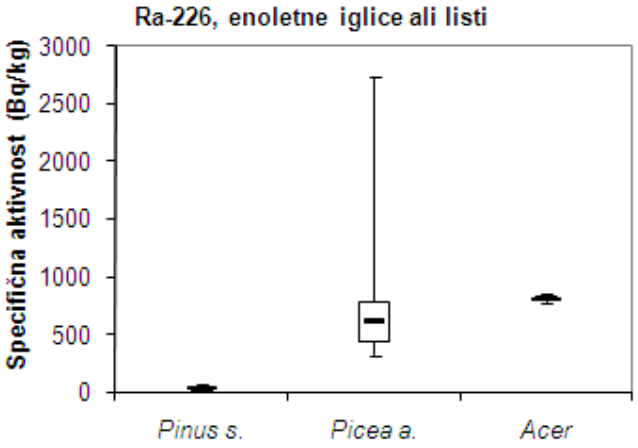

Slika 81: *Specifične aktivnosti ^{226}Ra v enoletnih iglicah ali listih.*

Tudi specifične aktivnosti ^{210}Pb so bile največje pri enoletnih iglicah ali listih, vendar pa so jim v primeru ^{210}Pb sledile specifične aktivnosti v lesu, najmanjše pa so bile v poganjkih (slike 82 – 84). Kruskal-Wallisov ANOVA test je tudi tukaj pokazal, da so rezultati za ^{210}Pb med enoletnimi iglicami ali listi, lesu in poganjkih statistično različne ($P_{\text{Pb-210}} < 0{,}0001$). Maksimalne specifične aktivnosti ^{210}Pb so bile največje v primeru poganjkov in enoletnih iglic ali listov pri smreki, njej pa sta sledila javor in bor. V lesu sem največje maksimalne specifične aktivnosti ^{210}Pb določil pri boru, temu pa sta sledila smreka in javor. Studentov t test je pokazal, da so pri ^{210}Pb med bori in smrekami ob 95 % zaupanju statistično različni le rezultati pri enoletnih iglicah ali listih (tabela 6).

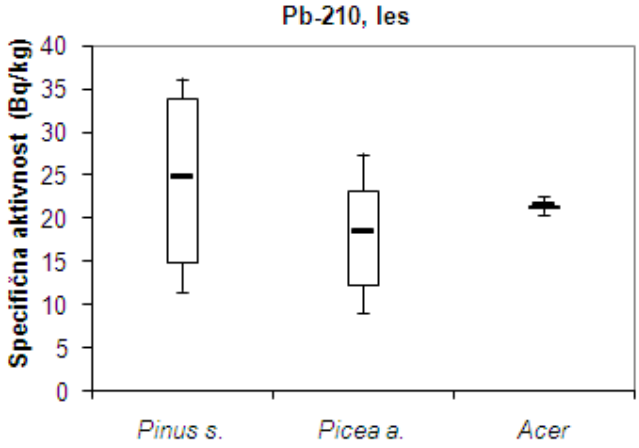

Slika 82: *Specifične aktivnosti ^{210}Pb v lesu.*

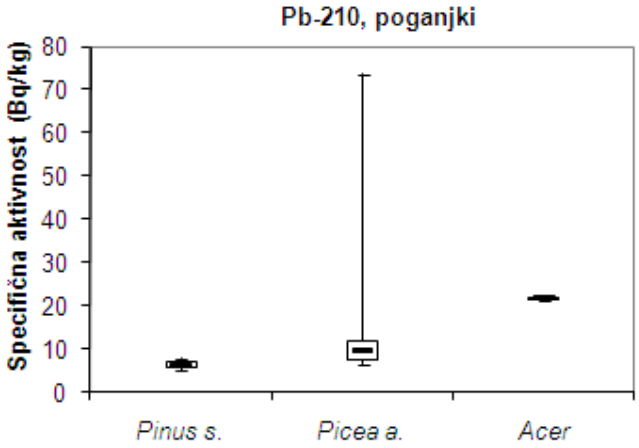

Slika 83: *Specifične aktivnosti ^{210}Pb v poganjkih.*

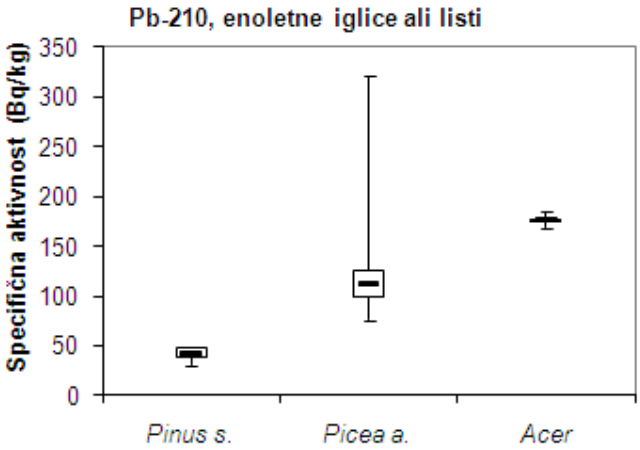

Slika 84: *Specifične aktivnosti ^{210}Pb v enoletnih iglicah ali listih.*

Pri pregledu slik 73 – 84 sem ugotovil, da so bile največje specifične aktivnosti v drevesih določene za ^{226}Ra (od 2,7 do 2728 Bq/kg), temu so sledili ^{210}Pb (od 5,1 do 321 Bq/kg), ^{230}Th (od 0,03 do 11,3 Bq/kg) in ^{228}U (od 0,01 do 5,4 Bq/kg).

V tabeli 7 so predstavljeni rezultati izračunov koncentracijskih razmerij med specifično aktivnostjo v HMJ in posameznimi deli dreves za ^{238}U, ^{230}Th, ^{226}Ra in ^{210}Pb. Pri borih in smrekah so podane minimalne in maksimalne vrednosti, kar pa ni bilo možno pri javorju, saj je bilo vzorčeno le eno drevo. Vrednosti specifičnih aktivnosti posameznih radionuklidov za HMJ, ki sem jih uporabil za preračun so bile (995 ± 80) Bq/kg za ^{238}U, (3930 ± 580) Bq/kg za ^{230}Th, (8630 ± 340) Bq/kg za ^{226}Ra (Križman et al., 1995) in (7610 ± 495) Bq/kg za ^{210}Pb. Največje vrednosti koncentracijskih razmerij sem določil za ^{226}Ra, temu pa so sledili ^{210}Pb, ^{238}U in ^{230}Th.

Tabela 7: *Koncentracijska razmerja (CR) za ^{238}U, ^{230}Th, ^{226}Ra in ^{210}Pb za drevesa Pinus sylvestris, Picea abies in Acer.*

Vrsta		*CR* (les)	*CR* (poganjki)	*CR* (enoletne iglice ali listi)
^{238}U				
Pinus sylvestris	min	1,4E-5 ± 0,3E-5	8,6E-5 ± 2,7E-5	1,1E-3 ± 0,2E-3
	maks	4,8E-5 ± 0,6E-5	1,5E-4 ± 0,3E-4	5,4E-3 ± 0,6E-3
Picea abies	min	1,1E-5 ± 0,3E-5	1,2E-4 ± 0,3E-5	9,8E-4 ± 1,3E-4
	maks	2,1E-5 ± 0,3E-5	2,9E-4 ± 0,5E-4	2,1E-3 ± 0,2E-3
Acer		2,7E-5 ± 0,5E-5	3,7E-4 ± 0,7E-4	3,0E-3 ± 0,4E-3
^{230}Th				
Pinus sylvestris	min	7,7E-6 ± 1,4E-6	8,7E-5 ± 1,5E-5	1,0E-4 ± 0,2E-4
	maks	1,4E-5 ± 0,3E-5	3,5E-4 ± 0,6E-4	6,6E-4 ± 1,0E-4
Picea abies	min	1,2E-5 ± 0,2E-5	8,1E-5 ± 1,6E-5	1,4E-4 ± 0,3E-4
	maks	6,7E-5 ± 1,1E-5	3,9E-4 ± 0,7E-4	2,9E-3 ± 0,5E-3
Acer		2,0E-5 ± 0,3E-5	4,7E-4 ± 0,8E-4	1,8E-3 ± 0,3E-3
^{226}Ra				
Pinus sylvestris	min	3,1E-4 ± 0,2E-4	5,4E-4 ± 0,4E-4	2,3E-3 ± 0,2E-3
	maks	6,5E-4 ± 0,4E-4	1,4E-3 ± 0,1E-3	7,5E-3 ± 0,6E-3
Picea abies	min	8,1E-3 ± 0,5E-3	1,5E-2 ± 0,1E-2	3,7E-2 ± 0,2E-2
	maks	4,0E-2 ± 0,2E-2	1,4E-1 ± 0,1E-1	3,2E-1 ± 0,2E-1
Acer		3,2E-3 ± 0,2E-3	1,6E-2 ± 0,1E-2	9,4E-2 ± 0,6E-2
^{210}Pb				
Pinus sylvestris	min	1,5E-3 ± 0,1E-3	6,7E-4 ± 0,6E-4	4,1E-3 ± 0,3E-3
	maks	4,8E-3 ± 0,4E-3	1,1E-3 ± 0,1E-3	6,4E-3 ± 0,5E-3
Picea abies	min	1,2E-3 ± 0,1E-3	8,7E-4 ± 0,7E-4	9,9E-3 ± 0,8E-3
	maks	3,6E-3 ± 0,3E-3	9,7E-3 ± 0,8E-3	4,2E-2 ± 0,3E-2
Acer		2,8E-3 ± 0,2E-3	2,9E-3 ± 0,2E-3	2,3E-2 ± 0,2E-2

4.6 Vsebnosti naravnih radionuklidov v mleku in izračun dozne obremenitve

Vsebnosti ^{238}U, ^{234}U, ^{226}Ra, ^{210}Pb in ^{210}Po v vzorcih mleka in mleka v prahu so predstavljene na sliki 85 in v tabelah 8 – 9. Kemijski izkoristki separacije so znašali od 47 do 86 % za ^{238}U in ^{234}U, od 36 do 81 % za ^{226}Ra, od 21 do 43 % za ^{210}Pb in od 47 do 85 % za ^{210}Po. Vzorci 1 – 4 so bili vzorčeni na območju bivšega rudnika urana Žirovski vrh,

vzorec 5 je bil vzorčen v Bukovščici in predstavlja referenčno lokacijo. Ostali štirje vzorci so vzorci mleka v prahu in sicer vzorec mleka v prahu iz Pomurskih mlekarn (Pom. mlek.) ter trije vzorci mleka v prahu podjetja Hipp (Hipp PRE, Hipp 2 in Hipp 3). Najvišje specifične aktivnosti ^{238}U in ^{234}U sem določil v vzorcu mleka v prahu iz Pomurskih mlekarn, najnižje pa v vzorcu mleka iz referenčne lokacije 5. Specifična aktivnost ^{226}Ra je bila v območju od 0,041 Bq/kg suhe mase za mleko v prahu iz Pomurskih mlekarn do 0,101 Bq/kg suhe mase za vzorec mleka iz območja bivšega rudnika urana Žirovski vrh (vzorec 2). Najnižjo specifično aktivnost ^{210}Pb sem določil v vzorcu mleka v prahu Hipp 3 in je znašala 0,290 Bq/kg suhe mase, najvišja pa je bila v primeru vzorca mleka v prahu Hipp PRE (0,652 Bq/kg suhe mase). Specifične aktivnosti ^{210}Po so bile v območju od 0,055 Bq/kg suhe mase za vzorec mleka v prahu Hipp PRE do 0,611 Bq/kg suhe mase za vzorec mleka številka 2 iz območja bivšega rudnika urana Žirovski vrh.

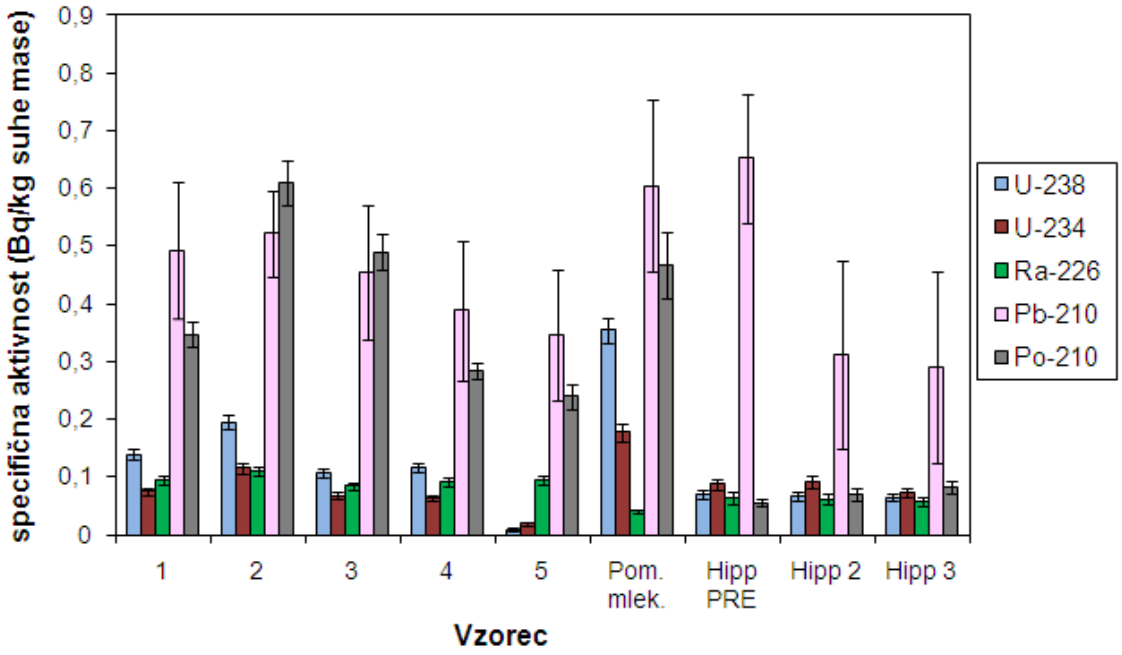

Slika 85: *Specifične aktivnosti ^{238}U, ^{234}U, ^{226}Ra, ^{210}Pb in ^{210}Po v vzorcih mleka in mleka v prahu (Pom. mlek. = Pomurske mlekarne).*

Tabela 8: *Vsebnosti ^{238}U, ^{234}U in ^{226}Ra v vzorcih mleka in mleka v prahu.*

Vzorec	Sveža masa /suha masa	*a* (Bq/kg suhe mase)		
		^{238}U	^{234}U	^{226}Ra
1	8,6	0,139 ± 0,009	0,075 ± 0,006	0,094 ± 0,008
2	9,4	0,195 ± 0,012	0,115 ± 0,009	0,110 ± 0,008
3	7,5	0,107 ± 0,008	0,067 ± 0,006	0,085 ± 0,006
4	7,3	0,116 ± 0,007	0,064 ± 0,005	0,091 ± 0,007
5	7,8	0,009 ± 0,002	0,019 ± 0,003	0,094 ± 0,007
Pomurske mlekarne	–	0,354 ± 0,023	0,177 ± 0,015	0,041 ± 0,004
Hipp PRE	–	0,071 ± 0,008	0,087 ± 0,009	0,063 ± 0,010
Hipp 2	–	0,066 ± 0,008	0,091 ± 0,010	0,062 ± 0,008
Hipp 3	–	0,065 ± 0,007	0,074 ± 0,008	0,057 ± 0,008

Tabela 9: *Vsebnosti ^{210}Pb in ^{210}Po v vzorcih mleka in mleka v prahu.*

Vzorec	Sveža masa /suha masa	*a* (Bq/kg suhe mase)	
		^{210}Pb	^{210}Po
1	8,6	0,492 ± 0,118	0,347 ± 0,021
2	9,4	0,522 ± 0,075	0,611 ± 0,039
3	7,5	0,454 ± 0,117	0,490 ± 0,030
4	7,3	0,388 ± 0,122	0,285 ± 0,014
5	7,8	0,345 ± 0,113	0,239 ± 0,021
Pomurske mlekarne	–	0,605 ± 0,148	0,467 ± 0,057
Hipp PRE	–	0,652 ± 0,111	0,055 ± 0,006
Hipp 2	–	0,312 ± 0,162	0,070 ± 0,010
Hipp 3	–	0,290 ± 0,165	0,082 ± 0,011

Povprečno izotopsko razmerje ^{234}U/^{238}U za vzorce 1 – 4 in mleko v prahu iz Pomurskih mlekarn je znašalo okrog 0,56. V primeru vzorcev mleka v prahu podjetja Hipp pa je bilo okrog 1,25.

Za izračun efektivne letne ingestijske doze zaradi zaužitja za posamezen radionuklid sem uporabil enačbo 36 in podatke iz tabel 8 – 10.

$$E_{\text{ing}} = h(g)_{\text{ing}}\, a\, m \tag{36}$$

Kjer je:

E_{ing} Efektivna letna ingestijska doza zaradi zaužitja za posamezen radionuklid v Sv/leto
$h(g)_{\text{ing}}$ Predvidena efektivna doza na enoto vnosa zaradi zaužitja v Sv/Bq
a Specifična aktivnost določenega radionuklida v vzorcu v Bq/kg suhe mase
m Letni vnos mleka v kg/leto

Tabela 10 prikazuje predvidene efektivne doze na enoto vnosa zaradi zaužitja za odrasle (osebe starejše od 17 let) in dojenčke mlajše od enega leta kot jih podaja Uradni list Republike Slovenije (2004) in so enake, kot v publikaciji IAEA International Basic Safety Standards (IAEA, 2003). Iz tabele je razvidno, da so največje vrednosti predvidenih efektivnih doz na enoto vnosa v primeru ^{210}Po. To pomeni, da posameznik, ki zaužije enako aktivnost ^{210}Po prejme večjo dozo, kot če zaužije enako aktivnost na primer ^{238}U.

Tabela 10: *Predvidena efektivna doza na enoto vnosa zaradi zaužitja za odrasle in dojenčke mlajše od enega leta.*

Radionuklid	$h(g)_{\text{ing}}$ (Sv/Bq)	
	Odrasli (> 17 let)	Dojenčki (≤ 1 leto)
^{238}U	4,5E-8	3,4E-7
^{234}U	4,9E-8	3,7E-7
^{226}Ra	2,8E-7	4,7E-6
^{210}Pb	6,9E-7	8,4E-6
^{210}Po	1,2E-6	2,6E-5

Efektivne letne ingestijske doze sem izračunal za dve skupini odraslega prebivalstva in sicer za prvo skupino, ki zaužije mleko iz vzorcev 1 – 4, ki so bili odvzeti iz okolice območja bivšega rudnika urana Žirovski vrh; druga skupina odraslega prebivalstva pa

zaužije mleko iz referenčnega vzorca 5 iz Bukovščice. Pri dojenčkih sem efektivne letne ingestijske doze izračunal za štiri skupine:

- dojenčki do enega leta starosti, ki zaužijejo mleko iz vzorcev 1 – 4, ki so bili odvzeti iz okolice območja bivšega rudnika urana Žirovski vrh,
- dojenčki do enega leta starosti, ki zaužijejo mleko iz referenčnega vzorca 5 iz Bukovščice,
- dojenčki do enega leta starosti, ki zaužijejo mleko v prahu iz Pomurskih mlekarn,
- dojenčki do enega leta starosti, ki zaužijejo mleko v prahu iz biološke pridelave proizvajalca Hipp.

Kot je razvidno iz enačbe 36, je efektivna letna ingestijska doza odvisna od zaužite mase mleka. Za izračun efektivne letne ingestijske doze za odrasle sem predpostavil, da odrasli človek letno zaužije 122 kg svežega mleka. Ta vrednost je ocena porabe, ki se uporablja tudi za nadzor radioaktivnosti v okolju bivšega rudnika urana Žirovski vrh in sem jo povzel po Omahen et al. (2006). V primeru dojenčkov, ki zaužijejo mleko iz biološke pridelave proizvajalca Hipp, sem maso mleka v prahu, ki ga dojenček zaužije, izračunal skladno z navodili proizvajalca za pripravo in število obrokov na dan. Znašala je 22,4 kg suhe mase za Hipp PRE, ki se uporablja od rojstva dojenčka do šestega meseca starosti; 10,8 kg suhe mase za Hipp 2, ki se uporablja za hrano dojenčkom od šestega do desetega meseca in 3,6 kg suhe mase za Hipp 3, ki se uporablja za hrano dojenčkom od desetega do dvanajstega meseca. Efektivne ingestijske doze teh treh produktov sem seštel, da bi dobil efektivno letno ingestijsko dozo. Za primerljivost rezultatov sem maso zaužitega mleka v prahu od Pomurskih mlekarn izračunal kot vsoto vseh treh mas produktov Hipp in je znašala 36,8 kg suhe mase. Ta masa pa odgovarja 294,5 kg sveže mase mleka v primeru vzorcev 1 – 4 in 5 in sem jo uporabil za izračun efektivne letne ingestijske doze dojenčkov iz teh dveh skupin.

Tabela 11 predstavlja vsoto efektivnih letnih ingestijskih doz za posamezne radionuklide, za v prejšnjem odstavku omenjene skupine odraslih populacij in dojenčkov. Vrednosti efektivnih letnih ingestijskih doz za posamezne radionuklide so razvidne iz slik 86 in 87 ter iz priloge 11. Iz tabele 11 je razvidno, da je vsota efektivnih letnih ingestijskih doz za vse analizirane radionuklide za odrasle pri vzorcih iz okolice bivšega rudnika urana Žirovski vrh za 4,3 μSv večja kot pri referenčnem vzorcu 5. Vsota efektivnih letnih ingestijskih doz za vse analizirane radionuklide v primeru dojenčkov pa je najvišja pri vzorcu mleka v prahu iz Pomurskih mlekarn (648 μSv/leto), temu sledijo vzorci 1 – 4 s 562 μSv/leto, vzorec 5 s 363 μSv/leto in vzorci mleka v prahu Hipp (195 μSv/leto).

Tabela 11: *Vsota efektivnih letnih ingestijskih doz za vse analizirane radionuklide za odrasle in dojenčke do enega leta starosti.*

Populacija	E_{ing} (μSv/leto)
Odrasli; 1 – 4	13,0 ± 1,7
Odrasli; 5	8,7 ± 1,6
Dojenčki; 1 – 4	562 ± 74
Dojenčki; 5	363 ± 66
Dojenčki; Pomurske mlekarne	648 ± 98
Dojenčki; Hipp	195 ± 40

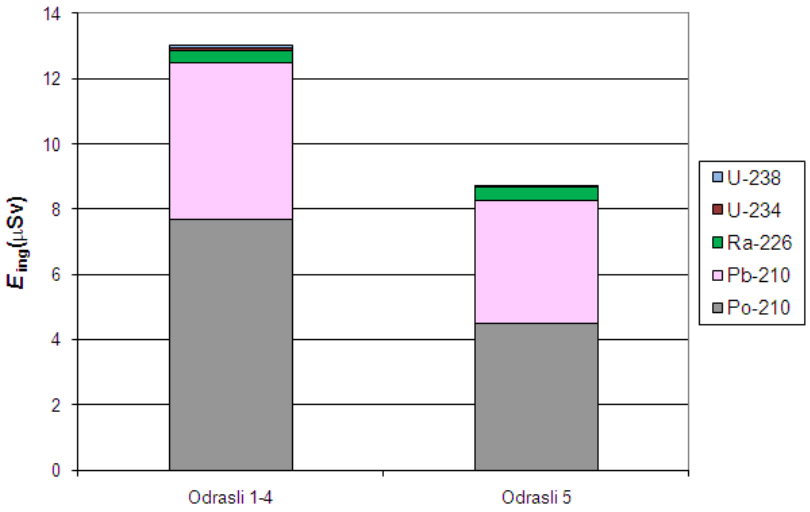

Slika 86: *Efektivna letna ingestijska doza za ^{238}U, ^{234}U, ^{226}Ra, ^{210}Pb in ^{210}Po za odrasle.*

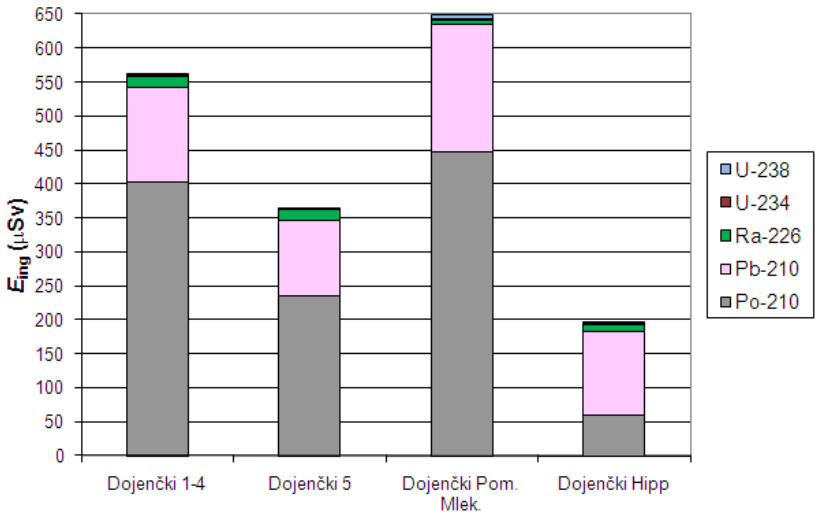

Slika 87: *Efektivna letna ingestijska doza za ^{238}U, ^{234}U, ^{226}Ra, ^{210}Pb in ^{210}Po za dojenčke.*

Slika 88 predstavlja delež posameznega radionuklida v vsoti efektivne letne ingestijske doze iz katere lahko ugotovimo, kateri radionuklidi največ prispevajo k dozi zaradi zaužitja mleka. Tako sem ugotovil, da največ prispeva k dozi zaradi zaužitja mleka ^{210}Po, ki predstavlja od 50 do 70 % doze pri vseh vzorcih, razen v primeru mleka v prahu Hipp. Pri mleku v prahu Hipp k dozi z okrog 60 % največ prispeva ^{210}Pb. Prispevek k dozi zaradi ^{210}Po in ^{210}Pb je v vseh primerih večji od 90 %.

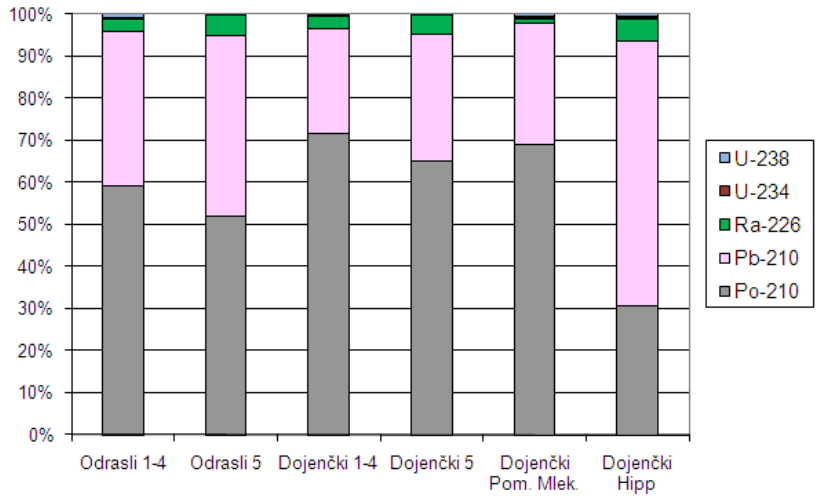

Slika 88: *Delež posameznega radionuklida v efektivni letni ingestijski dozi.*

4.7 Določitve koncentracijskih razmerij med krmo in mlekom

Specifične aktivnosti ^{238}U, ^{234}U, ^{230}Th, ^{226}Ra, ^{210}Pb in ^{210}Po v vzorcih tal, travne silaže, sena in mleka so predstavljene v tabelah 12 in 13. Trije vzorci tal reprezentativno predstavljajo tla, na katerih kmetija prideluje krmo za krave, vzorca silaže in trave pa krmo, s katero so bile krave krmljene ob času odvzema vzorca mleka. Iz tabel 12 in 13 je razvidno, da se specifične aktivnosti ^{238}U, ^{234}U, ^{230}Th in ^{226}Ra v treh vzorcih tal ne razlikujejo bistveno, v primeru ^{210}Pb in ^{210}Po pa so bile vrednosti v tretjem vzorcu tal za nekoliko več kot dvakrat višje v primerjavi s prvima dvema vzorcema tal. Če primerjam specifične aktivnosti radionuklidov med silažo in senom ugotovim, da so le te v primeru ^{230}Th in ^{210}Po skoraj petkrat višje v silaži, v primeru ^{226}Ra so v silaži dvakrat višje kot v senu, pri ^{238}U in ^{210}Pb pa so le te primerljive (tabeli 12 in 13).

Tabela 12: *Vsebnosti ^{238}U, ^{234}U in ^{230}Th v vzorcih tal, silaže, sena in mleka.*

Vzorec	Sveža masa /suha masa	*a* (Bq/kg suhe mase)		
		^{238}U	^{234}U	^{230}Th
Tla 1	–	65,0 ± 3,6	62,9 ± 3,5	58,1 ± 2,9
Tla 2	–	65,1 ± 3,6	69,0 ± 3,8	65,2 ± 3,2
Tla 3	–	60,5 ± 3,2	60,1 ± 3,2	64,6 ± 3,2
Silaža	–	0,213 ± 0,021	0,320 ± 0,027	0,561 ± 0,028
Seno	–	0,218 ± 0,017	0,209 ± 0,017	0,125 ± 0,010
Mleko	7,9	0,056 ± 0,008	0,062 ± 0,009	0,087 ± 0,004

Tabela 13: *Vsebnosti ^{226}Ra, ^{210}Pb in ^{210}Po v vzorcih tal, silaže, sena in mleka.*

Vzorec	Sveža masa /suha masa	*a* (Bq/kg suhe mase)		
		^{226}Ra	^{210}Pb	^{210}Po
Tla 1	–	83,1 ± 4,0	51,3 ± 1,9	59,6 ± 2,0
Tla 2	–	74,6 ± 3,7	48,7 ± 1,8	59,5 ± 2,2
Tla 3	–	79,6 ± 2,9	119 ± 4	134 ± 5
Silaža	–	1,28 ± 0,08	14,7 ± 0,9	22,6 ± 0,85
Seno	–	0,602 ± 0,036	14,4 ± 0,9	4,54 ± 0,19
Mleko	7,9	0,066 ± 0,005	0,302 ± 0,087	0,251 ± 0,019

Izotopsko razmerje ^{234}U/^{238}U je bilo v primeru vzorcev tal v povprečju enako 1, pri silaži je znašalo 1,5; v primeru sena je bilo okrog 1, pri mleku pa je znašalo 1,1. Pri izotopskem razmerju med ^{210}Po in ^{210}Pb lahko ugotovim, da sta le-ta v primeru vzorcev tal in mleka praktično v ravnotežju, kar pa ne morem trditi za vzorca silaže in sena. V primeru vzorca silaže je ^{210}Po približno 1,5 krat več, v primeru vzorca sena pa približno 3 krat manj kot ^{210}Pb.

Pri izračunu faktorjev prenosa iz tal v silažo in seno ter pri izračunu koncentracijskih razmerij med silažo in senom sem uporabil povprečne vredosti za tla in silažo ter za seno. Tako sem predpostavil, da trije vzorci tal reprezentativno predstavljajo tla, na katerih kmetija pridobiva krmo ter da pri kravah predstavlja polovica krme silaža in polovica krme seno. Faktorji prenosa iz tal v silažo in seno za določene radionuklide so predstavljeni na sliki 89 in v tabeli 14. Najvišje faktorje prenosa iz tal v silažo in seno sem določil pri ^{210}Pb, temu pa so sledili ^{210}Po, ^{226}Ra, ^{230}Th, ^{234}U, in ^{238}U.

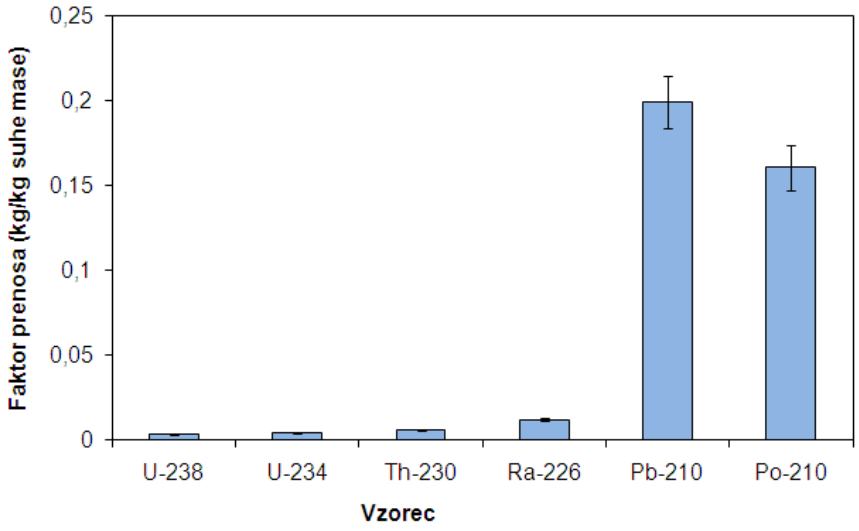

Slika 89: *Faktor prenosa tla – silaža in seno za posamezen radionuklid.*

Koncentracijska razmerja med silažo in senom ter mlekom so predstavljena na sliki 90 in v tabeli 14. Iz njih je razvidno, da so koncentracijska razmerja za ^{238}U, ^{234}U in ^{230}Th med seboj primerljiva in znašajo okrog 0,25. Koncentracijska razmerja za ^{226}Ra, ^{210}Pb in ^{210}Po pa so mnogo manjša in znašajo okrog 0,07 za ^{226}Ra in okrog 0,02 za ^{210}Pb ter ^{210}Po.

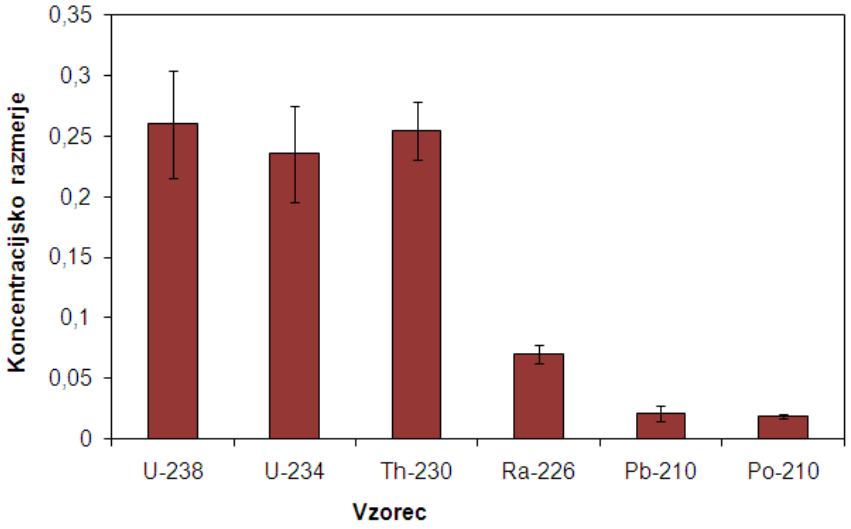

Slika 90: *Koncentracijsko razmerje silaža in seno – mleko za posamezen radionuklid.*

Tabela 14: *Faktorji prenosa (TF) tla – silaža in seno ter koncentracijska razmerja (CR) silaža in seno – mleko za ^{238}U, ^{234}U ^{230}Th, ^{226}Ra, ^{210}Pb in ^{210}Po.*

Radionuklid	*TF* (tla – silaža in seno)	*CR* (silaža in seno – mleko)
^{238}U	0,0034 ± 0,0004	0,260 ± 0,048
^{234}U	0,0041 ± 0,0008	0,235 ± 0,040
^{230}Th	0,0055 ± 0,0005	0,255 ± 0,024
^{226}Ra	0,0119 ± 0,0011	0,070 ± 0,008
^{210}Pb	0,199 ± 0,016	0,021 ± 0,006
^{210}Po	0,161 ± 0,014	0,019 ± 0,002

4.8 Rezultati medlaboratorijskih primerjav

V času trajanja doktorskega dela sem v sklopu zagotovitve kakovosti meritev opravil določitve radionuklidov v številnih medlaboratorijskih primerjavah. V tabeli 15 so predstavljeni rezultati teh primerjav. V prvi koloni je predstavljen naslov medlaboratorijske primerjave in organizator le-te, v drugi je predstavljena vrsta vzorca, v tretji koloni pa seznam analiziranih radionuklidov pri posamezni medlaboratorijski primerjavi. V četrti koloni so predstavljeni kriteriji za preverjanje ustreznosti rezultatov, v peti pa rezultati posameznih določitev. Zadnja kolona prikazuje ustreznost merilnih rezultatov, kjer črka Z pomeni, da so bili rezultati s strani organizatorja medlaboratorijske primerjave ocenjeni kot zadovoljivi, črka N pa, da le-ti niso bili zadovoljivi. Ob pregledu rezultatov v tabeli 15 tako lahko ugotovim, da so vsi rezultati dosegli zadovoljivo oceno.

Tabela 15: Rezultati medlaboratorijskih primerjav (R = radionuklid, U = ustreznost).

Medlaboratorijska primerjava; organizator	Vrsta vzorca	R	Kriterij	Rezultat	U
IAEA-CU-2007-09; IAEA	Voda	^{210}Po	52,8 ± 1,4 Bq/kg	49,3 ± 3,8 Bq/kg	Z
			101,6 ± 2,8 Bq/kg	99,9 ± 4,7 Bq/kg	Z
			52,8 ± 1,4 Bq/kg	51,7 ± 2,7 Bq/kg	Z
			101,6 ± 2,8 Bq/kg	102,9 ± 4,6 Bq/kg	Z
			Slep vzorec	0,019 ± 0,004 Bq/kg	Z
IAEA-CU-2007-04; IAEA	Zemlja	^{210}Pb	48 ± 1,5 Bq/kg	56 ± 8 Bq/kg	Z
	Voda	^{210}Pb	29,34 ± 0,5 Bq/kg	25 ± 1 Bq/kg	Z
	Špinača	^{234}U	1,02 ± 0,07 Bq/kg	1,4 ± 0,2 Bq/kg	Z
		^{238}U	0,95 ± 0,05 Bq/kg	1,1 ± 0,2 Bq/kg	Z
Ringversuch 2/2008; Bundesamt für Strahlenschutz	Modelna voda	^{234}U	1,41 ± 0,282 Bq/L	1,39 ± 0,07 Bq/L	Z
		^{238}U	1,44 ± 0,239 Bq/L	1,38 ± 0,07 Bq/L	Z
	Realna voda	^{234}U	0,753 ± 0,135 Bq/L	0,77 ± 0,04 Bq/L	Z
		^{238}U	0,753 ± 0,125 Bq/L	0,82 ± 0,04 Bq/L	Z
NPL Environmental radioactivity proficiency test exercise 2008; NPL	Voda AH	^{226}Ra	4,77 ± 0,38 Bq/g	5,4 ± 0,3 Bq/g	Z
		^{234}U	11,1 ± 0,5 Bq/g	11,1 ± 0,5 Bq/g	Z
	Voda AL	^{238}U	11,262 ± 0,57 Bq/g	11,3 ± 0,5 Bq/g	Z
		^{226}Ra	4,71 ± 0,33 Bq/kg	5,3 ± 0,3 Bq/kg	Z
		^{234}U	14,6 ± 0,88 Bq/kg	15,6 ± 0,7 Bq/kg	Z
		^{238}U	14,76 ± 0,89 Bq/kg	16,3 ± 0,8 Bq/kg	Z
Ringversuch 2/2009; Bundesamt für Strahlenschutz	Modelna voda	^{234}U	0,98 ± 0,14 Bq/L	1,02 ± 0,04 Bq/L	Z
		^{238}U	1,0 ± 0,14 Bq/L	1,03 ± 0,04 Bq/L	Z
	Realna voda	^{234}U	0,15 ± 0,026 Bq/L	0,150 ± 0,010 Bq/L	Z
		^{238}U	0,15 ± 0,024 Bq/L	0,153 ± 0,011 Bq/L	Z
IAEA-CU-2008-04; IAEA	Voda 01	^{234}U	0,56 ± 0,02 Bq/kg	0,61 ± 0,04 Bq/kg	Z
		^{238}U	0,36 ± 0,01 Bq/kg	0,39 ± 0,03 Bq/kg	Z
		^{226}Ra	0,69 ± 0,04 Bq/kg	0,79 ± 0,05 Bq/kg	Z
	Voda 02	^{234}U	1,2 ± 0,04 Bq/kg	1,20 ± 0,07 Bq/kg	Z
		^{238}U	1,25 ± 0,04 Bq/kg	1,26 ± 0,07 Bq/kg	Z
		^{226}Ra	1,93 ± 0,09 Bq/kg	2,26 ± 0,12 Bq/kg	Z
NPL Environmental radioactivity proficiency test exercise 2009; NPL	Voda AH	^{226}Ra	15,90 ± 0,21 Bq/kg	17,6 ± 0,8 Bq/kg	Z
	Voda AL	^{238}U	18,0 ± 0,4 Bq/kg	18,1 ± 0,9 Bq/kg	Z
IAEA-CU-2009-03; IAEA	Mah – zemlja	^{238}U	22,2 ± 0,8 Bq/kg	25 ± 2 Bq/kg	Z
		^{234}U	21,8 ± 0,8 Bq/kg	24 ± 2 Bq/kg	Z
		^{226}Ra	25,1 ± 2,0 Bq/kg	35 ± 4 Bq/kg	Z
		^{210}Pb	424 ± 20 Bq/kg	435 ± 13 Bq/kg	Z
		^{210}Po	423 ± 10 Bq/kg	406 ± 20 Bq/kg	Z

5 Razprava

Rezultati primerjave obeh sekvenčnih ekstrakcijskih postopkov so pokazali, da sta oba sekvenčna ekstrakcijska postopka statistično primerljiva le v primeru vsebnosti ^{238}U v organski frakciji in v preostanku (slike 24 – 53 in tabela 5). Torej lahko v splošnem ugotovim, da oba postopka med seboj nista primerljiva, kar je bilo tudi v skladu s pričakovanji. Med obema postopkoma so namreč opazne številne razlike (tabeli 1 in 2). Postopek S ima eno frakcijo več kot postopek B, prav tako je zaporedje frakcij različno (v primeru postopka S je organska frakcija postavljena pred karbonatno frakcijo in Fe/Mn oksidi). Različni so tudi posamezni reagenti in njihove koncentracije, kakor tudi razmerje med reagentom in vzorcem, ter čas stresanja. S samimi eksperimenti in s statistično primerjavo rezultatov sem tako le potrdil, da rezultati med seboj niso primerljivi. To je pomembno zato, ker rezultatom za posamezne frakcije ni mogoče dajati prevelike teže in na podlagi le teh sklepati določene zaključke, saj so ti rezultati odvisni od vrste sekvenčnega ekstrakcijskega postopka in se ne navezujejo na točno določeno frakcijo.

Pri primerjavi rezultatov obeh sekvenčnih ekstrakcijskih postopkov se je pokazalo, da je pri vseh radionuklidih postopek S dajal višje rezultate za karbonatno frakcijo kot postopek B. Razlog za to bi lahko bila uporaba 50 krat bolj koncentriranega reagenta v primeru postopka S (tabeli 1 in 2). Vendar sta čas ekstrakcije in razmerje med reagentom in vzorcem pri postopku B štirikrat večja kot pri postopku S. Prav tako je organska frakcija pri postopku S postavljena pred karbonatno. Razlog za to je, da lahko organska snov obdaja trdne delce v vzorcu in s tem preprečuje reakcijo le teh z reagentoma za karbonatno frakcijo in Fe/Mn okside (Schultz et al., 1998). Zato je najverjetnejši razlog višjih rezultatov postopka S za karbonatne frakcije postavitev organske frakcije pred karbonatno.

Postopek B je pri vseh radionuklidih dajal najvišje rezultate za Fe/Mn oksidno frakcijo. Razlog temu je dvanajstkrat bolj koncentriran reagent v primeru postopka B ter daljši čas stresanja in večje razmerje med vzorcem in reagentom (tabeli 1 in 2). Pomemben vpliv bi lahko imela tudi postavitev organske frakcije pred karbonatno in Fe/Mn oksidno frakcijo v primeru postopka S, saj La Force in Fendorf (2000) poročata, da lahko le to raztopi do 10 % železa in poveča specifično aktivnost v organski frakciji. Vendar rezultati primerjave obeh sekvenčnih ekstrakcijskih postopkov tega ne potrjujejo, saj dajeta oba postopka za ^{238}U primerljive rezultate, pri ^{230}Th, ^{210}Pb in ^{210}Po daje postopek B višje rezultate in le v primeru ^{226}Ra daje postopek S nekoliko višje rezultate od postopka B (slike 34 – 53 in tabela 5).

Kljub temu, da oba sekvenčna ekstrakcijska postopka v splošnem ne dajeta primerljivih rezultatov, je mogoče iz njih marsikaj zanimivega zaključiti. Tako so v primeru ^{238}U porazdelitveni profili med lokacijama 2 in 5 podobni kot pri nekontaminirani lokaciji 3 (slika 54). Pri tem je večina ^{238}U v preostanku (več od 80 % v primeru postopka B), kar pomeni, da je le manjši del ^{238}U v bolj mobilnih frakcijah. Iz tega sledi, da lokacija 2 ne vsebuje ^{238}U iz HMJ. Porazdelitveni profili v lokacijah 1, 4 in 6 so si podobni med seboj pri obeh postopkih (slika 54). ^{238}U se v teh lokacijah nahaja pretežno v bolj mobilnih frakcijah in ga je v preostanku le okrog 20 %. Tako lahko iz slik 54 in 55 zaključim, da se ^{238}U iz odlagališča HMJ zadržuje v lokaciji 1 in ne v lokaciji 2. Največjo celotno specifično aktivnost ^{238}U pa sem ugotovil na dnu odlagališča (lokacija

4), ki leži v smeri spiranja radionuklidov iz odlagališča. ^{238}U iz odlagališča HMJ se nahaja pretežno vezan na organsko snov (od 40 – 60 %), v ostalih primerih pa je pretežno vezan na preostanek (od 60 do 90 %).

Razlike med ^{230}Th iz odlagališča HMJ in naravno prisotnim ^{230}Th niso tako očitne, saj se v vseh lokacijah ^{230}Th nahaja pretežno v preostanku (od 50 do 86 %) (slika 56). Ti rezultati potrjujejo mnogo manjšo mobilnost ^{230}Th v primerjavi z ^{238}U, kar je znano tudi iz literature (Hyde, 1960). Torij je namreč v okolju povezan s trdnimi delci, le manjši delež pa je raztopljen v vodi. Tudi v primeru ^{230}Th sem največjo celotno specifično aktivnost ugotovil v primeru lokacije 4, kar je bilo pričakovano (slika 57). Višje celotne specifične aktivnosti ^{230}Th sem ugotovil tudi v primeru lokacij 5 in 6, ter v primeru postopka S tudi v lokaciji 1.

Slika 58 prikazuje porazdelitvene profile med posameznimi frakcijami za ^{226}Ra, iz katere je očitno, da ga je več v preostanku v lokacijah 1, 2 in 3, kot pa v lokacijah 4, 5 in 6. To je še posebno izrazito v primeru postopka B, kjer je v prvih treh lokacijah od 60 do 70 % ^{226}Ra v preostanku medtem, ko je v lokacijah 4, 5 in 6 ta delež od 30 do 40 %. Tako je iz slik 58 in 59 očitno, da se ^{226}Ra iz odlagališča HMJ ne zadržuje v lokacijah 1 in 2, saj so tako porazdelitveni profili, kot tudi celotne specifične aktivnosti ^{226}Ra podobne tistim v lokaciji 3. V primeru lokacij 4, 5 in 6 pa lahko ugotovimo večje celotne specifične aktivnosti ^{226}Ra v primerjavi z lokacijo 3, kar skupaj z drugačnimi porazdelitvenimi profili posameznih frakcij v teh lokacijah v primerjavi z lokacijo 3 pomeni, da je vir povečane vsebnosti ^{226}Ra HMJ.

V primeru obeh sekvenčnih ekstrakcijskih postopkov za ^{210}Pb, ki jih prikazujeta sliki 60 in 61, pa rezultati niso tako enoznačni. Oba postopka namreč tudi v primeru frakcije s prevladujočo vsebnostjo ^{210}Pb dajeta različne rezultate. Pri postopku S je namreč preostanek prevladujoča frakcija, v kateri se nahaja ^{210}Pb (od 55 do 70 %) preostanek, pri postopku B pa so to Fe/Mn oksidi (od 40 do 60 %). Tako je na podlagi porazdelitvenih profilov težko sklepati karkoli, ker so rezultati obeh postopkov preveč različni. Pri celotnih specifičnih aktivnostih ^{210}Pb lahko ugotovim, da so bile le te v primerjavi z lokacijo 3 večje v lokacijah 1, 4, 5 in 6.

Ker sem vzorce za določitev vsebnosti ^{210}Po analiziral približno tri leta po vzorčenju, so bile celotne specifične aktivnosti ^{210}Po že v trajnem radioaktivnem ravnotežju s ^{210}Pb in dejanske celotne specifične aktivnosti ^{210}Po ob vzorčenju ni bilo več mogoče določiti. Zato pa se rezultati porazdelitvenih profilov posameznih frakcij, ki jih prikazuje slika 62 zelo razlikujejo od rezultatov za ^{210}Pb (slika 60); polonij se namreč v okolju obnaša drugače kot svinec. Tako je večina ^{210}Po v vseh lokacijah povezana s preostankom (od 70 do 98 %). Te vrednosti so celo višje, kot v primeru ^{230}Th (slika 56), ki je znan kot slabo mobilen radionuklid. Sklepam lahko, da je ^{210}Po v okolju odlagališča Boršt zelo nemobilen in se nahaja pretežno v preostanku.

Pri primerjavi rezultatov porazdelitvenih profilov posameznih frakcij v lokaciji 4, kjer sem ugotovil največjo celotno specifično aktivnost za vse radionuklide, lahko ugotovim, da pripada največji delež vsote vseh frakcij brez preostanka ^{238}U (okrog 80 %), temu sledijo ^{226}Ra (od 70 do 50 %), ^{210}Pb (od 70 do 40 %), ^{230}Th (okrog 15 %) in ^{210}Po (okrog 5 %) (slike 54, 56, 58, 60 in 62). Iz tega lahko sklepam, da je na odlagališču Boršt najbolj mobilen ^{238}U, njemu pa sledijo ^{226}Ra, ^{210}Pb, ^{230}Th in ^{210}Po.

Rezultati izotopskih razmerij ^{234}U/^{238}U so pokazali, da je uran v mobilnih frakcijah in preostankih na lokacijah 2 in 3 naravnega izvora in ne prihaja iz odlagališča HMJ, saj je bilo izotopsko razmerje v mobilnih frakcijah večje od 1, v preostanku pa manjše od 1 (slika 64). V primeru lokacije 1 lahko ugotovim, da je izvor urana v mobilnih frakcijah iz odlagališča HMJ, saj je izotopsko razmerje enako 1, uran v preostanku pa je naravnega izvora, saj je izotopsko razmerje ^{234}U/^{238}U manjše od 1. Pri lokacijah 4, 5 in 6 pa lahko

ugotovim, da je tako pri mobilnih frakcijah, kot tudi pri preostanku, izotopsko razmerje $^{234}U/^{238}U$ enako 1, iz česar sledi, da je izvor urana v teh frakcijah iz odlagališča HMJ.

Slika 65 prikazuje faktorje prenosa iz tal v travo za ^{238}U, iz katerih je razvidno, da sta faktorja prenosa mnogo višja v prvih dveh lokacijah. Razlog temu je najverjetneje večji privzem ^{238}U iz izcedne vode iz odlagališča HMJ (specifična aktivnost ^{238}U v izcedni vodi znaša okrog 8 Bq/L), ki teče skozi ti dve lokaciji, kot pa privzem iz samih tal. Faktorji prenosa pri ostalih lokacijah so približno enaki. Tudi iz slike 66, ki prikazuje specifične aktivnosti ^{238}U v travi v odvisnosti od le teh v tleh, je razvidno, da lokaciji 1 in 2 odstopata, v ostalih štirih lokacijah pa so specifične aktivnosti ^{238}U v travi in v tleh linearno korelirane. Tako obstaja potencialna možnost uporabe trave pri sledenju migracije ^{238}U, saj obstaja povezava med specifično aktivnostjo v tleh in v travi. Vendar pa je potrebno še meritve izboljšati in izključiti morebitni prispevek kontaminacije, ker vzorci trav niso bili predhodno oprani z vodo.

V primeru ^{230}Th lahko ugotovim, da faktorji prenosa iz tal v travo padajo z naraščajočo specifično aktivnostjo ^{230}Th (slika 67). Po poročanju avtorjev Sheppard in Sheppard (1985) je takšno obnašanje značilno za esencialne elemente. Za razliko od ^{238}U pa pri ^{230}Th ni opaziti korelacije med specifično aktivnostjo ^{230}Th v tleh in v travi (slika 68). Zato v primeru ^{230}Th trave ni možno uporabiti za sledenje migracije, saj specifične aktivnosti v travi niso odvisne od specifičnih aktivnosti v tleh.

Drugače je v primeru ^{226}Ra, kjer so specifične aktivnosti ^{226}Ra v tleh in v travi v vzorcih iz lokacij 4, 5 in 6 med seboj linearno korelirane (slika 70). V vzorcih iz lokacij 1, 2 in 3 so faktorji prenosa iz tal v travo mnogo nižji kot v primerjavi z vzorci iz lokacij 4, 5 in 6 (slika 69). Razlog temu bi lahko bila večja biodostopnost ^{226}Ra v lokacijah 4, 5 in 6. Zanimivo je tudi, da se v primeru ^{226}Ra, za razliko od ^{238}U, v lokacijah 1 in 2 ne pozna vpliv izcednih vod iz odlagališča na specifično aktivnost ^{226}Ra v travi.

Podobno kot pri ^{230}Th, lahko tudi pri ^{210}Pb ugotovim padanje faktorjev prenosa iz tal v travo z naraščanjem specifične aktivnosti ^{210}Pb v tleh (slika 71). Tako se tudi ^{210}Pb obnaša kot esencialni element, kot to okarakterizirata Sheppard in Sheppard (1985). Tudi pri ^{210}Pb specifične aktivnosti v tleh in travi med seboj ne korelirajo (slika 72), zato tudi tukaj ni možno uporabiti trave za sledenje migracije ^{210}Pb.

Faktorji prenosa iz tal v travo so bili v glavnem primerljivi z vrednostmi, ki jih poroča Vandenhove et al. (2009). Nekoliko višji so bili le v primeru ^{210}Pb. Razlog temu je najverjetneje to, da vzorce trave po vzorčenju nisem opral, rezultati, ki jih poroča Vandenhove et al. (2009) pa vključujejo le predhodno oprane vzorce. ^{210}Pb se namreč, kot razpadni produkt ^{222}Rn odlaga iz zraka na rastline, kar bi lahko bil razlog za nekoliko večje faktorje prenosa ^{210}Pb. Faktorji prenosa iz tal v travo so bili v povprečju najvišji za ^{210}Pb, temu pa so sledili ^{226}Ra, in ^{238}U ter ^{230}Th (slike 65 – 72, priloga 8). V primeru ^{238}U in ^{230}Th so bili faktorji prenosa iz tal v travo v povprečju primerljivi med seboj.

V drevesih sem največje specifične aktivnosti določil za ^{226}Ra (od 2,7 do 2728 Bq/kg), temu pa so sledili ^{210}Pb (od 5,1 do 321 Bq/kg), ^{230}Th (od 0,03 do 11,3 Bq/kg) in ^{228}U (od 0,01 do 5,4 Bq/kg). Pri vseh radionuklidih sem največjo vsebnost določil v enoletnih iglicah ali listih, kar pritrjuje hipotezi, da drevesa kopičijo radionuklide v starejše liste in iglice (slike 73 – 84). Razlike med posameznimi deli rastlin so bile pri vseh analiziranih radionuklidih tudi statistično potrjene. V primeru ^{226}Ra pri smreki so bile vrednosti v enoletnih iglicah še posebno visoke saj so znašale tudi do 2728 Bq/kg, kar predstavlja eno tretjino specifične aktivnosti ^{226}Ra v HMJ. Zanimive so tudi do 100 krat nižje specifične aktivnosti ^{226}Ra pri borih v primerjavi s smrekami, čeprav gre v obeh primerih za iglasto drevo (slike 79 – 81). To verjetno priča o drugačnem mehanizmu privzema ^{226}Ra pri teh dveh vrstah dreves.

Koncentracijska razmerja med specifično aktivnostjo v HMJ in specifično aktivnostjo

v različnih delih dreves kažejo, da je ^{226}Ra na območju odlagališča Boršt za drevesa najbolj biodostopen, temu pa sledijo ^{210}Pb, ^{238}U in ^{230}Th (tabela 7). Primerjava koncentracijskih razmerij za ^{238}U in ^{226}Ra v enoletnih iglicah borov je pokazala, da so le ti rezultati primerljivi z rezultati, ki jih poroča Petrova (2006) in znašajo za ^{238}U od 0,0004 do 0,0159 ter za ^{226}Ra od 0,0013 do 0,1081.

Rezultati analiz radionuklidov v vzorcih mleka in mleka v prahu so pokazali, da sem najvišje specifične aktivnosti v vzorcih mleka 1 – 5 in v vzorcu mleka v prahu iz Pomurskih mlekarn ugotovil za ^{210}Pb in ^{210}Po (slika 85, tabeli 8 in 9). V teh vzorcih so bile razlike v specifičnih aktivnostih med ^{210}Pb in ^{210}Po znotraj kombinirane standardne negotovosti, iz česar lahko sklepam, da sta bila oba radionuklida v trajnem radioaktivnem ravnotežju. Zanimivo je, da so specifične aktivnosti ^{210}Po pri vseh vzorcih podjetja Hipp precej nižje od specifičnih aktivnosti ^{210}Pb. Razlogov za to je lahko več. Eden izmed njih je hlapnost ^{210}Po, ki bi lahko med postopkom predelave mleka in pridobivanja mleka v prahu izhlapel. Možen razlog pa je lahko tudi, da je ^{210}Pb prisoten v katerem izmed mlečnih dodatkov, ki niso dovolj stari, da bi prišlo do vzpostavitve trajnega radioaktivnega ravnotežja s ^{210}Po. Rezultati specifičnih aktivnosti za ^{226}Ra se med vsemi vzorci ne razlikujejo bistveno (slika 85, tabela 8). Pri rezultatih specifičnih aktivnosti za ^{238}U in ^{234}U pa so te razlike večje; vrednosti so bile pri vzorcu mleka 5 nižje v primerjavi z vzorci mleka 1 – 4 in vzorci mleka v prahu Hipp, vrednosti za vzorec mleka v prahu iz Pomurskih mlekarn pa višje (slika 85, tabela 8).

Zanimivi so tudi rezultati izotopskih razmerij med ^{234}U in ^{238}U v vzorcih mleka. Tako je bilo povprečno izotopsko razmerje ^{234}U/^{238}U za vzorce 1 – 4 in mleko v prahu iz Pomurskih mlekarn okrog 0,56. V primeru vzorcev mleka v prahu podjetja Hipp pa je bilo to razmerje okrog 1,25 (slika 85, tabela 8). ^{234}U je razpadni produkt ^{238}U zato sta ponavadi v pogojih, kjer ne prihaja do tako imenovanega odbojnega efekta, v trajnem radioaktivnem ravnotežju. Vendar v naravi temu pogosto ni tako, saj je zaradi odbojnega efekta izotopsko razmerje ^{234}U/^{238}U v trdnih delcih manjše od 1 in v vodi, ki obkroža te trdne delce večje od 1 (Bourdon et al., 2003; Adloff in Rössler, 1991; Suksi et al., 2006). Iz tega sledi, da lahko v vodi in posledično v rastlinah ter mleku pričakujemo izotopsko razmerje ^{234}U/^{238}U, ki je bodisi enako ali večje od 1. Tudi potencialna sistematična napaka meritve ^{234}U in ^{238}U s spektrometrijo alfa ne more biti vzrok za to, da je izotopsko razmerje ^{234}U/^{238}U manjše od 1. Iz slike 11, ki prikazuje spekter alfa uranovih izotopov je namreč razvidno, da je vrh ^{238}U bolj oddaljen od vrha kemijskega izkoristka ^{232}U, kot pa vrh ^{234}U. To pomeni, da je morebitni vpliv pri nepravilni izbiri količine sledilca kemijskega izkoristka ali pri preširokih vrhovih, večji pri ^{234}U, kot pri ^{238}U. Posledica tega je, da so lahko, zaradi vplivov sledilca kemijskega izkoristka ^{232}U, vrednosti izotopskega razmerja ^{234}U/^{238}U kvečjemu večje od 1 in ne manjše od 1. Tako vrednosti izotopskih razmerij ^{234}U/^{238}U za vzorce 1 – 4 in mleko v prahu iz Pomurskih mlekarn ne morem pripisati ne odbojnemu efektu, ne morebitni napaki pri meritvi. Eden od možnih vzrokov za izotopska razmerja manjša od 1 bi lahko bila prisotnost osiromašenega urana, vendar je to malo verjetno saj na območju bivšega rudnika urana Žirovski vrh ni virov osiromašenega urana. Zanimivo je, da so vrednosti izotopskega razmerja ^{234}U/^{238}U v vzorcih proizvajalca Hipp, ki so opredeljeni kot vzorci iz biološke pridelave, večji od 1. Zato bi bilo mogoče razloge za izotopsko razmerje ^{234}U/^{238}U manjše od 1 iskati v razlikah med klasično pridelavo in biološko pridelavo. Vendar je število meritev premajhno, da bi to lahko z gotovostjo potrdil. Zato bi bilo potrebno izvesti obširnejšo raziskavo, ki bi vključevala tako klasične pridelovalce kot tudi tiste z biološko pridelavo ter bi zajemala celotno verigo prenosa radionuklidov v mleko preko tal, umetnih gnojil in krme.

Na splošno lahko ugotovim, da so v povprečju specifične aktivnosti ^{226}Ra in ^{210}Pb v vzorcih mleka 1 – 4 iz okolice območja bivšega rudnika urana Žirovski vrh primerljive z referenčnim vzorcem mleka 5 (slika 85, tabeli 8 in 9). Specifične aktivnosti ^{238}U, ^{234}U in

^{210}Po pa so v vzrocih mleka 1 – 4 višje kot v vzorcu mleka iz referenčne lokacije. Tako so vrednosi za ^{238}U v povprečju 15 krat višje, za ^{234}U v povprečju 4 krat višje in za ^{210}Po v povprečju 1,8 krat višje kot pri referenčnem vzorcu 5. Vendar pa, če primerjam povprečne specifične aktivnosti ^{238}U, ^{234}U in ^{210}Po v vzorcih 1 – 4 z vzorcem mleka v prahu iz Pomurskih mlekarn, ugotovim, da so vrednosti za ^{238}U, ^{234}U v vzorcih 1 – 4 nižje, vrednosti za ^{210}Po pa primerljive s tistimi v vzorcu iz Pomurskih mlekarn. Tako ne morem enoznačno trditi, da so vsebnosti omenjenih radionuklidov v vzorcih mleka iz okolice bivšega rudnika urana Žirovski vrh višje kot drugod po Sloveniji.

Vsota efektivnih letnih ingestijskih doz analiziranih radionuklidov v mleku je bila za odrasle pri vzorcih iz okolice bivšega rudnika urana Žirovski vrh za 4,3 μSv/leto večja kot v referenčnem vzorcu 5 (tabela 11). Vendar pa bi bila, če bi preračunali dozo za odrasle tudi iz mleka v prahu Pomurskih mlekarn, vrednost v vzorcih iz okolice bivšega rudnika urana Žirovski vrh za 2,5 μSv/leto manjša. To pomeni, da ni mogoče potrditi, da dobi prebivalstvo, ki pije mleko iz okolice bivšega rudnika urana Žirovski vrh, večjo dozo kot prebivalstvo drugod po Sloveniji. Podobno velja za dojenčke do enega leta, kjer bi prejeli največjo dozo dojenčki, ki bi uživali mleko v prahu iz Pomurskih mlekarn in sicer 648 μSv/leto, zatem tisti, ki bi uživali mleko iz okolice bivšega rudnika urana Žirovski vrh (562 μSv/leto), iz referenčnega vzorca (363 μSv/leto), najmanjšo dozo (195 μSv/leto) pa bi prejeli tisti, ki bi uživali mleko v prahu podjetja Hipp (tabela 11).

Rezultati, ki prikazujejo deleže posameznih radionuklidov v vsoti efektivne letne ingestijske doze so pokazali, da predstavljata največji delež pri dozni obremenitvi posameznikov tako v primeru odraslih kot tudi dojenčkov ^{210}Po in ^{210}Pb. Njun skupni delež presega 90 % doze pri vseh obravnavanih ciljnih skupinah (slika 88). Pri skupinah odraslih in dojenčkov, ki zaužijejo mleko iz vzorcev 1 – 4, odraslih in dojenčkov, ki zaužijejo mleko iz vzorca 5 ter pri dojenčkih, ki zaužijejo mleko v prahu iz Pomurskih mlekarn, predstavlja ^{210}Po največji prispevek k dozi zaradi zaužitja mleka (50 do 70 % doze). Le v primeru dojenčkov, ki zaužijejo mleko v prahu Hipp predstavlja ^{210}Pb največji prispevek k dozi (okrog 60 % doze). Razlog za to je v povprečju šestkrat nižja specifična aktivnost ^{210}Po v primerjavi z ^{210}Pb v vzorcih mleka v prahu Hipp (slika 85, tabela 9). Deleži ostalih analiziranih radionuklidov v vsoti efektivne letne ingestijske doze so zanemarljivi. Razloga za tako visok delež ^{210}Po in ^{210}Pb v vsoti efektivne letne ingestijske doze sta višje specifične aktivnosti teh dveh radionuklidov v primerjavi z ostalimi (slika 85, tabeli 8 in 9) ter višji predvideni efektivni dozi na enoto vnosa zaradi zaužitja za ^{210}Po in ^{210}Pb v primerjavi z ostalimi radionuklidi (tabela 10).

Rezultati meritev specifičnih aktivnosti ^{238}U, ^{234}U, ^{230}Th, ^{226}Ra, ^{210}Pb in ^{210}Po v vzorcih tal, travne silaže, sena in mleka so pokazali, da so le te v treh vzorcih tal za vse radionuklide, razen za ^{210}Pb in ^{210}Po, med seboj primerljive (tabeli 12 in 13). Izotopska razmerja ^{234}U/^{238}U so bila v omenjenih vzorcih večja ali enaka 1 in skladna s pričakovanji. Meritve specifičnih aktivnosti ^{210}Po in ^{210}Pb so pokazale neravnotežje med tema dvema radionuklidoma v vzorcih silaže in sena. Tako je bilo v silaži ^{210}Po približno 1,5 krat več, v senu pa približno 3 krat manj kot ^{210}Pb (tabela 13). Razlog za takšno nesorazmerje ni jasen. ^{210}Po je sicer znan kot hlapen radionuklid (Mabuchi, 1958) vendar pa temperature sušenja trave na soncu verjetno ne presegajo 80 °C, ki glede na podatke iz literature, predstavlja temperaturo pri kateri ni pričakovati zaznavne hlapnosti ^{210}Po.

Faktorji prenosa iz tal v silažo in v seno iz kmetije v bližini bivšega rudnika urana Žirovski vrh za ^{238}U, ^{234}U, ^{230}Th, ^{226}Ra in ^{210}Pb so bili primerljivi s tistimi, ki sem jih določil za vzorce trave z območja odlagališča Boršt (slika 89 in tabela 14 ter slike 65 – 72 in priloga 8). Najvišje faktorje prenosa iz tal v silažo in v seno sem določil za ^{210}Pb in ^{210}Po. Razlog za to je najverjetneje zračna depozicija ^{210}Pb in ^{210}Po na travo kar posledično zvišjuje faktorje prenosa.

Koncentracijska razmerja med silažo in senom ter mlekom so bila najvišja v primeru

^{238}U, ^{234}U in ^{230}Th in so znašala okrog 0,25 (tabela 14). Koncentracijska razmerja za ^{226}Ra, ^{210}Pb in ^{210}Po so bila mnogo manjša in so znašala okrog 0,07 za ^{226}Ra in okrog 0,02 za ^{210}Pb ter ^{210}Po.

Rezultati analiz medlaboratorijskih primerjav, ki so predstavljeni v tabeli 15, kažejo na visoko kakovost meritev radionuklidov, saj so bili v vseh primerih s strani organizatorjev medlaboratorijskih primerjav ovrednoteni kot zadovoljivi. Na žalost pa za radionuklide ne obstaja nobena medlaboratorijska primerjava ali ustrezni referenčni material za določanje vsebnosti radionuklidov v posameznih frakcijah s pomočjo sekvenčnih ekstrakcijskih postopkov.

6 Zaključki

Primerjava obeh sekvenčnih ekstrakcijskih postopkov je pokazala, da sta primerljiva le v primeru organske frakcije in preostanka za ^{238}U. Pri vseh ostalih frakcijah in radionuklidih pa sta oba postopka dajala statistično različne rezultate. Kljub temu je iz rezultatov sekvenčnih ekstrakcijskih postopkov mogoče ugotoviti, da se ^{238}U, ^{230}Th in ^{210}Pb zadržujejo v tleh v lokaciji 1, skozi katero teče izcedna voda iz odlagališča Boršt s povišano vsebnostjo naravnih radionuklidov. V lokaciji 2, skozi katero prav tako teče izcedna voda iz odlagališča, pa se radionuklidi v tleh ne zadržujejo. Ugotovil sem tudi, da so najvišje celotne specifične aktivnosti za vse radionuklide na dnu odlagališča (lokacija 4). Glede na deleže mobilnih frakcij v lokaciji 4, je ^{238}U na območju odlagališča Boršt najbolj mobilen, sledijo pa mu ^{226}Ra, ^{210}Pb, ^{230}Th in ^{210}Po. Rezultati izotopskih razmerij ^{234}U/^{238}U kažejo, da je vir urana pri mobilnih frakcijah iz lokacije 1 odlagališče HMJ, pri preostanku pa gre za uran, ki je naravno prisoten v okolju. V lokacijah 2 in 3 sem ugotovil, da gre tako v mobilnih frakcijah, kot tudi v preostanku za uran, ki je naravno prisoten v okolju in ni posledica odložene HMJ. V lokacijah 4, 5 in 6 pa je iz izotopskega razmerja ^{234}U/^{238}U moč razbrati, da je vir urana tako v mobilnih frakcijah, kot tudi v preostanku pretežno HMJ.

Faktorji prenosa iz tal v travo so znašali od 1,40E-3 do 1,47E-2 za ^{238}U, od 3,90E-3 do 1,24E-2 za ^{230}Th, od 3,46E-2 do 4,65E-1 za ^{226}Ra in od 9,83E-2 do 1,52E+0 za ^{210}Pb in so bili v glavnem primerljivi z vrednostmi iz literature (Vandenhove et al., 2009). Faktorji prenosa iz tal v travo za ^{230}Th in ^{210}Pb so se zmanjševali z naraščajočo specifično aktivnostjo v tleh, kar je značilnost esencialnih elementov. Specifične aktivnosti v travi in v tleh so bile linearno korelirane v primeru ^{238}U za lokacije 3, 4, 5 in 6, ter v primeru ^{226}Ra za lokacije 4, 5 in 6. To dejstvo predstavlja potencial za uporabo trave za sledenje migracije teh dveh radionuklidov v tleh.

Najvišjo vsebnost radionuklidov v drevesih sem določil v enoletnih iglicah ali listih, kar pomeni, da drevesa koncentrirajo radionuklide v starejše liste in iglice. Pri smrekah so vrednosti ^{226}Ra v enoletnih iglicah še posebno visoke in so znašale v posameznih primerih tudi do tretjine specifične aktivnosti ^{226}Ra v jalovini. Tudi do 100 krat nižje specifične aktivnosti ^{226}Ra pri borih v primerjavi s smrekami nakazujejo drugačen mehanizem privzema ^{226}Ra pri teh dveh vrstah dreves. Koncentracijska razmerja med specifično aktivnostjo v HMJ in specifično aktivnostjo v različnih delih dreves so pokazala, da je ^{226}Ra na območju odlagališča Boršt za drevesa najbolj biološko dostopen, temu pa sledijo ^{210}Pb, ^{238}U in ^{230}Th. Primerjava koncentracijskih razmerij za ^{238}U in ^{226}Ra v enoletnih borovih iglicah je pokazala, da so vrednosti primerljive z rezultati, ki jih poroča Petrova (2006).

Rezultati analiz ^{238}U, ^{234}U, ^{226}Ra, ^{210}Pb in ^{210}Po v vzorcih mleka in mleka v prahu so pokazali, da na splošno specifične aktivnosti omenjenih radionuklidov v vzorcih mleka iz okolice območja bivšega rudnika urana Žirovski vrh niso povišane v primerjavi z ostalimi vzorci. Vsota efektivnih letnih ingestijskih doz analiziranih radionuklidov za odrasle je pri vzorcih iz okolice bivšega rudnika urana Žirovski vrh znašala 13 μSv/leto, pri vzorcu iz referenčne lokacije pa 8,7 μSv/leto. Vsota efektivnih letnih ingestijskih doz analiziranih radionuklidov za dojenčke do enega leta starosti je znašala 648 μSv/leto za vzorec mleka v prahu iz Pomurskih mlekarni, 562 μSv/leto za vzorce iz okolice bivšega rudnika urana

Žirovski vrh, 363 μSv/leto za referenčni vzorec in 195 μSv/leto za vzorce mleka v prahu podjetja Hipp.

Rezultati meritev izotopskih razmerij med ^{234}U in ^{238}U v vzorcih mleka iz okolice bivšega rudnika urana Žirovski vrh in mleka v prahu iz Pomurskih mlekarn so bili manjši od 1, kar ni mogoče razložiti ne s tako imenovanim odbojnim efektom ne z morebitno napako pri meritvi. Zato bi bile potrebne dodatne obsežnejše raziskave celotne prehranske verige krav, da bi ugotovili morebitni vzrok.

Delež ^{210}Po in ^{210}Pb v vsoti efektivne letne ingestijske doze tako v primeru odraslih kot tudi dojenčkov presega 90 % doze pri vseh obravnavanih ciljnih skupinah. Razloga za to sta višje specifične aktivnosti teh dveh radionuklidov v primerjavi z ostalimi v vzorcih mleka ter višji predvideni efektivni dozi na enoto vnosa zaradi zaužitja za ^{210}Po in ^{210}Pb v primerjavi z ostalimi radionuklidi.

Koncentracijska razmerja med silažo in senom ter mlekom iz vzorcev iz kmetije v bližini bivšega rudnika urana Žirovski vrh so bila najvišja v primeru ^{238}U, ^{234}U in ^{230}Th in so znašala okrog 0,25. Koncentracijska razmerja za ^{226}Ra, ^{210}Pb in ^{210}Po so bila mnogo manjša in so znašala okrog 0,07 za ^{226}Ra in okrog 0,02 za ^{210}Pb ter ^{210}Po.

7 Zahvale

Zahvaljujem se mentorju doc. dr. Borutu Smodišu za njegovo mentorstvo, pomoč in nasvete pri pripravi doktorske disertacije. Prav tako se zahvaljujem vsem sodelavcem Odseka za znanosti o okolju Instituta Jožef Stefan za vsakršno pomoč in podporo pri mojem doktorskem delu.

Zahvaljujem se tudi podjetju Rudnik Žirovski vrh in njihovim sodelavcem, med katerimi bi izpostavil predvsem gospoda Jožeta Rojca, da so mi omogočili vzorčenje na območju odlagališča Boršt in mi pomagali pri vzorčenju. Brez njihove kooperativnosti in pomoči moje doktorsko delo ne bi bilo mogoče.

Zahvalil bi se rad tudi dr. Klemenu Elerju iz Oddelka za Agronomijo Biotehniške fakultete v Ljubljani za njegovo pomoč pri vzorčenju in pripravi vzorcev.

Zahvala gre tudi Javni agenciji za raziskovalno dejavnost Republike Slovenije, ki je v sklopu programa mladih raziskovalcev financirala moje doktorsko delo.

Na koncu bi se še rad zahvalil moji družini, predvsem ženi Sanji, ki mi je vedno stala ob strani in me podpirala pri mojem delu, kljub temu, da je to pomenilo, da sem manj časa preživel z njimi.

8 Literatura in viri

Adloff, J. P.; Rössler, K. Recoil and transmutation effects in the migration behaviour of actinides. *Radiochimica Acta* **52/53**, 269-274 (1991).

Aguado, J. L.; Bolivar, J. P.; Tenorio, R. G. Sequential extraction of ^{226}Ra in sediments from an estuary affected historically by anthropogenic inputs of natural radionuclides. *Journal of Environmental Radioactivity* **74**, 117-126 (2004).

Al-Masri, M. S.; Al-Karfan, K.; Khalili, H.; Hassan, M. Speciation of ^{210}Po and ^{210}Pb in air particulates determined by sequential extraction. *Journal of Environmental Radioactivity* **91**, 103-112 (2006).

Bacon, J. R.; Davidson, C. M. Is there a future for sequential chemical extraction? *Analyst* **133**, 25-46 (2008).

Benedik, L.; Vreček, P. Determination of ^{210}Pb and ^{210}Po in environmental samples. *Acta Chimica Slovenica* **48**, 199-213 (2001).

Blanco, P.; Vera Tome, F.; Lozano, J. C. Fractionation of natural radionuclides in soils from a uranium mineralized area in the south-west of Spain. *Journal of Environmental Radioactivity* **79**, 315-330 (2005).

Bland, J. M.; Altman, D. G. Statistical methods for assessing agreement between two methods of clinical measurement. *Lancet* **327**, 307-310 (1986).

Bourdon, B.; Turner, S.; Henderson, G. M.; Lundstrom, C. C. Introduction to U-series geochemistry. *Reviews In Mineralogy & Geochemistry* **52**, 7-10 (2003).

Currie, L. A. Limits for qualitative detection and quantitative determination: Application to radiochemistry. *Analytical Chemistry* **40**, 586-592.

Desideri, D.; Roselli, C.; Meli, M. A.; Feduzi, L. Analytical methods for the characterization and the leachability evaluation of a solid waste generated in a phosphoric acid production plant. *Microchemical Journal* **88**, 67-73 (2008).

Eurachem. *Quantifying uncertainty in analytical measurement, second edition* (2000).

Florjančič, A. P. *Rudnik urana Žirovski vrh* (Didakta, Radovljica, 2000).

Galindo, C.; Mougin, L.; Fakhi, S.; Nourreddine, A.; Lamghari, A.; Hannache, H. Distribution of naturally occurring radionuclides (U, Th) in Timahdit black shale (Morocco). *Journal of Environmental Radioactivity* **92**, 41-54 (2007).

Gibson, W. M. *The radiochemistry of lead* (USDOE Technical Information Center, Oak Ridge, Tenessee, 1961).

Hampel, C. A. (edit.). *The encyclopedia of the chemical elements* (Reinhold Book Corporation, New York, 1968).

Hindman, F. D. Neodymium fluoride mounting for alpha spectrometric determination of uranium, plutonium, and americium. *Analytical Chemistry* **55**, 2460-2461 (1983).

Horwitz, E. P.; Chiarizia, R.; Dietz, M. L.; Diamond, H.; Nelson, D. M. Separation and preconcentration of actinides from acidic media by extraction chromatography. *Analytica Chimica Acta* **281**, 361-372 (1993).

Hyde, E. K., *The radiochemistry of thorium* (USDOE Technical Information Center, Oak Ridge, Tennessee, 1960).

IAEA. *International basic safety standards for protection against ionizing radiations and for the safety of radiation sources* (IAEA Safety Series No. 115, Vienna, 2003).

IAEA. *Quantifying uncertainty in nuclear analytical measurements* (IAEA-TECDOC-1401, Vienna, 2004).

ISO 11464:1994(E). *Soil quality – Pretreatment of samples for physico-chemical analyses* (International Organization for Standarisation, Geneve, 1994).

IUPAC. Guidelines for terms related to chemical speciation and fractionation of elements. Definitions, structural aspects, and methodological approaches. *Pure and Applied Chemistry* **72**, 1453-1470 (2000).

Jia, G.; Torri, G.; Innocenzi, P. An improved method for the determination of uranium isotopes in environmental samples by alpha-spectrometry. *Journal of Radioanalytical and Nuclear Chemistry* **262**, 433-441 (2004).

Jia, G.; Torri, G. Determination of ^{210}Pb and ^{210}Po in soil or rock samples containing refractory matrices. *Applied Radiation and Isotopes* **65**, 1-8 (2007).

Kirby, H. W.; Salutsky, M. L., *The radiochemistry of radium* (USDOE Technical Information Center, Oak Ridge, Tennessee, 1964).

Križman, M.; Byrne, A. R.; Benedik, L. Distribution of ^{230}Th in milling wastes from the Žirovski vrh uranium mine (Slovenia), and its radioecological implications. *Journal of Environmental Radioactivity* **26**, 223-235 (1995).

L'Annunziata, M. F. *Handbook of Radioactivity Analysis* (Academic Press, San Diego, 1998).

La Force, M. J.; Fendorf, S. Solid-phase iron characterization during common selective sequential extractions. *Soil Science Society of America Journal* **64**, 1608-1615 (2000).

Lozano, J. C.; Fernandez, F.; Gomez, J. M. G. Determination of radium isotopes by $BaSO_4$ coprecipitation for the preparation of alpha-spectrometric sources. *Journal of Radioanalytical and Nuclear Chemistry* **223**, 133-137 (1997).

Mabuchi, H. On the Volatility of Polonium Compounds. *Bulletin of the Chemical Society of Japan* **31**, 245-246 (1958).

Madruga, M. J.; Brogueira, A.; Alberto, G.; Cardoso, F. ^{226}Ra bioavailability to plants at the Urgeirica uranium mill tailings site. *Journal of Environmental Radioactivity* **54**, 175-188 (2001).

Omahen, G.; Benedik, L.; Repinc, U. *Nadzor radioaktivnosti v okolju rudnika urana Žirovski vrh med izvajanjem programa trajnega prenehanja izkoriščanja uranove rude in ocena vplivov na okolje – rezultati za leto 2005* (Institut Jožef Stefan, Ljubljana, IJS-DP-9342, 2006).

Petrova, R. Accumulation of natural radionuclides in wooden and grass vegetation from abandoned uranium mines. Opportunities for phytoremediation. V: Merkel, B. J., Hasche-Berger, A. (ed.) *Uranium in the environment, mining impact and consequences*. 507-518 (Springer-Verlag, Berlin Heidelberg, 2006).

Rauret, G.; Lopez-Sanchez, J. F.; Sahuquillo, A.; Rubio, R.; Davidson, C.; Ure, A.; Quevauviller, Ph. Improvement of the BCR three step sequential extraction procedure prior to the certification of new sediment and soil reference materials. *Journal of Environmental Monitoring* **1**, 57-61 (1999).

Rodríguez, P. B.; Tomé, F. V.; Lozano, J. C.; Fernández M. A. P. Transfer of ^{238}U, ^{230}Th,

^{226}Ra, and ^{210}Pb from soils to tree and shrub species in a Mediterranean area. *Applied Radiatation and Isotopes* **68**, 1154-1159 (2010).

Schultz, M. K.; Burnett, W. C.; Inn, K. G. W. Evaluation of a sequential extraction method for determining actinide fractionation in soils and sediments. *Journal of Environmental Radioactivity* **40**, 155-174 (1998).

Sheppard, M. I.; Sheppard, S. C. The plant concentration ratio concept as applied to natural U. *Health Physics* **48**, 494-500 (1985).

Sill, C. W. Decomposition of refractory silicates in ultramicro analysis. *Analytical Chemistry* **33**, 1684-1686 (1961).

Sill, C. W.; Williams, R. L. Preparation of actinides for alpha spectrometry without electrodeposition. *Analytical Chemistry* **53**, 412-415 (1981).

Suksi, J.; Rasilainen, K.; Pitkänen, P. Variations in ^{234}U/^{238}U activity ratios in groundwater – A key to flow system characterisation?. *Physics and Chemistry of the Earth* **31**, 556-571 (2006).

Tessier, A.; Campbell, P. G. C.; Bisson, M. Sequential extraction procedure for the speciation of particulate trace metals. *Analytical Chemistry* **51**, 844-851 (1979).

Thiry, Y.; Schmidt, P.; Hees, M. V.; Wannijn, J.; Bree, P. V.; Rufyikiri, G.; Vandenhove, H. Uranium distribution and cycling in Scots pine (Pinus sylvestris L.) growing on a revegetated U-mining heap. *Journal of Environmental Radioactivity* **81**, 201-219 (2005).

Trautmannsheimer, M.; Schramel, P.; Winkler, R.; Bunzl, K. Chemical fractionation of some natural radionuclides in a soil contaminated by slags. *Environmental Science & Technology* **32**, 238-243 (1998).

Uradni list Republike Slovenije. *Uredba o mejnih dozah, radioaktivni kontaminaciji in intervencijskih nivojih* (Uradni list Republike Slovenije, Ljubljana, **49**, 2004)

Ure, A. M.; Quevauviller, Ph.; Muntau, H.; Griepink, B. Speciation of heavy metals in soils and sediments. An account of the improvement and harmonization of extraction techniques undertaken under the auspices of the BCR of the Commission of the European Communities. *International Journal of Environmental Analytical Chemistry* **51**, 135-151 (1993).

Ure, A. M.; Davidson, C. M., *Chemical speciation in the environment, second edition* (Blackwell Science, Oxford, 2002).

Vajda, N.; LaRosa, J.; Zeisler, R.; Danesi, P.; Kis-Benedek, Gy. A novel technique for the simultaneous determination of ^{210}Pb and ^{210}Po using a crown ether. *Journal of Environmental Radioactivity* **37**, 355-372 (1997).

Vandenhove, H.; Olyslaegers, G.; Sanzharova, N.; Shubina, O.; Reed, E.; Shang, Z.; Velasco, H. Proposal for new best estimates of the soil-to-plant transfer factor of U, Th, Ra, Pb and Po. *Journal of Environmental Radioactivity* **100**, 721-732 (2009).

Vreček, P.; Benedik, L.; Pihlar, B. Determination of ^{210}Pb and ^{210}Po in sediment and soil leachates and in biological materials using a Sr-resin column and evaluation of column reuse. *Applied Radiation and Isotopes* **60**, 717-723 (2004).

Kazalo slik

Kazalo tabel

Priloge

Priloga 1: Lastne objave iz disertacije

Štrok, M., Smodiš, B. Fractionation of natural radionuclides in soils from the vicinity of a former uranium mine Žirovski vrh, Slovenia. Journal of Environmental Radioactivity **101**, 22-28 (2010).

Štrok, M., Smodiš, B. Comparison of two sequential extraction protocols for fractionation of natural radionuclides in soil samples. *Radiochimica acta* **98**, 221-229 (2010).

Benedik, L., Repinc, U., Štrok, M. Evaluation of procedures for determination of Ra-226 in water by α-particle spectrometry with emphasis on the recovery. *Applied Radiation and Isotopes* **68**, 1221-1225 (2010).

Štrok, M., Smodiš, B. Natural radionuclides in milk from the vicinity of a former uranium mine. *Nuclear Engineering and Design* v tisku, doi: 10.1016/j.nucengdes.2010.03.035 (2010).

Černe, M., Smodiš, B., Štrok, M., Jaćimović, R. Accumulation of ^{226}Ra, ^{238}U and ^{230}Th by wetland plants in a vicinity of U-mill tailings at Žirovski vrh (Slovenia). *Journal of Radioanalytical and Nuclear Chemistry* v tisku, doi: 10,1007/s10967-010-0708-0 (2010).

Černe, M., Smodiš, B., Štrok, M., Uptake of radionuclides by a common reed (*Phragmites australis* (Cav.) Trin. ex Steud.) grown in the vicinity of the former uranium mine at Žirovski vrh. *Nuclear Engineering and Design* v tisku, doi: 10.1016/j.nucengdes.2010.04.003 (2010).

Štrok, M., Repinc, U., Smodiš, B. Calibration and validation of a proportional counter for determining beta emitters. *Journal of Power and Energy Systems* **2**, 573-581 (2008).

V nadaljevanju so članki predstavljeni v celoti.

Priloga 1: Nadaljevanje

Journal of Environmental Radioactivity 101 (2010) 22–28

Contents lists available at ScienceDirect

Journal of Environmental Radioactivity

journal homepage: www.elsevier.com/locate/jenvrad

Fractionation of natural radionuclides in soils from the vicinity of a former uranium mine Žirovski vrh, Slovenia

Marko Štrok, Borut Smodiš*

Jožef Stefan Institute, Jamova 39, SI-1000 Ljubljana, Slovenia

ARTICLE INFO

Article history:
Received 24 March 2009
Received in revised form
27 July 2009
Accepted 4 August 2009
Available online 16 September 2009

Keywords:
Sequential extraction
Natural radionuclides
Alpha spectrometry
Radiochemical disequilibrium

ABSTRACT

As a result of former uranium mining and milling activities at Žirovski vrh, Slovenia, 0.6 million tons of uranium mill tailings (UMT) were deposited onto a nearby waste pile Boršt. Resulting enhanced levels of natural radionuclides in UMT could pose threat for the surrounding environment. Therefore, sequential extraction protocol was performed to assess mobility and bioavailability of ^{238}U, ^{234}U, ^{230}Th and ^{226}Ra in soils from the waste pile and its surrounding. The radionuclides associated with exchangeable, organic, carbonate, Fe/Mn oxides and residual fraction, respectively, were determined. Results showed that the highest activity concentrations for the studied radionuclides were on the bottom of the waste pile. In non-contaminated locations, about 80% of all radionuclides were in the residual fraction. Considering activity concentrations in the UMT, ^{238}U and ^{234}U are the most mobile. Mobility of ^{226}Ra is suppressed by high sulphate concentrations and is similar to mobility of ^{230}Th.

1. Introduction

Industrial excavations of the uranium ore in the area of Žirovski vrh, Slovenia were started in the year 1982. Yellowcake production was started two years later and lasted up to 1990, when the mining and milling activities were stopped. During this time, about 0.6 million tons of uranium ore and more than 2.5 million tons of other waste rocks and pore uranium ore were excavated. After the uranium ore was crushed and milled in a mill, it was leached with H_2SO_4 in order to obtain uranium from the ore. Remains after leaching are called uranium mill tailings (UMT). UMT is gray coloured waste product from leaching and contains enhanced levels of all decay products from the ^{238}U decay chain. Activity concentrations in the UMT at Boršt are: (995 ± 80) Bq/kg of ^{238}U, (3930 ± 580) Bq/kg of ^{230}Th and (8630 ± 340) Bq/kg of ^{226}Ra (Križman et al., 1995).

UMT was deposited onto the Boršt waste pile, which lies close to the uranium mine. The amount of UMT is about 0.6 million tons. In the time of sampling, the Boršt waste pile was covered with 30–40 cm thick soil cover and overgrown with grass and pine trees. The waste pile is situated in the subalpine region with relatively high rainfall and within a relatively densely populated area. Therefore, it is very important to assess mobility and bioavailability of natural radionuclides present in the tailings, both from radiation protection and long-term stability of waste pile viewpoints.

Sequential extraction is one of the powerful tools for assessing mobility and bioavailability of contaminants in the environment. Since their introduction in the late 1970s, sequential extraction procedures have experienced a rapid increase in use for a large number of potentially toxic elements in a wide range of sample types (Bacon and Davidson, 2008). Nowadays two procedures have attained almost a rank of standard, one is Tessier's method (Tessier et al., 1979) and the other is so called BCR method (Quevauviller et al., 1993). Use of sequential extraction procedures for natural radionuclide investigations is rather scarce (Bunzl et al., 1995; Blanco et al., 2005) and usually implies Tessier's method or Schultz modification of Tessier method (Schultz et al., 1998). Blanco et al. (2004) investigates both Tessier's method and Schultz modification of Tessier's method and concluded that the two procedures yield different results and that Schultz modifications better suit the objectives of this type of sequential protocol. Therefore, Schultz modification of Tessier's method was used in our study.

2. Materials and methods

2.1. Sampling and sample preparation

About 5 kg of each soil sample from six sites at the Boršt waste pile, presented in Fig. 1, were collected at the depth 10–15 cm. The sites 1 and 2 lie in two swampy areas through which seepage water from the Boršt waste pile with elevated radionuclides concentrations is flowing. It was expected that in these sites the radionuclides could be retained and consequently their activity concentrations elevated. The

* Corresponding author. Tel.: +38615885353; fax: +38615885346.
E-mail addresses: marko.strok@ijs.si (M. Štrok), borut.smodis@ijs.si (B. Smodiš).

0265-931X/$ – see front matter © 2009 Elsevier Ltd. All rights reserved.
doi:10.1016/j.jenvrad.2009.08.006

Priloga 1: Nadaljevanje

Fig. 1. Air picture of the Boršt waste pile; numbers represent sampling sites.

site 3 lies outside of the waste pile and should not be affected by the radionuclides from the waste pile. Therefore, it was considered as a non-contaminated site. The other three sites lie on the waste pile and represent basically UMT covered with soil.

Pretreatment of the samples was performed according to the ISO 11464 (1994). After sampling, the samples were weighed, dried in an oven at 80 °C and again weighed. Samples were then sieved through 2 mm sieve. Bigger clods were crushed with a mortar and pestle and again sieved through 2 mm sieve. Sample was then subsampled by hand quartering into representative portions of about 200 g to get a laboratory sample and stored until analysis. To obtain required amount of the sample for the analysis (i.e., 1.5 g), laboratory sample was further subsampled by hand quartering into representative portions. One part of each sample was sent to the Pedological Centre of the Department of Agronomy, Biotechnical Faculty, University of Ljubljana, for the pH, organic matter, carbonate content and particle size distribution determinations.

2.2. Sequential extraction procedure

1.5 g of the sample was weighed into a centrifuge tube and wetted overnight with deionized water. Then, sequential extraction procedure according to Table 1 was applied (Schultz et al., 1998). In each sequential extraction step, 22.5 mL of extractive reagent was added and samples were shaken at 180 rpm. Shaking times are presented in Table 1. For organic matter fraction, the samples were shaken in a shaking water bath at 96 °C. After each sequential extraction step, the samples were centrifuged for 30 min at 3000 rpm and filtered through a 0.1 μm pore diameter filter. The residue was reintroduced into the following sequential extraction step and the radionuclides in filtrate were separated according to the radiochemical separation procedure (Fig. 2).

2.3. Radiochemical separation procedure

Radiochemical separation procedure for solutions after each sequential extraction step is summarized in Fig. 2. ^{226}Ra was separated using principles described in Lozano et al. (1997). Uranium and thorium isotopes were separated on an UTEVA separation column.

To the filtered solution from each sequential extraction step ^{232}U, ^{229}Th and ^{133}Ba tracers were added in order to determine radiochemical recovery. Radium and barium were coprecipitated with $PbSO_4$ with addition of 1 mL concentrated H_2SO_4 and 1 mL of $Pb(NO_3)_2$ solution (50 mg/mL Pb^{2+}). After 10 min, sample was centrifuged for 10 min at 3000 rpm. Supernatant containing uranium and thorium was decanted. Precipitate containing radium and barium was washed with deionized water in order to remove excess H_2SO_4 and again centrifuged. This step was repeated until neutral pH was achieved. Then the precipitate was dissolved with addition of 4 mL 0.1 M EDTA/0.5 M NaOH with help of an ultrasound bath. If the amount of EDTA and NaOH was not sufficient for complete dissolution of $PbSO_4$, more EDTA and NaOH was added. Then 0.3 mL Ba carrier (0.3 mg/mL Ba^{2+}) and one drop of liquid pH 0–5 indicator were added. Then the pH was adjusted to acidic with addition of 1 mL 1:1 acetic acid. After that, 4 mL of saturated Na_2SO_4 was added in order to form $Ba(Ra)SO_4$ precipitate. Then 0.3 mL of 0.125 mg/mL $BaSO_4$ substrate was added. After 10 min, solution was filtered through a 0.1 μm pore diameter filter and after that the filter was washed two times with deionized water. The filter was then mounted on a stainless steel disc with water basis glue and dried under a heating lamp. After drying, the so prepared counting source was ready for measurement.

To the supernatant – containing uranium and thorium –, which was left after $PbSO_4$ precipitate centrifugation, ammonia solution was added until alkaline pH was achieved. Uranium and thorium were coprecipitated as $Fe(OH)_3$ with addition of three drops of 5 mg/mL Fe^{3+} solution. After 30 min, the sample was centrifuged for 10 min at 3000 rpm. Solution was decanted and precipitate was washed with deionized water and again centrifuged. This step was repeated until neutral pH was achieved. After that, precipitate was dissolved with 10 mL of 3 M HNO_3/1 M $Al(NO_3)_3$ and solution transferred onto a TEVA separation resin. TEVA separation resins were packed into column and pre-conditioned with 5 mL of 3 M HNO_3. Eluates were collected in centrifuge tubes. In this step, thorium was retained on TEVA separation column and uranium was eluted. The centrifuge tube was rinsed with 5 mL of 2.5 M HNO_3 and again processed through the column. Finally, the column was washed with 30 mL of 2.5 M HNO_3 and the eluate retained for further purification on an UTEVA separation column. Thorium was eluted from the TEVA column with consecutive addition of 20 mL 9 M HCl and 5 mL of 6 M HCl and the eluate collected in a centrifuge tube.

Uranium-containing eluate, which was left from separation on TEVA column, was transferred onto an UTEVA separation column that was previously conditioned with 5 mL of 3 M HNO_3. The centrifuge tube in which was uranium-containing eluate was rinsed with 5 mL of 3 M HNO_3 and processed through the column. The column was rinsed with consecutive addition of 5 mL of 3 M HNO_3, 5 mL of 9 M HCl and 20 mL of 5 M HCl/0.05 M oxalic acid. Eluates from all prior steps were discarded and uranium finally eluted with 15 mL of 1 M HCl into a centrifuge tube.

Thorium was microprecipitated with addition of 0.1 mL of 0.5 mg/mL Nd^{3+} and 1 mL of concentrated HF. Uranium was microprecipitated with addition of 0.1 mL 0.5 mg/mL Nd^{3+}, 1 mL of 15% $TiCl_3$ and 1 mL of concentrated HF. Both thorium and uranium microprecipitates were placed prior to filtration for at least 30 min into ice bath. Filtration was carried out through a 0.1 μm pore diameter filter that was previously rinsed twice with 5 mL of 10 μm/mL NdF_3 substrate solution. The centrifuge tube was rinsed twice with 2 mL of 0.58 M HF and twice with deionized water. Finally, the filter was mounted on stainless steel disc with water basis glue and dried under a heating lamp.

Procedure for the radiochemical separation of the residue that remained after the final sequential extraction step is summarized in Fig. 3. Residue was ashed for 5 h at 650 °C and afterwards digested using principles described by Jia et al. (2004) and Sill (1961). 0.5 g of ash was introduced into a glassy carbon crucible together with 2 g of Na_2CO_3 and 2 g of Na_2O_2, and melted in muffle furnace for 5 min at 900 °C. After cooling to the room temperature ^{232}U, ^{229}Th and ^{133}Ba tracers were added in order to trace radiochemical recovery. The melt was dissolved with 1 mL of deionized water and 4 mL of concentrated HNO_3, and transferred into a Teflon beaker. To the sample, 5 mL concentrated HCl, 5 mL concentrated HNO_3, 5 mL concentrated HF and 5 mL H_2O_2 were added and evaporated until incipient dryness on a hot plate. This procedure was repeated three times in order to remove silicates. Afterwards, 8 mL of concentrated H_2SO_4 was added and evaporated until incipient

Table 1
Modified Tessier sequential extraction procedure.

Target fraction	Extractive reagent	Reagent/sample ratio	Temp (°C)	Shaking time (h)
Exchangeable	0.4 M $MgCl_2$ pH5	15:1	Room temp.	1
Organic matter	5–6% NaOCl pH 7.5	15:1	96	0.5 × 2
Carbonates	1 M NaAc in 25% HAc pH4	15:1	Room temp.	2 × 2
Oxides (Fe/Mn)	0.04 M NH_2OH HCl pH 2 (HNO_3)	15:1	Room temp.	5
Residue	NaOH fusion and HNO_3/HCl/HF/$HClO_4$		900	

Priloga 1: Nadaljevanje

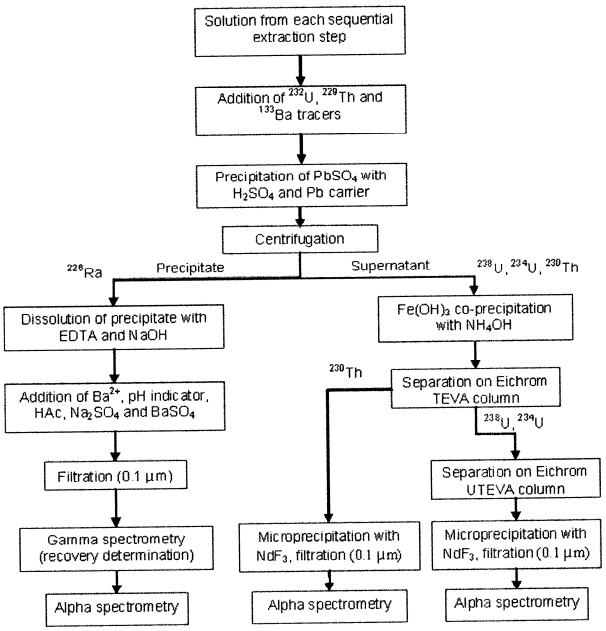

Fig. 2. Radiochemical separation procedure for solution from each sequential extraction step.

dryness. This step removed any residual HF and fluorosilicates and converted salts into sulphates. After final evaporation, the sample was dissolved with 2 mL deionized water and 2 mL concentrated HNO_3. Finally, the obtained solution was processed the same way as the other fractions of the sequential extraction steps.

2.4. Measurement system

All counting sources were measured on alpha spectrometric systems equipped with passivated implanted planar silicon (PIPS) detectors (Alpha Analyst, Canberra). Radiochemical recovery for ^{226}Ra was determined via measurement of ^{133}Ra tracer on gamma-ray spectrometer consisting of HP Ge detector connected to a multichannel analyser (Spectrum Master 919, Ortec).

3. Results and discussion

3.1. Physicochemical parameters

Results for physicochemical parameters are shown in Table 2. It can be observed that at almost all locations pH of soil is slightly acidic, only at location 4 the pH is neutral. This can be attributed to the highest carbonate content in that location. Organic matter content varies from 2.1 to 5.9%. Carbonates content is the highest at site four, 7.9%, and much lower (up to 1.6%) at other locations. Particle size distribution at sites 4 and 6, which lies on the waste pile, is almost identical. Silt fraction is dominant at site 3 and sand fraction at site 1. At site 2, soil particles are almost equally distributed among sand, silt and clay fractions.

3.2. Sequential extraction

Results of the applied sequential extraction are presented in Fig. 4. Uncertainties are not shown because of better clarity and are in the range from 4 to 15%, depending on the activity concentration. Radiochemical recovery varied from 47 to 95%, 46 to 92% and 54 to 87% for U, Th and Ra radionuclides, respectively.

Analytical determinations reveal that the studied radionuclides are not concentrated at site 2, as both total activity concentrations and distribution of radionuclides among different fraction are similar as in site 3 lying outside of the waste pile. On the other hand, elevated activity concentrations of $^{234/238}U$ in site 1 and its distribution profile among different fractions at that site that is similar to those at sites 4 and 6, indicates that uranium is retained in this site. ^{226}Ra is not retained in the swampy sites 1 and 2. Activity concentration profiles for ^{230}Th at sites 1 and 2 are similar as for $^{234/238}U$; ^{230}Th is retained in site 1 but not in site 2. However, difference in the distribution profile of ^{230}Th between the sites 1, 4, 5 and 6 with elevated activity concentrations and sites 2 and 3 are much smaller. Maximum activity concentrations for all the radionuclides were determined in site 4, which lies on the bottom of the waste pile and is therefore under direct influence of washout from the pile.

Approximately 80% of the ^{238}U, ^{234}U and ^{226}Ra in the non-contaminated sites were found in the residual fraction. This confirms the thesis that the radionuclides contained in the samples, which are not affected from mining and milling activities, are present mostly within primordial minerals. Oppositely, about 60% of $^{234/238}U$ in the

Priloga 1: Nadaljevanje

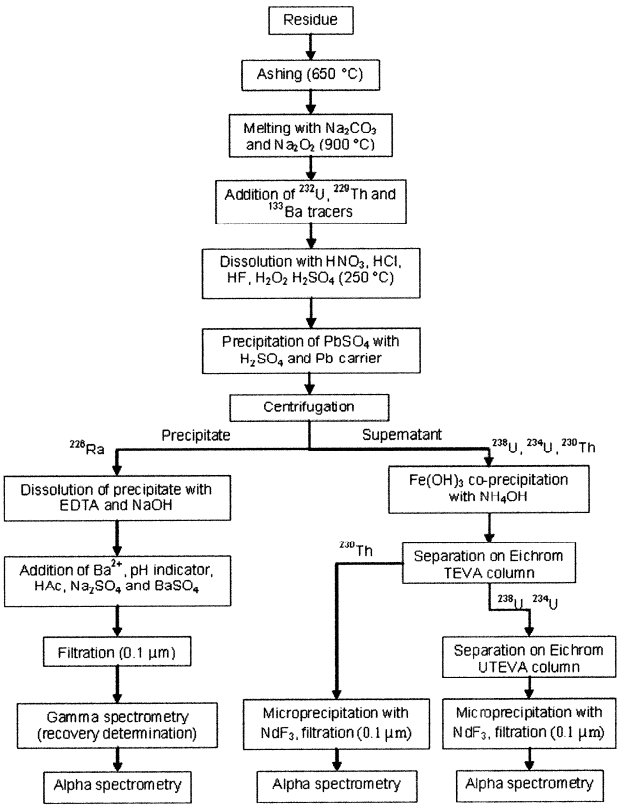

Fig. 3. Radiochemical separation procedure for residue after the final extraction step.

sites 4 and 6, and about 40% in the site 1 are present in the organic fraction, with only about 20% in the residual fraction. This could be attributed to the fact that those sites are contaminated with $^{234/238}U$ released from the deposited UMT. Similar conclusions can be drawn for ^{226}Ra, where 50–60% of ^{226}Ra is present in the residual fraction at the contaminated sites 4, 5 and 6; this is up to 30% lower than at the non-contaminated sites 1, 2 and 3.

Table 2
Physicochemical parameters for collected soil samples.

Location	pH in $CaCl_2$	Organic matter (%)	Carbonates (%)	Sand (%)	Silt (%)	Clay (%)
1	5.4	5.4	1.6	62.0	27.5	10.5
2	4.5	3.8	0.8	37.2	36.3	26.5
3	4.5	5.9	1.2	12.5	68.2	19.3
4	7	3.8	7.9	46.7	34.9	18.4
6	5.9	2.1	<0.5	49.9	31.3	18.8

This pattern is different for ^{230}Th, where its distribution among the different fractions at the sites 2–5 is similar, although the total activity concentrations are quite different. This confirms low solubility of thorium, which remains mostly in the residual fraction also in the contaminated areas; approximately 80% in sites 2–5, 60% in the site 6 and 50% in the site 1.

Activity concentration of ^{226}Ra in UMT is almost nine times higher than for ^{238}U, as shown in Section 1. However, uranium is shown to be much more mobile. Mobility of ^{226}Ra from UMT is suppressed by high concentrations of sulphate ions as a consequence of uranium extraction process, leading to the formation of stable $RaSO_4$, and thus reducing the mobility of radium.

3.3. $^{234}U/^{238}U$ ratios and radiochemical disequilibrium

Under undisturbed and steady conditions equilibrium would be expected between activity concentration of ^{238}U and ^{234}U;

Priloga 1: Nadaljevanje

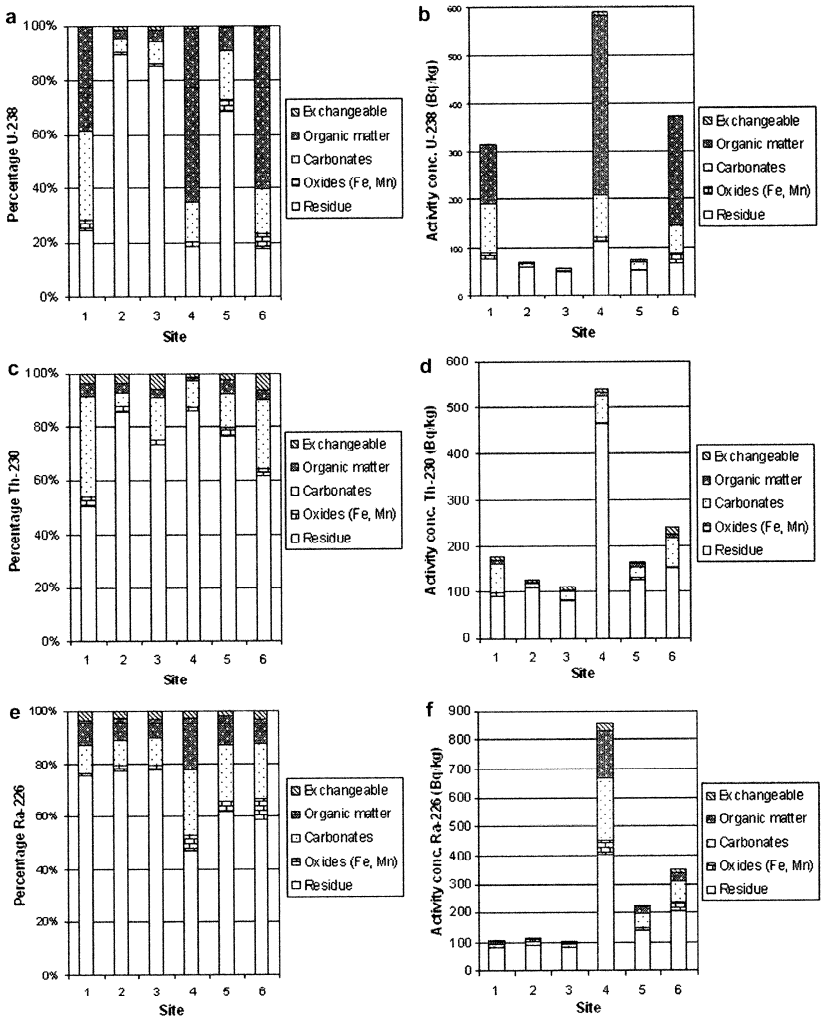

Fig. 4. Results of the sequential extraction.

however, this is not always the case. According to Bourdon et al. (2003), Adloff and Rössler (1991) and Suksi et al. (2006), the reason for $^{234}U/^{238}U$ disequilibrium is (1) recoil effect, which induces ejection of decay product from a particle into its environment, and (2) increased mobility of a decay product due to subsequent oxidation of ^{234}U in zones which are not close to phase boundary. This effect is evidenced by reduced $^{234}U/^{238}U$ ratio within the observed particle and increased ratio in its environment. According to the above-mentioned reasoning, within the Boršt waste pile, i.e., in UMT and in sites contaminated with UMT ^{234}U and ^{238}U should be in equilibrium, as the tailings are the remains of a crushed ore leached with H_2SO_4. Consequently, the recoil effect and oxidation

Priloga 1: Nadaljevanje

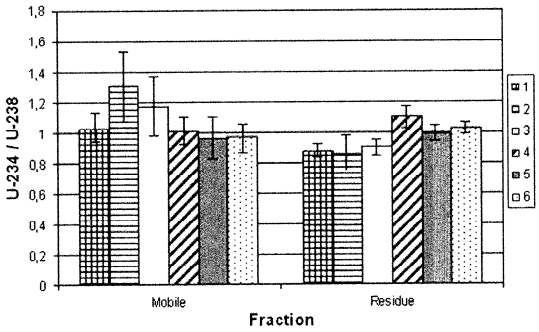

Fig. 5. $^{234}U/^{238}U$ ratios for mobile and residual fractions.

state impact are assumed to not have that important influence on the isotope ratio. In the undisturbed locations that are not affected with UMT, however, the ratio in residual fraction could be expected to be less than 1. Following the same reasoning for a mobile fraction, ^{234}U and ^{238}U could be expected to be in equilibrium in the areas contaminated by UMT leached-out water, but ^{234}U enrichment could be expected in non-contaminated locations.

In Fig. 5 $^{234}U/^{238}U$ ratios are shown for the mobile (referred to as summed measurement results for the exchangeable, organic matter, carbonate and Fe/Mn oxides fractions) and the residual fractions. In the sites 2 and 3 the ratio in mobile fraction is 1.2, supporting hypothesis that those sites are not influenced by the contaminated material. Further support to this hypothesis gives results for the residual fractions, where $^{234}U/^{238}U$ ratio is 0.9. The similar ratio was found in the site 1, giving supportive evidence that the residual fraction from that site is also not contaminated. In the mobile fractions at sites 1, 4 and 6, ^{234}U and ^{238}U are in equilibrium, i.e., their ratio is about 1. This finding suggests that the mobile fraction in the site 1 might be contaminated by the mobile material leached from the UMT containing pile.

4. Conclusions

Measurement results showed that uranium and ^{230}Th are retained in swampy site 1 but not in swampy site 2, whilst ^{226}Ra is not retained in any of the two sites. In the non-contaminated sites, the studied radionuclides are mainly concentrated in the residual fraction. In the contaminated sites uranium is mainly found in the organic fraction. ^{230}Th is very insoluble, and consequently found in both contaminated and non-contaminated sites mainly in the residual fraction. ^{226}Ra distribution in the contaminated sites is somewhere between uranium and ^{230}Th with about 60% found in the residual fraction. Considering activity concentrations in the UMT, it can be concluded that ^{238}U and ^{234}U are the most mobile radionuclides among the studied ones. Mobility of ^{226}Ra is suppressed by the high sulphate ion concentrations in the UMT and its distribution is similar to ^{230}Th.

$^{234}U/^{238}U$ ratio in the mobile fraction in the site 1 is the same as for the sites 4–6, thus giving support to the hypothesis that uranium in the mobile fraction from that location is result of the UMT leaching. Results for the sites 2 and 3 are similar, thus giving support to the assumption that the site 2 is not contaminated with uranium from the UMT. However, more profound studies should be carried out to definitely confirm the given hypothesis.

Sequential extraction proved to be a very useful tool for assessing radionuclide migration and mobility in soils. $^{234}U/^{238}U$ ratio determination yielded helpful evidence for identifying if uranium found at a specific sampling site is of natural origin or transported from the waste pile.

The obtained results will contribute to the further decisions on how to remediate the contaminated area of the former uranium mine in order to minimise the influence of the waste pile onto the nearby environment.

Acknowledgements

The authors would like to thank the staff of the Rudnik Žirovski vrh company for their cooperation and assistance. Financial support of the Slovenian Research Agency (Grant No. P2-0075) is highly appreciated.

References

Adloff, J.P., Rössler, K., 1991. Recoil and transmutation effects in the migration behaviour of actinides. Radiochim. Acta 52/53, 269–274.
Bacon, J.R., Davidson, C.M., 2008. Is there a future for sequential chemical extraction? Analyst 133, 25–46.
Blanco, P., Vera Tomé, F., Lozano, J.C., 2004. Sequential extraction for radionuclide fractionation in soil samples: a comparative study. Appl. Radiat. Isot. 61, 345–350.
Blanco, P., Vera Tomé, F., Lozano, J.C., 2005. Fractionation of natural radionuclides in soils from a uranium mineralized area in the south-west of Spain. J. Environ. Radioact. 79, 315–330.
Bourdon, B., Turner, S., Henderson, G.M., Lundstrom, C.C., 2003. Introduction to U-series geochemistry. In: Bourdon, B., Henderson, G.M., Lundstrom, C.C., Turner, S.P. (Eds.), Uranium-series Geochemistry. Rev. In Mineralogy & Geochemistry, vol. 52, pp. 7–10.
Bunzl, K., Kretner, R., Schramel, P., Szeles, M., Winkler, R., 1995. Speciation of ^{238}U, ^{226}Ra, ^{210}Pb, ^{228}Ra, and stable Pb in the soil near an exhaust ventilating shaft of a uranium mine. Geoderma 67, 45–53.
ISO 11464:1994(F). Soil quality – Pretreatment of samples for physico-chemical analyses.
Jia, G., Torri, G., Innocenzi, P., 2004. An improved method for the determination of uranium isotopes in environmental samples by alpha-spectrometry. J. Radioanal. Nucl. Chem. 262, 433–441.
Križman, M., Byrne, A.R., Benedik, L., 1995. Distribution of ^{230}Th in milling wastes from the Žirovski vrh uranium mine (Slovenia), and its radioecological implications. J. Environ. Radioact. 26, 223–235.
Lozano, J.C., Fernandez, F., Gomez, J.M.G., 1997. Determination of radium isotopes by $BaSO_4$ coprecipitation for the preparation of alpha-spectrometric sources. J. Radioanal. Nucl. Chem. 223, 133–137.

Priloga 1: Nadaljevanje

Quevauviller, P., Ure, A., Muntau, H., Griepink, G., 1993. Improvement of analytical measurements within the BCR-programme: single and sequential extraction procedures applied to soil and sediment analysis. Int. J. Environ. Anal. Chem. 51, 231–235.

Schultz, M.K., Burnett, W.C., Inn, K.G.W., 1998. Evaluation of a sequential extraction method for determining actinide fractionation in soils and sediments. J. Environ. Radioact. 40, 155–174.

Sill, C.W., 1961. Decomposition of refractory silicates in ultramicro analysis. Anal. Chem. 33 (12), 1684–1686.

Suksi, J., Rasilainen, K., Pitkänen, P., 2006. Variations in $^{234}U/^{238}U$ activity ratios in groundwater – a key to flow system characterisation? Phys. Chem. Earth 31, 556–571.

Tessier, A., Campbell, P.G.C., Bisson, M., 1979. Sequential extraction procedure for the speciation of particulate trace metals. Anal. Chem. 51, 844–851.

Priloga 1: Nadaljevanje

Radiochim. Acta 98, 221–229 (2010) / DOI 10.1524/ract.2010.1710

Comparison of two sequential extraction protocols for fractionation of natural radionuclides in soil samples

By M. Štrok and B. Smodiš*

Jožef Stefan Institute, Jamova 39, 1000 Ljubljana, Slovenia

(Received August 20, 2009; accepted in revised form November 26, 2009)

Sequential extraction / Natural radionuclides / Uranium / Thorium / Radium

Summary. Revised BCR (Bureau Communautaire de Référence) and the Schultz modification of Tessier's sequential extraction protocols are compared for fractionation of uranium, thorium and radium in soil samples. Six soil samples were collected near to the uranium mill tailings waste pile and some of them had enhanced levels of natural radionuclides. The samples were processed by both protocols and the radionuclide content assayed by alpha spectrometric determination. The analysis revealed that results obtained by the two protocols are not fully comparable as data are mostly protocol- and element-dependent. Nevertheless, general conclusions about potential source of the particular radionuclide, which could be drawn from the specific study carried out, are mostly similar for both protocols.

1. Introduction

Environmental behaviour of natural radionuclides depends on the chemical form in which they occur. Chemical form of a certain radionuclide is closely related to its mobility and bioavailability in the environment. There are many technologically enhanced naturally occurring radioactive material (NORM) waste piles worldwide, which are affected by weathering processes. This could cause migration of radionuclides from the controlled area into the surrounding environment and thus pose a radiological risk to people who live there. Specific radionuclide is in a certain chemical form more bioavailable than in the other, which may result in the higher plant uptake of that radionuclide. Consequently, higher portion of that radionuclide is transferred into the human food chain. Therefore, it is important to know how a particular radionuclide is mobile and bioavailable in the environment.

One powerful tool for assessing mobility and bioavailability of natural radionuclides in the environment is sequential extraction. Since its introduction in the late 1970s, sequential extraction procedures have experienced a rapid increase in use for a large number of potentially toxic elements in a wide range of sample types [1]. However, there is an ever-lasting dilemma and that is, which sequential extraction procedure is most suitable for a certain problem? In the past, there have been many efforts to derive a unique protocol for sequential extraction in order to achieve comparability and enhance quality of the results. In the case of toxic elements, these efforts lead to development of the revised BCR sequential extraction protocol [2]. However, the use of the sequential extraction protocols for natural radionuclides is scarce [3, 4] and most often involves the Tessier's protocol [5] or the Schultz modification of Tessier's protocol [6] rather than the revised BCR protocol. Blanco *et al.* investigated both the Tessier's protocol and the Schultz modification of Tessier's protocol and concluded that the two procedures yield different results and that the Schultz protocol better suits the objectives of this type of sequential protocol in terms of reproducibility and recovery [7].

In our study, the revised BCR protocol and the Schultz modification of Tessier's protocol were compared for uranium, thorium and radium radionuclides. Throughout the text, the revised BCR protocol is referred to as protocol B and the Schultz modification of Tessier's protocol as protocol S. The protocols were applied on real soil samples, which were collected in the area of a uranium mill tailings (UMT) waste pile of the former uranium mine Žirovski vrh, Slovenia. Due to different extractants used by the two sequential extraction protocols (Tables 1 and 2), it was expected that the obtained results could be different. Therefore, the purpose was to test whether the differences would be small enough to allow for similar conclusions concerning the mobility and bioavailability of the analysed radionuclides in soil samples. This would mean that both methods would fit the objectives of this type of sequential extraction protocol, although they do not yield exactly the same results.

2. Experimental

2.1 Sampling and sample preparation

About 5 kg of each soil sample from six sites at the Boršt waste pile, presented in Fig. 1, were collected at the depth 10–15 cm. Sites 1 and 2 lie in two swampy areas through which seepage water from the Boršt waste pile is flowing with elevated radionuclide concentrations. It was expected that in these sites the radionuclides could be retained and consequently their activity concentrations elevated. Site 3

*Author for correspondence (E-mail: borut.smodis@ijs.si).

Priloga 1: Nadaljevanje

Table 1. Schultz modification of Tessier sequential extraction protocol (protocol S).

Target fraction	Extractive reagent	Reagent/ sample ratio	Temp. (°C)	Shaking time (h)
Exchangeable	0.4 M $MgCl_2$ pH 5	15 : 1	Room temp.	1
Organic matter	5–6% NaOCl pH 7.5	15 : 1	96	0.5 × 2
Carbonates	1 M NaAc in 25% HAc pH 4	15 : 1	Room temp.	2 × 2
Oxides (Fe/Mn)	0.04 M $NH_2OH{\cdot}HCl$ pH 2 (HNO_3)	15 : 1	Room temp.	5
Residue	Na_2O_2 fusion and HNO_3/ $HCl/HF/H_2SO_4$		900	

Table 2. Revised BCR sequential extraction protocol (protocol B).

Target fraction	Extractive reagent	Reagent/ sample ratio	Temp. (°C)	Shaking time (h)
Carbonates	0.11 M HAc	40 : 1	Room temp.	16
Oxides (Fe/Mn)	0.5 M $NH_2OH{\cdot}HCl$ 0.05 M HNO_3	40 : 1	Room temp.	16
Organic matter	8.8 M H_2O_2	10 : 1	Room temp.	1
			85	1
	8.8 M H_2O_2	10 : 1	85	1
	1 M NH_4Ac	50 : 1	Room temp.	16
Residue	Na_2O_2 fusion and HNO_3/ $HCl/HF/H_2SO_4$		900	

Fig. 1. Air picture of the Boršt waste pile; numbers show the sampling sites.

lies outside of the waste pile and should not be affected by the radionuclides from the waste pile. Therefore, it was considered as a non-contaminated site. The other three sites lie on the waste pile and represent basically UMT covered with soil.

Pretreatment of the samples was performed according to the ISO 11464 [8]. After sampling, the samples were weighed, dried in an oven at 80 °C and again weighed. Samples were then sieved through a 2 mm sieve. Bigger clods were crushed with a mortar and pestle and again sieved through the 2 mm sieve. A sample was then subsampled by hand quartering into representative portions of about 200 g to get a laboratory sample and stored until analysis. To obtain the required amount of the sample for the analysis, laboratory sample was further subsampled by hand quartering into representative portions. One part of each sample was sent to the Pedological Centre of the Department of Agronomy, Biotechnical Faculty, University of Ljubljana, for the pH, organic matter, carbonate content and particle size distribution determinations.

2.2 Sequential extraction protocols

The two sequential extraction protocols shown in Tables 1–2 were performed according to references 2 and 6. All fractions in the protocols should be regarded as operationally defined and do not strictly correspond to certain chemical species.

Priloga 1: Nadaljevanje

In the case of protocol S, 1.5 g of the sample were weighed into a centrifuge tube and wetted overnight with deionized water. Then, one sequential extraction procedures according to the Table 1 were applied. In each sequential extraction step, 22.5 mL of extractive reagent were added and samples were shaken at 180 rpm according to the shaking times presented in Table 1. For organic matter fraction, the samples were shaken in a shaking water bath at 96 °C. After each sequential extraction step, the samples were centrifuged for 30 min at 3000 rpm and filtered through a 0.1 μm pore diameter filter. The residue was reintroduced into the following sequential extraction step and the radionuclides in filtrate were separated according to the radiochemical separation procedure.

In protocol B, 1 g of sample was weighed into the centrifuge tube and 40 mL of the first extraction reagent were added (Table 2). Then the sample was shaken for 16 h at 30 rpm. After that, the extract was separated from the solid residue with centrifugation for 20 min at 3000 rpm and subsequently filtered through a 0.1 μm pore diameter filter. Then radionuclides in the filtrate were separated according to the radiochemical separation procedure. Residue was washed with 20 mL of the deionized water with shaking for 15 min at 30 rpm and centrifuging for 20 min at 3000 rpm. After that, the next extraction reagent was introduced to the residue (Table 2) and all aforementioned extraction steps were repeated. For organic matter dissolution, 10 mL of H_2O_2 were added to the residue from previous step and digested at the room temperature for 1 h. Then the centrifuge tube was placed into the water bath at 85 °C and digested for 1 h, covered loosely with its cap. After that, the cap was removed and volume of the solution reduced to 3 mL. Then additional aliquot of 10 mL of H_2O_2 were added and again digested for 1 h, covered loosely with its cap at 85 °C. Then the cap was removed and volume of the solution reduced to 1 mL and after cooling down, 50 mL of 1 M NH_4Ac were added and shaken for 16 h at 30 rpm. The separation of the extract from the residue was the same as in previous steps.

2.3 Radiochemical separation procedure

For solutions that remained after each sequential extraction step for both sequential extraction protocols, the same radiochemical separation procedure was used and it is summarized in Fig. 2. ^{226}Ra was separated using principles described by Lozano *et al.* [9]. Uranium and thorium isotopes were separated on an UTEVA separation column.

To the filtered solution from each sequential extraction step, ^{232}U, ^{229}Th and ^{133}Ba tracers were added to determine radiochemical recovery. Radium and barium were coprecipitated with $PbSO_4$ with addition of 1 mL concentrated H_2SO_4 and 1 mL of $Pb(NO_3)_2$ solution (50 mg/mL Pb^{2+}). After 10 min, the sample was centrifuged for 10 min at 3000 rpm. Supernatant containing uranium and thorium was decanted. Precipitate containing radium and barium was washed with deionized water to remove excess H_2SO_4 and again centrifuged. This step was repeated until neutral pH was achieved. Then the precipitate was dissolved with addition of 4 mL 0.1 M EDTA/0.5 M NaOH with the help of an ultrasound bath. If the amount of EDTA and NaOH was not sufficient for the complete dissolution of $PbSO_4$,

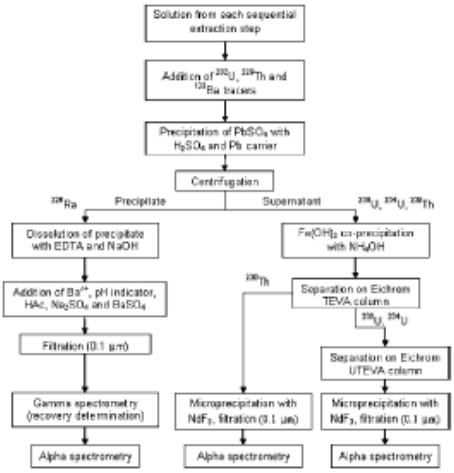

Fig. 2. Radiochemical separation procedure for solution from each sequential extraction step.

more EDTA and NaOH was added. Then 0.3 mL Ba carrier (0.3 mg/mL Ba^{2+}) and one drop of liquid pH 0–5 indicator were added. Then the pH was adjusted to acidic with the addition of 1 mL 1 : 1 acetic acid. After that, 4 mL of saturated Na_2SO_4 were added to form $Ba(Ra)SO_4$ precipitate. Then 0.3 mL of 0.125 mg/mL $BaSO_4$ substrate were added. After 10 min, the solution was filtered through the 0.1 μm pore diameter filter and then the filter was washed twice with deionised water. The filter was then mounted on a stainless steel disc with a water based glue and dried under a heating lamp. After drying, the so prepared counting source was ready for measurement.

To the supernatant – containing uranium and thorium, which was left after $PbSO_4$ precipitate centrifugation, ammonia solution was added until alkaline pH was achieved. Uranium and thorium were coprecipitated as $Fe(OH)_3$ with addition of three drops of 5 mg/mL Fe^{3+} solution. After 30 min, the sample was centrifuged for 10 min at 3000 rpm. Solution was decanted and the precipitate was washed with deionized water and again centrifuged. This step was repeated until neutral pH was achieved. After that, the precipitate was dissolved with 10 mL of 3 M HNO_3/1 M $Al(NO_3)_3$ and solution transferred onto a TEVA separation resin. The TEVA separation resins were packed into a column and preconditioned with 5 mL of 3 M HNO_3. The eluates were collected in centrifuge tubes. In this step, thorium was retained on the TEVA separation column and uranium was eluted. The centrifuge tube was rinsed with 5 mL of 2.5 M HNO_3 and again processed through the column. Finally, the column was washed with 30 mL of 2.5 M HNO_3 and the eluate retained for further purification on the UTEVA separation column. Thorium was eluted from the TEVA column with consecutive additions of 20 mL 9 M HCl and 5 mL of 6 M HCl and the eluate collected in a centrifuge tube.

The uranium-containing eluate, which was left from the separation on TEVA column, was transferred onto the

Priloga 1: Nadaljevanje

UTEVA separation column that was previously conditioned with 5 mL of 3 M HNO_3. The centrifuge tube which contained the uranium-containing eluate was rinsed with 5 mL of 3 M HNO_3 and processed through the column. The column was rinsed with consecutive additions of 5 mL of 3 M HNO_3, 5 mL of 9 M HCl and 20 mL of 5 M HCl/0.05 M oxalic acid. Eluates from all prior steps were discarded and uranium finally eluted with 15 mL of 1 M HCl into a centrifuge tube.

Thorium was microprecipitated with addition of 0.1 mL of 0.5 mg/mL Nd^{3+} and 1 mL of concentrated HF. Uranium was microprecipitated with addition of 0.1 mL of 0.5 mg/mL Nd^{3+}, 1 mL of 15% $TiCl_3$ and 1 mL of concentrated HF. Both thorium and uranium microprecipitates were placed prior to filtration for at least 30 min into an ice bath. Filtration was carried out through a 0.1 μm pore diameter filter that was previously rinsed twice with 5 mL of 10 μg/mL NdF_3 substrate solution. The centrifuge tube was rinsed twice with 2 mL of 0.58 M HF and twice with deionised water. Finally, the filter was mounted on a stainless steel disc with water based glue and dried under a heating lamp.

Procedure for the radiochemical separation of the residue that remained after the final sequential extraction step for both protocols is summarized in Fig. 3. Residue was ashed for 5 h at 650 °C and afterwards digested using the principles described by Jia *et al.* [10] and Sill [11]. 0.5 g of ash was introduced into a glassy carbon crucible together with 2 g of Na_2CO_3 and 2 g of Na_2O_2, and melted in muffle furnace for 5 min at 900 °C. After cooling to room temperature,

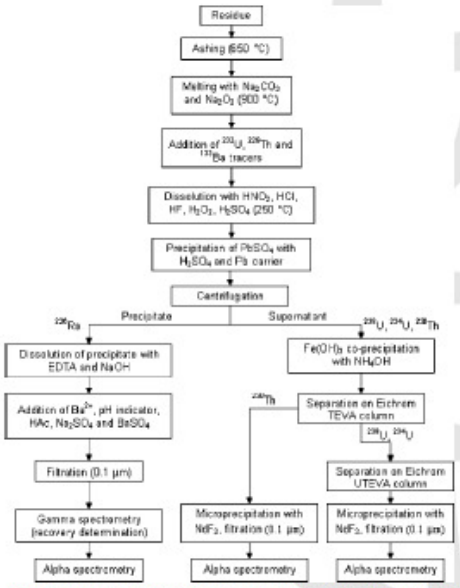

Fig. 3. Radiochemical separation procedure for residue after the final extraction step.

^{232}U, ^{229}Th and ^{133}Ba tracers were added to determine radiochemical recovery. The melt was dissolved with 1 mL of deionised water and 4 mL of concentrated HNO_3, and transferred into a Teflon beaker. To the sample, 5 mL concentrated HCl, 5 mL concentrated HNO_3, 5 mL concentrated HF and 5 mL H_2O_2 were added and evaporated until incipient dryness on a hot plate. This procedure was repeated three times in order to remove silicates. Afterwards, 8 mL of concentrated H_2SO_4 were added and evaporated until incipient dryness. This step removed any residual HF and fluorosilicates and converted salts into sulphates. After final evaporation, the sample was dissolved with 2 mL deionized water and 2 mL concentrated HNO_3. Finally, the obtained solution was processed the same way as the other fractions of the sequential extraction steps.

2.4 Measurement system

All counting sources were measured on an alpha spectrometric system equipped with passivated implanted planar silicon (PIPS) detectors (Alpha Analyst, Canberra). Radiochemical recovery for ^{226}Ra was determined *via* measurement of ^{133}Ba tracer on a gamma-ray spectrometer consisting of HP Ge detector connected to a multichannel analyser (Spectrum Master 919, Ortec).

3. Results and discussion

3.1 Physicochemical parameters

Results for physicochemical parameters are shown in Table 3. It can be observed that at almost all locations the pH of the soil is slightly acidic; only at location 4 the pH is neutral. This can be attributed to the highest carbonate content in that location. Organic matter content varies from 2.1 to 5.9%. Carbonate content is highest at site 4, 7.9%, and much lower (up to 1.6%) at other locations. Particle size distribution at sites 4 and 6, which lies on the waste pile, is almost identical. Silt fraction is dominant at site 3 and sand fraction at site 1. At site 2, soil particles are almost equally distributed among sand, silt and clay fractions.

3.2 Comparison of the sequential extraction protocols

A comparison of both sequential extraction protocols is presented in Fig. 4a–f. Radiochemical recoveries varied from 47–95%, 46–92% and 54–87% for U, Th and Ra radionuclides, respectively. On each graph, activity concentrations of a certain fraction for the protocol S are presented on *x* axis and for the protocol B on *y* axis. For better clarity, the results

Table 3. Physicochemical parameters of the collected soil samples.

Location	pH in $CaCl_2$	Organic matter (%)	Carbonates (%)	Sand (%)	Silt (%)	Clay (%)
1	5.4	5.4	1.6	62.0	27.5	10.5
2	4.5	3.8	0.8	37.2	36.3	26.5
3	4.5	5.9	1.2	12.5	68.2	19.3
4	7	3.8	7.9	46.7	34.9	18.4
6	5.9	2.1	< 0.5	49.9	31.3	18.8

Priloga 1: Nadaljevanje

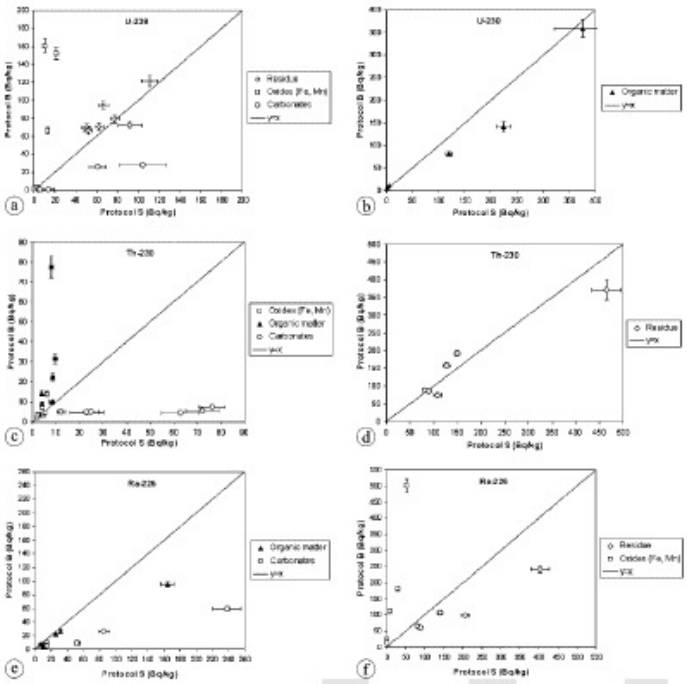

Fig. 4. Comparison of Schultz modification of Tessier sequential extraction protocol (protocol S) and revised BCR sequential extraction protocol (protocol B) for all fractions and six sampling sites; carbonate fraction for Schultz modification of Tessier sequential extraction protocol include exchangeable fraction.

for each radionuclide are shown on two graphs. Uncertainty bars refer to combined standard uncertainty; if the bar is not visible, uncertainty is smaller than the symbol size. As the protocol S involves exchangeable fraction, which is not the case for the protocol B, the exchangeable and carbonate fractions for protocol S are summed and presented as carbonate fraction.

Fig. 4a–f help in assessing if the results for both protocols are comparable; if they would be the same, they would lie on the line $y = x$. However, it is difficult to make visual judgements whether certain point is close enough to the line or not. Therefore statistical approach for assessing of agreement between the two methods was applied [12]. Figs. 5–7 show differences between the two protocols against average values for the two protocols for specific fraction and radionuclide. If the difference is zero or close to zero, it means that both protocols are in good agreement. Mean value of the differences is also calculated and presented together with ± 2 times standard deviation of those difference values (2SD) at 95% confidence level. Those figures reveal the differences between both protocols more clearly. However, it should also be assessed whether differences are small enough to ensure agreement between two protocols or not. In our case, combined standard uncertainties of the measured results for both protocols were in the range from 4 to 15%, depending on the activity concentration and with most of the results around 10%. Therefore, the value of 10% was applied, finally resulting in relative expanded uncertainty of 20% (coverage factor of 2 for 95% confidence level). As the value for 2SD is expressed in absolute form, it was necessary to transform it into relative form. This was accomplished by dividing it with the largest average value for both protocols for the certain fraction. Protocols were considered comparable if this value was smaller than 20%. Table 4 shows data for the means of differences between the two protocols, 2SD values, largest average values of the both protocols (max (aver(S,B))), 2SD values for the largest average values and if the results for both protocols for certain fraction are in agreement according to the adopted criterion.

Figs. 4a–b, 5 and Table 4 show that the two protocols for ^{238}U give similar results for both organic matter and the residue fraction. That is not the case for carbonates and Fe/Mn oxides; protocol S resulted in higher values for the carbonate fraction and protocol B for Fe/Mn oxides. For ^{230}Th (Figs. 4c–d, 6 and Table 4), results for all fractions are not comparable. Protocol S yielded higher values for carbonates and residue fraction, protocol B for organic matter and Fe/Mn oxides. Results for ^{226}Ra (Figs. 4e–f, 7 and Table 4) showed no agreement for any fraction; application of protocol S resulted in higher values for organic matter, carbonates and residue, whilst the values for the Fe/Mn oxides were higher for protocol B.

The results for protocol S for carbonate fraction are all higher than for protocol B. This could be attributed to the stronger extraction reagent used in protocol S (Tables 1, 2), which is about 50 times more concentrated than in proto-

Priloga 1: Nadaljevanje

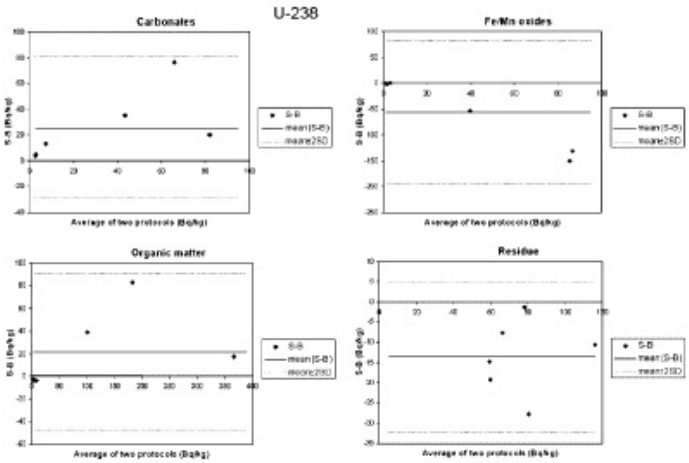

Fig. 5. Differences between protocols S and B against average of the two protocols for ^{238}U for all samples and fractions; mean line indicates mean of all difference values for one fraction; mean ± 2SD line indicates 2 times standard deviation (95% confidence interval).

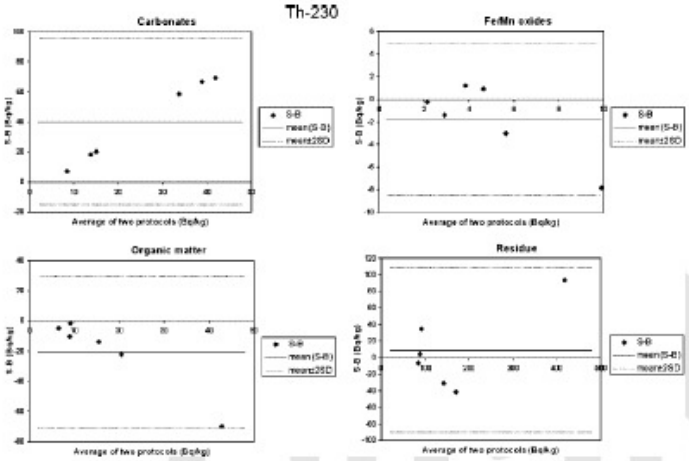

Fig. 6. Differences between protocols S and B against average of the two protocols for ^{230}Th for all samples and fractions; mean line indicates mean of all difference values for one fraction; mean ± 2SD line indicates 2 times standard deviation (95% confidence interval).

col B. However, the extraction time and reagent to sample ratio are about four times lower than in the case of protocol B. Furthermore, protocol S involves the organic fraction extraction step before the carbonate fraction step. The reason for placing the organic fraction before the carbonate and Fe/Mn oxide fractions is in fact that solid particles are often coated with a layer of organic matter, which may inhibit reaction of the other geochemical phases targeted by subsequent reagents applied in the experimental sequence [6]. Therefore, the reason for higher carbonate content found in the case of protocol S could be attributed to placement of the organic matter step early in the sequential extraction protocol.

Protocol B yielded higher results for Fe/Mn oxides than protocol S in all cases. Reasons for that could be the fact that (1) extraction reagent for this fraction in both protocols (Tables 1, 2) is about 12 times more concentrated in protocol B and that (2) shaking time and reagent to sample ratio is also higher. Further reason for that could be in the placement of the organic fraction in early stages of the sequential extraction sequence for the protocol S, which could dissolve up to 10% of iron and thus increase the activity concentrations in the organic fraction [13]. However, our results did not prove that as the results for ^{238}U in the organic fraction were similar for both protocols, for ^{230}Th higher by protocol B and for ^{226}Ra slightly higher by protocol S.

When comparing the three analysed radionuclides presented in Fig. 4a–f, it is evident that the activity concentrations of ^{230}Th in the organic fraction obtained by protocol B are substantially higher compared to protocol S, which is

Priloga 1: Nadaljevanje

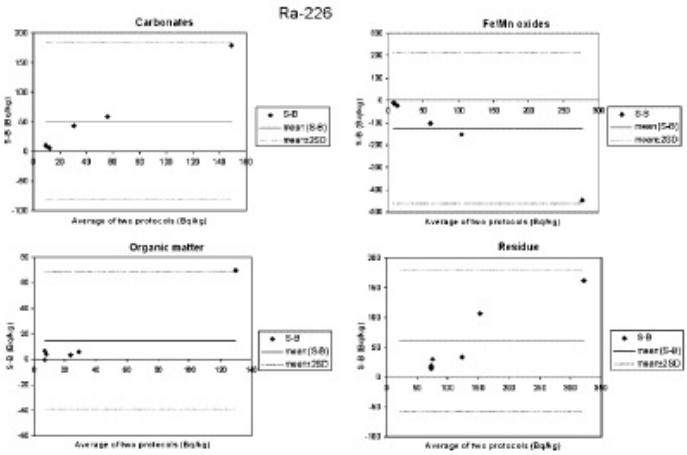

Fig. 7. Differences between protocols S and B against average of the two protocols for ^{226}Ra for all samples and fractions; mean line indicates mean of all difference values for one fraction; mean ± 2SD line indicates 2 times standard deviation (95% confidence interval).

Table 4. Statistical assessment of agreement between protocol S and B.

Radionuclide	Fraction	mean (S-B) [Bq/kg]	2SD [Bq/kg]	max (aver(S,B)) [Bq/kg]	2SD/max (S,B) [%]	Agreement
^{238}U	Carbonates	25.7	54.9	82.0	67	NO
	Fe/Mn oxides	−56.2	137.6	86.7	159	NO
	Organic matter	21.6	68.9	367.0	19	YES
	Residue	−13.6	18.5	116.3	16	YES
^{230}Th	Carbonates	40.0	55.5	41.9	132	NO
	Fe/Mn oxides	−1.7	6.7	9.9	68	NO
	Organic matter	−20.4	50.1	42.9	117	NO
	Residue	8.9	99.3	417.8	24	NO
^{226}Ra	Carbonates	50.8	132.7	149.0	89	NO
	Fe/Mn oxides	−125.9	335.3	276.7	121	NO
	Organic matter	15.0	53.9	129.8	42	NO
	Residue	60.7	119.6	321.7	37	NO

not the case for the other two radionuclides. Other observable difference is that the results for ^{226}Ra in all fractions were the most scattered among the three radionuclides, and the smallest level of similarities could be found between the two protocols.

Fig. 8a–f show results for both sequential extraction protocols according to the sampling sites. Analytical uncertainties that were in the range from 4 to 15%, depending on the activity concentration, are not shown for better clarity. Graph b in Fig. 8 shows results for ^{238}U. Both protocols reveal that elevated levels of total activity concentrations (defined as a sum of all fractions) for uranium are in sites 1, 4 and 6. The two protocols also show that in sites 2 and 5 total activity concentrations are similar as for site 3, which is referred to as a reference, non-contaminated location. Different results can be observed for ^{230}Th (Fig. 8d). In both protocols, higher total activity concentrations of ^{230}Th are on sites 4, 5 and 6 compared with site 3. In addition, protocol S yields elevated total activity concentration of ^{230}Th for site 1, whereas protocol B yields results similar to the site 3. However, both protocols reveal that total activity concentration of ^{230}Th in site 2 is similar to site 3. Results of both protocols for ^{226}Ra (Fig. 8f) show elevated total activity concentrations in sites 4, 5 and 6 with respect to site 3. In other two sites (1 and 2) total activity concentrations are similar to site 3.

In terms of particular fractions, in sites 2 and 3 more than 80% of ^{238}U is in the residue for both protocols (Fig. 8a). Differences between the two protocols for residual fraction are higher in site 5. At sites 1, 4 and 6, the residual fraction contains about 20% of ^{238}U for both protocols. Therefore, majority of ^{238}U in locations with elevated total activity concentrations is present in potentially mobile fractions. Application of the two protocols at sites 1, 4 and 6 results in different distribution among the mobile fractions: protocol B yields higher activity concentrations for Fe/Mn oxides, and lower values for organic matter and carbonates. Variability can also be observed in more mobile fractions in sites 2, 3 and 5, with the highest differences for the residual fraction. Nevertheless, distribution profiles for each protocol for sites with elevated levels (1, 4 and 6), as well as for site 2 with total activity concentration close to site 3, are similar. This means that both protocols give comparable information on the potential source of ^{238}U. Distribution profiles for ^{230}Th showed in Fig. 8c reveal that for both protocols most of the

Priloga 1: Nadaljevanje

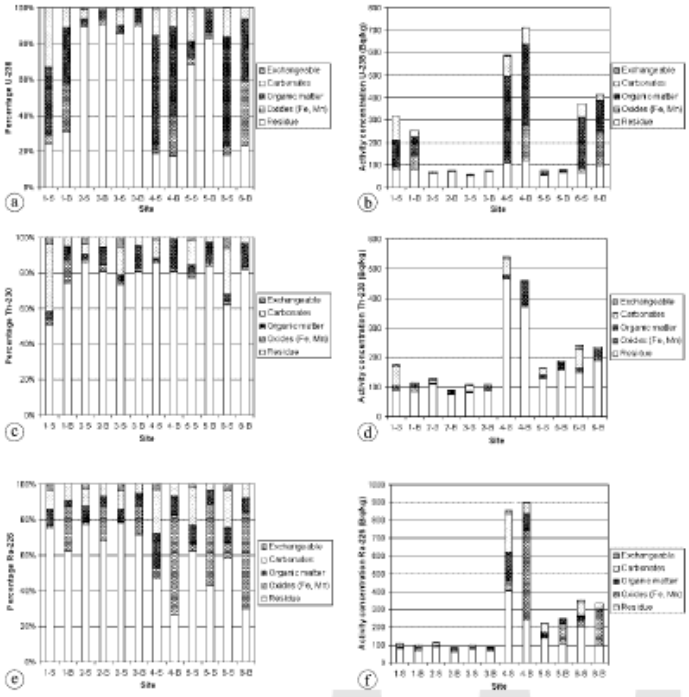

Fig. 8. Results of both sequential extraction protocols for six sampling sites; S – results for Schultz modification of Tessier sequential extraction protocol, B – BCR sequential extraction protocol.

^{230}Th is in the residue fraction (50–85%); protocol S gives relatively higher results for the carbonates and protocol B for the organic matter. From the distribution profiles for ^{230}Th it is not possible to identify any differences between site 3 (referred as non-contaminated site) and sites 4, 5 and 6 with elevated total activity concentrations. Distribution profiles for ^{226}Ra (Fig. 8e) in particular fractions differ between the two protocols. Nevertheless, distribution profiles for each protocol for sites with elevated levels (4, 5 and 6), as well as for sites 1 and 2 with total activity concentration close to site 3, are similar. Consequently, both protocols give comparable information on the potential source of ^{226}Ra.

4. Conclusions

The results obtained by the Schultz modification of Tessier's sequential extraction protocol (protocol S) and the revised BCR protocol (protocol B) revealed that different activity concentrations of a particular radionuclide could be expected to be found in comparable fractions. In particular, systematically higher values could be found for all the three radionuclides studied, *i.e.* ^{238}U, ^{230}Th and ^{226}Ra, for carbonate fraction processed by protocol S and for Fe/Mn oxides fraction processed by protocol B. For other fractions, the results are variable and no such systematic trends could be observed. The variations could be attributed to different extractants and target fractions used by the two protocols. The findings prove that the particular fractions of each protocol are operationally defined and should in principle not be applied as alternatives in the same study.

Similar conclusion could be drawn regarding fractionation of the three studied radionuclides; different activity concentrations obtained by the two protocols could be expected in the particular comparable extraction fractions. The most extreme case was observed for ^{230}Th in the organic fraction, where the results for protocol B were 2 to 11 times higher than for protocol S. That was not the case for the other two radionuclides, where activity concentrations in organic fraction were lower (^{226}Ra) or equal (^{238}U) compared to protocol S. In the case of ^{226}Ra it is interesting that all the values were lower for protocol B except for the Fe/Mn oxides fraction. So the fractionation studies using different extraction protocols are strongly element-dependent.

Comparison of the results regarding the sampling sites showed that both protocols yield comparable evidence (except for ^{230}Th in site 1) in determining elevated total activity concentrations of particular radionuclides and in comparing the distribution profiles of contaminated sites with the reference site 3. However, one should be careful in interpreting the measurement results for specific fractions as they are mostly protocol dependent. Nevertheless, when considering the exchangeable, carbonates, organic matter and Fe/Mn oxides fractions as potentially mobile fraction, similar con-

Priloga 1: Nadaljevanje

clusions about the potential source of the particular radionuclide could be derived by using either protocol as evidenced by the specific case presented in this paper.

Acknowledgment. The authors would like to thank the staff of the Rudnik Žirovski vrh company for their cooperation and assistance. Financial support of the Slovenian Research Agency (Grant No. P2-0075) is highly appreciated. Pedological Centre of the Department of Agronomy, Biotechnical Faculty, University of Ljubljana is acknowledged for the analysis of physicochemical parameters of soil samples.

References

1. Bacon, J. R., Davidson, C. M.: Is there a future for sequential chemical extraction? The Analyst **133**, 25 (2008).
2. Rauret, G., López-Sánchez, J. F., Sahuquillo, A., Rubio, R., Davidson, C., Ure, A., Quevauviller, Ph.: Improvement of the BCR three step sequential extraction procedure prior to the certification of new sediment and soil reference materials. J. Environ. Monit. **1**, 57 (1999).
3. Bunzl, K., Kretner, R., Schramel, P., Szeles, M., Winkler, R.: Speciation of ^{238}U, ^{226}Ra, ^{210}Pb, ^{228}Ra, and stable Pb in the soil near an exhaust ventilating shaft of a uranium mine. Geoderma **67**, 45 (1995).
4. Blanco, P., Vera Tomé, F., Lozano, J. C.: Fractionation of natural radionuclides in soils from a uranium mineralized area in the south-west of Spain. J. Environ. Radioact. **79**, 315 (2005).
5. Tessier, A., Campbell, P. G. C., Bisson, M.: Sequential extraction procedure for the speciation of particulate trace metals. Anal. Chem. **51**, 844 (1979).
6. Schultz, M. K., Burnett, W. C., Inn, K. G. W.: Evaluation of a sequential extraction method for determining actinide fractionation in soils and sediments. J. Environ. Radioact. **40**, 155 (1998).
7. Blanco, P., Vera Tomé, F., Lozano, J. C.: Sequential extraction for radionuclide fractionation in soil samples: a comparative study. Appl. Radiat. Isot. **61**, 345 (2004).
8. ISO 11464:1994(E): Soil quality – Pretreatment of samples for physico-chemical analyses. International Organization for Standarisation, Geneve (1994).
9. Lozano, J. C., Fernandez, F., Gomez, J. M. G.: Determination of radium isotopes by $BaSO_4$ coprecipitation for the preparation of alpha-spectrometric sources. J. Radioanal. Nucl. Chem. **223**, 133 (1997).
10. Jia, G., Torri, G., Innocenzi, P.: An improved method for the determination of uranium isotopes in environmental samples by alpha-spectrometry. J. Radioanal. Nucl. Chem. **262**, 433 (2004).
11. Sill, C. W.: Decomposition of refractory silicates in ultramicro analysis. Anal. Chem. **33**, 1684 (1961).
12. Bland, J. M., Altman, D. G.: Statistical methods for assessing agreement between two methods of clinical measurement. Lancet **327**, 307 (1986).
13. La Force, M. J., Fendorf, S.: Solid-phase iron characterization during common selective sequential extractions. Soil Sci. Soc. Am. J. **64**, 1608 (2000).

Priloga 1: Nadaljevanje

Applied Radiation and Isotopes 68 (2010) 1221–1225

Contents lists available at ScienceDirect

Applied Radiation and Isotopes

journal homepage: www.elsevier.com/locate/apradiso

Evaluation of procedures for determination of Ra-226 in water by α-particle spectrometry with emphasis on the recovery

L. Benedik *, U. Repinc, M. Štrok

Jozef Stefan Institute, Jamova 39, SI-1000 Ljubljana, Slovenia

ARTICLE INFO

Keywords:
Radium
Radiochemistry
Recovery
α-particle spectrometry
γ-ray spectrometry

ABSTRACT

Radium-226 is one of the best known long-lived α-emitters abundantly present in the environment. The determination of radium isotopes in environmental samples usually requires a demanding chemical separation before measurement and quantification. Each step in the chemical separation process can involve losses of the analyte, therefore it is of vital importance that the recovery of the whole radiochemical procedure is evaluated. The emphasis of the work presented was determination of the chemical recovery using the different yield tracers Ra-223, Ra-225 and Ba-133.

1. Introduction

There are four radium isotopes present in the natural decay series: α-emitting Ra-226 in the uranium series, α-emitting Ra-223 in the actinium series and β-emitting Ra-228 and α-emitting Ra-224 in the thorium series. Radium-226 is one of the most widespread α-emitters present in environmental samples. The activity concentration of Ra-226 has to be determined in order to evaluate its potential contribution to the internal dose. Since Ra-226 is an α- and γ-emitter, the most frequently used analytical methods for its determination in water samples are α-particle spectrometry, liquid scintillation counting (LSC), the sorption-emanation technique and γ-ray spectrometry.

Alpha-particle spectrometry in combination with radiochemical separation allows determination of very low activity concentration of Ra-226. Direct measurement of isolated Ra-226 independent of any considerations of nonequilibrium due to loss of gaseous intermediates can be performed (Lawrie et al., 2000). Some simple and specific separation methods for radium have been reported, but the preparation of sources of sufficient spectrometric quality, which requires many chemical operations, is difficult. Each step in the chemical separation process can result in unavoidable losses of the analyte, therefore yield tracers must be used to evaluate the chemical yield. For the preparation of the thin sources for high resolution α-particle spectrometry electrodeposition and/or micro-coprecipitation with rare earths are the most often used methods.

In the case of Ra-226, several tracers such as Ba-133, Ra-225, Ra-224 and Ra-223 were applied. Ra-224 ($T_{1/2}$=3.627 d), which occurs naturally as a descendant of the Th-232 decay scheme, is an α-emitter. Ra-225 ($T_{1/2}$=14.8 d), the first descendant of Th-229, is a β- and γ-emitter and it does not occur naturally (Crespo, 2000). Its γ line at 40.09 keV is rather intensive (P_γ=30.0%) and allows its measurement with a low-level energy γ-ray detector. On the other hand, its immediate descendants (Ac-225, Fr-221, At-217) are α-emitters and evaluation of the recovery is possible via indirect measurement via At-217 at 7066.9 keV (P_α=99.932%) using ingrowth-decay equations. Ra-223 ($T_{1/2}$=11.4 d) originates from U-235, whereas Ra-226 is formed from decay of U-238. Since the chemical properties of the progenitor nuclides are comparable and the terrestrial activity ratio of U-235/U-238 is 0.047, the conclusion would be that Ra-223 activity is very small compared to Ra-226. The main α lines of Ra-223 lie in the range from 5433 to 5871 keV with major α peak at 5716 keV, but are affected by ingrowing Rn-222 ($T_{1/2}$=3.8232 d, E_α=5489.48 keV, P_α=99.22%). Due to the short half-life of Rn-222 it is necessary to take the contribution of Rn-222 to the Ra-223 α lines into account. When using the α-emitting isotopic Ra-223 tracer, the chemical yield can also be determined from Po-215 peak at 7386 keV (P_α=99.99%), since equilibrium between Ra-223 and its descendants is established immediately after separation. Po-215 does not interfere with the peaks in the spectrum produced by α-emitting radium radionuclides and the ingrowth of Rn-222, Po-218 and Po-214. In addition, Ra-223 is also a γ-emitter (E_γ=154.7 keV, P_γ=5.7%) and evaluation of the recovery is possible through its measurement by γ-ray spectrometry. Ba-133 is often used as a yield tracer for radium. In this case, the analyst should be aware that experimental evidence has been reported that barium does not exactly follow the chemical behaviour of radium in all reactions. Sill (1987) demonstrated that Ra-226 and Ba-133 suffer from differences in quantitative chemistry, which could culminate in an inaccurate calculation of the chemical yield.

The experimental design of our study was to evaluate the stages of separation and thin source preparation by micro-coprecipitation,

* Corresponding author. Tel.: +386 1 5885347; fax: +386 1 5885346.
E-mail address: ljudmila.benedik@ijs.si (L. Benedik).

0969-8043/$ - see front matter © 2009 Elsevier Ltd. All rights reserved.
doi:10.1016/j.apradiso.2009.12.005

Priloga 1: Nadaljevanje

investigating the use of the tracers Ra-225, Ra-223 and Ba-133 for chemical yield evaluation for determination of Ra-226 by α-particle spectrometry. Determination of recovery was based on γ measurement of Ra-225, Ra-223 and Ba-133 at 40.09, 154.7 and 356.0 keV, respectively. Direct measurement by α-particle spectrometry for Ra-223 and its descendant Po-215 immediately after source preparation and indirect measurement of At-217 by α-particle spectrometry after approximately three weeks can also be applied.

2. Experimental

Water samples were collected in the vicinity of the former uranium mine at Žirovski vrh, Slovenia. Ra-226 standard solution and tracer solutions (Ba-133, Th-229, Pa-231) used in the study were prepared from calibrated solutions purchased from Analytics, Inc. (Atlanta, GA, USA) and AEA Technology UK. Both producers maintain traceability to the NIST.

2.1. Instruments

An α spectrometer (EG&G ORTEC) with a passivated implanted planar silicon (PIPS) semiconductor detector with an active area of 450 mm^2 and 28% efficiency for 25 mm diameter discs was used for α spectrometry measurements. The calibration of the detector was made with a standard radionuclide source, containing U-238, U-234, Pu-239 and Am-241 (code: 67978-121), obtained from Analytics, Inc. A low energy HP Ge detector was used for measurement of γ-emitting nuclides after microprecipitation. For evaluation of gamma spectra, the HyperLab (2005) program was used.

2.2. Separation techniques

The preconcentration and separation method used for α spectrometric determination of Ra-226 depends on source preparation (micro-coprecipitation or electrodeposition), as well as the use of an appropriate tracer. Test studies with a single tracer and source preparation by micro-coprecipitation were done previously.

We determined the activity concentration of Ra-226 in the selected water samples, where recoveries were evaluated using Ba-133, Ra-225 and Ra-223 tracers. The analytical scheme was adapted from Lozano (Lozano et al., 1997). Ba-133, Ra-225 and Ra-223 tracers were used as a single tracers or their combination was used. The procedure is based on coprecipitation of Pb(Ra)(Ba)SO_4 from acidified water samples. The precipitate was dissolved, purified and finally radium was micro-coprecipitated with $BaSO_4$. The suspension was filtered through a 25 mm 0.1 μm polypropylene filter. The filter with $BaSO_4$ deposit was mounted on a stainless steel disc and measured by α-particle spectrometry for determination of Ra-226 and yield determination via Ra-223 and Po-215.

The yield was also evaluated using γ-ray spectrometry of Ba-133 at 356.0 keV, Ra-225 at 40.0 keV and Ra-223 at 154.7 keV. The filter was remeasured by α-particle spectrometry after two weeks for determination of recovery via At-217.

If At-217 (decay product of Ra-225) is used, it is important that before adding Ra-225 tracer into the sample or during the sample separation procedure, Th-229 and Ac-225 are selectively removed. In our study we purified Ra-225 tracer before use, its activity concentration has been determined by alpha spectrometry using standard radionuclide source to determine the counting efficiency. The separation was performed using extraction (Horwitz et al., 1993) and cation exchange chromatography (Cabell, 1959), as described in the literature.

3. Results and discussion

Fig. 1 shows the γ spectrum of the isolated radium isotopes measured by a low-level HP germanium γ detector when tracers Ba-133, Ra-223 and Ra-225 in the same sample were used. Determination of recovery using Ba-133 is very simple. Ba-133 and Ra-226 have conveniently long half-lives of 10.66 and 1600 yr, respectively. The γ measurement of Ba-133 can be done before or after α measurement. Furthermore, since it is a pure β- and γ-emitter, there are no interferences in α spectrum of radium radionuclides. For calculation of recovery with Ra-223, the γ energy at 154.7 keV was used. Ra-225 emits γ rays at 40.0 keV (P_γ=30.0%). When using α-emitting isotopic Ra-223 as a tracer, the recovery can be determined from the Ra-223 peaks. Fig. 2 shows α spectrum of a water sample of Ra-226 and Ra-223 and their daughters. The measurement started immediately after source preparation and the time of measurement was 20 h. The

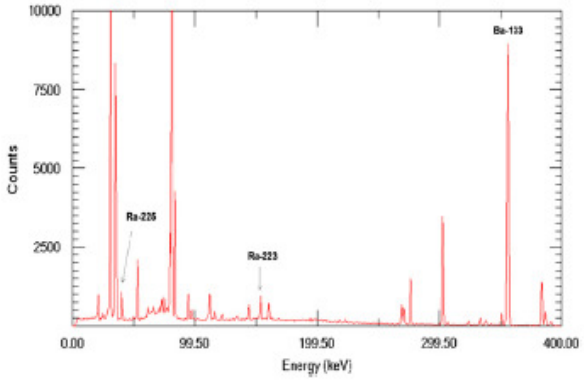

Fig. 1. γ-ray spectrum of isolated Ra isotopes, where Ba-133, Th-229 and Ra-223 tracers were added.

Priloga 1: Nadaljevanje

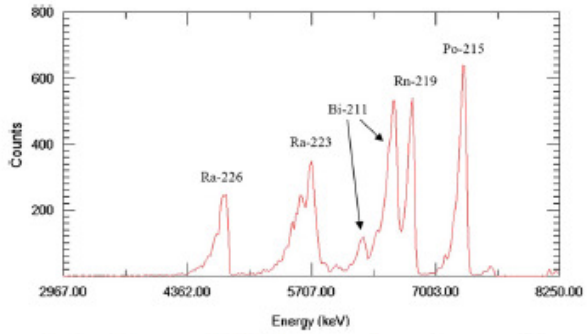

Fig. 2. α-particle spectrum of isolated radium isotopes where Ra-223 tracer was added.

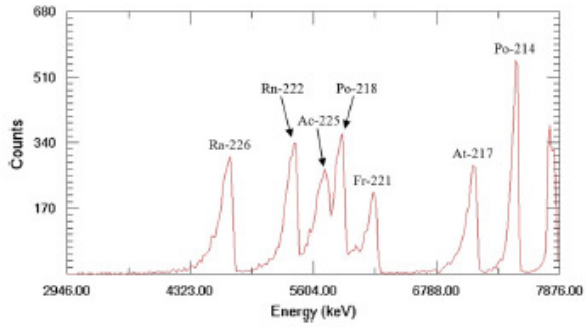

Fig. 3. α-particle spectrum of isolated radium isotopes where Ra-225 was added.

ingrowth of Rn-222 in 20h is more than 10%. In the case of recovery evaluation via At-217, the waiting time between source preparation and α spectrometric measurement of At-217 is approximately three weeks, at which time the At-217/Ra-225 ratio attains its maximum. In the calculation it is necessary to take into account the time of preconcentration of radium, the starting time of measurements, the duration of measurements, as well as ingrowth of At-217 and decay of Ra-225 during the measurement. Fig. 3 shows α spectrum of separated radium isotopes measured three weeks after source preparation.

The results with corresponding uncertainties for the determination of the activity concentration of Ra-226 in water samples obtained using various tracers are presented in Tables 1–3. When recoveries were determined by γ-ray spectrometry, relative measurements based on the comparison of the measured peak areas of the Ba-133, Ra-223 and Ra-225 tracers in the water samples and Ba-133, Ra-223 and Ra-225 in standard sources were used. A detailed description of the uncertainty budget calculation for determination of Ra-226 activity concentration in water, when recovery is determined by γ-ray spectrometry, was given by Spasova et al. (2007). In the case of determination of recovery with Ra-223 and Ra-225, their decay during sample preparation and measurement must be taken into account. When recoveries were determined by α-particle spectrometry via Po-215 from the well-resolved α peak at 7386 keV, the recoveries were calculated according to Eq. (1):

$$R = \frac{P}{A_0 m_{std} \varepsilon_{det}} \left\{ \frac{1}{\lambda} [e^{-\lambda(t_1 - t_0)} - e^{-\lambda(t_2 - t_0)}] \right\}^{-1} \times 100 \quad (1)$$

where is P a net area of Po-215 in the sample; t_0 is a time of the beginning of the separation where we know the activity A_0 of added Ra-223; m_{std} is a mass of added Ra-223 tracer; ε_{det} is an efficiency of detector; λ is a decay constant of Ra-223; t_1 and t_2 are the time of beginning and end of measurement, respectively.

When recoveries were determined by α-particle spectrometry via At-217 from the well-resolved peak at 7066.9 keV the recovery was calculated according to Eq. (2):

$$R = \frac{P(\lambda_2 - \lambda_1)}{\lambda_2 A_0 m_{std} \varepsilon_{det}} \times \left\{ \frac{1}{\lambda_1} [e^{-\lambda_1(t_1 - t_0)} - e^{-\lambda_1(t_2 - t_0)}] - \frac{1}{\lambda_2} [e^{-\lambda_2(t_1 - t_0)} - e^{-\lambda_2(t_2 - t_0)}] \right\}^{-1} \times 100 \quad (2)$$

where is P a net area of At-217 in the sample; t_0 is a time of the beginning of the separation where we know the activity A_0 of added Ra-225; m_{std} is a mass of added Ra-225 tracer; ε_{det} is an efficiency of detector; λ_1 is a decay constant of Ra-225; λ_2 is a decay constant of Ac-225; t_1 and t_2 are the time of beginning and end of measurement, respectively.

Priloga 1: Nadaljevanje

Table 1
Comparison of the results for Ra-226 obtained using Ba-133, Ra-223 and Ra-225 tracers, in the same water samples in mBq/L.[a]

Sample	Ba-133		Ra-223		Ra-225	
	Recovery (%)	Ra-226 (mBq/L)	Recovery (%)	Ra-226 (mBq/L)	Recovery (%)	Ra-226 (mBq/L)
1	70.2 ± 2.8	1887 ± 193	77.6 ± 2.9	1707 ± 157	73.5 ± 3.2	1802 ± 143
2	71.2 ± 3.0	1019 ± 146	79.4 ± 4.1	914 ± 134	76.9 ± 2.9	943 ± 130
3	83.3 ± 3.2	318 ± 44	87.6 ± 3.5	302 ± 40	87.1 ± 3.6	304 ± 41
4	68.8 ± 3.0	242 ± 35	80.1 ± 3.4	208 ± 29	75.1 ± 3.9	222 ± 31
5	32.8 ± 2.3	203 ± 19	36.7 ± 2.0	180 ± 17	32.6 ± 2.8	204 ± 25

[a] Uncertainty values reported as combined uncertainty expanded by a coverage factor $k=2$.

Table 2
Comparison of the results for Ra-226 obtained using Ba-133, and Ra-223 tracers in the same water samples in mBq/L.[a]

Sample	Ba-133		Po-215	
	Recovery (%)	Ra-226 (mBq/L)	Recovery (%)	Ra-226 (mBq/L)
6	60.2 ± 3.6	245 ± 23	74.4 ± 3.5	199 ± 18
7	75.0 ± 6.0	439 ± 50	93.0 ± 7.0	375 ± 41
8	57.0 ± 3.5	883 ± 130	64.4 ± 4.2	781 ± 111
9	90.0 ± 7.0	1555 ± 60	100.0 ± 3.0	1404 ± 40
10	74.0 ± 4.0	3080 ± 120	94.0 ± 8.0	2462 ± 120

[a] Uncertainty values reported as combined uncertainty expanded by a coverage factor $k=2$.

Table 3
Comparison of the results for Ra-226 obtained using Ba-133, and Ra-225 tracers in the same water samples in mBq/L.[a]

Sample	Ba-133		At-217	
	Recovery (%)	Ra-226 (mBq/L)	Recovery (%)	Ra-226 (mBq/L)
11	77.9 ± 3.8	220 ± 21	87.5 ± 4.0	196 ± 18
12	64.7 ± 3.2	225 ± 23	89.0 ± 7.9	185 ± 21
13	39.4 ± 3.9	315 ± 32	48.9 ± 5.3	254 ± 26
14	75.0 ± 3.2	387 ± 35	87.5 ± 3.8	332 ± 29
15	81.1 ± 3.2	674 ± 57	86.9 ± 8.4	629 ± 60
16	91.7 ± 3.1	764 ± 64	99.6 ± 10.3	703 ± 68
17	57.2 ± 2.9	817 ± 111	64.3 ± 3.6	726 ± 100

[a] Uncertainty values reported as combined uncertainty expanded by a coverage factor $k=2$.

The main causes of uncertainties in determination of recovery by α-particle spectroscopic measurements via Po-215 and At-217 are peak areas of Po-215 and At-217, efficiency of the detector, activity and mass of added tracers.

In Table 1 results are presented, when Ba-133, Ra-225 and Ra-223 were added to the same sample. The source was measured by γ-ray spectrometry for evaluation of recovery by measurement of Ba-133, Ra-225 and Ra-223 and α-particle spectrometry for determination of Ra-226. From the results it is evident that slightly lower recoveries are always obtained with Ba-133 tracer than those evaluated with Ra-225 and Ra-223. The results for Ra-226 are higher when recovery was calculated from Ba-133. The recoveries obtained were more than 10% higher than when calculation via Po-215 was made. Also in the case when the tracers Ba-133 and Ra-223 were added to the same sample (Table 2), the obtained results show similar pattern. Table 3 shows the results obtained when the recovery was evaluated with Ba-133 and indirect measurement of At-217. For this study we purified the Ra-225 tracer, since Th-229 and Ac-225 cannot be selectively removed during the sample separation procedure.

4. Conclusion

Recoveries obtained when the tracers Ba-133, Ra-225 and Ra-223 were measured by γ spectrometry are comparable. The differences in the recovery when Ba-133 or radium tracers (Ra-225 and Ra-223) are used were less than 10%. But all the measurements showed that the recovery is lower when Ba-133 was used for its evaluation, as also reported Lozano et al. (1997). Reported yield ratio $Y_{Ra\text{-}226}/Y_{Ba\text{-}133} \approx 1.04$ with a typical uncertainty of 8% is comparable with our values for yield ratios of $Y_{Ra\text{-}223}/Y_{Ba\text{-}133}$ ($1.03 \pm 11.7\%$) and $Y_{Ra\text{-}225}/Y_{Ba\text{-}133}$ ($1.02 \pm 11.7\%$).

Evaluation of the α spectra and the results of yield determinations from the well-resolved Po-215 peak at 7386 keV showed deviation between the Ra-223 and Po-215 peak areas. Due to ingrowth of Rn-222 during the time-consuming measurement it is only possible to use the Po-215 peak for calculation of recovery. Yield ratio $Y_{Ra\text{-}223}/Y_{Ba\text{-}133}$ obtained shows the value ($1.17 \pm 8.5\%$). On the other hand, it is necessary to note that Po-215 is the progenitor of Rn-219 and it is possible that Rn-219 emanation from the source occurs. The same range of difference was found in the case of determination of recovery via At-217. Yield ratio $Y_{Ra\text{-}225}/Y_{Ba\text{-}133}$ obtained shows the value ($1.17 \pm 11.4\%$). It is important to point out that Ra-225 does not exist in the natural environment and that its decay does not produce radon.

The main purpose of our study was to compare the results of activity concentration of Ra-226 in water where Ba-133, Ra-225 and Ra-223 tracers would be used for evaluation of the overall recovery. The results obtained showed that the activity concentrations of Ra-226 are within measurement uncertainties for all tracers used. A lower recovery was always found when Ba-133 was used. The use of Ra-223 and Ra-225 is also possible, but due to their short half-lives, their decays should be taken into account, as well as the ingrowth of their decay products.

Acknowledgements

This work was supported by the Ministry of Higher Education, Science and Technology of the Republic of Slovenia within the research programme P1-0143.

References

Cabell, M.J., 1959. The purification, determination, and neutron capture cross section of actinium-227. Can. J. Chem. 37, 1094–1103.
Crespo, M.T., 2000. On the determination of Ra-226 in environmental and geological samples by α-spectrometry using Ra-225 as yield tracer. Appl. Radiat. Isot. 53, 109–114.
Horwitz, E.P., Chiarizia, R., Dietz, M.L., Diamond, H., 1993. Separation and preconcentration of actinides from acidic media by extraction chromatography. Anal. Chim. Acta 281, 361–372.
HyperLab, 2005. System, Installation and Quick Start Guide, HyperLabs Software, Budapest, Hungary.

Priloga 1: Nadaljevanje

Lawrie, W.C., Desmond, J.A., Spence, D., Anderson, S., Edmondson, C., 2000. Determination of Ra-226 in environmental and personal monitoring samples. Appl. Radiat. Isot. 53, 133–137.
Lozano, J.C., Fernandez, F., Gomez, J.M.G., 1997. Determination of radium isotopes by $BaSO_4$ coprecipitation for the preparation of α-spectrometric sources. J. Radioanal. Nucl. Chem. 223 (1–2), 133–137.
Sill, C.W., 1987. Determination of Ra-226 in ores, nuclear wastes and environmental samples by high resolution α-spectrometry. Nucl. Chem. Waste Manage. 7, 239–256.
Spasova, Y., Pommé, S., Benedik, L., Wätjen, U., 2007. Uncertainty budget for Ra-226 activity concentration in water by alpha spectrometry. Acta Chim. Slov. 54, 845–858.

Discussion:

Q(Christian Hurtgen): What did you take for the time of measurements?

A(Ljudmila Benedik): In some cases we measured more than 20 h; we measured up to 100 h.

Q(Pierino De Felice): On the basis of your experience in this work, can you comment on the use of a stable barium as a carrier for radium?

A(Ljudmila Benedik): We checked the amount of stable barium in the samples. We added as a carrier barium, but barium is also present in all our samples because as I said we collected this water in the surroundings of a former uranium mine and in some cases it was also the wastewater so this water also contained barium.

Q(Dirk Arnold): I would like to come again to the point of barium 133 as a tracer. You mentioned the differences. And now again to your conclusions or recommendations: Would you say that it is an appropriate method to use barium 133 as a tracer or with respect to your result would you more recommend the use of radium 225 or 223 as a tracer?

A(Ljudmila Benedik): So if you ask for my personal opinion, the best way is barium. I prefer barium 133. But on the other hand I think that radium 225 is also an appropriate tracer because it is not complicated; just add thorium 229. But the problem occurs if you want to measure with γ-ray spectrometry. Then the activity must be higher and then in the case of α-particle spectrometry, the in-growth of actinium from radium 225 could be the problem. The tailing of actinium could overlap the radium 226.

Priloga 1: Nadaljevanje

G Model
NED-5722; No. of Pages 5

Nuclear Engineering and Design xxx (2010) xxx–xxx

Contents lists available at ScienceDirect

Nuclear Engineering and Design

journal homepage: www.elsevier.com/locate/nucengdes

Natural radionuclides in milk from the vicinity of a former uranium mine

Marko Štrok, Borut Smodiš*

"Jožef Stefan" Institute, Jamova 39, SI-1000 Ljubljana, Slovenia

ARTICLE INFO

Article history:
Received 5 January 2010
Received in revised form 19 March 2010
Accepted 24 March 2010
Available online xxx

ABSTRACT

Natural radionuclides in milk from farms in the vicinity of a former uranium mine Žirovski vrh in Slovenia, from a farm on the reference location, in powdered milk purchased from Ljubljana shops and in milk intended for infant food, were determined. In the milk samples, ^{238}U, ^{234}U, ^{226}Ra, ^{210}Pb and ^{210}Po were determined. After sample preparation, radiochemical separation and preparation of counting sources, ^{238}U, ^{234}U, ^{226}Ra and ^{210}Po were measured by alpha spectrometric system equipped with passivated implanted planar silicon detectors (PIPS) and ^{210}Pb by a gas-flow proportional counter. Activity concentrations varied from 0.009 to 0.354 Bq/kg dry weight for ^{238}U, 0.019–0.177 Bq/kg dry weight for ^{234}U, 0.041–0.110 Bq/kg dry weight for ^{226}Ra, 0.290–0.652 Bq/kg dry weight for ^{210}Pb and 0.055–0.611 Bq/kg dry weight for ^{210}Po. Assessed combined annual effective doses per unit of intake were from 8.7 to 13.0 μSv/year for adults and from 195 to 648 μSv/year for infants.

1. Introduction

Milk is one of the basic foodstuffs for many people, especially for infants. Radionuclides come into cows and consequently in milk through cow's food. In the areas with higher natural radioactivity levels, like in the area of the former uranium mine Žirovski vrh in Slovenia, one could reasonably expect higher activity concentrations of natural radionuclides in milk than in other areas. Man made radionuclides such as ^{90}Sr and ^{131}I, which can be released due to different human activities can also come into milk and consequently increase the radiation dose for humans.

Natural radionuclides of concern in the area of uranium mine are long-lived radionuclides ^{238}U, ^{234}U, ^{230}Th, ^{226}Ra, ^{210}Pb and ^{210}Po. With except of ^{210}Po and ^{234}U all of these radionuclides can be determined by gamma spectrometry although determinations are sometimes difficult because of low emission probability (^{238}U, ^{230}Th), low gamma ray energy (^{210}Pb) and problems with the determination via decay products or via peak subtraction (^{226}Ra). With except of ^{210}Pb, which is beta emitter, all others radionuclides are alpha emitters and can be determined by alpha spectrometry which requires previous radiochemical separation. In addition, ^{210}Pb can be determined by low background proportional counter, which also requires previous radiochemical separation.

In the past, natural radionuclides in milk from the vicinity of the former uranium mine Žirovski vrh were determined by gamma spectrometry and values found were below the detection limit (Omahen et al., 2006). Measurements included ^{226}Ra and ^{210}Pb and results were <0.03 Bq/kg fresh weight for ^{226}Ra and <0.2 Bq/kg fresh weight for ^{210}Pb (Omahen et al., 2006). As consequence, effective ingestion doses could not be assessed properly as the detection limits, which were higher than the actual activity concentrations, are used for dose calculations in annual monitoring reports for the mine. In addition ^{210}Po, although having one of the highest committed effective dose per unit of intake by ingestion and consequently contributing substantially to the effective dose due to milk consumption, has not been measured in the past. ^{210}Po is a pure alpha emitter and therefore it can be determined only by measurement of alpha particles. Radiotoxicity of ^{210}Po is connected with the fact that it emits alpha particles with relatively high energy of about 5.3 MeV and that it is concentrated in the soft tissues, such as muscles, livers and others. Radiotoxicity of other natural radionuclides are also connected with the fact that they are alpha (^{238}U, ^{234}U, ^{226}Ra) or beta (^{210}Pb) emitters and that they can be also concentrated in the different parts of the human body.

In our study ^{238}U, ^{234}U, ^{226}Ra, ^{210}Po and ^{210}Pb were determined in milk samples with the help of the radiochemical separation followed by the measurements with alpha spectrometry or a gas-flow proportional counter. These methods have about 10 times lower detection limit as gamma spectrometry and allows more accurate determination of radionuclides of interest. Consequently, this allows for more proper assessment of ingestion doses due to milk consumption.

The aim of the study was to compare selected radionuclide activity concentrations in milk samples from the farms near to the former uranium mine Žirovski vrh with a sample from the reference location. In addition, these activity concentrations were also compared to the powdered milk samples which are used for infant diets and were bought in Ljubljana shops. Afterwards, combined annual

* Corresponding author.
E-mail addresses: Marko.Strok@ijs.si (M. Štrok), Borut.Smodis@ijs.si (B. Smodiš).

0029-5493/$ – see front matter © 2010 Elsevier B.V. All rights reserved.
doi:10.1016/j.nucengdes.2010.03.035

Please cite this article in press as: Štrok, M., Smodiš, B., Natural radionuclides in milk from the vicinity of a former uranium mine. Nucl. Eng. Des. (2010), doi:10.1016/j.nucengdes.2010.03.035

Priloga 1: Nadaljevanje

G Model
NED-5722; No. of Pages 5

Nomenclature

a	activity concentration (Bq/kg dry weight)
E_{ing}	annual effective ingestion dose due to particular radionuclide in Sv/year
$h(g)_{ing}$	committed effective dose per unit of intake by ingestion (Sv/Bq)
m	annual intake of milk for certain group of individuals (kg/year)

effective ingestion doses were calculated for adults and infants and radionuclides, which contribute the major part to the dose, were identified.

2. Experiment

2.1. Sampling and sample preparation

Four milk samples from the farms near to the former uranium mine Žirovski vrh and one milk sample from the reference location was collected by the company Rudnik Žirovski vrh, which is responsible for the closure of the uranium mine. The volume of each collected milk sample was about 5 L. In addition, four powdered milk samples, which are used for infant diets were purchased in a shop in Ljubljana. One of the purchased powdered milk samples was from Slovenian Dairy Pomurske mlekarne with no additives. The other three powdered milk samples were intended for infant food and were produced by the Hipp company from Gmunden in Austria. These products were from organic production and differed in their composition according to the infant age. The Hipp PRE is intended for food for newborns from first day up to 6 months, the Hipp 2 for infants from 6 to 10 months and the Hipp 3 for infants after 10 months of age. Ingredients of the Hipp infant diet are skimmed milk, vegetable oils, lactose, starch, sweet whey powder partially demineralised (all from organic production) and calcium chloride, vitamin C, calcium hydroxide, iron lactate, zinc sulphate, niacin, vitamin E, pantothemic acid, copper sulphate, folic acid, vitamin K, vitamin A, potassium iodate, vitamin B_6, vitamin B_1, manganese sulphate, sodium selenite, biotin and vitamin D.

Milk samples were weighed and then evaporated at 60 °C until dryness and again weighed in order to determine the wet weight/dry weight ratio. Evaporation of milk samples was performed at the Department for low and intermediate energy physics, Jožef Stefan Institute. Samples were sealed in plastic bags and stored into the refrigerator until analysis.

For the determination of ^{238}U, ^{234}U and ^{226}Ra, samples were ashed at 650 °C for 4 h in order to eliminate organic matter and to reduce the sample size. This was not the case for the determination of ^{210}Po and ^{210}Pb due to their potential volatilization at higher temperatures.

2.2. Radiochemical separation of ^{238}U, ^{234}U and ^{226}Ra

All samples were analysed in duplicates. To the 3 g of ashed milk sample, known activities of ^{232}U and ^{133}Ba were added in order to trace chemical recovery of the radiochemical separation. Activity concentrations of both tracers were traceable to SI units. After that, sample was digested with 4 mL HNO_3 and 4 mL HCl and then evaporated until incipient dryness at 200 °C. Then 2 mL of H_2O_2 was added and sample again evaporated until incipient dryness. After that, the sample was dissolved in 2 mL HNO_3 and 10 mL of deionised water and filtered through black ribbon filter paper. Radium and barium were precipitated with addition of 2 mL H_2SO_4 and 1 ml Pb carrier (50 mg/mL Pb^{2+}). After 30 min, sample was centrifuged and supernatant with uranium was decanted and stored for uranium separation. Precipitate with radium and barium was further washed with deionised water and centrifuged until neutral pH was achieved. Then the precipitate was dissolved and Ra was microprecipitated using principles described in Lozano et al. (1997). To the precipitate, 4 mL of 0.1 M EDTA/0.5 M NaOH were added and precipitate was shaken until complete dissolution. After that, 0.3 mL 0.3 mg/mL Ba^{2+} carrier, 1 drop of pH indicator, 2 mL of 1:1 acetic acid, 4 mL of saturated solution of Na_2SO_4 and 0.3 mL of 0.125 mg/mL $BaSO_4$ were added in order to microprecipitate radium as $Ba(Ra)SO_4$. After 30 min, sample was filtered through a 0.1 μm filter, which was then glued onto an Al disc in order to prepare counting source for alpha spectrometric measurement.

To the supernatant, which was decanted for uranium separation, ammonia was added until alkaline pH was achieved. Then five drops of 5 mg/mL Fe^{3+} was added in order to coprecipitate uranium with iron hydroxides. After 30 min, sample was centrifuged, supernatant was discarded, precipitate washed with deionised water and again centrifuged until neutral pH was achieved. Then the precipitate was dissolved with 3 M HNO_3/1 M $Al(NO_3)_3$ and solution poured through the UTEVA separation column, which was previously washed with 5 mL of 3 M HNO_3. After pouring the sample, centrifuge tube was washed twice with 2 mL 3 M HNO_3 and the washing was transferred onto the separation column. This process was followed by another 6 mL of 3 M HNO_3 was transferred onto the column. After that, the column was washed with consecutive addition of 2 mL 9 M HCl and 20 mL 5 M HCl/0.05 M oxalic acid. Eluates from all prior steps were discarded and uranium eluted with 15 mL 1 M HCl. Uranium was microprecipitated with addition of 0.1 mL 0.5 mg/mL Nd^{3+}, 1 mL of 15% $TiCl_3$ and 1 mL HF. Then the sample was placed for 30 min on ice bath and after that filtered through a 0.1 μm filter, which was prior to filtration conditioned with 10 mL of 5 μg/mL NdF_3 substrate solution. After filtration, counting source for alpha spectrometry was prepared with mounting the filter onto an Al disc.

2.3. Radiochemical separation of ^{210}Po

All samples were analysed in duplicates. To the 15 g of powdered or dried milk sample, known activity of the Po-209 tracer was added in order to determine chemical recovery of the radiochemical separation. Activity concentration of Po-209 tracer was traceable to SI units. Sample was transferred into the Erlenmeyer flask and digested with 30 mL HNO_3 and 5 mL HCl at 200 °C for 1 h. During the digestion period, the flask was covered with a watch glass. After the digestion, the solution was cooled down, watch glass was removed and the solution evaporated to dryness at 100 °C. Then 10 mL H_2O_2 and 1 mL HCl was added to the dried residue and again evaporated until dryness at 100 °C. After that 10 mL HCl was added and evaporated until dryness at 100 °C. Then 5 mL H_2O_2 was added and again evaporated to dryness. This was followed with addition of 1 mL HCl, 15 mL of deionised water and 1 g NH_2OHHCl. Finally the sample was cooled down, filtered through the black ribbon filter paper and diluted to 100 mL with deionised water. After that the counting source was prepared with spontaneous deposition of Po onto a copper disc for 4 h at 80 °C. At the end of the Po spontaneous deposition, the copper disc was washed with deionised water and dried on the air.

2.4. Radiochemical separation of ^{210}Pb

All samples were analysed in duplicates. To the 100 g of powdered or dried milk sample 25 mg Pb^{2+} was added in order to trace chemical recovery of the radiochemical separation. Mass of the added Pb^{2+} was traceable to SI units. Then 200 mL HNO_3 and 40 mL HCl were added and sample was heated up to 200 °C for 1 h

Please cite this article in press as: Štrok, M., Smodiš, B., Natural radionuclides in milk from the vicinity of a former uranium mine. Nucl. Eng. Des. (2010), doi:10.1016/j.nucengdes.2010.03.035

Priloga 1: Nadaljevanje

G Model
NED-5722; No. of Pages 5

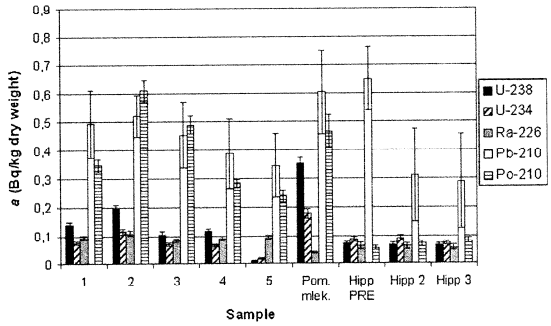

Fig. 1. Activity concentrations of the analysed radionuclides in milk samples (Pom. mlek. is the abbreviation for Pomurske mlekarne).

in order to digest the sample. After cooling to the 100 °C, 20 mL H_2O_2 was added and further digested for 1 h at the same temperature. Then the sample was cooled down and filtered through the black ribbon filter paper. After that, the filtrate was evaporated until incipient dryness at 100 °C. The dried residue was dissolved in 100 mL 2 M HCl and filtered through the black ribbon filter paper. ^{210}Pb was separated from other radionuclides according to Tavčar and Benedik (2002). Filtrate was introduced onto the Eichrom Sr resin separation column, which was previously rinsed with 100 mL 2 M HCl. After pouring the sample, column was washed with 90 mL 2 M HCl and consecutive addition of 60 mL 6 M HNO_3. All eluates until now were discarded. Pb was stripped from the column with addition of 90 mL 6 M HCl. The eluate was collected in a beaker and the solution was evaporated until incipient dryness. The sample was then dissolved with 40 mL of deionised water and 3 mL of H_2SO_4 was added in order to precipitate lead as $PbSO_4$. After 1 h sample was centrifuged, supernatant discarded and precipitate washed with deionised water until neutral pH was achieved. After that, precipitate was transferred onto a counting planchet and dried under the heating lamp. Radiochemical recovery was determined by weighing the precipitate.

2.5. Measurements

Uranium isotopes and ^{210}Po were measured by an alpha spectrometry system equipped with PIPS detectors. Results were corrected for chemical recovery, which was determined with help of the added ^{232}U tracer for uranium isotopes and ^{209}Po tracer for ^{210}Po. Chemical recovery for ^{226}Ra was determined via gamma spectrometric measurement of ^{133}Ba and ^{226}Ra was measured by the same alpha spectrometry system as in case of uranium and polonium. ^{210}Pb was measured onto a low background gas-flow proportional counter previously calibrated as described in Štrok et al. (2008). Chemical recovery for ^{210}Pb was determined via weighing the $PbSO_4$ precipitate. All results were corrected for blanks. Blanks were prepared following the same radiochemical separation procedure as for samples.

3. Results and discussion

3.1. Activity concentrations of analysed radionuclides in milk samples

Results for the analysed radionuclides are presented in Fig. 1 and Table 1 with combined standard uncertainties with coverage factor $k = 1$. Fig. 1 shows activity concentration of particular radionuclide for particular sample. Radiochemical recoveries were in the range 47–86% for uranium isotopes, 36–81% for ^{226}Ra, 21–43% for ^{210}Pb and 47–85% for ^{210}Po. Milk samples 1–4 are from the farms near to the former uranium mine Žirovski vrh and milk sample 5 from the reference location. The highest activity concentrations (a) of ^{238}U and ^{234}U were found in powdered milk sample from the Pomurske mlekarne dairy and lowest in the milk sample 5 from the reference location. Activity concentration of ^{226}Ra was in the range from 0.041 Bq/kg dry weight for the powdered milk sample from the Pomurske mlekarne dairy up to 0.110 Bq/kg dry weight for milk sample 2. The lowest activity concentration of ^{210}Pb was found in Hipp 3 infant diet (0.290 Bq/kg dry weight) and the highest in Hipp PRE infant diet (0.652 Bq/kg dry weight). ^{210}Po activity concentrations were in the range from 0.055 Bq/kg dry weight for Hipp PRE up to 0.611 Bq/kg dry weight for the milk sample 2.

The average ^{234}U/^{238}U ratio for milk samples 1–4 and powdered milk from Pomurske mlekarne is about 0.56, which is not the case for the Hipp samples, where it is about 1.25. ^{234}U is a decay product from the ^{238}U decay chain and usually it is supposed that under undisturbed and steady conditions, they are in a secular radioactive equilibrium. However, the so-called recoil effect can cause disruption of equilibrium in soil and water (Bourdon et al., 2003; Adloff and Rössler, 1991; Suksi et al., 2006). This effect is evidenced by reduced ^{234}U/^{238}U ratio within the observed particle and increased ratio in its environment. This would mean that if this effect is present, ratios higher than 1 can be expected in water and the ratio of about 1 if this is not the case. Consequently, plants that take up such water could have ratios which are higher or equal to 1 and similar could hold for cow's milk. However, it is not possible to attribute ratios that are substantially lower than 1 to this effect. Consequently recoil effect cannot explain ^{34}U/^{238}U ratio for milk samples 1–4 and powdered milk from Pomurske mlekarne. Therefore, further research is needed in order to identify reason for low ^{234}U/^{238}U ratios observed in some milk samples.

Interestingly, ^{210}Po activity concentrations for all Hipp infant diet samples are substantially lower than ^{210}Pb activity concentrations, which is not the case for other samples where, taking into account uncertainties, activity concentrations of these two radionuclides are similar. The reason for that difference is not evident. Namely, ^{210}Pb decays into ^{210}Bi and then into ^{210}Po. Relatively short half lives of ^{210}Bi and ^{210}Po (5 and 138 days, respectively) would mean that if there would be difference in uptake of ^{210}Pb and ^{210}Po, this should be evident from the results from milk samples 1–5, which were collected directly from farmers and therefore,

Please cite this article in press as: Štrok, M., Smodiš, B., Natural radionuclides in milk from the vicinity of a former uranium mine. Nucl. Eng. Des. (2010), doi:10.1016/j.nucengdes.2010.03.035

Priloga 1: Nadaljevanje

G Model
NED-5722; No. of Pages 5

Table 1
Results of analysed radionuclides in milk, powdered milk and infant diet samples with combined standard uncertainties ($k = 1$).

Sample	Fresh weight/dry weight	a (Bq/kg dry weight)				
		^{238}U	^{234}U	^{226}Ra	^{210}Pb	^{210}Po
1	8.6	0.139 ± 0.009	0.075 ± 0.006	0.094 ± 0.008	0.492 ± 0.118	0.347 ± 0.021
2	9.4	0.195 ± 0.012	0.115 ± 0.009	0.110 ± 0.008	0.522 ± 0.075	0.611 ± 0.039
3	7.5	0.107 ± 0.008	0.067 ± 0.006	0.085 ± 0.006	0.454 ± 0.117	0.490 ± 0.030
4	7.3	0.116 ± 0.007	0.064 ± 0.005	0.091 ± 0.007	0.388 ± 0.122	0.285 ± 0.014
5	7.8	0.009 ± 0.002	0.019 ± 0.003	0.094 ± 0.007	0.345 ± 0.113	0.239 ± 0.021
Pomurske mlekarne	–	0.354 ± 0.023	0.177 ± 0.015	0.041 ± 0.004	0.605 ± 0.148	0.467 ± 0.057
Hipp PRE	–	0.071 ± 0.008	0.087 ± 0.009	0.063 ± 0.010	0.652 ± 0.111	0.055 ± 0.006
Hipp 2	–	0.066 ± 0.008	0.091 ± 0.010	0.062 ± 0.008	0.312 ± 0.162	0.070 ± 0.010
Hipp 3	–	0.065 ± 0.007	0.074 ± 0.008	0.057 ± 0.008	0.290 ± 0.165	0.082 ± 0.011

time to establish secular radioactive equilibrium was too short. More likely, the reason for this discrepancy could be that ^{210}Pb is present in some of the additives, which are not old enough that secular radioactive equilibrium could be achieved or that milk drying and reprocessing removes polonium from the powdered milk.

3.2. Assessment of annual effective ingestion dose due to radionuclides in milk

For calculation of the annual effective ingestion dose due to radionuclides in milk, Eq. (1) was used.

$$E_{ing} = h(g)_{ing} a m \quad (1)$$

where E_{ing} is the annual effective ingestion dose due to particular radionuclide in Sv/year, $h(g)_{ing}$ is committed effective dose per unit of intake by ingestion in Sv/Bq, a is activity concentration of a particular radionuclide in the sample in Bq/kg dry weight and m is the annual intake of milk for certain group of individuals in kg/year. For the calculation, data from Tables 1 and 2 were used. Committed effective dose per unit of intake by ingestion were from the Official Gazzete of the Republic of Slovenia (2004) and are consistent with the IAEA International Basic Safety Standards (IAEA, 2003). Annual effective ingestion doses were calculated for adults (average of the samples 1–4 and sample 5) and infants (average of the samples 1–4, sample 5, powdered milk from Pomurske mlekarne and Hipp infant diet). Annual effective ingestion dose due to milk consumption strongly depends on the milk consumption. In our study mass of the milk consumed by the adults was 122 kg fresh weight (Omahen et al., 2006). Mass of the milk consumed by the infant for Hipp infant diet was calculated according to the instructions on the products and it was 22.4 kg dry weight for Hipp PRE (from birth to the 6 months), 10.8 kg dry weight for Hipp 2 (from 6 to 10 months) and 3.6 kg dry weight for Hipp 3 (from 10 to 12 months). Effective ingestion doses of the three products were summed in order to obtain annual effective ingestion dose. In order to obtain comparable results, mass of the powdered milk from Pomurske mlekarne diary was calculated as sum of all Hipp products and was 36.8 kg dry weight. This mass correspond to the 294.5 kg of fresh milk samples 1–4 and milk sample 5, which was used for the calculation of the annual ingestion dose for the infants for that samples.

Table 2
Committed effective dose per unit of intake by ingestion for adults and infants (Official Gazette of the Republic of Slovenia, 2004).

Radionuclide	$h(g)_{ing}$ (Sv/Bq)	
	Adults	Infants (≤1 year)
^{238}U	4.5×10^{-8}	3.4×10^{-7}
^{234}U	4.9×10^{-8}	3.7×10^{-7}
^{226}Ra	2.8×10^{-7}	4.7×10^{-6}
^{210}Pb	6.9×10^{-7}	8.4×10^{-6}
^{210}Po	1.2×10^{-6}	2.6×10^{-5}

Table 3
Combined annual effective ingestion dose per unit of intake for all radionuclides for adults and infants.

	E_{ing} (μSv/year)
Adults; 1–4	13.0 ± 1.7
Adults; 5	8.7 ± 1.6
Infants; 1–4	562 ± 74
Infants; 5	363 ± 66
Infants; Pomurske mlekarne	648 ± 98
Infants; Hipp	195 ± 40

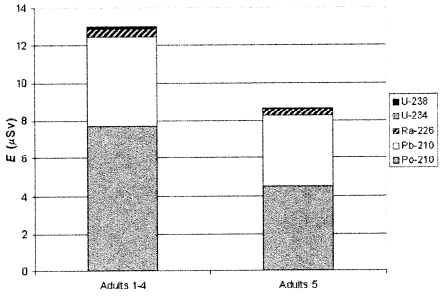

Fig. 2. Effective annual ingestion doses for particular radionuclides for adults.

Results of the dose calculations are presented in Table 3 and Figs. 2–4. Fig. 2 shows effective annual ingestion doses for particular radionuclides for adults and Fig. 3 effective annual ingestion doses for particular radionuclides for infants. Fig. 4 shows contribution

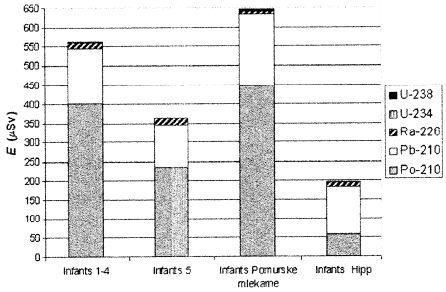

Fig. 3. Effective annual ingestion doses for particular radionuclides for infants.

Please cite this article in press as: Štrok, M., Smodiš, B., Natural radionuclides in milk from the vicinity of a former uranium mine. Nucl. Eng. Des. (2010), doi:10.1016/j.nucengdes.2010.03.035

Priloga 1: Nadaljevanje

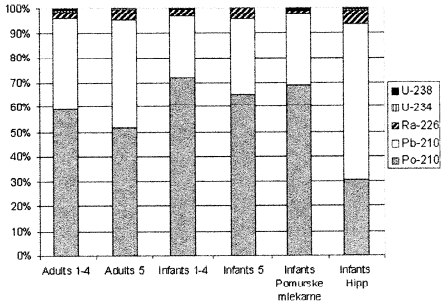

Fig. 4. Contributions of particular radionuclides to the combined effective annual ingestion dose.

of particular radionuclide to the combined effective annual ingestion dose for different analysed samples. Combined annual effective ingestion dose for adults consuming milk from the vicinity of the former uranium mine Žirovski vrh (samples 1–4) is 4.3 μSv/year higher than for adults consuming milk from the reference site (sample 5). This is due to higher ^{210}Pb and ^{210}Po activity concentrations in samples 1–4. However, for infants, the highest combined annual effective ingestion dose was calculated for powdered milk sample from the Pomurske mlekarne diary (648 μSv/year). The lowest dose was calculated for the Hipp diet (195 μSv/year). Reason for that is low ^{210}Po activity concentration found in the latter samples.

Fig. 4 shows contribution of particular radionuclide to the combined annual effective dose, expressed in percent. It is evident that ^{210}Po annual effective dose represents from 50 up to 70% of the combined dose for all samples except for Hipp diet. This is clear evidence of importance of the ^{210}Po determination for any dose assessment involving natural radionuclides. From Fig. 3 it is also evident that only two radionuclides (^{210}Pb and ^{210}Po) are responsible for more than 90% of the combined annual ingestion dose due to milk consumption.

4. Conclusions

Results of our study showed that levels of measured radionuclides in milk from the area of former uranium mine Žirovski vrh are comparable to the reference location, with exception of uranium; activity concentration of uranium was lower at the reference location. Combined annual effective ingestion dose for adults was higher in milk from the area of former uranium mine Žirovski vrh (13.0 ± 1.7 μSv/year) than in milk from the reference location (8.7 ± 1.6 μSv/year). On the other hand, the highest combined annual effective ingestion dose for infants was found for the powdered milk sample from Pomurske mlekarne diary (648 ± 98 μSv/year). Main contributors to the combined annual effective ingestion dose are ^{210}Po and ^{210}Pb, which are responsible for more than 90% of the dose.

Acknowledgments

This work was supported by the Rudnik Žirovski vrh company. The Slovenian Research Agency (contract no. P2-0075) is acknowledged. Assistance of the Department for low and intermediate energy physics, Jožef Stefan Institute for drying of milk samples is greatly appreciated.

References

Adloff, J.P., Rössler, K., 1991. Recoil and transmutation effects in the migration behaviour of actinides. Radiochim. Acta 52/53, 269–274.
Bourdon, B., Turner, S., Henderson, G.M., Lundstrom, C.C., 2003. Introduction to U-series Geochemistry. Rev. Mineral. Geochem. 52, 7–10.
IAEA, 2003. International Basic Safety Standards for Protection against Ionizing Radiations and for the Safety of Radiation Sources. Safety Series No. 115.
Lozano, J.C., Fernandez, F., Gomez, J.M.G., 1997. Determination of radium isotopes by $BaSO_4$ coprecipitation for the preparation of alpha-spectrometric sources. J. Radioanal. Nucl. Chem. 223, 133–137.
Official Gazette of the Republic of Slovenia, 2004. Decree on dose limits, radioactive contamination and intervention levels, 49/2004 (in Slovene).
Omahen, G., Benedik, L., Repinc, U., 2006. Measurements of the radioactivity in the Žirovski vrh uranium mine environment and assessment of its environmental impacts—results for 2005. Jožef Stefan institute, Ljubljana, IJS-DP-9342 (in Slovene).
Suksi, J., Rasilainen, K., Pitkänen, P., 2006. Variations in $^{234}U/^{238}U$ activity ratios in groundwater—a key to flow system characterisation? Phys. Chem. Earth 31, 556–571.
Štrok, M., Repinc, U., Smodiš, B., 2008. Calibration and validation of a proportional counter for determining beta emitters. J. Power Energy Syst. 2, 573–581.
Tavčar, P., Benedik, L., 2002. Determination of ^{210}Pb and ^{210}Po in sediments, water, and plants in an area contaminated with mine waste. Mine Water Environ. 21, 156–159.

Please cite this article in press as: Štrok, M., Smodiš, B., Natural radionuclides in milk from the vicinity of a former uranium mine. Nucl. Eng. Des. (2010), doi:10.1016/j.nucengdes.2010.03.035

Priloga 1: Nadaljevanje

J Radioanal Nucl Chem
DOI 10.1007/s10967-010-0708-0

Accumulation of ^{226}Ra, ^{238}U and ^{230}Th by wetland plants in a vicinity of U-mill tailings at Žirovski vrh (Slovenia)

Marko Černe · Borut Smodiš · Marko Štrok · Radojko Jaćimović

Received: 8 July 2010

Abstract The impact of a U-mill tailing on radionuclide accumulation by plants was assayed. In particular, a preliminary screening of ^{226}Ra, ^{238}U and ^{230}Th in Marsh marigold (*Caltha palustris* L.), soft rush (*Juncus effusus* L.) and Tall Moor grass (*Molinia arundinacea* (L.) Moench) grown in a marsh habitat is presented. Activity concentrations for the studied radionuclides and their transfer factors for the particular plants are shown and discussed.

Keywords ^{238}U · ^{226}Ra · ^{230}Th · Uranium mine · Plants · Accumulation

Introduction

Uranium mines tailings are one of the important sources of natural radionuclides from U-decay chain in the environment. The uranium mine at Žirovski vrh in Slovenia has two tailings sites with U-mill tailings deposited on the Boršt and red mud on the Jazbec site. Tailings from the Boršt site contain 995 ± 80 Bq kg^{-1} d.w. of ^{238}U, 8630 ± 340 Bq kg^{-1} of ^{226}Ra and 3930 ± 580 Bq kg^{-1} d.w. of ^{230}Th [1]. Transfer of the three radionuclides from that site to the surrounding environment is probable due to flow of seepage waters from the tailings pile. Radionuclides are first bound by the soil particles and subsequently taken up by organisms [2]. Several studies confirmed accumulation of U [3, 4] and Ra [5–7] in plants, while accumulation of Th is known to be less effective [8]. U is most often accumulated in roots and less in shoots [9]. The uptake of Ra is supposed to be similar to the uptake of Ca due to their similar chemical activity [10, 11]. The accumulation of radionuclides in plants may pose risk to humans and herbivore animals due to ingestion. Evaluation of radionuclide transfer through a soil–plant system is therefore important for better radiological risk assessment.

The aim of this study was preliminary screening of ^{238}U, ^{226}Ra and ^{230}Th accumulation by Tall Moor grass (*Molinia arundinacea* (L.) Moench), Marsh marigold (*Caltha palustris* L.) and soft rush (*Juncus effusus* L.), grown on a small marsh area continuously flooded by tailings seepage waters.

M. Černe · B. Smodiš (✉) · M. Štrok · R. Jaćimović
Jožef Stefan Institute, Jamova cesta 39,
1000 Ljubljana, Slovenia
e-mail: borut.smodis@ijs.si

Published online: 19 August 2010

Materials and methods

Study location

The uranium mine at Žirovski vrh operated from 1985 to 1990 and about 600,000 tons of U-ore were processed during that period. The U-mill tailings with high activity concentrations of ^{238}U, ^{230}Th and ^{226}Ra were disposed at the Boršt site. The sampled plants (*J. effusus*, *C. palustris* and *M. arundinacea*) were grown on a small marsh (mark 2 on Figs. 1, 2) which was created downwards the disposal site (mark 1 on Fig. 1). The marsh lies outside of the controlled area and is constantly flooded by tailings seepage waters.

Sampling and sample preparation

The plants (*J. effusus*, *C. palustris* and *M. arundinacea*) grown on contaminated marsh (Fig. 2) were taken in July 2009 from the whole marsh area at places with sufficient vegetation cover. The contaminated marsh was located

Priloga 1: Nadaljevanje

Fig. 1 Air picture of Boršt tailings pile and contaminated marsh (latitude = 46°05′07.40″, altitude = 14°10′52.15″)

Fig. 2 Contaminated marsh

some tens of metres distant from a tailings pile. Grasses, soft rush and marsh marigolds were taken as composite samples (composed of about 200 plants) from one location. The grasses were in the vegetative stage, while some plants of soft rush and marsh marigolds were already in the flowering stage. The control plants, which also represented a composite sample (about 200 plants of each plant species) were taken from the marsh in the vicinity of Ljubljana, the capital of Slovenia. About 50 individual plants for each plant species were used for alpha spectrometric measurements. Soil samples were taken from two places of the rooting zone (20 cm). The two samples taken were approximately 5 meters apart from each other. One sample of seepage tailings water (20 L) was taken at the same site.

The plants of marsh marigold were separated on stems and leaves. In case of grasses and soft rush the whole aboveground parts were taken. The roots were not analysed due to low amount of samples. The plant samples were first air dried and than for two days in an oven dried at 80 °C. The dried samples were milled with a rotor speed mill and than ashed at 650 °C. Soil samples were dried at 60 °C, sieved through 2 mm sieve and than ashed at 650 °C.

Determination of radionuclides by alpha spectrometric measurements

Plant and soil samples

Determination of ^{226}Ra, ^{238}U and ^{230}Th radionuclides in plants and soils comprised radiochemical separation followed by alpha spectrometric measurement. About 0.5 g of ashed samples, together with 2 g of Na_2O_2 and 2 g of Na_2CO_3, were melted at 900 °C to get the alkaline melt. The radiotracers ^{133}Ba for ^{226}Ra, ^{232}U for ^{238}U and ^{229}Th for ^{230}Th were added after melting for recovery determination. Then, the dedicated procedures for U, Th and Ra determination were followed, as described by Štrok et al. [12].

Water samples

Procedures for ^{226}Ra, ^{238}U and ^{230}Th determination in seepage tailings waters were adopted from the literature [13, 14] and modified by Štrok et al. [12].

Measurement of activity concentrations

The activity concentrations of ^{238}U, ^{226}Ra and ^{230}Th were measured by an alpha spectrometer (Alpha-Analyst, Canberra) equipped with PIPS semiconductor detectors having efficiency of 28%. The calibration was done with electroplated certified standard sources containing ^{239}Pu, ^{238}U, ^{234}U and ^{241}Am. The measurements were validated by participation in interlaboratory comparisons and proficiency tests organised by the International Atomic Energy Agency, Austria, the Institute for Reference Materials and Measurements, Belgium, and the National Physical Laboratory, UK. The results were in all cases satisfactory. The alpha spectrometric results were also crosschecked with gamma spectrometric measurements wherever possible. Detection limits for plants depended on the sample quantity and were in the range from 0.01 to 0.40 Bq kg^{-1} d.w. for ^{226}Ra, from 0.01 to 0.17 Bq kg^{-1} d.w. for ^{238}U and from 0.01 to 0.12 Bq kg^{-1} d.w. for ^{230}Th.

Complementary determinations

Organic matter content, clay content, pH value, exchangeable cations, available phosphorus and potassium, and CEC of soils were assayed in the Centre for Pedology of the Agronomy Department, Biotechnical faculty, University of Ljubljana. For these determinations, the standard ISO recommended procedures were applied.

The macro elements K, Ca and Mg in plants were determined by neutron activation analysis [15].

Priloga 1: Nadaljevanje

Transfer factors

Transfer factor or transfer coefficient is the ratio between activity concentration in a plant (Bq kg^{-1} d.w. of a plant) and activity concentration in soil (Bq kg^{-1} d.w. of soil) and is used as a parameter for describing accumulation of radionuclides [10]. Transfer factors were calculated as ratio of activity concentration in pooled plant samples (about 50 plants) and average activity concentration in soil.

Results and discussion

Radionuclides in the contaminated marsh soil

Relatively higher activity concentrations in the contaminated marsh soil are attributed to permanent flooding of marsh by contaminated seepage tailings waters from the tailings pile. This hypothesis can reasonably be confirmed by relatively high activity concentrations, in particular ^{238}U and ^{226}Ra, as shown in Table 1. Activity concentrations of ^{238}U, ^{230}Th and ^{226}Ra in the marsh soil taken at the two microlocations are quite different and were 320 ± 60 and 450 ± 90 Bq kg^{-1} d.w., respectively for ^{238}U, 160 ± 30 and 1650 ± 350 Bq kg^{-1} d.w., respectively for ^{226}Ra, and 120 ± 20 and 600 ± 120 Bq kg^{-1} d.w, respectively for ^{230}Th (Table 2). Soil characteristics were also different, especially pH value (4.2 and 6.5, respectively), organic matter content (24.1 and 8.0%, respectively), clay content (25.2 and 12.0%, respectively), CEC (45.2 and 26.9 mmol C+/100 g, respectively), available phosphorus (9.4 and 2.1 mg/100 g, respectively), available potassium (17.3 and 10.3 mg/100 g, respectively) and exchangeable calcium (8.2 and 19.0 mmol C+/100 g, respectively).

Table 1 Activity concentrations in the tailings seepage water (expanded uncertainties, $k = 2$)

Radionuclide	a (Bq m^{-3})
^{238}U	8200 ± 758
^{230}Th	1.1 ± 0.2
^{226}Ra	193 ± 14

Table 2 Activity concentrations (average and range) in two contaminated marsh soil samples

Radionuclide	Average a (Bq kg^{-1} d.w.)	Range (Bq kg^{-1} d.w.)
^{238}U	385	320–450
^{226}Ra	900	160–1650
^{230}Th	360	120–600

Radionuclides in the plants

Activity concentrations of ^{238}U, ^{230}Th and ^{226}Ra in plants from the contaminated marsh were evidently higher compared to the control plants (Table 3).

^{226}Ra in plants

The highest activity concentration of ^{226}Ra (35 times higher compared to the control site) was found in *J. effusus* (Table 3) which resulted in the highest transfer factor calculated for this plant (Table 4). It should be mentioned, however, that the metal accumulation capacity for *J. effusus* was proved in several studies [16–18]. It is interesting that in *C. palustris* the ^{226}Ra activity concentration was almost three times higher in stems than in leaves (Fig. 3). This fact could be attributed to higher content of Ca in leaves and lower content of Ca in stems of the same plant (Fig. 4), as reported in several studies [11, 19, 20]. ^{226}Ra activity concentration in *M. arundinacea* was 40 times higher compared to the control site (Table 3) and could be affected by Ca content in shoots [10]. Transfer factor for this grass species (Table 4) is comparable to the literature data for grasses [21]. Soil-to-plant transfer factors increase in the following order: *C. palustris* < *M. arundinacea* < *J. effusus* (Table 4).

^{238}U in plants

Relatively low content of U in soil resulted in low activity concentrations of ^{238}U in all three plant species. Transfer factor was the highest for *J. effusus* which could be explained by its ability to accumulate toxic metals. Soil-to-plant transfer factors increase in the following order: *M. arundinacea* = *C. palustris* < *J. effusus* (Table 4).

^{230}Th in plants

The lowest activity concentration of ^{230}Th was found in *M. arundinacea* which is probably related to low thorium mobility in soil [8] and metal-excluding mechanism as known for several grass species growing on metalliferous or metal-contaminated soil [22, 23]. Transfer factor for *M. arundinacea* is in the same range as found in the literature for grasses [21]. Soil-to-plant transfer factors increase in the following order: *M. arundinacea* < *J. effusus* < *C. palustris* (Table 4).

One should also consider probability for the contamination of plants due to soil resuspension as result of wind blowing. However, in our specific case this was less probable due to the coverage of the tailings pile with a thick layer of non-contaminated soil and dense vegetation of trees around the marsh. So the root uptake of ^{238}U, ^{230}Th

Priloga 1: Nadaljevanje

Table 3 Activity concentrations in plants (pooled samples, about 50 plants) from the contaminated and control sites (expanded uncertainties, $k = 2$)

Bq kg^{-1} d.w.	*Caltha palustris*-leaves	*Caltha palustris*-stems	*Juncus effusus*	*Molinia arundinacea*
Contaminated site				
^{238}U	1.9 ± 0.3	3.9 ± 0.8	7.8 ± 0.6	2.9 ± 0.4
^{226}Ra	12.4 ± 1.1	34 ± 3	70 ± 7	40 ± 3
^{230}Th	6.6 ± 0.7	7.9 ± 0.9	3.8 ± 0.4	1.1 ± 0.2
Control site				
^{238}U	0.6 ± 0.2	0.4 ± 0.1	1.0 ± 0.2	0.10 ± 0.04
^{226}Ra	2.0 ± 0.3	4.4 ± 0.6	2.0 ± 0.2	1.0 ± 0.1
^{230}Th	2.2 ± 0.2	1.5 ± 0.3	1.0 ± 0.1	0.40 ± 0.04

Table 4 Transfer factors of plants (pooled samples, about 50 plants) from the contaminated site (Activity concentration in *C. palustris*, used for TF calculation is an average of activity concentration in stems and leaves)

	TF (kg kg^{-1})		
	Caltha palustris	*Juncus effusus*	*Molinia arundinacea*
Contaminated site			
^{238}U	0.008	0.020	0.008
^{226}Ra	0.026	0.078	0.044
^{230}Th	0.020	0.011	0.003

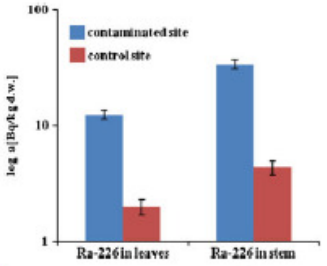

Fig. 3 ^{226}Ra activity concentrations (Bq kg^{-1} d.w.) in leaves and stems of *Caltha palustris* from contaminated and control sites

and ^{226}Ra remains the only reliable explanation for the elevated activity concentrations observed in the studied area.

There is a need for further studies on transfer factors for the three radionuclides in the studied plants, as there is a general lack of relevant data. This is particularly needed for ^{226}Ra and ^{238}U in *C. palustris*, and ^{230}Th in all studied plants.

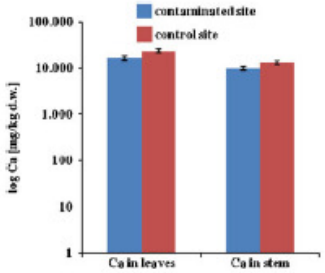

Fig. 4 Calcium content (mg kg^{-1} d.w.) in leaves and stems of *Caltha palustris* from contaminated and control sites

Conclusions

Seepage tailings waters contribute to increased activity concentrations of uranium, radium and thorium in plants (*J. effusus*, *C. palustris*, *M. arundinacea*) from contaminated marsh at the studied area, but this does not pose risk to the environment as the content of radionuclides in the tested plants is nevertheless relatively low. The obtained results show the highest ^{226}Ra and the lowest ^{230}Th activity concentrations in all three plant species. This is comparable to the literature data for other plants and is probably consequence of higher radium mobility in the soil and low thorium mobility due to strong binding capacity. Activity concentrations were different for each plant species. The influence of calcium content on radium activity concentration in plants was observed in *C. palustris*, but further investigation is required to appropriately evaluate this phenomenon. Further studies should also be carried out for *J. effusus*, which is already known to accumulate toxic metals, and for the less investigated *M. arundinacea*. It would be interesting to include *J. effusus* as a biomonitor of water contamination around the former uranium mine due to its potential accumulation ability. As the flow of mine

Priloga 1: Nadaljevanje

waters through the Boršt tailings site is expected to be relatively constant also in the future, the dispersion of uranium and its decay products within the nearby waters could thus be bio-monitored. In the future, similar investigations should be focused on radium screening in other plants from the area around the former uranium mine at Žirovski vrh in Slovenia.

Acknowledgments This work was financially supported by the Slovenian Research Agency (contract no. P2-0075). The authors would like to thank Mr. Jože Rojc of the Rudnik Žirovski vrh company for his cooperation and to the Centre for Pedology of the Agronomy Department, Biotechnical faculty, University of Ljubljana, for soil characteristics determination.

References

1. Križman M, Byrne AR, Benedik L (1995) Distribution of ^{230}Th in milling wastes from Žirovski vrh uranium mine (Slovenia), and its radioecological implications. J Environ Radioact 26:223–235
2. Tamponnet C, Martin-Garin A, Gonze M-A, Parekh N, Vallejo R, Sauras-Yera T, Casadesus J, Plassard C, Staunton S, Norden M, Avila R, Shaw G (2008) An overview of BORIS: bioavailability of radionuclides in soils. J Environ Radioact 99:820–830
3. Shahandeh H, Hossner L (2002) Role of soil properties in phytoaccumulation of uranium. Water Air Soil Pollut 141:165–180
4. Vera Tome F, Blanco Rodríguez P, Lozano JC (2009) The ability of *Helianthus annus* L. and *Brassica juncea* to uptake and translocate natural uranium and ^{226}Ra under different milieu conditions. Chemosphere 74:293–300
5. Chao JH, Lee HP, Chiu CY (2006) Measurement of ^{226}Ra uptake in a fern actively accumulating radium. Chemosphere 62: 1656–1664
6. Soudek P, Podracká E, Vágner M, Vaněk T, Petřík P, Tykva R (2004) ^{226}Ra uptake from soils into different plant species. J Radioanal Nucl Chem 262:187–189
7. Soudek P, Petrová Š, Benešová D, Kotyza J, Vágner M, Vaňková R, Vaněk T (2010) Study of soil-plant transfer of ^{226}Ra under greenhouse conditions. J Environ Radioact 101:446–450
8. Syed HS (1999) Comparison studies adsorption of thorium and uranium on pure clay minerals and local Malaysian soil sediments. J Radioanal Nucl Chem 241(1):11–14
9. Huang JW, Blaylock MJ, Kapulnik Y, Ensley BD (1998) Phytoremediation of uranium-contaminated soils: role of organic acids in triggering uranium hyperaccumulation in plants. J Environ Sci Technol 32:2004–2008
10. Gerzabek MH, Strebl F, Temmel B (1998) Plant uptake of radionuclides in lysimeter experiments. Environ Pollut 99:93–103
11. Million JB, Sartain JB, Gonzales RX, Carrier WD (1994) Radium-226 and calcium uptake by crops grown in mixtures of sand and clay tailings from phosphate mining. J Environ Qual 23:671–676
12. Štrok M, Smodiš B (2010) Fractionation of natural radionuclides in soils from the vicinity of a former uranium mine Žirovski vrh, Slovenia. J Environ Radioact 101:22–28
13. Sill CW, Williams RL (1981) Preparation of actinides for alpha spectrometry without electrodeposition. Anal Chem 53:415–421
14. Lozano JC, Fernandez F, Gomez JMG (1997) Determination of radium isotopes by $BaSO_4$ coprecipitation for the preparation of alpha-spectrometric sources. J Radioanal Nucl Chem 223:133–137
15. Jačimović R, Smodiš B, Bučar T, Stegnar P (2003) k_0-NAA quality assessment by analysis of different certified reference materials using the KAYZERO/SOLCOI software. J Radioanal Nucl Chem 257:659–663
16. Deng H, Ye ZH, Wong MH (2004) Accumulation of lead, zinc, copper and cadmium by 12 wetland plant species thriving in metal-contaminated sites in China. Environ Pollut 132:29–40
17. Archer MJG, Caldwell RA (2004) Response of six australian plant species to heavy metal contamination at an abandoned mine site. Water Air Soil Pollut 167:257–267
18. Anawar HM, Garcia-Sanchez A, Murciego A, Buyolo T (2006) Exposure and bioavailability of arsenic in contaminated soils from the La Parrilla mine, Spain. Environ Geol 50:170–179
19. Kopp P, Oestling P, Burkart W (1989) Availability and uptake by plants of radionuclides under different environmental conditions. Toxicol Environ Chem 23:53–63
20. Linsalata P, Mores RS, Ford H, Eisenbud M, Penna Franca E, De Castro MB, Lobao N, Sachett I, Carlos M (1989) An assessment of soil-to plant concentration ratios for some natural anlogues of the transuranic elements. Health Phys 56(1):33–46
21. Vandenhove H, Olyslaegers G, Sanzharova N, Shubina O, Reed E, Shang Z, Velasco H (2009) Proposal for new best estimates of the soil-to-plant transfer factor of U, Th, Ra, Pb and Po. J Environ Radioact 100:721–732
22. Baker AJM (1981) Accumulators and excluders – strategies in the response of plants to heavy metals. J Plant Nutr 3:643–654
23. Ebbs SD, Lasat MM, Brandy DJ, Cornish J, Gordon R, Kochian LV (1997) Heavy metals in the environment: phytoextraction of cadmium and zinc from a contaminated soil. J Environ Qual 26:1424–1430

Priloga 1: Nadaljevanje

G Model
NED-5735; No. of Pages 5

Nuclear Engineering and Design xxx (2010) xxx–xxx

Contents lists available at ScienceDirect

Nuclear Engineering and Design

journal homepage: www.elsevier.com/locate/nucengdes

Uptake of radionuclides by a common reed (*Phragmites australis* (Cav.) Trin. ex Steud.) grown in the vicinity of the former uranium mine at Žirovski vrh

Marko Černe, Borut Smodiš*, Marko Štrok

Jožef Stefan Institute, Jamova cesta 39, SI-1000 Ljubljana, Slovenia

ARTICLE INFO

Article history:
Received 19 January 2010
Received in revised form 7 April 2010
Accepted 8 April 2010
Available online xxx

ABSTRACT

From uranium mining areas, in particular, the radionuclides are usually discharged to the environment during the mining and milling process. At the former uranium mine Žirovski vrh, Slovenia, mine waste and mill tailings were deposited at the Jazbec site and the Boršt site, respectively. Plants grown in soils contaminated with the seepage waters from tailings may represent radiological concern if radionuclides from the uranium decay chain are transferred into the food chain. Uranium is usually accumulated in the roots and translocated to the shoots in limited amounts. Uranium plant accumulators are usually plants from Brassicaceae and Poaceae families. A common reed (*Phragmites australis* (Cav.) Trin. ex Steud.), a tall perennial grass, growing in a wetland habitats, accumulates metals in the above-ground parts. It may be used for phytoremediation of uranium-contaminated soils, because of high biomass production and high metal-accumulation potential. Preliminary results of radionuclide contents measured in such plants, growing on the deposit tailings are presented. A common reed, that was grown on the Boršt tailings pile accumulated 8.6 ± 8 mBq/g dry weight (d.w.) and 2.4 ± 2 mBq/g dry weight (d.w.) of ^{238}U in leaves and stems, respectively. In the paper, activity concentrations of other nuclides, i.e. ^{226}Ra, ^{210}Pb and ^{40}K are also shown and discussed.

1. Introduction

Radioactive contamination of the environment is a global concern. The mining and the milling processes of raw material containing uranium and thorium are one of the main causes of discharging of radionuclides into the environment, mainly from the tailings. The other processes include the coal combustion, cement production, phosphate fertilizers production and its use in agriculture management and the nuclear fuel cycle operations (Pöschl and Nollet, 2007). Discharged radionuclides in the environment may pose a threat to the humans, due to inhalation of contaminated aerosols, ingestion of contaminated water or food and external irradiation (Howard et al., 1996; IAEA, 1994; Pöschl and Nollet, 2007). The migration of radionuclides in the environment depends on many factors, such us physico-chemical, biological, geochemical and microbial influences, soil and water properties, air flows and specific interactions of radionuclides with vegetation or other organisms where they accumulate (Pöschl and Nollet, 2007). Uranium for example, can be effectively bounded to the clay minerals, humic substances (Vandenhove et al., 2009) or accumulated by plants (Huang et al., 1998; Vera Tome et al., 2009; Shahandeh and Hossner, 2002) or microorganisms (Tabak et al., 2005).

The uptake of radionuclides by plants is observed by some metal-accumulating plants that grow on soils contaminated with uranium tailings (Soudek et al., 2007a,b). These are metal-tolerant plants, having toxic metal hyperaccumulation potential, which could be beneficial in phytoremediation for cleanup of soil and water (Prasad and De Oliveira Freitas, 2003). Metal hyperaccumulation is defined as uptake of metals in the aboveground tissues of a plant under field conditions (Pollard, 2000). Most plants on metalliferous soils accumulate low concentrations of metal ions in their upper tissues, while few species, endemic to metalliferous sites may accumulate high concentrations (Baker and Brooks, 1989). Plants growing on metal-contaminated and metalliferous soils developed three basic strategies of survival: metal excluders, metal indicators and metal accumulators (Peer et al., 2005). Metal excluders are metal-tolerant plants, that prevent metal from entering their aerial parts over a broad range of metal concentrations in soils, but some may still contain large amounts of metals in their roots. Metal indicators accumulate metals in their aboveground tissues and the metal levels in the tissues of these plants reflect metal levels in the soil. Metal accumulators or hyperaccumulators concentrate metals in above-ground tissues to levels far exceeding those present in the soil or in nonaccumulating plants growing nearby (Baker and Walker, 1990). The accumulation of uranium in plants is proved in several studies (Huang et al., 1998;

* Corresponding author.
E-mail addresses: marko.cerne@ijs.si (M. Černe), borut.smodis@ijs.si (B. Smodiš), marko.strok@ijs.si (M. Štrok).

0029-5493/$ – see front matter © 2010 Elsevier B.V. All rights reserved.
doi:10.1016/j.nucengdes.2010.04.003

Please cite this article in press as: Černe, M., et al., Uptake of radionuclides by a common reed (*Phragmites australis* (Cav.) Trin. ex Steud.) grown in the vicinity of the former uranium mine at Žirovski vrh. Nucl. Eng. Des. (2010), doi:10.1016/j.nucengdes.2010.04.003

Priloga 1: Nadaljevanje

G Model
NED-5735; No. of Pages 5
ARTICLE IN PRESS
2 M. Černe et al. / Nuclear Engineering and Design xxx (2010) xxx–xxx

Shahandeh and Hossner, 2002; Chao et al., 2006; Vera Tome et al., 2009). Uranium is usually accumulated in the roots and less in the shoots. Other nuclides from uranium decay chain, such us ^{210}Pb and ^{226}Ra can also be accumulated in the plants (Hovmand et al., 2009; Soudek et al., 2008). The levels of ^{210}Pb concentrations in native and cultivated plants are very low. Bioavailability of ^{210}Pb in the soil is rather low due to the ability of solid phase of soil to strongly adsorb lead ions (Usman, 2008; Veeresh et al., 2003; Irha et al., 2009). Accumulation of ^{210}Pb in the plants is investigated in very few studies (Pietrzak-Flis and Skowrońska-Smolak, 1995; Hovmand et al., 2009), where authors agreed that atmospheric deposition contribute to the major part of plant contamination with ^{210}Pb. Root uptake of ^{210}Pb is proved for mushrooms, where 30% of ^{210}Pb present in the soil was available for transfer to mushrooms (Guillén et al., 2009). Radium is known to be more mobile than lead in soil (Simon and Ibrahim, 1990). Radium is an easily dissolved salt and could be readily absorbed by plant roots and accumulated in the roots and shoots (Soudek et al., 2007a,b). Radium is chemically analogues to the essential element Ca and considered to participate in the similar physiological processes in the plants (Gerzabek et al., 1998; Million et al., 1994). The understanding of transport of uranium and its decay products through a soil–plant system is thus important for better radiological assessment of human and environmental exposure to radioactive elements through ingestion.

The aim of this study was to assess the uptake of ^{238}U, ^{226}Ra, ^{210}Pb and ^{40}K by a common reed. We assume that accumulation of radium would be the highest. The plants were grown on the deposit tailings on the tailings pile.

2. Materials and methods

2.1. Fieldwork

The sampled plants (common reed) were grown on the tailings pile at deposited tailings which originated from the pond (site 2 of Fig. 1) where loading of U-mill tailings constantly occurred due to flowing of seepage waters from the tailings pile to the pond. During the pond cleaning, the loaded tailings were removed and deposited on the tailings pile (site 1 of Fig. 1). Deposited tailings contained higher amount of moisture, seeds and obviously enough nutrients, because the same plants grew also in the pond on this loaded tailings material. The plants of common reed which represent a composite sample of 200 plants were surrounded by bare tailing material where they were taken from 3 places in the area of 100 m^2 of site 1 (Figure 1). Plants were in the fully grown stage and were sampled in the late autumn 2006. The control group of plants were taken from the marsh in the vicinity of Ljubljana, the capital.

Fig. 1. Air picture of the Boršt tailings pile.

2.2. Study area

The uranium mine at Žirovski vrh operated from 1985 to 1990 and about 600,000 tons of U-ore were processed during that period. The U-mill tailings with high concentrations of uranium decay products such as ^{230}Th, ^{226}Ra and ^{210}Pb were disposed at the Boršt site. The map of the Boršt disposal site with indicated sampling points is given in Fig. 1. Site 1 represents the location of the sampled plants, site 2 represents the pond—the origin of deposited tailings.

2.3. Sample preparation

The average of 20 plants of common reed was used for alpha and gamma spectrometric measurement. Plants were firstly separated on stems and leaves, to observe the difference in radionuclide content in both parts. The samples were then air dried for a longer period of time and finally for 2 days in an oven (model ST-05—Instrumentaria, Zagreb) at 80 °C. Dried samples were than ashed in a laboratory furnace (model Bosio—Štore) to 650 °C for few days to attain the complete mineralization. The samples intended for gamma spectrometric measurements of ^{210}Pb and ^{40}K were not ashed. Soil samples were dried on 60 °C in the oven for 1 week, sieved to pass through 1 mm sieve and packed into 150 mL plastic cylindrical containers for at least 4 weeks to achieve radioactive equilibrium.Determination of radionuclides in the samples

Determination of radionuclides in the plant samples of common reed comprised radio-chemical separation and measurement of activity concentrations using alpha-spectrometer for ^{226}Ra and ^{238}U and gamma-spectrometer for ^{210}Pb and ^{40}K determination.

2.4.1. Radio-chemical separation

Environmental samples containing alpha emitters must undergo specific procedures before being counted. All sample preparations are designed to remove as many impurities from the sample as possible and convert it into a form suitable for chemical separation. Chemical separation isolates specific elements in the sample to minimize interferences among multiple alpha emitting nuclides and concentrates/purifies the sample for the element to be measured. The 0.5 g of ashed samples, together with 2 g of Na_2O_2 and 2 g of Na_2CO_3 were melted at 900 °C to get the alkaline melt. The radiotracers ^{133}Ba for ^{226}Ra and ^{232}U for ^{238}U were added after melting for recovery determination. The procedures for uranium and radium determination are described below.

2.4.1.1. Determination of uranium. The procedure was modified as described in Štrok and Smodiš (2010). The alkaline melt was dissolved with 6 mL HNO_3, 6 mL HCl and 6 mL HF. After dissolution sample was evaporated until incipient dryness, followed by the addition of 2 mL H_2O_2 and the sample was again evaporated. These steps were repeated three times to ensure the complete digestion. The residue was dissolved with 8 mL H_2SO_4 and evaporated until incipient dryness. After that, NH_4OH and five drops of 5 mg/mL Fe^{3+} were added in order to co-precipitate uranium with $Fe(OH)_3$. The sample was centrifugated and supernatant was discarded. The precipitate was centrifuged until neutral pH was achieved. Then the precipitate was dissolved with 10 mL of 3 M HNO_3–1 M $Al(NO_3)$ and loaded onto UTEVA separation column, which was previously conditioned with 5 mL 3 M HNO_3. The column was rinsed with consecutive addition of 5 mL 3 M HNO_3, 5 mL of 9 M HCl and 20 mL of 5 M HCl/0.05 M oxalic acid uranium was eluted from the column with 15 mL of 1 M HCl and microprecipitated with 0.1 mL of

Please cite this article in press as: Černe, M., et al., Uptake of radionuclides by a common reed (*Phragmites australis* (Cav.) Trin. ex Steud.) grown in the vicinity of the former uranium mine at Žirovski vrh. Nucl. Eng. Des. (2010), doi:10.1016/j.nucengdes.2010.04.003

Priloga 1: Nadaljevanje

0.5 mg/mL Nd^{3+}, 1 mL of 15% $TiCl_3$ and 1 mL HF. Prior to filtration the solution was placed for 30 min into ice bath, followed by the filtration through 0.1 μm membrane filter, which was previously rinsed twice with 5 mL of 10 μg/mL NdF_3. After filtration, the membrane filter was mounted on an aluminium disc, dried with a heating light and measured on an alpha-spectrometer for uranium determination.

2.4.1.2. Determination of radium. The procedure was modified as described in Štrok and Smodiš (2010). The alkaline melt was dissolved with 6 mL HNO_3, 6 mL HCl and 6 mL HF. After dissolution sample was evaporated until incipient dryness, followed by the addition of 2 mL H_2O_2 and the sample was again evaporated. These steps were repeated three times to ensure the complete digestion. The residue was dissolved in 2 mL HNO_3 and deionized water and filtered through black ribbon filter paper. After that, radium was co-precipitated as $Pb(Ra)SO_4$ from the filtered solution, with addition of 2 mL H_2SO_4 and 1 mL of 50 mg/mL Pb^{2+} carrier. The sample was centrifuged and supernatant was discarded. The precipitate was washed with deionized water and again centrifuged until neutral pH was achieved. Then the precipitate was dissolved with addition of 4 mL 0.1 M EDTA/0.5 M NaOH. After that, radium was microprecipitated with addition of 0.3 mL Ba-carrier (0.3 mg/mL Ba^{2+}), one drop of liquid pH 0–5 indicator, 1 mL of 1:1 acetic acid, 4 mL of saturated Na_2SO_4 and 0.3 mL of 0.125 mg/mL $BaSO_4$ substrate. After 30 min, the solution was filtered through 0.1 μm membrane filter. After filtration, membrane filter was mounted on an aluminium disc, dried with a heating light and measured on a gamma-spectrometer for chemical recovery determination through ^{133}Ba and later on an alpha-spectrometer for ^{226}Ra determination.

2.4.2. Measurement of activity concentration in the samples

The activity concentrations of the ^{238}U and ^{226}Ra were measured by the alpha-spectrometer equipped with PIPS semiconductor detectors (Alpha-Analyst–Canberra) having an efficiency of 28%. The calibration was done with electroplated certified standard source containing ^{239}Pu, ^{238}U, ^{234}U and ^{241}Am.

^{210}Pb and ^{40}K in the plant samples were determined by gamma spectrometry using a well-type HP germanium detector. The dried samples were transferred to a 10 mL vials and hermetically sealed. ^{210}Pb was measured at 46.5 keV and ^{40}K at 1460.8 keV. The gamma-ray spectrometry system was calibrated with KCl powder and certified liquid solution of ^{210}Pb spiked on cellulose powder. Radionuclides in the soil samples were also measured by gamma spectrometry, after being hermetically sealed for at least 4 weeks to achieve radioactive equilibrium.

3. Results and discussion

3.1. Radionuclides in the deposit tailings

Deposit tailings, contained very high activity concentrations of ^{226}Ra and ^{210}Pb and rather elevated high activity concentrations of ^{40}K (Table 1).

The radium content is double compared to radium content found in U-mill tailings deposited on the Boršt tailings pile (8.63 ± 0.34 Bq/g d.w.) (Križman et al., 1995). Radium was obviously concentrated, presumably due to constant loading of ^{226}Ra on fine particles (Simon and Ibrahim, 1990) in the pond from contaminated seepage water, but this process should be further investigated. Radionuclide content in the marsh soil from the control site was significantly lower and below the detection limit for ^{210}Pb.

Table 1
Radionuclide concentrations in the deposit tailings (expanded uncertainties, $k = 2$).

Bq/g d.w.	^{238}U	^{226}Ra	^{210}Pb	^{40}K
Boršt site	1.38 ± 0.28	14.9 ± 2.0	7.1 ± 4.6	0.78 ± 0.14
Control	0.07 ± 0.02	0.056 ± 0.008	<0.15	0.42 ± 0.08

Table 2
Activity concentrations in leaves and stems of plants (average of 20 plants) grown at the study site (expanded uncertainties, $k = 2$).

mBq/g d.w.	^{238}U	^{226}Ra	^{210}Pb	^{40}K
Leaves	8.6 ± 0.8	1200 ± 100	780 ± 10	13.3 ± 0.5
Stems	2.4 ± 0.2	270 ± 20	190 ± 10	98 ± 4

3.2. Radionuclides in leaves

Our results for ^{238}U, ^{226}Ra, ^{210}Pb and ^{40}K activity concentrations of common reed represent preliminary values of a composite sample consisting of about 200 plants from one location. Obtained values were determined separately in leaves and stems (but not in the roots) so the classical transfer factors where the activity concentration in plant (Bq/g d.w. of a plant) is divided with the activity concentration in soil (Bq/g d.w. of soil) (Chen et al., 2005) were not determined. The radionuclide concentrations were significantly different between control plants (Table 3) and plants from the study site (Table 2). Our measurements show higher amounts of ^{226}Ra (by a factor 30.000 compared to the control plants) and ^{210}Pb (by a factor 78 compared to the control plants) in leaves of plants (common reed) from study site, with activity concentrations of 1200 ± 100 and 780 ± 10 mBq/g d.w., respectively (Table 2). Several studies confirm the accumulation of radium in plants (Chao et al., 2006; Soudek et al., 2004, 2007a,b). Accumulation of ^{210}Pb is less known phenomenon and should be further investigated. In the literature it is indicated that the major pathways of lead transfer to the plants are usually dry or wet deposition (Hovmand et al., 2009) and rarely root uptake. Radionuclide ^{210}Pb is permanently present in the atmosphere due to decay of radon short-lived decay products. High activity concentrations of ^{210}Pb in the leaves from the plants grown on deposit tailings at the Boršt site may be observed due to several reasons. Contamination of leaves with U-mill tailings during the wind blowing at the Boršt site is probable since most of the bare tailings were surrounded the plants, but root uptake of ^{226}Ra and ^{210}Pb remains more reliable option because in the case of wind contamination the content of ^{238}U should also be higher. Common reed is a helophyte and has a high transpiration capacity, which is a possible reason for higher root uptake of radium and lead, just like by mineral nutrients (Casadesus et al., 2001, 2008). Concentrations of ^{226}Ra and ^{210}Pb in the control plants were below the detection limits, being 0.04 mBq/g d.w. for ^{226}Ra and 10 mBq/g d.w. for ^{210}Pb. Lower limit of detection for ^{210}Pb is, because the measured gamma line for ^{210}Pb has low intensity (4%) and relatively low signal-to-noise ratio due to low gamma energy (46.5 keV), higher than for the other measured gamma emitters. The amount of ^{238}U in the leaves of plants from contaminated area was lower and is probably due to lower activity concentration of uranium in the deposited tailings, where the radium and lead levels were high. The accumulation properties of a common reed for uranium were already confirmed by other studies (Soudek et al., 2007a,b; Gerth et al., 2005). Uranium in the soil is most often bioavailable for plants in the form of uranyl cations, uranyl–carbonate complexes, uranyl–phosphate complexes (Vandenhove et al., 2007) and uranyl–citrate complexes (Huang et al., 1998). Potassium activity concentrations in the leaves of plants from contaminated area were significantly lower (by a factor 47 compared to the control plants) compared to the control plants, in spite of that the activity concentrations of ^{40}K in deposit tailings were doubled when compared to the control site. It is possible the ^{40}K was not bioavailable in U-mill tailings or that tailings had

Please cite this article in press as: Černe, M., et al., Uptake of radionuclides by a common reed (*Phragmites australis* (Cav.) Trin. ex Steud.) grown in the vicinity of the former uranium mine at Žirovski vrh. Nucl. Eng. Des. (2010), doi:10.1016/j.nucengdes.2010.04.003

Priloga 1: Nadaljevanje

G Model
NED-5735; No. of Pages 5
ARTICLE IN PRESS
4 M. Černe et al. / Nuclear Engineering and Design xxx (2010) xxx–xxx

Table 3
Activity concentrations in leaves and stems of control plants (average of 20 plants) grown in the marsh in the vicinity of Ljubljana, the capital (expanded uncertainties, $k = 2$).

mBq/g d.w.	^{238}U	^{226}Ra	^{210}Pb	^{40}K
Leaves	0.27 ± 0.11	<0.04	<10	630 ± 11
Stems	0.3 ± 0.1	1.0 ± 0.2	<10	780 ± 14

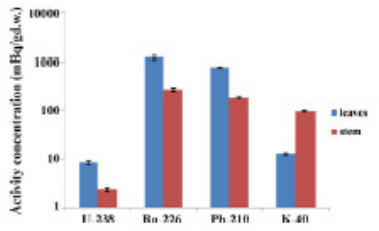

Fig. 2. Radionuclide content in leaves and stems of plants (common reed) form the study site.

some negative or phytotoxic effect (Bhagawati and Pankaj, 2006) which impact the uptake of ^{40}K. Further investigation is required to clarify this phenomenon. ^{40}K is a naturally abundant nuclide in a plants and its content is specific from one plant to another (Pulhani et al., 2005; Badran et al., 2003). Higher amounts of potassium in the plants are normal, because of its essential role in almost all physiological processes needed to sustain plant growth and reproduction. Potassium is a cation, with the highest concentration in cytoplasm and plays a vital role in photosynthesis, translocation of sugars and starches, protein synthesis, control of ionic balance, maintain of turgor, reduction of water loss, activation of plant enzymes, resistance do plant disease and many other processes (Lambers et al., 2008).

3.3. *Radionuclides in stems*

Activity concentrations of ^{238}U, ^{226}Ra and ^{210}Pb in the stems of plants from study site, were lower than in the leaves, except for ^{40}K (Table 2). Activity concentrations of radionuclides in control plants were lower than at the study site, except for ^{40}K (Table 3). Activity concentrations of radionuclides in samples from the study site are graphically presented in Fig. 2.

4. Conclusions

The results indicated a possible radio-accumulating ability of a common reed grown on a deposit U-mill tailings. Specific physiological characteristics of common reed could influence to higher content of ^{210}Pb in the leaves, although it is known that lead ions hardly accumulate in the plant tissues due to strong binding capacity of lead to solid phase of soil. Low content of uranium in the leaves and stems may be connected to not bioavailable form of uranium in the deposit tailings. Presence of small amounts of radionuclides in the stems is logical, because of the fact that a stem has a transport function and translocates nutrients to different tissues. Higher potassium content in the deposit tailings could be related to higher potassium content in the uranium ore and it was obviously not in bioavailable form as potassium in the marsh soil of control site, where one or two orders of magnitude higher activity concentrations of potassium were measured in the plants.

The accumulation properties of common reed could be useful in phytoremediation of mine waters or for bioindication of radionuclides in such waters. However, the specific location of ^{226}Ra and ^{210}Pb in the plant tissues of common reed should be further investigated. High activity concentrations of radionuclides in the U-mill tailings did not negatively impact on plants growth, which means that common reed belongs to the metal-resistant plants with a metal-tolerance mechanism against toxic elements.

Acknowledgments

This work was supported by the Rudnik Žirovski vrh company. The Slovenian Research Agency (contract no. P2-0075) is also acknowledged.

References

Badran, H.M., Sharshar, T., Elnimer, T., 2003. Levels of ^{137}Cs and ^{40}K in edible parts of some vegetables consumed in Egypt. Journal of Environmental Radioactivity 67, 181–190.
Baker, A.J.M., Brooks, R.R., 1989. Terrestial higher plants which hyper accumulate metallic elements. Review of their distribution, ecology and phytochemistry. Biorecovery 1, 81–126.
Baker, A.J.M., Walker, P.L., 1990. Ecophysiology of metal uptake by tolerant plants. In: Shaw, A.J. (Ed.), Heavy Metal Tolerance in Plants: Evolutionary Aspects. CRC Press, Boca Raton, pp. 155–177.
Bhagawati, L.J., Pankaj, P., 2006. Effects of various concentrations of uranium tailings on certain growth and biochemical parameters in sunflower. Biologia Bratislava 61 (1), 103–107.
Casadesus, J., Sauras, T., Gonze, M.A., Vallejo, R., Bréchignac, F., 2001. A nutrient-based mechanistic model for predicting the root uptake of radionuclides. In: Bréchignac, F., Howard, B. (Eds.), Radioactive Pollutants: Impact on the Environment. EDP Sciences, Les Ulis, pp. 209–239.
Casadesus, J., Sauras-Year, T., Vallejo, V.R., 2008. Predicting soil-to plant transfer of radionuclides with a mechanistic model (BIORUR). Journal of Environmental Radioactivity 99 (5), 864–871.
Chao, J.H., Lee, H.P., Chiu, C.Y., 2006. Measurement of ^{224}Ra uptake in a fern actively accumulating radium. Chemosphere 62, 1656–1664.
Chen, S.B., Zhu, Y.G., Hu, Q.H., 2005. Soil to plant transfer of ^{238}U, ^{226}Ra and ^{232}Th on a uranium mining—impacted soil from southeastern China. Journal of Environmental Radioactivity 82, 223–236.
Gerth, A., Hebner, A., Kiessig, G., Zellemer, A., 2005. Passive treatment of minewater at the Schlema Alberoda site. In: Merkel, B., Hasche-Berge, A. (Eds.), Uranium in the Environment: Mining Impact and Concequences. Springer-Verlag, Berlin, pp. 409–414.
Gerzabek, M.H., Strebl, F., Temmel, B., 1998. Plant uptake of radionuclides in lysimeter experiments. Environmental Pollution 99, 93–103.
Guillén, J., Baeza, A., Ontalba, M.A., Miguez, M.P., 2009. ^{210}Pb and stable lead content in fungi: its transfer from soil. Science of the Total Environment 407, 4320–4326.
Hovmand, M.F., Nielsen, S.P., Johnsen, I., 2009. Root uptake of lead by Norway spruce grown on ^{210}Pb spiked soils. Environmental Pollution 157, 404–409.
Howard, B.J., Johanson, K.J., Linsley, G.S., Hove, K., Pröhl, G., Horyna, J., 1996. Transfer of radionuclides by terrestial food products from semi-natural ecosystems. In: Second Report on the VAMP Terrestial Working Group, IAEA, Vienna, IAEA-TECDOC-857, pp. 49–79.
Huang, J.W., Blaylock, M.J., Kapulnik, Y., Ensley, B., 1998. Phytoremediation of uranium-contaminated soils: role of organic acids in triggering uranium hyperaccumulation in plants. Environmental Science and Technology 32, 2004–2008.
IAEA, 1994. Handbook of transfer parameter values for the prediction of radionuclide transfer in temperate environments. IAEA, Vienna, Technical Reports Series No. 364.
Irha, N., Steinnes, E., Kirso, U., Petersell, V., 2009. Mobility of Cd, Pb, Cu and Cr in some Estonian soil types. Estonian Journal of Earth Sciences 58 (3), 209–214.
Križman, N., Byrne, A.R., Benedik, L., 1995. Distribution of ^{230}Th in milling wastes from Žirovski vrh uranium mine (Slovenia), and its radioecological implications. Journal of Environmental Monitoring 26, 223–235.
Lambers, H., Chapin, F.S., Pons, T.L., 2008. Plant Physiological Ecology. Springer Science + Business Media, LLC, New York, p. 604.
Million, J.B., Sartain, J.B., Gonzales, R.X., Carrier, W.D., 1994. Radium-226 and calcium uptake by crops grown in mixtures of sand and clay tailings from phosphate mining. Journal of Environmental Quality 23, 671–676.
Peer, W.A., Baxter, I.R., Richards, E.L., Freeman, J.L., Murphy, A.S., 2005. Phytoremediation and hyperaccumulator plants. In: Tamás, M.J., Martinoia, E. (Eds.), Molecular Biology of Metal Homeostasis and Detoxification: Topics in Current Genetics. Springer-Verlag, Berlin/Heidelberg, p. 14.
Pietrzak-Flis, Z., Skowrońska-Smolak, M., 1995. Transfer of ^{210}Pb and ^{210}Po to plants via root system and above-ground interception. The Science of the Total Environment 162, 139–147.
Pollard, A.J., 2000. Metal hyperaccumulation. New Phytologist 146, 179–181.
Pöschl, M., Nollet, L.M.L., 2007. Radionuclide Concentrations in Food and the Environment. CRC Press/Taylor & Francis Group, Boca Raton, p. 458.

Please cite this article in press as: Černe, M., et al., Uptake of radionuclides by a common reed (*Phragmites australis* (Cav.) Trin. ex Steud.) grown in the vicinity of the former uranium mine at Žirovski vrh. Nucl. Eng. Des. (2010), doi:10.1016/j.nucengdes.2010.04.003

Priloga 1: Nadaljevanje

Prasad, M.N.V., De Oliveira Freitas, H.M., 2003. Metal hyperaccumulation in plants—biodiversity prospecting for phytoremediation technology. Electronic Journal of Biotechnology 3, 110–146.
Pulhani, V.A., Dafauti, S., Hegde, A.G., Sharma, R.M., Mishra, U.C., 2005. Uptake and distribution of natural radioactivity in wheat plants from soil. Journal of Environmental Radioactivity 79, 331–346.
Shahandeh, H., Hossner, L., 2002. Role of soil properties in phytoaccumulation of uranium. Water, Air and Soil Pollution 141, 165–180.
Simon, S.L., Ibrahim, S.A., 1990. Biological uptake of radium by terrestrial plants. In: The Environmental Behaviour of Radium, vol. 1, IAEA. Technical report series no., 310, pp. 545–599.
Soudek, P., Valenová, Š., Benešová, D., Vaněk, T., 2007. From laboratory experiments to large scale application—an example of the phytoremediation of radionuclides. In: Advanced Science and Technology for Biological Decontamination of Sites Affected by Chemical and Radiological Nuclear Agents. Springer, pp. 139–158.
Soudek, P., Petřik, P., Vágner, M., Tykva, R., Plojhar, V., Petrová, Š., Vaněk, T., 2007b. Botanical survey and screening of plant species which accumulate ^{226}Ra from contaminated soil of uranium waste depot. European Journal of Soil Biology 43, 251–261.
Soudek, P., Petrová, Š., Benešová, D., Kotyza, J., Vágner, M., Vaňková, R., Vaněk, T., 2008. Study of soil–plant transfer of ^{226}Ra under greenhouse conditions. Journal of Environmental Radioactivity, 1–5.
Soudek, P., Podracká, E., Vágner, M., Vaněk, T., Petřík, P., Tykva, R., 2004. ^{226}Ra uptake from soils into different plant species. Journal of Radioanalytical and Nuclear Chemistry 262, 187–189.
Štrok, M., Smodiš, B., 2010. Fractionation of natural radionuclides in soils from the vicinity of a former uranium mine Žirovski vrh, Slovenia. Journal of Environmental Radioactivity 101, 22–28.
Tabak, H.H., Lens, P., Van Hullebusch, E.D., Dejonghe, W., 2005. Developments in bioremediation of soils and sediments polluted with metals and radionuclides. 1. Microbial processes and mechanisms affecting bioremediation of metal contamination and influencing metal toxicity and transport. Reviews in Environmental Science and Biotechnology 4, 115–156.
Usman, A.R.A., 2008. The relative adsorption selectivities of Pb, Cu, Zn, Cd and Ni by soils developed on shale in New Valley, Egypt. Geoderma 144, 334–343.
Vandenhove, H., Van Hees, M., Wannijn, J., Wouters, K., Wang, L., 2007. Can we predict uranium bioavailability based on soil parameters? Part 2. Soil solution uranium concentration is not a good bioavailability index. Environmental Pollution 145, 577–586.
Vandenhove, H., Gil-García, C., Vidal, M., 2009. New best estimates for radionuclide solid–liquid distribution coefficients in soils. Part 2. Naturally occurring radionuclides. Journal of Environmental Radioactivity 100, 697–703.
Veeresh, H., Tripathy, S., Chaudhuri, D., Hart, B.R., Powell, M.A., 2003. Competitive adsorption behaviour of selected heavy metals in three soil types of India amended with fly ash and sewage sludge. Environmental Geology 44, 363–370.
Vera Tome, F., Blanco Rodríguez, P., Lozano, J.C., 2009. The ability of *Helianthus annus* L. and *Brassica Juncea* to uptake and translocate natural uranium and ^{226}Ra under different milieu conditions. Chemosphere 74, 293–300.

Please cite this article in press as: Černe, M., et al., Uptake of radionuclides by a common reed (*Phragmites australis* (Cav.) Trin. ex Steud.) grown in the vicinity of the former uranium mine at Žirovski vrh. Nucl. Eng. Des. (2010), doi:10.1016/j.nucengdes.2010.04.003

Priloga 1: Nadaljevanje

Journal of Power and Energy Systems

Vol. 2, No. 2, 2008

Calibration and Validation of a Proportional Counter for Determining Beta Emitters*

Marko ŠTROK**, Urška REPINC** and Borut SMODIŠ**
**Department of Environmental Sciences, Jožef Stefan Institute
Jamova 39, SI-1000 Ljubljana, Slovenia
E-mail: Marko.Strok@ijs.si

Abstract
Calibration of recently installed proportional counter at the Hot Cells Facility of the Jožef Stefan Institute was performed. Instrument was calibrated for determination of total beta activity, Sr–90 and Pb–210. Detection efficiencies for K–40, Sr–90, Y–90, Pb–210 and Bi–210 were determined, allowing for more accurate determination of the particular nuclide as a single K–40 efficiency. In addition, self-absorption curves for different surface densities for the nuclides mentioned were derived. Two empirical equations for faster and more accurate determination of Sr–90 and Pb–210 were derived. These two equations consider differences in surface density and in-growth of Y–90 and Bi–210, respectively. The detection efficiencies obtained ranged from 10 to 52 %, depending on the nuclide, surface density and chemical compositions of the salts used or precipitates obtained following radiochemical separation in the experiment. As a performance test of derived empirical equation for the determination of detection efficiency for Pb–210, specific activity of Pb 210 in IAEA 385 and IAEA 414 intercomparison materials were determined. All procedures and formulae developed include calculation of minimal detectable activities and uncertainty budgets for the determinations concerned.

Key words: Proportional Counter, Detection Efficiency, Beta Emitters, Total Beta Activity, Sr–90, Pb–210

1. Introduction

Accurate and fast determination of different beta emitters in various samples is very important for monitoring of possible releases of these nuclides into the environment. Part of this determination is also related to proper and accurate calibration of a proportional counter, which in general includes determination of background of the proportional counter and determination of detection efficiency.

In this work we focused on the determination of detection efficiency. The detection efficiency for beta emitters depends on the type of the nuclide, the type of precipitate and surface density. According to that we must prepare and measure calibration standards for determining detection efficiency in the same manner as we prepare and measure samples.

The preparation of standards and samples is not a problem with respect to the type of the nuclide and type of precipitate. But on the other hand it is very difficult to achieve the same surface density for the standards and samples, because we cannot always achieve the same chemical yield for radiochemical separation procedure. The best way to overcome this problem is to measure detection efficiencies for different surface densities and to construct a self-absorption curve and find an equation, which will describe dependence of the detection efficiency on the surface density. After that we can apply this equation to calculate detection

*Received 30 July, 2007 (No. 07-0332)
[DOI: 10.1299/jpes.2.573]

Priloga 1: Nadaljevanje

Journal of Power and Energy Systems

Vol. 2, No. 2, 2008

efficiencies for different surface densities of the prepared samples.

Determination of Sr–90 and Pb–210, having beta emitting daughters Y–90 and Bi–210, respectively, represents another difficulty. In this case, activity and also the detection efficiency grows up after radiochemical separation so long as they achieve secular radioactive equilibrium. For Y–90 this time is approximately 14 days and for Bi–210 approximately 30 days.

Usual procedures for the determination of Sr–90 involve its measurement in secular radioactive equilibrium with Y–90 [1] or separation of Y–90 from Sr–90 followed by Y–90 measurement [2]. These procedures usually neglect the effect of surface density because it is expected that samples have the same surface densities as the standard. But in laboratory practice it is very difficult to obtain the same surface densities for both the sample and standard. It is also assumed that the effect of surface density, because of high-energy beta particles from Y–90, can be neglected. Pb–210 is usually determined with a proportional counter by measuring its daughter nuclide Bi–210 [3].

In our case the detection efficiencies were determined based on empirical equation that allows for accurate determination of Sr–90 over a whole in-growth period of Y–90 and for different surface densities. With this improvement we can define the detection efficiency for Sr–90 independently of time elapsed after the radiochemical separation of Y–90 and independently of the surface density. Equations (1) to (4) describes the detection efficiency where $\varepsilon_{Sr-90+Y-90}$ is total detection efficiency, ε_{Sr-90} is detection efficiency for Sr–90, ε_{Y-90} is detection efficiency for Y–90, λ_{Y-90} is decay constant for Y–90, $t_{2,Sr-90}$ is the time elapsed from the separation of Sr–90, $N_{Sr\text{-}90\text{-}Y\text{-}90}$ is number of counts for Sr-90 and Y-90, $A_{Sr\text{-}90}$ is the activity of Sr-90 in the standard, t_m is measuring time of the standard, $N_{Sr\text{-}90}$ is number of counts for Sr-90 and $N_{Y\text{-}90}$ is number of counts for Y-90.

$$\varepsilon_{Sr-90+Y-90} = \varepsilon_{Sr-90} + \varepsilon_{Y-90}\left(1-\exp\left(-\lambda_{Y-90}t_{2,Sr-90}\right)\right) \quad (1)$$

$$\varepsilon_{Sr\text{-}90+Y\text{-}90} = \frac{N_{Sr\text{-}90+Y\text{-}90}}{A_{Sr\text{-}90}t_m} \quad (2)$$

$$\varepsilon_{Sr\text{-}90} = \frac{N_{Sr\text{-}90}}{A_{Sr\text{-}90}t_m} \quad (3)$$

$$\varepsilon_{Y\text{-}90} = \frac{N_{Y\text{-}90}}{A_{Sr\text{-}90}t_m} \quad (4)$$

If we substitute ε_{Sr-90} and ε_{Y-90} in Eq. (1) with empirical equations for self-absorption curves, we obtain Eq. (7), which allows for the determination of Sr–90 detection efficiency for different surface densities and for various times elapsed from the separation. Empirical equation for the Pb–210 detection efficiency is derived in the same manner.

Performance test of derived empirical equation for the determination of detection efficiency for Pb–210 was also performed. Specific activities of Pb–210 in IAEA 385 and IAEA 414 intercomparison materials were determined. IAEA 385 is Irish Sea sediment material and IAEA 414 is mixed fish material from Irish and the North Sea. In this determination, detection efficiencies for Pb–210 were calculated with the derived Eq. (8). Performance test contained measurements of specific activity of Pb–210 in different times after radiochemical separation. Measured specific activities were plotted versus time after radiochemical separation and compared with the information value.

Priloga 1: Nadaljevanje

Journal of Power and Energy Systems

Vol. 2, No. 2, 2008

2. Experimental

2.1 Proportional Counter

A Canberra Tennelec LB4100-W low background gas flow proportional counter having eight proportional detectors in two drawers was used. As a counting gas, mixture of 90 % argon and 10 % methane was used.

2.2 Detection Efficiency for K–40

KCl was weighted onto stainless steel planchets using an analytical balance. KCl was dispersed onto planchets by adding small amount of acetone to achieve homogenous deposit of KCl. When the acetone was evaporated, KCl was mounted with the glue and the detection efficiency was measured with proportional counter. This procedure was applied for different surface densities. Self-absorption curve was fitted to the experimental data with program CurveExpert 1.3.

2.3 Detection Efficiency for Sr–90 and Y–90

Detection efficiency for Sr–90 and Y–90 was determined by two methods, differing in the way of separation of Sr–90 from Y–90. The first procedure involved extraction process and the second procedure precipitation. These two procedures were applied to ensure that separation process of Sr–90 from Y–90 was really selective.

The extraction procedure involved addition of different amounts of 20 mg/mL Sr carrier to the standard Sr–90/Y–90 solution in order to achieve different surface densities of $SrCO_3$. To these solutions 15 mL of 0.15 mol/L HNO_3 were added and then Y–90 extracted with 15 mL of 0.2 mol/L dibutylphosphate in chlorophorm. The time of this extraction was the separation time of Sr–90 from Y–90. The water phase was stored. The organic phase was washed three more times by adding 10 mL of 0.15 mol/L HNO_3 and the organic phase discarded. The water phases were filtered through filter paper and then 0.2 g $(NH_4)_2CO_3$ and NH_4OH were added to make the solution alkaline. This solution was heated on a hot plate to accomplish precipitation of $SrCO_3$.

This precipitate was then transferred to a plastic centrifuge beaker and centrifuged. Supernatant was discarded. The precipitate was washed with deionized water and again centrifuged. Supernatant was discarded and the precipitate quantitatively transferred to a plastic tube with aluminium planchet on the bottom. 2 mL of ethanol was added to the tube and then centrifuged. Supernatant was discarded, the precipitate deposited on planchet and dried up under a heating lamp. So prepared precipitates were weighted on an analytical balance to determine chemical yield of the procedure and then measured in the proportional counter over a whole in-growth period of Y–90.

The precipitation procedure involved the same quantities of Sr carrier and standard Sr–90/Y–90 solution as for the extraction method. 10 mL of deionized water was added to the standards and heated on a hot plate. Then 1 mL of 10 mg/mL Ba carrier and 1 ml of 5 mg/mL Fe carrier were added. After $Fe(OH)_3$ coagulated, solution was filtered through a filter paper. Precipitate was discarded and time of filtration was registered as a separation time of Sr–90 from Y–90. 1 mL of concentrated CH_3COOH, 2 mL 25% NH_3 acetate and 1 mL of saturated $(NH_4)_2CrO_4$ solution were added to the filtrate. Then the solution was heated for 10 min on a hot plate and filtered through a filter paper. The $BaCrO_4$ precipitate was discarded. To the filtrate 0.2 g of $(NH_4)_2CO_3$ and NH_4OH were added to achieve alkalinity. This solution was heated on a hot plate to accomplish precipitation of $SrCO_3$.

The precipitate was centrifuged, washed, dried up, weighted and measured in the proportional counter in the same way as in the extraction procedure.

The experimental data obtained from extraction and precipitation procedures were plotted versus time after separation and fitted with the CurveExpert 1.3 program to the Eq. (1) in order to determine detection efficiencies for Sr–90 at the time of separation and for

Priloga 1: Nadaljevanje

Journal of Power and Energy Systems

Vol. 2, No. 2, 2008

Y–90 at the time when Y–90 was in secular equilibrium with Sr–90. These detection efficiencies were plotted to the different surface densities obtained and fitted with the CurveExpert 1.3 to obtain the self-absorption equations for Sr–90 and Y–90. These self-absorption equations were inserted into Eq. (1), replacing the detection efficiencies for Sr–90 and Y–90. As result the empirical equation describing the detection efficiency for Sr–90 was obtained, which is function of the $SrCO_3$ surface density and the time elapsed after the Y–90 separation.

2.4 Detection Efficiency for Pb–210 and Bi–210

Different amounts of $PbCl_2$ were added to the standard solution of Pb–210/Bi–210 to achieve different surface densities of $PbSO_4$. Then HNO_3 and H_2O_2 were added and evaporated. Sample was dissolved in HCl. Pb was separated on a Sr Resin column and again evaporated and dissolved in H_2O. Then the sample was precipitated with sulfuric acid to form $PbSO_4$. This precipitate was quantitatively transferred into a plastic tube having an aluminium planchet on the bottom; 2 mL of ethanol was added and then centrifuged. Supernatant was discarded. The precipitate, deposited on the planchet, was dried up under a heating lamp. So prepared precipitates were weighted on an analytical balance to determine chemical yield of the separation and then measured in the proportional counter over a whole in-growth period of Bi–210.

Experimental data was processed in the same way as for Sr–90, yielding the empirical equation for the detection efficiency for Pb–210 as function of the $PbSO_4$ surface density and the time elapsed after the separation from Bi–210.

2.5 Determination of Pb–210 Specific Activity

For the determination of Pb–210 specific activity in an IAEA intercomparison sample, $PbCl_2$ carrier was added to the sample and sample was digested in HNO_3 and H_2O_2. After digestion, HNO_3 and H_2O_2 were evaporated and the sample was dissolved in HCl. Pb was separated on the Sr Resin column and again evaporated and dissolved in H_2O. Then this sample was precipitated with sulfuric acid to form $PbSO_4$. This precipitate was quantitatively transferred into a plastic tube having an aluminium planchet on the bottom; 2 mL of ethanol was added and then centrifuged. Supernatant was discarded. The precipitate, deposited on the planchet, was dried up under a heating lamp. So prepared precipitate was weighted on an analytical balance to determine chemical yield of the separation and then measured in the proportional counter over a whole in-growth period of Bi–210.

Specific activity was calculated with the help of Eq. (5). In this equation a_S is specific activity of the sample, R_S is count rate the sample, R_B is background count rate, m_S is mass of the sample, $\varepsilon_{Pb\text{-}210+Bi\text{-}210}$ is from Eq. (8) calculated total detection efficiency and η_S is chemical recovery of the sample.

$$a_S = \frac{R_S - R_B}{m_S \varepsilon_{Pb\text{-}210+Bi\text{-}210} \eta_S} \tag{5}$$

3 Results and Discussion

3.1 Detection Efficiency for K–40

Detection efficiency and self-absorption curve derived from experimental data for K–40 is shown in Fig. 1. Surface densities from 10 mg/cm^2 to 235 mg/cm^2 were considered. Detection efficiency ranged from 47 % for the lowest surface density to 18 % for the greatest surface density. Equation (6) shows plotted self-absorption curve that was calculated by the CurveExpert 1.3. In this equation $\varepsilon_{K\text{-}40}$ is detection efficiency of K–40 and

Priloga 1: Nadaljevanje

Journal of Power and Energy Systems
Vol. 2, No. 2, 2008

$\rho_{A,KCl}$ is surface density of the KCl. Good agreement between the experimental results and the derived self-absorption curve can be observed.

$$\varepsilon_{K-40} = 0.4215\left(0.1804 + \exp\left(-0.0060\rho_{A,KCl}\right)\right) \quad (6)$$

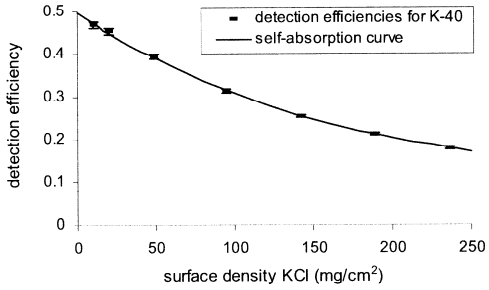

Fig. 1 Detection efficiency for K–40 in KCl and self-absorption curve

3.2 Detection Efficiency for Sr–90 and Y–90

Detection efficiencies for Sr–90 and Y–90 and self-absorption curves obtained by the CurveExpert 1.3 program are presented in Fig. 2. Surface densities ranged from 10 mg/cm^2 to 72 mg/cm^2. Detection efficiency for Sr–90 ranged from 32 % for the smallest surface density to 17 % for the greatest one. The detection efficiency for Y–90 ranged from 52 % to 44 %. Equation (7) represents the empirical equation for the determination of total detection efficiency as function of the $SrCO_3$ surface density and the time elapsed after the separation from Y–90.

$$\begin{aligned}\varepsilon_{Sr-90+Y-90} = {} & 0.3449\left(0.0854 + \exp\left(-0.0159\rho_{A,SrCO3}\right)\right) \\ & + 0.1881\left(1.8751 + \exp\left(-0.0130\rho_{A,SrCO3}\right)\right) \\ & \cdot\left(1 - \exp\left(-\lambda_{Y-90}t_{2,Sr-90}\right)\right)\end{aligned} \quad (7)$$

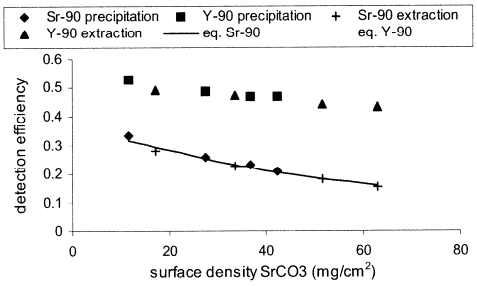

Fig. 2 Detection efficiencies for Sr–90 and Y–90 versus surface density of $SrCO_3$

Priloga 1: Nadaljevanje

Journal of Power and Energy Systems

Vol. 2, No. 2, 2008

Figures 3 and 4 present in-growth of Y–90 from Sr–90 indicated as increase in the total detection efficiency. The curves in the figures are derived from Eq. (7) and show good agreement with the experimental data. By comparing detection efficiencies for Sr–90 and Y–90 for the precipitation and extraction procedures, it is evident that the detection efficiencies for the precipitation procedure are slightly higher than for the extraction one, as evident from Fig. 2. Accordingly, the curves derived from Eq. (7) in Fig. 3 are below the experimental data and in Fig. 4 above the experimental data.

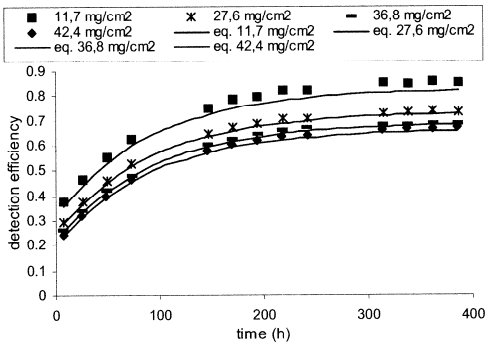

Fig. 3 In-growth of total detection efficiency for different surface densities of $SrCO_3$; precipitation

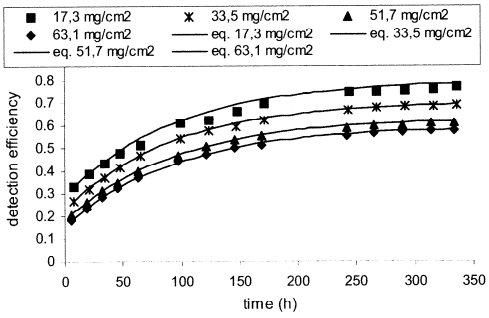

Fig. 4 In-growth of total detection efficiency for different surface densities of $SrCO_3$; extraction

3.3 Detection efficiency for Pb–210 and Bi–210

Detection efficiencies for Pb–210 and Bi 210 versus surface density are presented in Fig. 5. Self-absorption curves, obtained by the program CurveExpert 1.3, are also shown in the figure. Surface densities ranged from 2.7 mg/cm^2 to 21 mg/cm^2. The detection efficiency for Pb–210 ranged from 13 % for the lowest surface density to 11 % for the greatest. The detection efficiency for Bi–210 ranged from 36 % to 20 %. Equation (8) shows the empirical equation for the total detection efficiency ($\varepsilon_{Pb\text{-}210,Bi\text{-}210}$) as function of

Priloga 1: Nadaljevanje

Journal of Power and Energy Systems
Vol. 2, No. 2, 2008

the surface density ($\rho_{A,PbSO4}$) and the time elapsed after separation from Bi–210 ($t_{2,Pb-210}$). This equation was also obtained by the program CurveExpert 1.3.

$$\varepsilon_{Pb-210+Bi-210} = 0.0492\left(1.8007+\exp\left(-0.0373\rho_{A,PbSO4}\right)\right) + 0.2648\left(0.7469+\exp\left(-0.1811\rho_{A,PbSO4}\right)\right) \cdot\left(1-\exp\left(-\lambda_{Bi-210}t_{2,Pb-210}\right)\right) \quad (8)$$

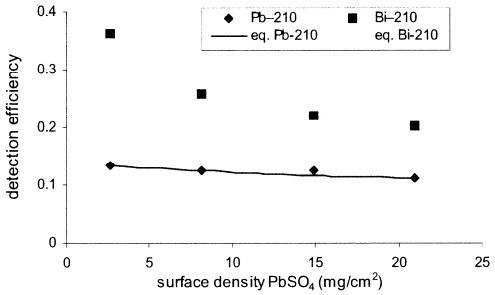

Fig. 5 Detection efficiencies for Pb–210 and Bi–210 versus surface density of $PbSO_4$

Figure 6 shows in-growth of Bi–210 from the Pb–210 indicated as the in-growth of the total detection efficiency. Curves in this figure are derived from Eq. (8) and are in good agreement with the experimental data shown as points.

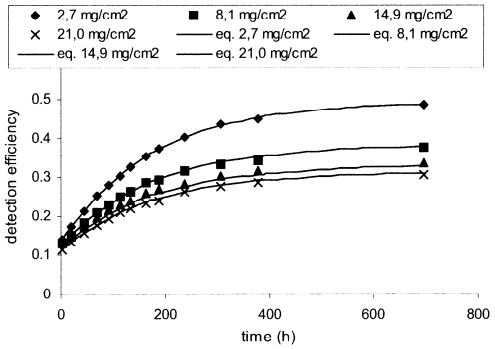

Fig. 6 In-growth of total detection efficiency for different surface densities of $PbSO_4$

3.4 Comparison of detection efficiencies

The results obtained show that beta detection efficiency varies with the surface density and with the type of the precipitate as revealed in Fig. 7. The detection efficiency for Bi–210 in $PbSO_4$ is lower than the one for Sr–90 in $SrCO_3$, although Sr–90 has lower maximum beta energy than Bi–210. This is due to greater molecular mass of the $PbSO_4$.

Priloga 1: Nadaljevanje

Journal of Power and Energy Systems

Vol. 2, No. 2, 2008

From Fig. 7 it can be seen that the detection efficiency for Pb–210 is almost independent of the surface density but that is due to the low energy of the beta particles emitted by Pb–210, which are almost completely absorbed in $PbSO_4$ precipitate. Due to that, a detector can detect only the beta particles emitted by Pb–210, which are on the surface of the sample.

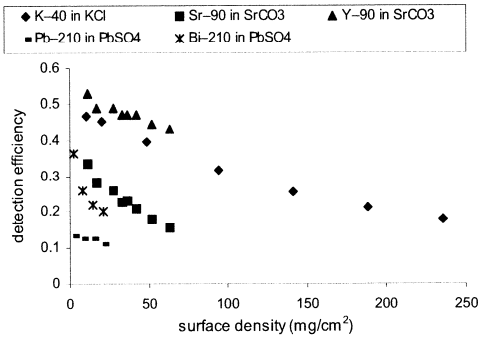

Fig. 7 Detection efficiencies versus surface density

3.5 Determination of Pb–210 Specific Activity

Figures 8 and 9 present performance test results involving the derived empirical equation for determination of detection efficiency for Pb–210. These two figures show Pb–210 specific activities obtained for the two IAEA intercomparison materials versus time after radiochemical separation. It is noticeable that in both cases uncertainties decrease with time after radiochemical separation due to in-growth of Bi–210 from Pb–210; the increase in count rate causes reduction of uncertainty. All results except the first ones are in good agreement with the information values. Greater deviation from the information values in the first and second measurement after radiochemical separation is due to the relatively low count rate at the beginning of in-growth of Bi–210.

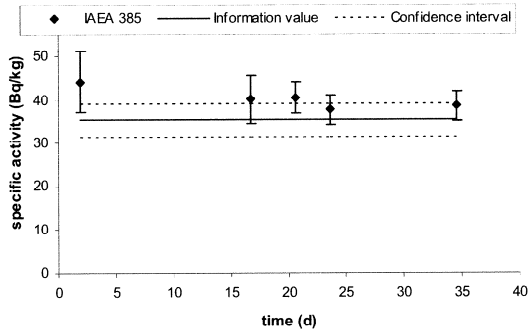

Fig. 8 Pb–210 specific activity of IAEA 385

Priloga 1: Nadaljevanje

Journal of Power and Energy Systems

Vol. 2, No. 2, 2008

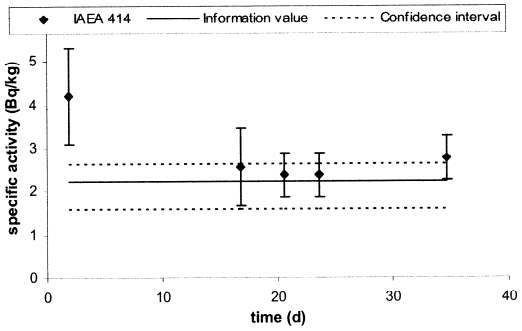

Fig. 9 Pb–210 specific activity of IAEA 414

4. Conclusion

All the obtained self-absorption curves and empirical equations follow well experimental results. The derived empirical equations offer possibility for accurate and faster determination of beta emitters, having beta-emitting daughters that come into secular radioactive equilibrium with their parents. The main advantage of using these empirical equations are the facts that one does not need to wait for achieving secular radioactive equilibrium (approximately 14 days for Sr–90 and approximately 30 days for Pb–210) and worry if the surface density of the sample is the same as the one for the standard. The performance test showed that calculation of detection efficiencies with help of the derived empirical equation is a suitable and very helpful method, which improves accuracy and flexibility in the determination of Pb–210 or Sr–90 using a proportional counter.

Acknowledgement

The financial support of the Slovenian Research Agency (Grant No. P2-0075) is highly appreciated.

References

(1) Manjon, G., El-Daoushy, F. and Garcia-Tenorio, R., Sr–90 in lake sediments, *Journal of Radioanalytical and Nuclear Chemistry*, Vol. 209, No. 1 (1997), pp 95-98.
(2) Goutleard, F., Nazard, R., Bocquet, C., Coquenlorge, N., Letessier, P. and Calmet, D., Improvement in Sr–90 measurements at very low levels in environmental samples, *Applied Radiation and Isotopes*, Vol. 53 (2000), pp 145-151.
(3) Peck, G. A. and Smith, J. D., Determination of Po–210 and Pb–210 using measurement of Po–210 and Pb–210, *Analytica Chimica Acta*, Vol. 422 (2000), pp 113-120

Priloga 2: Rezultati sekvenčnega ekstrakcijskega postopka S za ^{238}U, ^{230}Th in ^{226}Ra

Frakcija	Lokacija	$a_{U\text{-}238}$ (Bq/kg)	$a_{Th\text{-}230}$ (Bq/kg)	$a_{Ra\text{-}226}$ (Bq/kg)
Izmenljiva	1	0,44 ± 0,09	6,36 ± 0,48	4,03 ± 0,26
	2	0,91 ± 0,21	4,96 ± 0,70	3,19 ± 0,18
	3	0,92 ± 0,22	5,98 ± 1,01	3,59 ± 0,25
	4	5,74 ± 0,60	7,85 ± 0,92	25,5 ± 1,4
	5	0,44 ± 0,17	3,46 ± 0,39	4,16 ± 0,24
	6	1,13 ± 0,11	14,5 ± 0,8	12,1 ± 0,6
Organska snov	1	120 ± 6	8,28 ± 1,04	10,5 ± 0,7
	2	2,31 ± 0,18	3,95 ± 0,38	10,1 ± 0,6
	3	2,39 ± 0,15	3,83 ± 0,32	6,85± 0,45
	4	376 ± 54	8,08 ± 0,74	165 ± 9
	5	6,64 ± 0,50	8,55 ± 0,70	25,3 ± 1,4
	6	225 ± 14	9,43 ± 0,92	31,9 ± 1,3
Karbnonati	1	104 ± 11	65,9 ± 4,2	11,1 ± 0,8
	2	3,56 ± 0,35	7,07 ± 0,40	10,8 ± 0,7
	3	4,66 ± 0,58	17,0 ± 4,5	10,9 ± 0,7
	4	86,3 ± 5,6	54,9 ± 2,9	213 ± 11
	5	13,7 ± 1,2	21,5 ± 1,5	47,8 ± 2,4
	6	60,0 ± 5,6	62,1 ± 3,3	73,1 ± 4,7
Fe/Mn oksidi	1	12,9 ± 1,1	5,98 ± 0,63	1,20 ± 0,10
	2	0,49 ± 0,19	2,22 ± 0,18	2,10 ± 0,16
	3	0,60 ± 0,24	2,01 ± 0,22	1,59 ± 0,12
	4	10,2 ± 0,9	4,13 ± 0,51	52,7 ± 2,0
	5	3,04 ± 0,23	4,44 ± 0,35	8,03 ± 0,52
	6	21,1 ± 1,9	5,12 ± 0,61	29,0 ± 1,4
Preostanek	1	77,6 ± 4,6	90,3 ± 4,6	82,2 ± 3,5
	2	62,5 ± 4,4	109 ± 8	89,9 ± 5,4
	3	50,2 ± 3,8	80,6 ± 4,4	80,0 ± 3,4
	4	111 ± 8	465 ± 31	402 ± 24
	5	52,0 ± 3,5	128 ± 9	140 ± 7
	6	66,6 ± 4,4	150 ± 7	206 ± 11

Priloga 3: Rezultati sekvenčnega ekstrakcijskega postopka S za ^{210}Pb in ^{210}Po

Frakcija	Lokacija	$a_{Pb\text{-}210}$ (Bq/kg)	$a_{Po\text{-}210}$ (Bq/kg)
Izmenljiva	1	5,40 ± 2,08	0,128 ± 0,023
	2	1,39 ± 1,03	0,040 ± 0,020
	3	5,43 ± 2,23	0,252 ± 0,043
	4	5,87 ± 2,69	0,173 ± 0,021
	5	0,71 ± 0,51	0,0018 ± 0,0005
	6	4,86 ± 2,38	0,011 ± 0,004
Organska snov	1	2,70 ± 2,07	0,060 ± 0,045
	2	0,83 ± 0,51	0,040 ± 0,030
	3	0,21 ± 0,18	0,011 ± 0,009
	4	1,29 ± 1,03	0,018 ± 0,010
	5	0,18 ± 0,16	0,008 ± 0,002
	6	7,57 ± 2,48	0,723 ± 0,151
Karbnonati	1	48,7 ± 3,0	14,6 ± 0,9
	2	10,4 ± 2,4	1,15 ± 0,11
	3	14,5 ± 2,4	3,41 ± 0,22
	4	150 ± 5	26,2 ± 0,9
	5	35,0 ± 2,8	5,87 ± 0,30
	6	44,2 ± 2,9	6,01 ± 0,33
Fe/Mn oksidi	1	4,23 ± 2,28	1,29 ± 0,11
	2	4,83 ± 2,51	0,09 ± 0,04
	3	5,41 ± 2,24	0,08 ± 0,06
	4	46,6 ± 3,0	5,57 ± 0,31
	5	7,26 ± 2,42	0,43 ± 0,08
	6	24,1 ± 2,8	0,31 ± 0,08
Preostanek	1	73,6 ± 3,7	92,8 ± 4,9
	2	30,6 ± 2,9	45,8 ± 2,6
	3	35,3 ± 2,7	52,9 ± 2,9
	4	254 ± 8	301 ± 25
	5	83,4 ± 3,7	125 ± 9
	6	168 ± 6	161 ± 9

Priloga 4: Rezultati sekvenčnega ekstrakcijskega postopka B za ^{238}U, ^{230}Th in ^{226}Ra

Frakcija	Lokacija	$a_{U\text{-}238}$ (Bq/kg)	$a_{Th\text{-}230}$ (Bq/kg)	$a_{Ra\text{-}226}$ (Bq/kg)
Karbnonati	1	27,8 ± 1,2	5,46 ± 0,40	9,26 ± 0,66
	2	0,85 ± 0,12	4,84 ± 0,34	5,90 ± 0,38
	3	0,40 ± 0,10	4,54 ± 0,53	4,53 ± 0,33
	4	72,0 ± 3,9	4,45 ± 0,46	59,6 ± 3,0
	5	0,63 ± 0,18	4,93 ± 0,52	8,70 ± 0,62
	6	25,9 ± 1,7	7,25 ± 0,78	26,2 ± 1,6
Fe/Mn oksidi	1	66,3 ± 3,3	13,8 ± 1,3	25,5 ± 1,3
	2	2,28 ± 0,25	3,63 ± 0,31	16,5 ± 0,8
	3	1,26 ± 0,19	2,28 ± 0,28	14,2 ± 0,8
	4	160 ± 8	7,14 ± 0,63	501 ± 22
	5	2,95 ± 0,25	3,26 ± 0,33	112 ± 6
	6	152 ± 8	4,20 ± 0,44	181 ± 7
Organska snov	1	81,4 ± 4,3	10,0 ± 0,7	3,59 ± 0,30
	2	4,39 ± 0,34	8,99 ± 1,06	5,85 ± 0,45
	3	6,17 ± 0,43	14,1 ± 1,2	7,29 ± 0,57
	4	358 ± 20	77,6 ± 5,3	95,0 ± 3,9
	5	10,4 ± 0,7	22,4 ± 2,0	22,0 ± 1,3
	6	142 ± 11	31,5 ± 2,8	26,0 ± 1,5
Preostanek	1	79,0 ± 4,5	85,8 ± 6,0	63,4 ± 3,5
	2	70,3 ± 4,0	74,1 ± 5,8	60,4 ± 3,7
	3	69,4 ± 4,4	87,6 ± 3,6	65,5 ± 2,9
	4	122 ± 6	371 ± 30	241 ± 11
	5	66,7 ± 4,1	159 ± 8	107 ± 7
	6	94,4 ± 4,4	191 ± 8	99,4 ± 5,3

Priloga 5: Rezultati sekvenčnega ekstrakcijskega postopka B za ^{210}Pb in ^{210}Po

Frakcija	Lokacija	$a_{Pb\text{-}210}$ (Bq/kg)	$a_{Po\text{-}210}$ (Bq/kg)
Karbnonati	1	5,20 ± 3,38	0,33 ± 0,08
	2	0,27 ± 0,15	0,030 ± 0,016
	3	0,78 ± 0,52	0,018 ± 0,008
	4	16,5 ± 3,4	0,20 ± 0,08
	5	4,70 ± 3,34	0,004 ± 0,002
	6	4,15 ± 3,35	0,08 ± 0,05
Fe/Mn oksidi	1	83,4 ± 5,0	6,64 ± 0,41
	2	19,1 ± 3,8	4,36 ± 0,34
	3	32,2 ± 4,0	3,55 ± 0,38
	4	261 ± 9	6,58 ± 0,50
	5	93,6 ± 4,9	3,58 ± 0,30
	6	147 ± 9	66,3 ± 2,2
Organska snov	1	28,5 ± 3,2	3,00 ± 0,35
	2	19,1 ± 3,6	0,55 ± 0,12
	3	19,9 ± 3,3	0,48 ± 0,26
	4	82,2 ± 4,2	3,54 ± 0,70
	5	24,5 ± 3,0	1,13 ± 0,26
	6	41,2 ± 3,2	1,03 ± 0,13
Preostanek	1	19,8 ± 3,4	90,5 ± 4,4
	2	12,1 ± 3,2	45,1 ± 2,7
	3	22,7 ± 3,5	54,3 ± 3,3
	4	138 ± 9	384 ± 35
	5	40,1 ± 4,0	133 ± 7
	6	66,1 ± 3,9	134 ± 8

Priloga 6: Vsebnosti ^{238}U, ^{230}Th, ^{226}Ra in ^{210}Pb v vzorcih trav

Lokacija	$a_{U\text{-}238}$ (Bq/kg suhe mase)	$a_{Th\text{-}230}$ (Bq/kg suhe mase)	$a_{Ra\text{-}226}$ (Bq/kg suhe mase)	$a_{Pb\text{-}210}$ (Bq/kg suhe mase)
1	4,65 ± 0,31	1,50 ± 0,08	8,10 ± 0,68	43,3 ± 1,5
2	0,979 ± 0,076	1,22 ± 0,11	4,02 ± 0,21	72,9 ± 2,2
3	0,142 ± 0,029	1,36 ± 0,15	3,88 ± 0,22	42,5 ± 1,5
4	1,03 ± 0,16	2,10 ± 0,22	170 ± 8	45,0 ± 1,6
5	0,213 ± 0,041	0,93 ± 0,08	105 ± 5	94,7 ± 2,5
6	0,523 ± 0,081	1,04 ± 0,10	112 ± 6	77,9 ± 2,2

Priloga 7: Vsebnosti ^{238}U, ^{230}Th, ^{226}Ra in ^{210}Pb v vzorcih tal

Lokacija	$a_{U\text{-}238}$ (Bq/kg)	$a_{Th\text{-}230}$ (Bq/kg)	$a_{Ra\text{-}226}$ (Bq/kg)	$a_{Pb\text{-}210}$ (Bq/kg)
1	315 ± 31	177 ± 15	109 ± 7	135 ± 7
2	69,8 ± 12,1	127 ± 12	116 ± 7	48,1 ± 4,5
3	58,7 ± 10,6	109 ± 15	103 ± 7	60,7 ± 4,7
4	589 ± 54	540 ± 49	858 ± 43	457 ± 14
5	75,8 ± 10,3	165 ± 14	226 ± 13	126 ± 6
6	373 ± 31	241 ± 18	352 ± 18	249 ± 9

Priloga 8: Faktorji prenosa med tlemi in travo za ^{238}U, ^{230}Th, ^{226}Ra in ^{210}Pb

Lokacija	$TF_{\text{U-238}}$ (kg/kg suhe mase)	$TF_{\text{Th-230}}$ (kg/kg suhe mase)	$TF_{\text{Ra-226}}$ (kg/kg suhe mase)	$TF_{\text{Pb-210}}$ (kg/kg suhe mase)
1	0,015 ± 0,002	0,0085 ± 0,0008	0,074 ± 0,008	0,32± 0,02
2	0,014 ± 0,003	0,0096 ± 0,0012	0,035 ± 0,003	1,52 ± 0,15
3	0,0024 ± 0,0007	0,012 ± 0,002	0,038 ± 0,003	0,70 ± 0,06
4	0,0018 ± 0,0003	0,0039 ± 0,0005	0,198 ± 0,014	0,098 ± 0,005
5	0,0028 ± 0,0007	0,0056 ± 0,0007	0,465 ± 0,033	0,74 ± 0,04
6	0,0014 ± 0,0003	0,0043 ± 0,0005	0,319 ± 0,022	0,31 ± 0,01

Priloga 9: Vsebnosti ^{238}U, ^{230}Th in ^{226}Ra v drevesih

Vrsta	Drevo	a (Bq/kg suhe mase)		
		Les	Poganjki	enoletne iglice ali listi
^{238}U				
Pinus sylvestris	1	0,023 ± 0,003	0,09 ± 0,02	1,51 ± 0,11
	2	0,048 ± 0,005	0,13 ± 0,02	4,12 ± 0,26
	3	0,042 ± 0,005	0,15 ± 0,03	5,36 ± 0,35
	4	0,018 ± 0,003	0,11 ± 0,03	1,80 ± 0,09
	5	0,020 ± 0,003	0,09 ± 0,03	1,12 ± 0,12
	6	0,014 ± 0,003	0,10 ± 0,03	2,20 ± 0,16
Picea abies	1	0,018 ± 0,003	0,13 ± 0,03	1,36 ± 0,11
	2	0,020 ± 0,003	0,16 ± 0,03	0,98 ± 0,10
	3	0,010 ± 0,003	0,14 ± 0,03	1,10 ± 0,11
	4	0,012 ± 0,002	0,12 ± 0,03	2,06 ± 0,15
	5	0,021 ± 0,003	0,16 ± 0,02	1,14 ± 0,08
	6	0,019 ± 0,002	0,29 ± 0,04	1,16 ± 0,13
Acer	1	0,027 ± 0,004	0,37 ± 0,06	2,99 ± 0,28
^{230}Th				
Pinus sylvestris	1	0,041 ± 0,005	0,64 ± 0,07	0,98 ± 0,10
	2	0,039 ± 0,004	0,50 ± 0,05	1,37 ± 0,11
	3	0,046 ± 0,007	0,59 ± 0,06	1,79 ± 0,14
	4	0,035 ± 0,004	0,34 ± 0,03	0,40 ± 0,04
	5	0,030 ± 0,004	0,56 ± 0,04	0,60 ± 0,06
	6	0,053 ± 0,005	1,36 ± 0,11	2,59 ± 0,15
Picea abies	1	0,20 ± 0,01	1,53 ± 0,16	11,3 ± 0,8
	2	0,17 ± 0,01	0,32 ± 0,04	0,61 ± 0,07
	3	0,18 ± 0,01	1,52 ± 0,15	1,54 ± 0,15
	4	0,078 ± 0,005	1,29 ± 0,11	0,56 ± 0,06
	5	0,045 ± 0,006	0,56 ± 0,04	1,24 ± 0,12
	6	0,26 ± 0,015	0,90 ± 0,09	2,37 ± 0,18
Acer	1	0,077 ± 0,007	1,85 ± 0,19	7,03 ± 0,62
^{226}Ra				
Pinus sylvestris	1	5,62 ± 0,27	9,86 ± 054	20,0 ± 1,9
	2	2,68 ± 0,14	7,71 ± 0,43	20,5 ± 1,0
	3	5,20 ± 0,29	9,26 ± 0,48	64,9 ± 4,4
	4	4,22 ± 0,23	4,65 ± 0,27	25,3 ± 1,1
	5	5,00 ± 0,25	12,2 ± 0,7	45,2 ± 2,1
	6	2,96 ± 0,16	6,41 ± 0,42	21,0 ± 1,0
Picea abies	1	124 ± 6	127 ± 7	704 ± 31
	2	69,9 ± 3,1	163 ± 8	392 ± 45
	3	91,3 ± 4,0	228 ± 11	809 ± 34
	4	82,0 ± 3,6	290 ± 12	535 ± 23
	5	347 ± 15	1239 ± 81	2728 ± 113
	6	73,4 ± 3,2	140 ± 6	320 ± 14
Acer	1	27,3 ± 1,5	137 ± 7	809 ± 39

Priloga 10: Vsebnosti ^{210}Pb v drevesih

Vrsta	Drevo	a (Bq/kg suhe mase)		
		les	poganjki	enoletne iglice ali listi
^{210}Pb				
Pinus sylvestris	1	30,6 ± 1,5	5,4 ± 0,3	46 ± 2
	2	13,5 ± 0,8	8,0 ± 0,5	41 ± 2
	3	36,1 ± 1,8	6,1 ± 0,4	31 ± 1
	4	11,6 ± 0,7	6,6 ± 0,4	39 ± 1
	5	34,8 ± 2,2	7,4 ± 0,5	48 ± 2
	6	19,1 ± 1,1	5,1 ± 0,4	49 ± 2
Picea abies	1	20,2 ± 1,1	6,7 ± 0,3	76 ± 4
	2	16,8 ± 0,9	8,7 ± 0,5	96 ± 4
	3	10,8 ± 0,5	10,6 ± 0,7	116 ± 5
	4	27,4 ± 1,5	12,6 ± 0,8	130 ± 5
	5	23,8 ± 0,8	73,6 ± 3,1	321 ±15
	6	9,0 ± 0,5	7,4 ± 0,5	108 ± 5
Acer	1	21,5 ± 1,1	21,8 ± 0,6	177 ± 9

Priloga 11: Efektivne letne ingestijske doze za ^{238}U, ^{234}U, ^{226}Ra, ^{210}Pb in ^{210}Po za odrasle in dojenčke (P. m. = Pomurske mlekarne)

Populacija	E_{ing} (µSv/leto)				
	^{238}U	^{234}U	^{226}Ra	^{210}Pb	^{210}Po
Odrasli; 1 – 4	0,092 ± 0,015	0,058 ± 0,011	0,30 ± 0,07	4,8 ± 2,8	7,7 ± 1,3
Odrasli; 5	0,006 ± 0,003	0,015 ± 0,005	0,41 ± 0,06	3,7 ± 2,5	4,5 ± 0,8
Dojenčki; 1 – 4	1,68 ± 0,28	1,06 ± 0,16	16,1 ± 2,8	140 ± 83	402 ± 69
Dojenčki; 5	0,111 ± 0,052	0,269 ± 0,087	16,8 ± 2,6	110 ± 73	236 ± 43
Dojenčki; P. m.	4,44 ± 0,62	2,41 ± 0,41	7,08 ± 1,39	187 ± 92	447 ± 112
Dojenčki; Hipp	0,865 ± 0,060	1,18 ± 0,21	10,7 ± 2,1	123 ± 43	59,5 ± 6,8